

Fakultät Wissenschaftszentrum Weihenstephan für Ernährung, Landnutzung und Umwelt
Campus Straubing für Biotechnologie und Nachhaltigkeit
Lehrstuhl für Chemie Biogener Rohstoffe

Exopolysaccharides by *Paenibacilli*: from Genetic Strain Engineering to Industrial Application

Marius Paul Rütering

Vollständiger Abdruck der von der Fakultät Wissenschaftszentrum Weihenstephan für Ernährung, Landnutzung und Umwelt der Technischen Universität München zur Erlangung des akademischen Grades eines

Doktors der Naturwissenschaften

genehmigten Dissertation.

Vorsitzender: Prof. Dr. Cordt Zollfrank

Prüfer der Dissertation: 1. Prof. Dr. Volker Sieber
2. Prof. Dr. Wolfgang Liebl
3. Prof. Dr. Jochen Schmid

Die Dissertation wurde am 01.04.2019 bei der Technischen Universität München eingereicht und durch die Fakultät Wissenschaftszentrum Weihenstephan für Ernährung, Landnutzung und Umwelt am 16.12.2019 angenommen.



Dissertation



Marius Rütering

Exopolysaccharides by *Paenibacilli*:
from Genetic Strain Engineering to
Industrial Application

Danksagung

An erster Stelle möchte ich meinem Doktorvater Prof. Dr. Volker Sieber danken. Du hast durch deine Laufbahn den Weg von Nordrhein-Westfalen nach Niederbayern gepflastert, welchem ich später folgen durfte. Stets hast du mir das richtige Maß an individueller Freiheit und wissenschaftlicher Unterstützung zukommen lassen und somit maßgeblich dazu beigetragen, dass ich die Zeit in Straubing immer in guter Erinnerung behalten werde. Ich bin dankbar, dass ich in deiner Arbeitsgruppe promovieren durfte.

Mein Dank gilt auch Prof. Wolfgang Liebl für die Übernahme des Korreferats und Prof. Cordt Zollfrank für die Übernahme des Prüfungsvorsitzes.

Prof. Dr. Jochen Schmid - dir gilt ein ganz besonderes und herzliches Dankeschön. Über die gesamte Zeit meiner Promotion warst du weit mehr, als nur mein direkter wissenschaftlicher Betreuer. Du hattest immer ein offenes Ohr für Fragestellungen jeder Art – auch nach meiner Zeit am Lehrstuhl. Von Auslandsaufenthalten über Nachtschichten am Fermenter bis hin zu angeregten Diskussionen bei einem Glas Bier – auf deine Unterstützung konnte ich immer zählen. Dafür danke ich dir von ganzem Herzen.

Ein weiterer besonderer Dank gebührt Dr. Martin Schilling. Seit Beginn meiner Masterarbeit bist du ein wichtiger Mentor für mich. Du hast einen großen Teil dazu beigetragen, dass ich diese Sätze schreiben darf. Dr. Petra Allef danke ich für die initiale Projektidee und die essentielle Unterstützung dieser Kooperationsarbeit.

Bei Prof. Mattheos Koffas und Dr. Brady Cress möchte ich mich für eine wissenschaftlich, wie auch persönlich sehr lehrreiche Zeit am Rensselaer Polytechnic Institute in Troy bedanken. Bei euch durfte ich die wahre Macht der Molekularbiologie begreifen und erlernen.

Des Weiteren danke ich Dr. Broder Rühmann für die professionelle Unterstützung bei analytischen Untersuchungen, Steven Koenig für die Einführung in die faszinierende Welt der Rheologie und Sumanth Ranganathan für das Korrekturlesen dieser Arbeit. Für das überaus angenehme Arbeitsklima und viele schöne Stunden möchte ich allen Kollegen danken, mit denen ich während meiner Zeit in Straubing zusammenarbeiten durfte. Ganz besonders möchte ich hier meine guten Freunde José Guillermo Ortiz Tena, Hendrik Hohagen, Daniel Bauer und Dominik Schwarz erwähnen.

Meinen Eltern Hiltrud und Ulrich Rütering kann ich gar nicht genug danken für dieses wunderschöne Leben, das ihr mir geschenkt habt. Die Sicherheit, dass ihr mich jederzeit auffangen würdet verleiht mir grenzenlose Freiheit. Auch euren Partnern Klaus Wandjo und Elisabeth Reiter, meiner Schwester Jennifer, Burkhardt Ross und „den Dudes“ möchte ich dafür danken, dass ihr jeden Tag meines Lebens bereichert. Mögen wir noch viele Feste feiern.

Danke auch an Elke, Torsten und Carolin Diekmann. Ihr habt mich aufgenommen wie einen Sohn und Bruder und ward immer mein Ruhepol in bewegten Zeiten. Das werde ich euch nie vergessen.

Mein größter Dank geht an meine Ehefrau Sandra Rütering. Danke, dass du mir nach Bayern gefolgt bist, mich immer wieder auffängst und seit mehr als 12 Jahren tapfer und treu an meiner Seite stehst. Du bist das Glück meines Lebens.

Table of Contents

1	Introduction	13
1.1	Polysaccharides.....	13
1.2	Microbial Polysaccharides	14
1.2.1	Structure of exopolysaccharides	15
1.2.2	Rheology of polysaccharides	17
1.2.3	Biosynthesis of exopolysaccharides	19
1.2.4	Characteristics and challenges of exopolysaccharide production.....	21
1.2.5	Application of exopolysaccharides.....	23
1.2.6	Exopolysaccharide engineering	25
1.3	Genome editing and CRISPR-Cas	26
1.3.1	Functionality of CRISPR-Cas.....	27
1.3.2	CRISPR Editing.....	28
1.4	<i>Paenibacillus spp.</i>	29
1.4.1	Exopolysaccharides by <i>Paenibacilli</i>	31
1.5	Scope of the work.....	33
2	Material and Methods	34
2.1	Material	34
2.1.1	Equipment.....	34
2.1.2	Software and databases.....	35
2.1.3	Bacterial strains	36
2.1.4	Chemicals and reagents	37
2.1.5	Kits, enzymes and special consumables	38
2.1.6	Plasmids, primer and oligos.....	39
2.2	Media and Buffer.....	40
2.2.1	Media preparation.....	40
2.2.2	Cultivation media	40
2.2.3	Trace element solution.....	41
2.2.4	Buffers for chemical competent <i>E. coli</i> cells.....	41
2.3	Microbiological methods.....	41
2.3.1	Bacterial strain storage	41
2.3.2	Strain cultivation.....	41
2.3.3	Antibiotic sensitivity tests.....	41
2.3.4	Fermentations	42
2.3.5	EPS extraction	42
2.3.6	Chemically competent <i>E. coli</i> cells	42
2.3.7	Conjugation	43
2.4	Molecular biological methods.....	43
2.4.1	Agarose gel electrophoresis.....	43
2.4.2	Bacterial strain identification.....	43
2.4.3	Isolation of genomic DNA from bacterial strains.....	43
2.4.4	Genome editing in <i>P. polymyxa</i>	44
2.4.5	pCasPP plasmid construction	46
2.4.6	Bioinformatics	46

2.5 Analytical methods	46
2.5.1 Sugar monomer composition	46
2.5.2 Molecular weight determinations	47
2.5.3 Fourier transform infrared spectroscopy	47
2.5.4 Pyruvate assay	47
2.5.5 Glucose assay	47
2.5.6 Total sugar analysis	48
2.5.7 Protein content	48
2.6 Rheometry	48
2.6.1 Sample preparation	48
2.6.2 Dynamic viscosity	49
2.6.3 Viscosity curves.....	49
2.6.4 Amplitude sweeps.....	49
2.6.5 Frequency sweeps.....	50
2.6.6 Thixotropy	50
3 Results.....	51
3.1 Selection of an EPS production strain	51
3.2 Controlled production of polysaccharides – exploiting nutrient supply for levan and heteropolysaccharide production in <i>Paenibacillus</i> sp.	53
3.3 Rheological characterization of the exopolysaccharide Paenan in surfactant systems....	66
3.4 Genome sequencing – <i>Paenibacillus</i> sp. 2H2.....	79
3.5 Tailor-made Exopolysaccharides – CRISPR-Cas9 mediated genome editing in <i>Paenibacillus polymyxa</i>	81
4 Discussion	105
4.1 Strain selection.....	105
4.2 The potential of Paenan	106
4.2.1 Production and purification	107
4.2.2 Polymer characterization	110
4.3 Genome editing in <i>P. polymyxa</i>	112
5 Conclusions	113
6 References.....	115
7 Abbreviations	129
8 List of Figures	132
9 List of Tables.....	133

Summary

Limited fossil resources and an arising awareness for the importance of sustainability triggered an increasing demand for bio-based substances to replace petro-based chemicals. Microbial exopolysaccharides (EPSs) represent a promising alternative to synthetic rheological additives, when it comes to thickening, gelling, or emulsifying applications. Since the already available bio-based solutions do not cover all required application profiles, there is a high need for novel products that can compete with synthetic compounds in demanding industrial applications. This work describes the identification and characterization of a novel EPS and its bacterial producer.

Paenibacillus sp. 2H2 was selected as a promising bacterial EPS producer from a diverse strain collection using a high-throughput assisted screening platform followed by an in-depth strain characterization. The main selection criteria were: (i) the heterogeneous carbohydrate fingerprint of secreted EPS, (ii) outstanding growth characteristics, and (iii) a high initial polymer viscosity.

Fermentative EPS production in a production scale of 30 L was characterized by an EPS yield of 16%, a titer of $4.5 \text{ g} \cdot \text{L}^{-1}$, and a volumetric specific productivity competitive with commercial processes ($0.27 \text{ g} \cdot \text{L}^{-1} \cdot \text{h}^{-1}$). Analytical investigations using HPLC-MS/MS revealed that the heteropolysaccharide, named Paenan, comprises glucose, mannose, galactose, and glucuronic acid at a ratio of 3.5:2:1:0.1. In addition to heteropolysaccharide formation, the strain could be harnessed to produce levan-type polymer as well upon supplying the organism with specific carbon and nitrogen sources.

Paenans' rheology was characterized in aqueous solutions and in surfactant containing systems, which is of special relevance to the personal care industry. Due to a pronounced intermolecular network, Paenan forms stable weak-gels already at concentrations $\geq 0.1\%$, thereby delivering elasticity and thixotropy. This represents a novel application profile that lies between rigid gels as obtained by Gellan gum and viscous fluids, as produced by Xanthan gum. Furthermore, Paenan showed unique compatibilities with every class of surfactant, including cationic ones, and retained its weak-gel character in three out of four systems, rendering it interesting for several industrial applications.

To unravel the genetic basis for EPS production in *Paenibacillus* sp. 2H2, the genome was sequenced, and the putative EPS biosynthesis cluster was annotated. The functionality of the locus was subsequently proven in the closely related *Paenibacillus polymyxa* type strain DSM 365. For this, a CRISPR-Cas9 based genome-editing tool was developed, allowing for highly efficient deletions of single genes and large regions, as well as for integrations into the genome. By employing the system, several putative biochemical functions of glycosyltransferases involved in EPS biosynthesis could be identified. Furthermore, numerous EPS variants with altered physicochemical properties were generated through genetic recoding. These are the first published results on the genetic basis of EPS biosynthesis in *Paenibacilli* and an important step towards tailor-made EPSs using synthetic biology tools.

Future work should focus on the in-depth structural characterization of Paenan by e.g. NMR in order to link certain enzymatic functions encoded within the gene cluster to structural features of the polymer, thereby paving the way for rational EPS engineering.

List of Publications

Rütering M, Cress BF, Schilling M, Rühmann B, Koffas MAG, Sieber V & Schmid J (2017) Tailor-made exopolysaccharides – CRISPR-Cas9 mediated genome editing in *Paenibacillus polymyxa*. *Synthetic Biology* 2(1):ysx007. doi: 10.1093/synbio/ysx007

Rütering M, Schmid J, Gansbiller M, Braun A, Kleinen J, Schilling M, & Sieber V (2018) Rheological characterization of the exopolysaccharide Paenan in surfactant systems. *Carbohydrate Polymers* 181(1):719-726. doi: 10.1016/j.carbpol.2017.11.086

Rütering M, Schmid J, Rühmann B, Schilling M, & Sieber V (2016) Controlled production of polysaccharides—exploiting nutrient supply for levan and heteropolysaccharide formation in *Paenibacillus* sp. *Carbohydrate Polymers* 148:326-334. doi: 10.1016/j.carbpol.2016.04.074

Schmid J, Koenig S, Rühmann B, **Rütering M**, & Sieber V (2014) Biosynthese und Genomik mikrobieller Polysaccharide. *Biospektrum* 20(3):288-290. doi: 10.1007/s12268-014-0443-0

1 Introduction

“Increasingly, sustainability considerations will shape future technological, socio-economic, political and cultural change to define the boundaries of what is acceptable.” (1)

Twenty years later, this prediction made by Hall and Roome in 1996 has come true. Limited fossil resources and the progressing destruction of our environment triggered new global megatrends, such as sustainability and environmental awareness. The intentional, sustainable use of our resources has become an important element of people’s mindset in the western hemisphere and society wants to participate in the protection of our planet. Besides revolutions in power generation and the automotive industry, this lifestyle also resulted in an increasing demand for “all-natural” products in daily use commodities. The ingredients of these products are primarily provided by the chemical industry, which significantly contributed to achieving the present quality of life. However, conventional chemistry faces a great challenge in replacing commonly used synthetic chemicals with green alternatives (2).

Biotechnology – the technological application that uses biological systems, living organisms, or derivatives thereof, to make or modify products or processes for specific use – has great potential in providing renewable alternatives to petro-based chemicals or even entirely new substances with application profiles that are still to be defined. In the past 40 years, biotechnology has already affected several industrial sectors substantially, including healthcare, food, and agriculture. Scientific progress in adjacent fields, such as synthetic biology, will further accelerate the development of novel, bio-based solutions and help us to build a more sustainable “tomorrow”.

This work focuses on the development of a polysaccharide-based thickener to replace commonly used synthetic additives.

1.1 Polysaccharides

Polysaccharides are universal biopolymers found in every domain of life and amount to approximately 90 % of all existing carbohydrates (3). The variety in tasks they fulfill in nature is as impressive as their high abundance.

In the form of cellulose, chitin, xylans or mannans, polysaccharides form hard, solid structures giving mechanical strength to plants, insects or fungi. Starch and glycogen however, are efficient energy storage polysaccharides accumulated in animals, algae or plants. Hydrated, cross-linked three-dimensional networks formed by pectins (land plants) or carrageenans, agar and alginate (marine species) contribute to the structural integrity. In mammals, hyaluronate, chondroitin sulfate and other glycosaminoglycans essentially participate in structure buildup of the intercellular matrix and determine solution properties of physiological fluids. Further polysaccharide functions include wound sealing in tree bark (exudate gums) and protection against environmental stressors in microbes.

From the biotechnological point of view, microbial polysaccharides are of special interest, since they can be produced independent of seasons and location in variable scales.

1.2 Microbial Polysaccharides

Microorganisms are a diverse group of single-celled or multicellular organisms, comprising bacteria, archaea, microalgae, some fungi and protozoa. Polysaccharide production has primarily been reported for bacteria, fungi and some microalgae, with the first two being the most relevant groups. Based on their morphological localization, polysaccharides produced by microorganisms can be divided into three different categories:

- 1) Intracellular polysaccharides
- 2) Structural polysaccharides
- 3) Extracellular polysaccharides

Microorganisms accumulate “intracellular polysaccharides” during times of nutrient excess as a mean of energy storage for starvation periods. Glycogen is a well-known example for the group of intracellular polysaccharides and several studies describe glycogen storage in bacteria and fungi (4, 5).

“Structural polysaccharides” are integral parts of the cell structure or membrane. Lipopolysaccharides (LPSs) for example, play an important role in the integrity of the outer membrane in Gram-negative bacteria and extensively participate in host-pathogen interplay. In a broad sense, also peptidoglycan – the major component of most bacterial cell walls – can be regarded as polysaccharide-based, since alternating amino sugars form the backbone of this polymer.

The category of “extracellular polysaccharides” covers all polysaccharides, which are secreted into the extracellular space. This group can again be subdivided based on the location of the secreted polymer relative to the cell. Polysaccharides forming covalently bound, cohesive layers around the cell are termed capsular polysaccharides (CPSs) (6). If the polysaccharides are entirely secreted into the external environment or are synthesized extracellularly, they may be referred to as exopolysaccharides (EPSs). In reality however, the differentiation between CPSs and EPSs can be quite challenging, since capsules are sometimes only loosely attached to the membrane, or secreted EPSs stay within close proximity to the cell (7). The physiological functions of extracellular polysaccharides are diverse and largely associated to protection against environmental stressors, such as freezing (8), antibiotics, suboptimal pH, temperature, drying or high salt loads (9, 10). Furthermore, they were reported to deliver resistance against invasive species or against immunological reactions (11, 12). In biofilm matrices, they were shown to be involved in quorum sensing regulated processes (13). Under high nutrient conditions, overproduction of CPSs and EPSs can be induced to build up carbohydrate sinks for subsequent metabolism (14).

This summary of physiological functions is by far not complete and only gives a rough overview of the huge range of tasks extracellular polysaccharides in nature. Key to this functional variety of EPSs/CPSs is the seemingly endless structural diversity amongst these polymers.

Since easily separable EPSs are of greater interest when it comes to industrial utilization, the following sections will focus exclusively on EPSs.

1.2.1 Structure of exopolysaccharides

All polysaccharides are composed of carbohydrate building blocks. The secret for the inconceivable complexity of EPSs lies in the type and number of incorporated monomers and in the linkages between these monomers. Endless combinations yield uncountable polymer variants with unique structural and physiochemical properties.

Monomeric sugars and their derivatives form the building blocks for natural polysaccharides. The most frequently found neutral sugars in microbial EPSs are glucose, galactose, mannose, fructose, xylose, arabinose, fucose and rhamnose. Furthermore, several sugar derivatives, such as uronic acids, deoxy-sugars, anhydro-sugars, amino- or acetylated amino-sugars are common elements of EPSs. In addition to these regularly appearing building blocks, numerous rare sugars, such as N-acetyl-L-fucosamine, N-acetyl-D-glucosaminuronic acid, 2-deoxy-D-arabino-hexuronic acid and 2-acetamido-4-amino-2,4,6-trideoxy-D-galactose, were also found to be part of EPSs structures (15). In theory, conformational variants (pyranose and furanose) and stereoisomers (D- or L-configuration) of sugar monomers could raise the number of incorporable building blocks to even higher level (7). However, many of these variants have not yet been described for microbial EPSs and the unambiguous differentiation of these compounds poses a great challenge to analytical chemistry. Organic and inorganic substituents attached to sugar monomers add further complexity to the construction kit of polysaccharides. Pyruvate ketals or ester-linked acetate, hydroxybutanoate, succinate and glycerate are common organic representatives. Phosphate and sulfate are inorganic examples, which were described manifold for EPSs from bacteria, yeasts and cyanobacteria, respectively (16).

Based on the combination of monomers, EPSs can be divided into two classes. Homopolysaccharide-polymers containing only one type of sugar and heteropolysaccharide-polymers comprising two or more different monosaccharides. Microbial heteropolysaccharides, unlike their plant-based counterparts, are usually regular in structure and built from repetitive elements with a consistent monomer sequence – the so-called repeating units. Depending on species and strain, these repeating units usually consist of two to eight sugar monomers with extremes of up to fourteen residues (17).

One factor that is common among all polysaccharides is that their monomers are linked via glycosidic bonds. These linkages are formed during a condensation reaction of an anomeric hydroxyl group of one sugar with an alcohol group of another residue. Since glycosidic bonds can have two stereochemical configurations (α , β) and can occur at different hydroxylated carbons (for glucose e.g.: C-1, C-2, C-3, C-4 and C-6), the number of possible linkages increase exponentially with increasing number of involved partners. This complexity is increased further when taking into account that many polysaccharides are not linear, but branched molecules.

The repeating unit of Xanthan is shown in figure 1.1 to exemplify the above-described structural features of microbial heteropolysaccharides. Xanthan is an anionic polymer produced by the Gram-negative bacterium *Xanthomonas campestris*, which is by far the most successful representative of all bacterial EPSs. Its repeating unit is a pentasaccharide comprising a backbone of two β -1,4 linked glucose molecules and a tri-saccharide side-chain composed of α -(1,3)-mannose, β -(1,4)-glucuronic acid and β -(1,2)-mannose. Terminal mannoses of the side chain are either substituted with a pyruvic acid moiety joined by a ketal linkage or with an acetyl group. Internal mannoses also carry a 6-O-acetyl substituent.

For Xanthan, decoration with the substituent varies with bacterial growth conditions and other parameters (18).

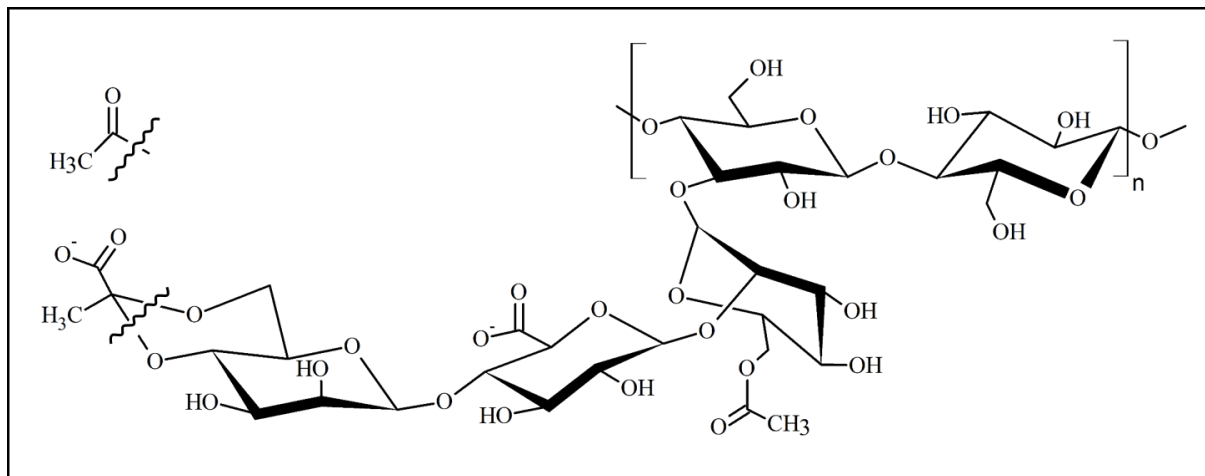


Figure 1.1 Chemical structure of Xanthan repeating unit. Two β-1,4 linked glucose molecules form the backbone of the pentasaccharide. The side-chain is connected to the O-3 of every other glucose molecule and comprises a glucuronic acid between two mannoses. The terminal mannose is substituted with a pyruvate ketal or an acetyl group and the internal mannose residue also carries a 6-O-acetyl substituent.

Up to here, we have only covered the basic primary structure of polysaccharides – the covalent sequence of monomer residues in the backbone. Similar to proteins and other biopolymers, the idea of a secondary and tertiary structure applies to polysaccharides as well (19). The conformation of individual sugar molecules within the polymer is relatively fixed, however, sugar monomers linked via glycosidic bonds can rotate around this linkage and will typically adopt the lowest energy state. Hence, specific primary structures will assume characteristic geometrical shapes in space, such as ribbons or helices. This regular arrangement is known as the secondary structure. The tertiary structure characterizes the way in which these arrangements pack together. Some polysaccharides exist as bundles containing up to tens of polysaccharide chains. These ordered entities can further aggregate, yielding large, three-dimensional networks – the quaternary structure. Superior structural characteristics are crucial for the physicochemical behavior and for the application profile of a polysaccharide as well (20).

Cellulose, for example, is a linear homopolysaccharide composed of β-1,4 linked glucose molecules, which adopt a ribbon-like secondary structure. The chains are closely packed and stabilized by hydrogen bonds and van der Waals forces, thereby resulting in a compact structure that is insoluble even in alkaline solvents. Contrarily, curdlan, which is also a linear glucan, forms coaxial triple helices resulting in a polymer that forms elastic gels in water upon heating and is soluble in DMSO and alkaline solvents. The only difference between curdlan and cellulose is the position of the glycosidic bond, which is β-1,3 in curdlan (19).

Absolute conformations of more complex polysaccharides are more difficult to elucidate and are significantly influenced by the degree and type of branching. The interruptions of regular structures, by occasionally occurring substituents or alternating sugar conformations for instance, drastically affect the overall structure. Interruptions generally force polymer chains into cross-linked networks, which consequently result in the formation of a higher level of ordered structure, resulting in e.g. gelation (19). Figure 1.2 illustrates a generalized scheme for the network formation of interrupted polysaccharide types based on the concept of junction zones, as proposed by Rees et al. (20).

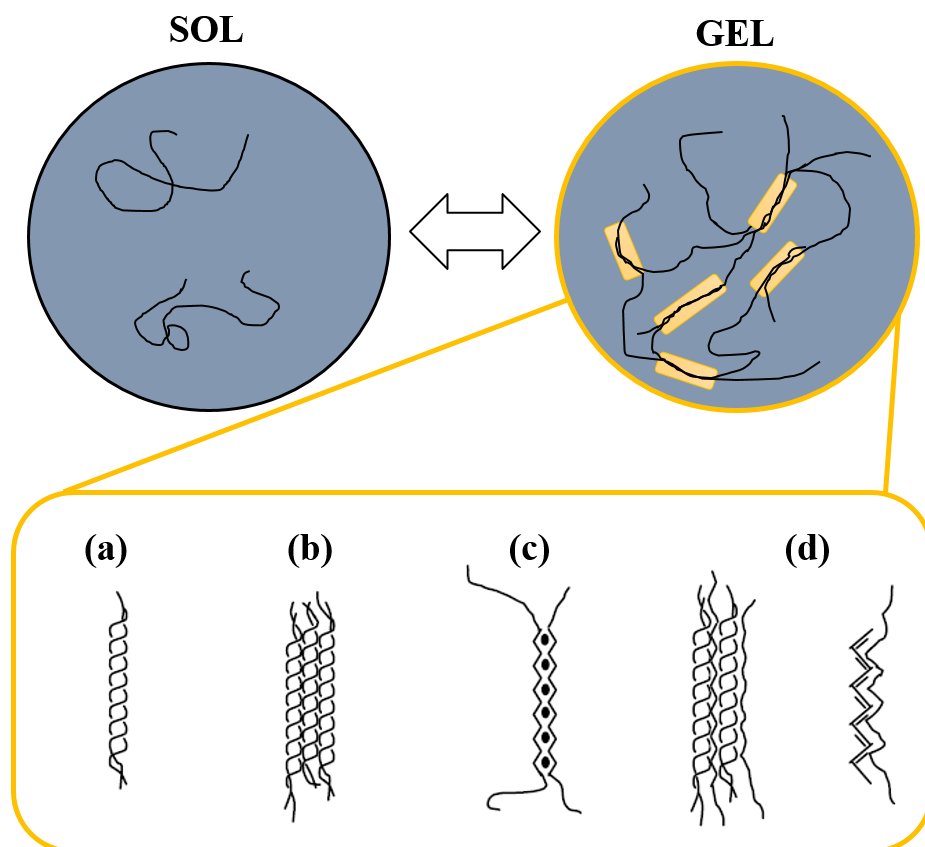


Figure 1.2. Higher ordered structures formed by interrupted polysaccharides, based on the theory of junction zones. Connections resulting in cross-linked networks can occur via (a) double-helices as in ι -carrageenan (b) bundles of helices as in agarose (c) ribbon-ribbon associations as in Ca^{2+} bridged alginates (d) helix-ribbon conformations as in mixed systems containing agarose and galactomannans or Xanthan and glucomannan.

Thorough characterization of secondary, tertiary and quaternary structures is essential to understand the influence of the monomeric composition on the functional properties of a polysaccharide. Although developments in computer and software technology has significantly eased data analysis, most studies are still based on empirical models and the results obtained are only partially adaptable to other systems. However, the combination of advanced computational modeling with experimental approaches has initiated a new trend in conformation analysis of polysaccharides. Together with state-of-the-art visual techniques, such as atomic force microscopy, this will greatly contribute to our understanding of the structure-function relationship of polysaccharides.

1.2.2 Rheology of polysaccharides

Rheology was first defined by Bingham in 1929 as the study of deformation and flow of matter (21). The development of precise controlled stress and controlled shear rheometers that are capable of measuring very low shear and stress rates has dramatically contributed to our understanding of polysaccharide rheology. Above all, the concentration of a polymer in solution determines the systems' rheology. Below the critical polymer concentration (C^*), polymer strands can move independently from each other and the solution exhibits Newtonian behavior. The viscosity of the system is independent of

the applied shear. This regime is called the “dilute region”. Above the C^* , polymer molecules start to entangle, overlap and interpenetrate each other, which results in a considerable increase in viscosity and the transition from Newtonian to non-Newtonian behavior. This regime is called “semi-dilute region” (22). Figure 1.3A exemplifies the zero-shear viscosity of a polysaccharide solution as a function of polymer concentration. Polymer solutions in the semi-dilute region typically exhibit a characteristic viscosity-shear rate profile, which can be divided into three distinct regions (Fig. 1.3B). At very low shear rates, polymer molecules ravel and unravel simultaneously and the solution shows a high, constant viscosity, the zero-shear viscosity (a). On increasing the applied shear, polymer strands align along the streamline of the flow and the viscosity drops (b). This property is also known as shear-thinning. At infinite shear rates, all molecules are arranged in parallel, no entanglement occurs and the solutions shows a high-shear Newtonian plateau (23).

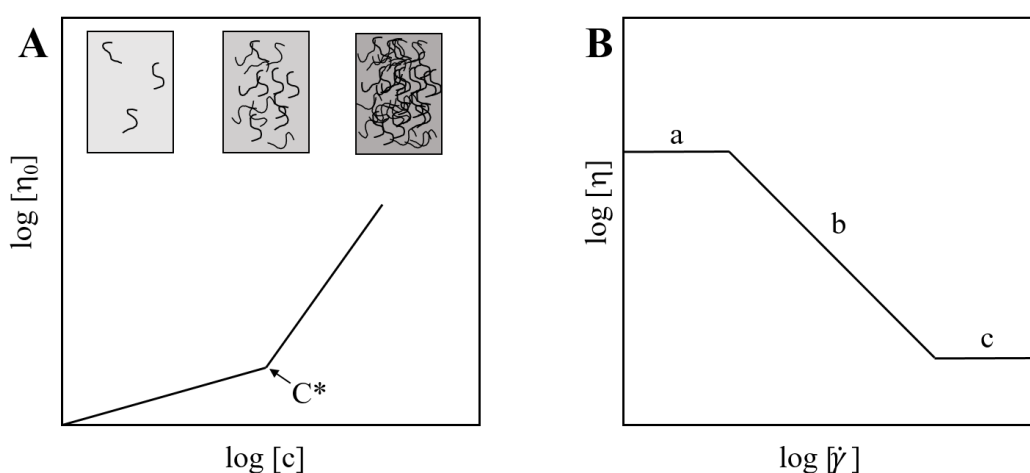


Figure 1.3. Rheological behavior of thickening polysaccharides. (A) Concentration dependency of the zero-shear viscosity (η_0). (B) Viscosity-shear rate profile of a polymer solution above the critical concentration C^* .

This generalized, theoretical concept of polymer rheology is applicable to most thickening hydrocolloids without a pronounced intermolecular network. However, in reality, the actual flow behavior is influenced by several other factors and not solely the polymer concentration. The molecular mass, for example, is usually proportional to the viscosity, meaning that flow resistance increases with increasing molecular mass of the molecules (24). In addition, the molecular structure strongly affects the rheology of a polymer. Linear and stiff molecules have large hydrodynamic radii resulting in higher viscosities as compared to branched polymers of the same molecular mass, which occupy less space in solution. Furthermore, parameters such as polymer charge, ionic strength, solvent, temperature, and pH significantly influence the degree and type of interaction between polymer molecules and thereby the rheology of the entire system. If individual molecules do not entangle with one another, but also interact via physical interaction (hydrogen bonding, hydrophobic association, cation-mediated crosslinking, etc.), three-dimensional network structures are formed, leading to the formation of hydrogels. Depending on the type and degree of interaction, hydrogels can either be soft and flexible, so-called “weak-gels”, or firm and brittle, also known as “strong-gels”. Different hydrogels and a qualitative comparison of their structures is given in figure 1.4.

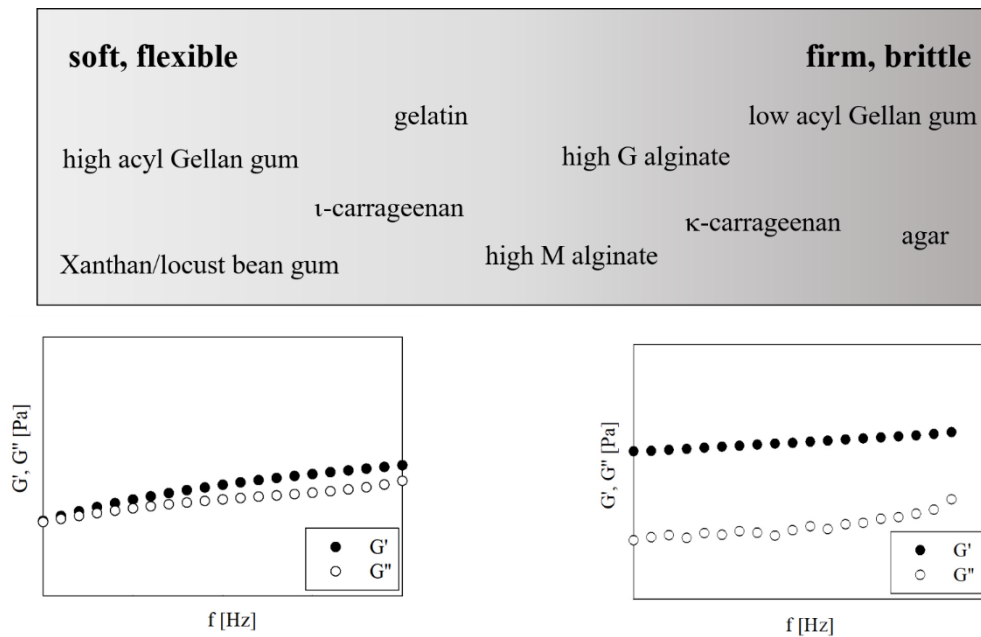


Figure 1.4. Gel textures produced by various hydrocolloids (adapted from William et al., 2009). Weak-gel forming polymers are depicted at the left, strong-gel forming polysaccharides at the right. Representative plots of frequency tests for soft gels (left) and firm gels (right) are shown at the lower part. The storage module G' is a measure of elasticity (solid behavior), the loss module G'' represents the viscous behavior.

1.2.3 Biosynthesis of exopolysaccharides

Exopolysaccharide biosynthesis is a multistep process (25). It starts with the intracellular synthesis of nucleotide sugar precursors, which serve as activated donors for the subsequent EPS assembly. Depending on the mechanism used, either oligosaccharide repeating-units or the entire polymer chain is assembled from the precursors by the action of one or more glycosyl transferases (GTs). Following the assembly of monosaccharide units, the mature EPS is secreted into the extracellular space. In contrast to the enormous structural diversity of polysaccharides, the number of underlying molecular mechanisms for EPS biosynthesis is limited. At present, four different pathways are described by which these biopolymers are assembled. Three of these are intracellular mechanisms and one is an extracellular catalysis mediated by a single enzyme.

- 1) Wzx/Wzy-dependent pathway (26)
- 2) ABC transporter-dependent pathway (27)
- 3) Synthase-dependent pathway (28)
- 4) The extracellular synthesis catalyzed by sucrases (29)

Figure 1.5 gives a schematic overview of the three intracellular pathways.

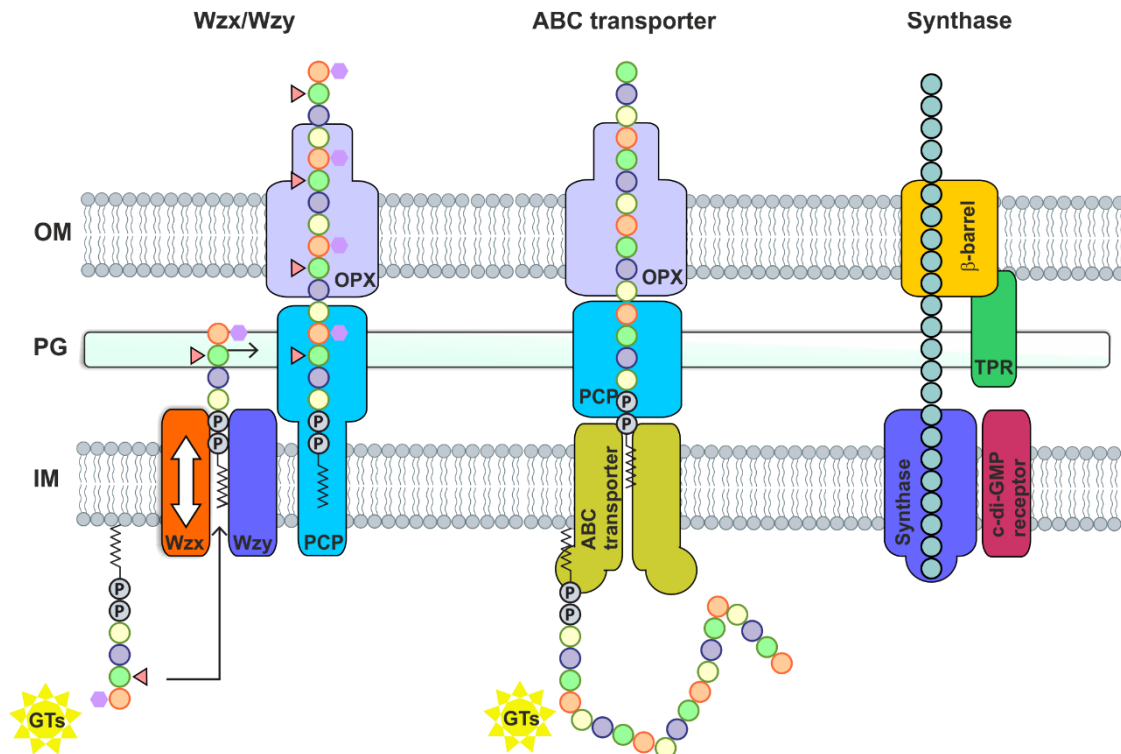


Figure 1.5. Molecular mechanisms of polysaccharide synthesis. In the Wzx/Wzy- dependent pathway, glycosyltransferases (GTs) assemble the repeating units at a membrane-anchored C₅₅-lipid linker. Subsequent to the flippase-mediated (Wzx) translocation over the inner membrane, repeating units are assembled by a polymerase (Wzy) yielding the mature polymer. Final secretion is enabled by outer-membrane polysaccharide export (OPX) and polysaccharide copolymerase (PCP) protein families. In ABC transporter dependent secretion, the entire polymer is synthesized on a lipid carrier located in the inner leaflet of the inner membrane by GTs and then transported across the membranes and cell wall by members of the PCP and OPX protein families. For synthase-dependent polysaccharide production, polymerization and export is catalyzed by a cell wall spanning synthase complex. Regulation of synthase activity occasionally occurs by a c-di-GMP receptor. Abbreviations: TPR, tetratricopeptide repeat proteins; IM, inner membrane; PG, peptidoglycan sacculus; OM, outer membrane; c-di-GMP, bis-(3'-5')-cyclic dimeric guanosine monophosphate.

The Wzx/Wzy-dependent pathway is very common in many Gram-positive and Gram-negative bacteria and is utilized for EPS formation in *Lactococci*, *Streptococci* and *Escherichia* (30-32). Through this pathway, individual repeating units are assembled on the inner side of the cytoplasmic membrane by membrane-associated or membrane embedded GTs. After the attachment of the initial sugar unit to a membrane bound lipid undecaprenyl carrier, the nascent repeating unit is elongated through successive addition of distinct sugars by other GTs. The transportation of the finished repeating units across the membrane is enabled by a flippase (Wzx,) followed by a Wzy polymerase-mediated assembly of the mature EPS in the periplasmic space (33). The secretion of the polymerized repeating units from the periplasm to the cell surface is supported by additional proteins of the polysaccharide co-polymerase (PCP) and the outer membrane polysaccharide export (OPX) families (34). Typically, EPSs synthesized via the Wzx/Wzy-dependent pathway belong to the group of heteropolysaccharides with highly diverse sugar patterns (e.g. Xanthan).

The ABC transporter-dependent systems are mainly found in CPS biosynthesis (28). Similar to the Wzx/Wzy-dependent pathway, GTs are responsible for the assembly of the polymer. However, in ABC transporter-dependent systems, the entire polysaccharide chain is assembled at the inner side of the cytoplasmic membrane. Depending on the number of involved GTs, either homopolysaccharides, or

heteropolysaccharides are formed (28). A membrane-spanning protein complex including ABC-transporters and periplasmic proteins of the PCP and OPX families realize the export of the polysaccharide chain across the cell wall. Although ABC transporter-dependent secretion differs from Wzx/Wzy-dependent systems mechanistically, protein families involved in the translocation across the periplasm (PCP) and outer-membrane (OPX) show high similarities (33).

In synthase-dependent systems, a membrane-embedded synthase performs both, the polymerization reaction and the translocation process over the membrane (35). This mechanism is frequently found in the biosynthesis of homopolysaccharides, which requires only one type of a sugar precursor. Bacterial cellulose and curdlan are examples of homopolysaccharides produced via the synthase-dependent pathway (29). In some cases, the synthase is only a subunit of an envelope-spanning multiprotein complex, which can also include enzymes for subsequent polymer modification, as observed for alginates (36). The hyaluronan synthase, which is responsible for the production of hyaluronic acid, is a fusion of two GTs, thereby capable of accepting two different precursors, glucuronic acid (GlcA) and N-acetyl-D-glucosamine (GlcNAc), and hence secreting a heteropolysaccharide (37).

Most microbial polysaccharides are synthesized according to one of the aforementioned pathways. The required precursors and activated nucleotide-sugars are produced inside the cell, whereas polymerization and transport are located on the membrane. However, some polysaccharides are entirely produced in the extracellular space. Synthesis of these EPSs occurs by action of sucrases that are secreted or bound to the cell wall (29). Dextran and levan are best-known representatives of this group (38, 39). In contrast to the intracellular pathways, sucrases do not require nucleotide precursors. These enzymes accept di- or trisaccharides such as sucrose or raffinose, as substrate and directly transfer one of the sugar moieties to a growing polymer chain by use of the energy obtained from the cleaved glycosylic bond.

The genes encoding the various functional elements involved in EPS biosynthesis are usually found clustered in the producers' genome or on large plasmids (35, 40). The clusters typically include GTs, polymerases, enzymes involved in the synthesis of nucleotide precursors and enzymes responsible for sugar-modification or the addition of sugar substituents. The accumulation of EPS-related genes significantly facilitates the discovery of novel EPS operons, even if only draft genome sequences are available (29). However, in-depth biochemical investigations are required to assign exact functions of contained genes. Although numerous EPS operons and pathways have been known for decades, several details on molecular and regulatory mechanisms of EPS biosynthesis are still unknown and if or to what extent a gene contributes to EPS biosynthesis can vary from strain to strain. Furthermore, annotation of several genes, especially GTs, is often ambiguous and putative substrates or acceptors can only be hypothesized until experimentally proven (25, 41).

1.2.4 Characteristics and challenges of exopolysaccharide production

The commercial production of microbial exopolysaccharides is typically carried out by growing cells in submerged cultures in large-scale fermenters, under standardized and highly controlled conditions. This guarantees reproducible product qualities and yields, independent of seasons, geographical location or climatic conditions (42). Very much alike every other product, also EPSs must compete with similar

substances recovered from other natural sources, such as polysaccharides from macroalgae or plants, in terms of quality and profitability. The high viscosity of most EPS-containing fermentation broth complicate cost-efficient production, recovery, and purification and make these fermentations one of the most challenging and complex processes at all (43).

During the early process development stage, the media optimization step poses the biggest challenge. Although some factors, such as nitrogen (N) limitation and carbon (C) excess, are known to favor EPS production, no general rules for the support of high yields for all production strains exists (44, 45). Media compositions are either determined arbitrarily or by using statistically based experimental design methods (46, 47). Several studies describe the utilization of complex natural sources, such as waste streams from sugar cane bagasse, cheese whey or biodiesel production, to replace expensive, pure substrates (48-50). However, these substrates suffer from several drawbacks, as for example impurities present or fluctuating nutrient compositions, which can result in the formation of different polymers or various byproducts (51, 52). Once a suitable fermentation media is developed, the challenges shift from the chemical to the physical environment of the EPS fermentation. The scaling-up of nutrient conditions is straightforward, but reproducing the physical surrounding during scale-up can be quite difficult, especially for highly viscous products (53). Initial media screenings are typically performed in shake flask cultures, wherein pH and PO₂ controls are not possible - parameters that significantly affect EPS production in most organisms (54). Continuously stirred tank reactors are the fermentation strategy of choice when it comes to EPS production at larger scale. The change in the rheological character of the process fluid from water-like to Newtonian flow behavior and then to highly viscous non-Newtonian behavior, because of the secreted EPS, is the most dominating processing factor (55). During the first period of low viscosity, a homogeneous mixing of the entire bioreactor allows process parameters to be monitored and controlled easily. By adjusting the gas flow rate and stirrer speed, the increased demand for oxygen and nutrient supply of the growing cell population can be satisfied (56). The whole culture media is homogeneous, and samples taken are representative of the actual fermentation conditions. When EPS formation is initiated, which can either be associated to cell growth (Gellan gum, bacterial cellulose), or to the late logarithmic or stationary phase (curdlan), the fermentation broth becomes more and more viscous (57, 58). There is a direct relationship between the viscosity of the fermentation broth and the mixing in the fermentation vessel, *i.e.* the thicker the broth, the more uneven is the mixing; thereby leading to a less tractable culture medium. High shear zones near the impeller remain well-mixed, whereas distant regions start to stagnate (59). Therefore, oxygen transfer rates collapse, nutrient transport is prevented and pH and pO₂ measurements are no longer reliable, since the system is heterogeneous. The process is not controllable any more at this stage and mass, momentum and heat transfer limitations lower the productivity (60).

Figure 1.6 illustrates the two extremes of a homogeneously mixed reactor and a poorly mixed EPS broth. The described issues complicate even further when increasing the process scale from the laboratory to production capacities. Moreover, a successful scale-up of EPS bioprocesses requires a high degree of empiricism, as the understanding of the real-time process is lacking (61).

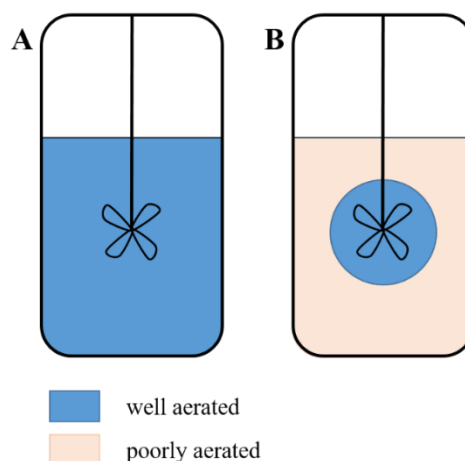


Figure 1.6. Mixing in stirred tank fermenters. (A) At the beginning of fermentative EPS production. (B) After EPS accumulation.

Subsequent to the fermentation process, the secreted EPS has to be recovered from the culture broth and purified. This is typically achieved by processes involving (50):

- (i) cell removal (centrifugation or filtration)
- (ii) polymer precipitation (addition of methanol, ethanol, isopropanol, or acetone)
- (iii) drying (freeze drying, drum drying)

Additional downstream processing steps, such as heat inactivation of the culture broth, dilution with deionized water to decrease viscosity and facilitate purification, or enzymatic treatments in order to lyse cells are employed depending on the polymer produced and the purity grade needed (62). Since EPS separation and purification contribute largely to the overall costs of the polymer, the procedures utilized must be chosen carefully and individually for each EPS as a compromise of recovery, purity and expenses (50).

Despite these problems, several EPS bioprocesses were commercialized, with Xanthan being the most prominent example. This versatile polymer is produced in batch fermentations, which achieve productivities of $0.4 - 0.7 \text{ g} \cdot \text{L}^{-1} \cdot \text{h}^{-1}$ and final product titers of 3-5% within 48-72 hours (63). Xanthan's major producers include CP Kelco, Merck, Pfizer, Rhône Poulenc, Sanofi-Elf, and Jungbunzlauer and the annual production is around 100,000 t (64, 65). The following section (section 1.2.5) will cover the numerous applications of Xanthan and other marketed EPSs.

1.2.5 Application of exopolysaccharides

Only a small proportion of the entirety of microbial polysaccharides utilized was commercialized in a way that they hold relevant shares of the global market for hydrocolloids. Plant and algae derived polymers, such as alginates, carrageenan and starch, still dominate the bulk business and the diversity of marketed microbial EPSs is found in high value, niche applications (66).

Table 1.1. Important marketed bacterial exopolysaccharides with corresponding application fields and properties (adapted from Freitas et al. 2011).

EPS	Monomer Composition ^a	Characteristics	Applications	Market (metric tons)	Price (US\$/kg)	Ref
Alginate	GlcA, ManA, Ac	<ul style="list-style-type: none"> Film formation Gelling capacity 	<ul style="list-style-type: none"> Food hydrocolloid Surgical dressings Wound management Drug release 	30,000	5-20	(66-68)
Cellulose	Glc	<ul style="list-style-type: none"> Water insoluble High crystallinity High tensile strength Moldability 	<ul style="list-style-type: none"> Food Wound healing Tissue engineering 	N.A. ^b	5.8-20	(67, 69)
Curdlan	Glc	<ul style="list-style-type: none"> Gelling capacity Insolubility in water Edible Biological activity 	<ul style="list-style-type: none"> Food Pharmaceutical industry Concrete additive Heavy metal removal 	N.A.	55	(58, 67, 70)
Dextran	Glc	<ul style="list-style-type: none"> Neutral High stability Newtonian flow behavior 	<ul style="list-style-type: none"> Food Blood volume expander Chromatography 	2,000	N.A.	(35, 67, 70)
Gellan	Glc, Rha, GlcA, Ac, Gl	<ul style="list-style-type: none"> Gelling capacity Thermoreversible gels pH stability 	<ul style="list-style-type: none"> Food Pharmaceuticals Agar substitution 	N.A.	55-66	(62, 66, 67)
Hyaluronan	GlcA, GlcNAc	<ul style="list-style-type: none"> Biocompatibility Biological activity 	<ul style="list-style-type: none"> Medicine 	N.A.	100,000	(67)
Levan	Fru	<ul style="list-style-type: none"> Low viscosity Biological activity High water solubility Film formation Adhesive strength 	<ul style="list-style-type: none"> Food Feed Medicine Cosmetics 	N.A.	N.A.	(51, 67)
Succinoglycan	Glc, Gal, Ac, Pyr, Succ, HB	<ul style="list-style-type: none"> Shear thinning Acid stability 	<ul style="list-style-type: none"> Food Oil recovery 	N.A.	N.A.	(67, 71)
Xanthan	Glc, Man, GlcA, Ac, Pyr	<ul style="list-style-type: none"> Highly viscous and shear thinning even at low concentrations Temperature, pH and salt stability 	<ul style="list-style-type: none"> Food Petroleum industry Pharmaceuticals Personal care Agriculture 	96,000	3-5	(66, 67, 70, 72)

^amannose (Man), galactose (Gal), glucose (Glc), glucuronic acid (GlcA), mannuronic acid (ManA), acetate (Ac), glycerate (Gl) pyruvate (Pyr), fructose (Fru), rhamnose (Rha), N-acetyl-D-glucosamine (GlcNAc), succinate (Succ), 3-hydroxybutyrate (HB)

^bN.A. – no data available

Excellent rheological properties combined with high stabilities towards temperature, ionic strength or pH are common traits qualifying EPSs for usage as thickening, stabilizing, emulsifying or gelling agent (73). Encapsulation of bioactive compounds in food, film formation with tuned barrier properties for packaging purposes or formation of polymeric matrix structures in tissue engineering are further specialized applications (74-77). Table 1.1 gives an overview on the most important, commercially available, bacterial EPSs.

The diverse properties and applications of bacterial EPSs impressively show their huge potential to replace petro-based products, or even possess entirely new functionalities. Their biocompatibility, biodegradability and their outstanding rheological properties render these polymers interesting for several applications. However, industrial demands in terms of product quality and performance are high and lots of work has to be done to keep or even make EPSs competitive. Two strategies to tackle this challenge are (i) harvesting the huge diversity of EPSs in nature to discover new polymers with superior properties and (ii) employing emerging and highly promising biotechnological techniques to engineer tailor-made EPS variants that exactly meet the customers' requirements.

1.2.6 Exopolysaccharide engineering

The diverse application profiles of EPSs in food, cosmetics, pharmaceutical, and construction industries render polysaccharides interesting targets for genetic engineering approaches. The strategies applied can be divided into two groups and aim either at the improvement of EPS production or at the generation of novel polymer variants.

Studies targeting the optimization of cost-efficient EPS production mostly focus on increasing volumetric EPS productivities of fermentative production processes. Boosting the pool of available nucleotide sugars was found to be an effective strategy to direct the carbon flux toward EPS biosynthesis, thereby increasing product titers and overall productivities (78, 79). More precisely, the overexpression of genes or gene clusters responsible for precursor biosynthesis or EPS assembly (GTs, Wzy, Wzx) was successfully employed to increase precursor conversion rates and product yields (80-83). The detrimental effects on EPS yields, which were occasionally observed in overexpression studies, can presumably be attributed to the disordering of multidomain protein complexes involved in polymerization and secretion (80). Another strategy that was successfully applied to increase sugar precursor availability and thereby EPS productivities is the disruption or knockdown of competing pathways (84, 85). Regulatory genes could be a further promising target to push EPS yields by increasing transcription rates of entire EPS operons (29).

The second engineering strategy addresses the development of tailor-made polysaccharide variants with novel or superior material properties. Changing the molecular weight of the polymers produced or altering the degree and type of substituent decoration are the most commonly followed routes. For instance, mutating or overexpressing genes involved in polymerization or polysaccharide degradation (e.g. Wzy, synthase, glucosidases) was successfully applied to generate EPS variants with varied molecular mass and altered rheological properties (86, 87). Modifying the type and degree of decoration was also found to affect the physico-chemical behavior of polysaccharides and significantly contributed to our understanding of structure-function relationships of EPSs. Hassler and Doherty performed first

engineering experiments on the biosynthesis of Xanthan in 1990 and found out, that the degree of acetylation and pyruvylation significantly influenced the viscosity of the polymer (88). The observed effect can be attributed to the polymer charge density that varies with degree of pyruvylation and to the occurrence of conformational changes, which were described manifold for side chain alterations (89-91). In case of Xanthan, not only the decoration patterns with substituents, but also the lengths of the side chain were subject to engineering approaches. By inactivating the GT that transfers the terminal mannose unit to the sidechain, a truncated tetramer version of Xanthan could be produced, exhibiting much lower viscosities than the wildtype (88).

However, the adjustment of substituent patterns and sidechain lengths only allows for alterations in the degree of superficial decorations while leaving the core, underlying glycan structure and sequence unchanged. Here, GTs represent a highly interesting engineering target, since they transfer defined sugar moieties to the nascent repeating units or growing polymer chain and thereby ultimately determine the composition and linkage pattern of the mature EPS (92, 93). Complementation experiments have shown that exchange of GTs with distinct monosaccharide preferences is feasible, indicating that the EPS polymerization and secretion machinery of one organism can potentially be harnessed for the production of various polymers with disparate structures and properties (29). However, exchanging native GTs with heterologous variants to incorporate new sugar monomers is not as straight forward as it seems. CAZY, the biggest database for GTs, comprises tens of thousands of putatively annotated GT genes. Only few of these described genes are sufficiently characterized and generally, substrate and acceptor specificities are unknown. This tremendously complicates the annotation of newly discovered GTs and obscures the search for alternative GTs that could be utilized to produce altered polymer variants (25). Nonetheless, progress in linking sequence information to enzyme specificities will accelerate this field and facilitate the rational search for GTs to replace native enzymes. On the long run, this will eventually yield a catalog of enzymes, which can be used for the directed incorporation of user-specified sugars imparting desired properties (41). Polymer variants produced in this fashion will successively contribute to the still superficial understanding of EPS structure-function relationships and thereby ultimately allowing the rational design of application-defined properties (94). Modern synthetic biology tools, such as CRISPR-Cas9, will not only facilitate engineering of structural features but will also drastically accelerate strain improvements, spurring the rise of robust and economical production processes for competitive, custom-made EPSs.

1.3 Genome editing and CRISPR-Cas

Ever since the discovery of the DNA double helix, researchers have tried to introduce site-specific changes to genomes. Studies on DNA recombination and DNA repair mechanisms unveiled the ability of cells to repair double-strand DNA breaks and the idea was born to introduce precise breaks at sites, which were to be changed (95, 96). During the second half of the 20th century, the discovery of various enzyme classes (restriction endonucleases, polymerases, ligases) and the development of new methods, such as the polymerase chain reaction and DNA sequencing, granted scientists access to modern molecular biology. Coupling chemical reagents to oligonucleotides were early approaches of targeted DNA alteration and were used successfully for chromosome modifications in eukaryotic cells (97-99).

Although these methods lacked robustness, they demonstrated the utility of base-pairing for targeted DNA modifications. Over the last two decades, methods using principles of DNA-protein recognition were developed and evolved, enabling the effective introduction of genomic sequence changes in eukaryotes and prokaryotes. For higher organisms, zinc finger nucleases (ZFNs) and TAL effector nucleases (TALENs) were found to be useful tools (100, 101) and in case of bacteria, mobile group II introns, transposon-based tools, and integrative plasmids represent well-established genome editing strategies (102). However, low efficiencies, tedious implementations, and difficulties in protein design, synthesis, and validation limit the widespread adoption of these techniques for routine use across various species.

Now, biology is being revolutionized in pro- and eukaryotes by harnessing of the bacterial adaptive immune system CRISPR-Cas as a tool for genetic engineering. Within a few years after the discovery of the potential of CRISPR-Cas, more than a thousand studies on this topic have been published (103), impressively illustrating the fast-paced development in this field.

1.3.1 Functionality of CRISPR-Cas

Bacteria and archaea have evolved a genetic adaptive immune system to defend against invading DNA. This system, termed CRISPR-Cas (**clustered regularly interspaced short palindromic repeats – CRISPR associated**), uses short RNA to direct degradation of foreign nucleic acids (104-106). By incorporating fragments of invading phage or plasmid DNA, so-called “spacers” into a defined locus of the own genome, the invader can be recognized during subsequent encounters (107). Spacer sequences are separated by identical repeats, yielding the crRNA (CRISPR RNA). An operon of *cas* genes encodes the Cas protein components and a sequence encoding the tracrRNA (trans-activating crRNA) complete the functional CRISPR locus (108). Up to now, three different types of CRISPR-systems are known. Type I and type III CRISPR-systems use multiple Cas proteins to target and degrade DNA, whereas type II only requires a single protein (109, 110). Due to this simplicity, the type II system was the starting point for the exploitation of CRISPR-Cas for genetic engineering. The functioning of the type II CRISPR-Cas system in bacteria is a multistep process (111), which can be divided into three steps:

- (i) Insertion of invading DNA fragments (spacers) into the CRISPR array
- (ii) Transcription and maturation of the array
- (iii) RNA guided cleavage of foreign DNA

During the immunization phase (i), the molecular signature of the invading species is stored by integrating DNA fragments into the CRISPR array. Expression of the CRISPR locus (ii) yields a long pre-crRNA from the spacer-repeat region, the tracrRNA and the multifunctional Cas9 protein. As a first step of the following maturation, the tracrRNA hybridizes to the repeat region of the pre-crRNA. Subsequently, RNase III activity cleaves the complex, resulting in the formation of mature crRNAs. Finally, the crRNA guides the Cas endonuclease to the complementary site of the foreign DNA and the double-strand break is initiated by HNH- and RuvC-like nuclease domains (iii). To prevent self-targeting of the own CRISPR locus, DNA cleavage only occurs in the presence of a protospacer-adjacent motif (PAM), which is a short nucleotide sequence, located upstream of the targeting region on the foreign

DNA. For recent reviews on CRISPR functionality, see (112-114). Figure 1.7 gives an overview on the mechanisms involved in CRISPR-Cas mediated adaptive immunity.

The utilization of this natural DNA cleavage machinery as a tool for site-directed mutagenesis *in vivo*, has dramatically increased the accessibility and throughput of genetic engineering studies in eukaryotes, not only in mammals, but also prokaryotes.

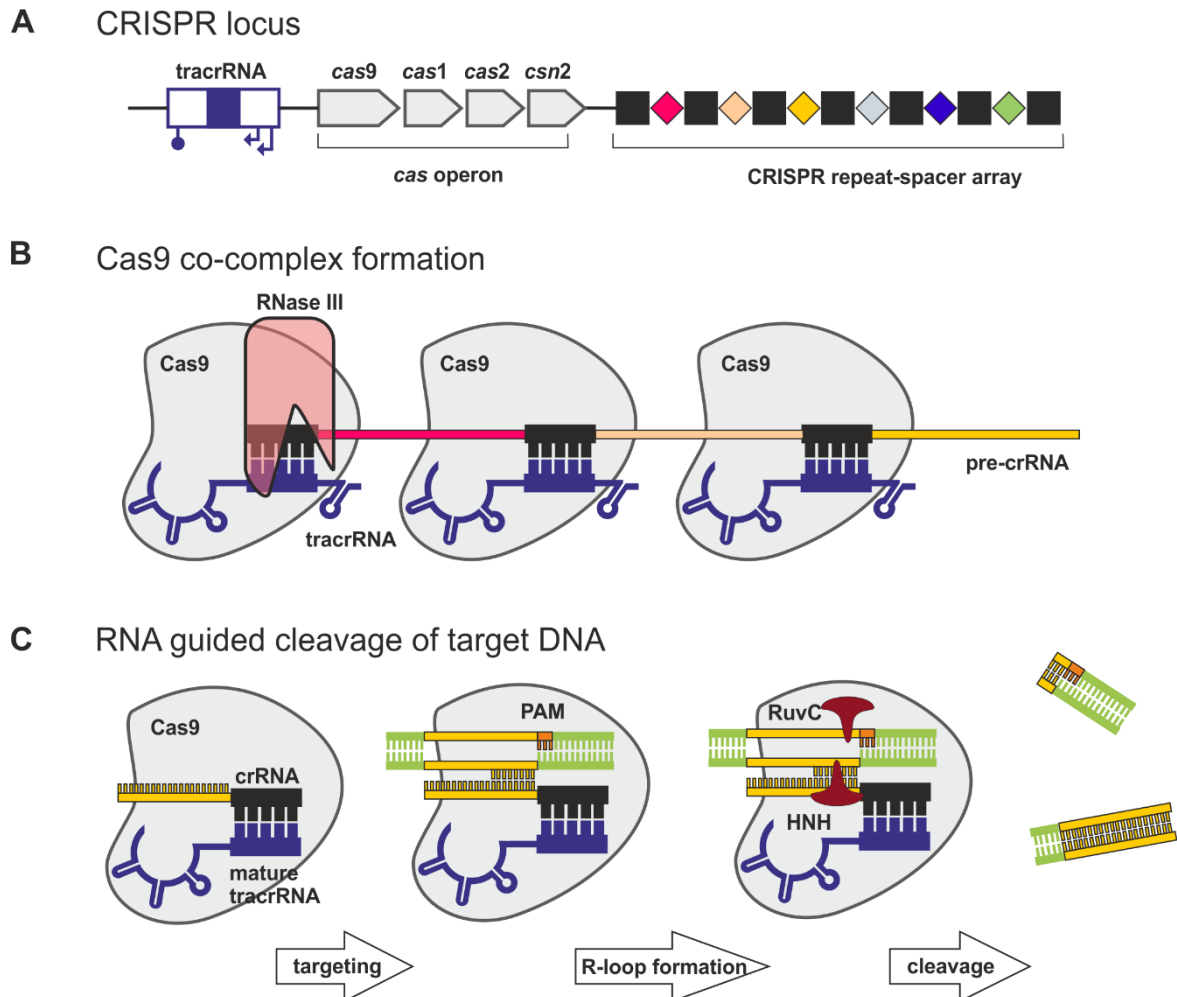


Figure 1.7. Mechanisms involved in adaptive immunity of type II CRISPR-Cas system. (A) The genomic locus including *cas* genes, tracrRNA and CRISPR array. (B) Association of Cas9 with tracrRNA:crRNA duplexes and RNase III mediated cleavage yielding mature Cas9 complexes. (C) The tracrRNA/crRNA/Cas9 ribonucleoprotein complex scans invading DNA for PAM sequences. Upon binding of the mature Cas9 complex, the target sequence upstream of the motif is unwound and crRNA annealing results in the formation of a crRNA:target R-loop that triggers cleavage by HNH and RuvC nuclease domains of Cas9.

1.3.2 CRISPR Editing

The type II CRISPR-Cas9 system of *Streptococcus pyogenes* is the best-studied representative and has been used manifold as template for the implementation of CRISPR-Cas in new organisms (115). In order to reduce the number of required elements, the natural two RNA duplex (pre-crRNA – tracrRNA) was combined to a chimeric single guide RNA (sgRNA), which retains the two critical features: a 20-nucleotide sequence at the 5' end that determines binding to the target DNA, and the double-stranded RNA structure at the 3' required for Cas9 binding (110). Hence, a two-component system (sgRNA,

Cas9) is sufficient to unleash the full potential of CRISPR-Cas9. In comparison to eukaryotes, this technique has only been sporadically used in bacteria. However, the technology is a highly promising opportunity to make bacterial strains accessible to genetic engineering that previously lacked efficient tools. The great potential lies in the combination of the high Cas9 activity and the fact that double-strand DNA breaks within the genome are mostly lethal to the host (116). Since Cas9 is targeted to genomic loci in case of editing approaches, bacteria with un-edited genomes are very unlikely to survive. The combination of this CRISPR-based negative selection with traditional recombination methods is the fundamental strategy for Cas9 mediated engineering in bacteria. DNA repair by endogenous repair machineries (e.g. Ku, LigD) via non-homologous end joining (NHEJ), usually results in indel mutations and thereby a disruption of the target gene. Homology directed repair (HDR) can be used to perform gene corrections or insertions by providing a tailored repair template (103, 115). Completely or partially inactivated Cas9 variants were designed to expand the possibilities of Cas9 engineering. Mutation of both endonuclease sites (Asp¹⁰ → Ala, His⁸⁴⁰ → Ala) results in a DNA binding protein without cleavage activity that can be used to label, activate or inactivate certain DNA regions by binding Cas9 to an effector domain, such as green fluorescent protein, transcriptional activators or repressors (103, 117). Inactivation of a single site yields nickases, which can be used to generate staggered double-strand breaks, resulting in decreased off-targeting effects (118).

1.4 *Paenibacillus* spp.

The genus *Paenibacillus* currently comprises around 200 bacterial species that have been isolated from various environments, ranging from Polar Regions to tropical forests and from aquatic habitats to dry deserts. However, the majority of *Paenibacillus* strains was discovered as plant root associated rhizobacteria and many of them are important to animals, plants, and humans (119).

The name *Paenibacillus* refers to the historical phylogenetic classification of the genus. The Latin adverb *paene* means almost and hence *Paenibacillus* stands for “almost bacillus” (120). Originally, *Paenibacillus* species were included in the *Bacillus* genus, as they showed morphological similarities to *Bacillus* bacteria and were able to form endospores. In the early 1990th, the phylogenetic relationship of *Bacillus* bacteria was redefined using 16S rDNA sequencing and the novel *Paenibacillus* genus was assigned with its type strain *Paenibacillus polymyxa* (121, 122). According to a refinement proposed in 1997, *Paenibacillus* strains have a 16S rDNA sequence similarity of ≥ 89.6%, are peritrichous flagella, can be Gram-positive, Gram-negative or Gram-variable and share further basal characteristics ascribed to *Bacillus* (123). The *Paenibacillaceae* family, which the genus *Paenibacillus* belongs to, comprises seven further genera, and it is expected that family and genera will undergo a significant taxonomic subdivision in the future (124). Several species of the *Paenibacillus* genus positively or negatively affect our environment and most important aspects are covered in the following.

Since most *Paenibacillus* species are found in soil, frequently associated with plant roots, it does not astonish that many of them promote plant growth in various ways. Positive effects were already shown for numerous plants including pumpkin and rice (125, 126). The ability to increase the bioavailability of essential elements, such as nitrogen and phosphorus, is one of the ways by which *Paenibacilli* promote plant growth. Over 20 species were reported to fix nitrogen by the nitrogenase-catalyzed

reduction of N_2 to bioavailable NH_3 (127) and genomic analyses suggest that most *Paenibacillus* species are able to solubilize inorganic phosphorus via gluconic acid production (128). For several representatives, this was already confirmed experimentally (129, 130). Another strategy of direct plant growth promotion is the secretion of phytohormones, which participate in the regulation of various steps in a plant's life cycle. Indole-3-acetic acid (IAA) is the first identified and most abundant auxin in nature (131). Although plants are able to produce IAA themselves, they can also utilize exogenous sources and many plant-associated organisms, including *Paenibacilli*, can produce IAA thereby contributing to plant growth (132).

An entirely different, but by no means less important way of supporting the growth of plants is the protection against insect herbivores or phytopathogens and the stimulation of endogenous resistance mechanisms. *Paenibacilli* possess an impressive arsenal of biocontrol features, which were shown to protect various plants, including cucumber, chickpea, peanut, soybean, pepper and many more (133-137). When present in sufficiently high population densities, *Paenibacilli* can, for example, trigger induced systemic resistances in plants – a defense mechanism relying on the hypersensitization to potential threats, which results in a faster and stronger immune response when exposed (138, 139). Furthermore, *Paenibacillus* species were reported to control pest insects like beetles (140) and lepidopterans (141), by expressing chitinases that degrade structural polysaccharides of insects or crystal proteins, which form lethal pores in the insect midgut epithelial cells.

Another property of *Paenibacilli* making this genus relevant especially to the pharmaceutical industry is their capability to produce different antimicrobial agents. Polymyxins are the best-described antibiotics produced by *Paenibacillus*. Since their first description in 1947, diverse polymyxin variants were identified and they were used extensively until 1970th to treat bacterial infections (142). Due to their toxicity to the human central nervous system and kidneys, their use is limited nowadays. However, synthetic approaches aim at the production of novel polymyxin variants with improved pharmacokinetic properties (143). Lantibiotics, pediocins, and fusaricidins are further examples of antimicrobial substances that are produced by *Paenibacillus* to inhibit the growth of related competitors (144-146).

Besides the described agricultural and medical aspects, *Paenibacilli* also exhibit properties interesting for the biotechnological industry. They are equipped with a wide set of enzymes, including amylases, cellulases, hemicellulases, lipases, pectinases, and ligning-modifying enzymes, which could potentially be used in the detergent, food and feed or paper industry (119). Furthermore, several *Paenibacillus* species were described to degrade contaminants in wastewaters or at sites of environmental spill using their enzyme repertoire. Various aliphatic and aromatic organic pollutants can be metabolized by *Paenibacilli* by the action of oxygenases, dehydrogenases, and ligninolytic enzymes (147, 148), rendering *Paenibacilli* interesting for bioremediation purposes. *Paenibacilli* can also produce and tolerate high levels of commercially relevant chemicals like 2,3-butanediol, making the genus interesting for the fermentative production of platform chemicals (149). Finally yet importantly, *Paenibacilli* produce a class of highly promising but still underappreciated EPSs, possessing various industrially relevant properties. This aspect is covered in section 1.4.1.

On the downside, some *Paenibacillus* species are known to be infectious to honeybees and occasionally to immune suppressed humans. Especially the American Foulbrood, a destructive disease of honeybee larvae, which is caused by *P. larvae* strains, poses a global threat to hives (150). Once infected, the most virulent *P. larvae* strains only need 7 days to erase entire honeybee larvae colonies (151). Since adult

honeybees are not susceptible, *P. larvae* spores are spread horizontally within and between hives in the process of cleaning contaminated cells, making this disease so virulent and devastating (152).

1.4.1 Exopolysaccharides by *Paenibacilli*

In 1969, Ninomya and Kizaki already described the fermentative production, monomeric composition, rheological properties and water holding capacity of a polysaccharide secreted by *P. polymyxa* (153). In the subsequent 50 years, several other studies were published, dealing with the discovery, production, as well as physiological and physicochemical properties of novel EPSs from *Paenibacilli*. When compared to the entirety of *Paenibacillus* species described, the number of EPS producing species is rather small. Most reports deal with strains of *P. polymyxa* or phylogenetically closely related representatives. Although these species share a high evolutionary similarity, the structural differences among their characterized EPSs is huge. Descriptions range from homopolysaccharides, such as glucanes (154) and levan-type polymers (155), to complex heteropolysaccharides comprising various sugars, including mannose, glucose, galactose, rhamnose, xylose, fucose, fructose and more (156, 157). Furthermore, some authors also describe the existence of two or even three polymer fractions of different molecular weights, charges, and monomer compositions (158). However, the majority of published monomer compositions is similar to the one reported by Ninomya and Kizaki, which comprises mannose, glucose, galactose and glucuronic acid. The structural diversity of *Paenibacillus* EPSs results in a variety of physicochemical properties and hence numerous potential applications. Due to a shear thinning, highly viscous flow behavior, several researchers proposed the usage of certain *Paenibacillus* EPSs as thickeners or rheological agents (159). Frequently reported bioactivities, such as antioxidative potential, antitumor activity, improvement of skin hydration, and enhancement of immunity, render EPSs from *Paenibacilli* interesting for medical applications (160). Further suggested fields of application include bioremediation, emulsification, animal feed additive, and cement mortar admixture. As for most bacteria, also *Paenibacillus* EPSs are typically produced via batch fermentations. Usually, bioreactors are operated between 20 – 40 °C, at a controlled pH of 6 – 8, for a duration of 24 h up to 10 days. Mostly, sucrose or glucose is used as carbon sources and yeast extract as nitrogen source. However, reports on numerous different nutrient sources can be found, also including complex media, such as waste streams from olive-mills (161) or squid pen powder (162). Obtained EPS titer range from 0.15 g·L⁻¹ to 54 g·L⁻¹ (163, 164), with fermentations on sucrose being the most productive in terms of absolute EPS titer. This can be explained by the activity of levansucrases, which catalyze the production of levan polysaccharide when sucrose is present. Table 1.2 gives an overview on some EPSs produced by *Paenibacilli*. For more information on EPSs of *Paenibacilli*, see reference (160).

Table 1.2. Summary of exopolysaccharides produced by *Paenibacillus* strains.

Strain	EPS Structure		Fermentation			Properties		Reference
	Monomer Composition ^a	Molecular Weight [MDa]	Duration	C-Source	N-Source	Titer [g·L ⁻¹]	Rheology	
<i>P. polymyxa</i> SQR-21	Man, Gal, Glc, GlcA	0.9	96 h	Gal	yeast extract	3.44	N.A. ^b	(165)
<i>P. polymyxa</i> A49 KCTC 8648P	Man, Gal, Glc, GlcA, Fuc	1.6	24 h	Glc	NH ₄ NO ₃ , yeast extract, tryptone, soytone	7	Shear thinning Highly viscous	(159, 166)
<i>P. polymyxa</i> NCIB 11429	Man, Gal, Glc, GlcA, Fuc, Pyr	N.A.	70 h	Suc	yeast extract	10	Thermos-reversible gels Highly viscous	(167)
<i>P. polymyxa</i> NRRL B-18475	Fru	2	10 days	Suc	yeast extract	36	N.A.	(155)
<i>P. polymyxa</i> EJS-3	Man, Glc, Fru (two EPSs)	EPS1: 1.2 EPS2: 0.9	60 h	Suc	yeast extract	35.26	N.A.	(168, 169)
<i>P. polymyxa</i> JB115	Glc	0.6	3 days	Suc	NH ₄ Cl	10.6	N.A.	(154, 170)
<i>P. jamilae</i> CECT 5266	Man, Gal, Glc, UAs, Fuc, Rha (two EPSs)	EPS1: 2 EPS2: 0.5	5 days	olive-mill wastewater, NH ₄ Cl, yeast extract		5.5	N.A.	(157, 161, 171, 172)
<i>P. elgii</i> B69	Man, Glc, GlcA, Xyl	3.5	96 h	Suc	peptone, yeast extract	25.63	High viscosity	(156)
<i>P. polymyxa</i> 1465	Man, Gal, Glc, UAs	0.07 - 2	7 days	Glc	(NH ₄) ₂ SO ₄	2.1	High viscosity	(173, 174)
<i>P. sp.</i> WN9 KCTC 8951P	Man, Glc, Tyr	31.5	48 h	Glc	yeast extract	4.0	Pseudoplasticity Temperature and pH stability	(175, 176)
<i>P. velaei</i> sp. nov.	Man, Gal, Glc, Fuc	2	5 days	Glc	NH ₄ Cl	1.4	N.A.	(177)
<i>P. sp.</i> TKU023	Glc, Mal	N.A.	5 days	squid pen powder		4.55	N.A.	(162)
<i>P. polymyxa</i> No.271	Man, Gal, Glc, GlcA, Pyr	1.3	60 h	Glc	peptone, urea	14	Highly viscous Gelling capacity	(153)

^amannose (Man), galactose (Gal), glucose (Glc), glucuronic acid (GlcA), fucose (Fuc), pyruvate (Pyr), fructose (Fru), uronic acids (UAs), rhamnose (Rha), xylose (Xyl), tyrosine (Tyr), maltose (Mal)^bno data available

1.5 Scope of the work

The aim of this work is to establish a bacterial strain as a new EPS production host, in order to develop, characterize and provide novel, bio-based thickeners for industrial applications.

As the first step, a potential production strain has to be chosen based on a high throughput screening approach, which was already developed by the institute to identify novel EPS producers. Strain selection criteria could include, but are not limited to the carbohydrate fingerprint of secreted EPS, broth viscosity and growth characteristics.

Subsequently, the chosen strain should be characterized phylogenetically and microbiologically, including 16S rDNA sequencing, carbon source acceptance, antibiotics resistances, growth preferences, and media optimization for the production of EPSs.

Afterwards, a fermentative production process in bioreactor systems has to be implemented, in order to produce consistent batches of polymer and to describe the growth and EPS secretion behavior under controlled and reproducible conditions. For this, the results obtained during the basic strain characterization should be transferred to small volume bioreactors and adapted if necessary. In parallel, a suitable downstream procedure has to be developed, allowing for the efficient and reproducible purification of EPS from the fermentation broth.

The EPSs obtained have to be characterized in detail using analytical and rheometrical techniques. The analytical part should include the identification of the monomeric composition (HPLC-ESI-MS/MS), ash and protein content, as well as molecular mass analyses (SEC-MALLS). The rheological characterization of the polymer should be performed using rotational and oscillatory measuring protocols, in order to describe viscous and elastic behavior of the samples. Since the study aims at the development of an industrially relevant EPS, especially for personal care formulations, rheological measurements of benchmark products have to be performed as well.

A last milestone of the dissertation is the genetic modification of the production strain, in order to describe the biosynthetic basis for EPS production and to produce different polymer variants. To implement this, at first a suitable transformation procedure has to be established, enabling the robust and efficient transfer of foreign DNA to the target strain. Secondly, a whole genome sequencing should be performed in order to identify and annotate the putative EPS biosynthesis cluster. Subsequently, a reliable genome-editing tool needs to be established, allowing for the targeted deletion and if possible even insertion of DNA sequences in the producers genome. Ideally, the developed tool can be utilized to proof experimentally that the hypothesized EPS cluster encodes biosynthesis machinery for polymer production. Furthermore, EPS variants could be generated by deleting or inserting certain enzymatic functionalities involved in the assembly of secreted EPSs. If successful, this approach could serve as a proof of concept that tailoring EPS structures via genetic engineering is feasible and that the selected production host might serve as chassis organism for the production of novel, tailored EPS variants.

2 Material and Methods

2.1 Material

2.1.1 Equipment

Table 2.1. Equipment used in this study.

Equipment name	Manufacturer / Model
Agarose gel electrophoresis apparatus	Bio-Rad (München), Mini-Sub Cell GT System
Autoclave	Thermo Scientific (Ulm) Varioklav 135S
Centrifuge	Thermo Scientific (Ulm) Sorvall RC-6 Plus
Clean bench	Thermo Scientific (Ulm) MSC-Advantage
Cross flow filtration system	Sartorius AG (Göttingen) SartoJet
Drying oven	Thermo Scientific (Ulm) Function line T12
Electroporator	Bio-Rad (München), MicroPulser™
Fermenter	Sartorius AG (Göttingen) Biostat® Bplus 2-L UniVessel® Sartorius AG (Göttingen) Biostat® Cplus 30-L
Fermentation sensors	BlueSens gas sensor GmbH (Herten) BCP-CO2 BlueSens gas sensor GmbH (Herten) BCP-O2
Freezer -20 °C	Liebherr-Hausgeräte (Ochsenhausen)
Freezer -80 °C	Thermo Scientific (Ulm) Forma 906 -86 °C ULT
FT-IR	Thermo Scientific (Ulm) Nicolet 380™
Gel documentation system	Intas Science Imaging (Göttingen), Gel iX Imager
Gel permeation chromatography (GPC)	Agilent Technologies (Waldbronn) 1260 Infinity
GPC-Detector	PSS Polymer Standards Service GmbH (Mainz) SECcurity SLD7000MALLS PSS (Mainz) SECcurity GPC1260 RI detector
GPC-Columns	PSS (Mainz) Suprema guard column PSS (Mainz) Suprema 10000 Å PSS (Mainz) Suprema 100 Å
Heating block	VLM (Bielefeld), EC model series Tmix (Jena) Jenaanalytik
Hydraulic press	Specac Inc (Fort Washington) ATLAS Manual Hydraulic Press
Incubator	Binder (Tuttlingen) KBF 240 E5.1/C Infors HT (Bottmingen-CH) Minitron
Magnetic stirrer	Thermo Scientific (Ulm) Variomag Telesystem
Microplate shaker	Edmund Bühler (Hechingen) TiMix 5 control and TH 15
Mixer Mill	Retsch (Haan) MM400
Nanophotometer	Implen (München), P-330
Overhead stirrer	Heidolph Instruments GmbH & Co. KG (Schwabach)

pH-meter and electrode	Mettler-Toledo (Giessen) Five Easy™ and InLab® Expert Pro
Pipettes	BRAND (Wertheim) Transferpetten
Rheometer	Anton Paar GmbH (Graz) MCR 300
Rheometer-Measuring System	Anton Paar GmbH (Graz) CP 50-1
Rheometer-Temperature control	Anton Paar GmbH (Graz) TEK 150P
Rotor	Thermo Scientific (Ulm) SS-34, SH-3000, F9-4x 1000y
Scale	Sartorius (Göttingen) TE1502 and TE6101
Shaker	Thermo Scientific (Ulm) MaxQ 2000
Spectrophotometer	Thermo Scientific (Ulm) Varioskan Flash and Multiskan
Table centrifuge	Thermo Scientific (Ulm) Heraeus Fresco 21
Thermo cycler	Bio-Rad (München) MyCycler™ Bio-Rad (München) MJ Mini™
UHPLC	Dionex (Idstein) Ultimate 3000RS
UHPLC-Autosampler	Dionex (Idstein) WPS 3000TRS
UHPLC-Column compartment	Dionex (Idstein) TCC 3000RS
UHPLC-Degasser	Dionex (Idstein) SRD 3400
UHPLC-Diode array detector	Dionex (Idstein) DAD 3000RS
UHPLC-High capacity ion trap	Bruker Daltonics (Bremen) HCT
UHPLC-Pump module	Dionex (Idstein) HPG 3400RS
UHPLC-Columns	Macherey Nagel (Düren) NUCLEODUR C18 Gravity, 1.8 µm, 100 mm, ID: 2 mm Bio-Rad (München) Aminex IEC HPX-87P; 300 × 7.8 mm
UHPLC-Refractive index detector	Shodex (Tokyo) RI 101
Ultrapure water system	ELGA LabWater (Celle) PURELAB classic
Vortexer	Scientific Industries (Bohemia) Vortex Genie 2
Water bath	Huber (Offenburg) CC1

2.1.2 Software and databases

Table 2.2. Software and databases used in this study.

Product	Manufacturer	Application
Basic Local Alignment Search Tool (BLAST)	National Center for Biotechnology Information	Protein sequence alignment
BioEdit	Tom A. Hall	Sequence alignment editor
Cello v.2.5	National Chiao Tung University	Protein localization analysis
Chromeleon	Dionex	Data analysis UHPLC
Clone Manager 9	Scientific & Educational Software	<i>In silico</i> DNA sequence analysis
Corel Draw 2017	Corel Corporation	Data visualization

DataAnalysis	Bruker	Data analysis MS
EndNote X7	Clarivate Analytics	Literature citing managing
MS Office 2016	Microsoft Corporation	Text processing (MS Word) Data analysis (MS Excel) Visualization (MS PowerPoint)
PSS WinGPC UniChrom 8.1	PSS Polymer Standards Services GmbH	Data analysis GPC
QuantAnalysis	Bruker	Quantification of MS-data
RAST V2	see reference (178)	DNA sequence annotation
Rheoplus/32 V3.61	Anton Paar GmbH	Data analysis rheometry
ScanIt	Thermo Scientific	MTP-reader control software
SigmaPlot 12.0	Systat Software	Data visualization
SnapGene 2.3.2	GSL Biotech	<i>In silico</i> cloning and sequence alignments
Web of Knowledge	Thomson Reuters	Literature research

2.1.3 Bacterial strains

Table 2.3. Bacterial strains used in this study.

Strain	Description	Reference
<i>E. coli</i> DH5 α	F ⁻ Φ 80lacZ Δ M15 Δ (lacZYA-argF) 169 recA1 endA1 hsd R17 (rK ⁻ , K ⁺) phoA supE44 λ - thi-1 gyrA96 relA1	NEB
<i>E. coli</i> S17-1	Conjugation strain; recA pro hsdR RP42Tc::Mu-Km::Tn7 integrated into the chromosome	ATCC 47055
<i>P. polymyxa</i> DSM-365	Wild type	DSMZ365
<i>P. polymyxa</i> 2H2	Wild type	This study
<i>Rhodobacter</i> sp. 1F2	Wild type	This study
<i>Rhizobium</i> sp. 2A7	Wild type	This study
<i>Micrococcus luteus</i> 1E6	Wild type	This study
<i>Paenibacillus</i> sp. 1E6	Wild type	This study
<i>P. polymyxa</i> DSM-365pepC	DSM-365 Δ pepC	This study
<i>P. polymyxa</i> DSM-365pepF	DSM-365 Δ pepF	This study
<i>P. polymyxa</i> DSM-365pepJ	DSM-365 Δ pepJ	This study
<i>P. polymyxa</i> DSM-365ugdH1	DSM-365 Δ ugdH1	This study
<i>P. polymyxa</i> DSM-365manC	DSM-365 Δ manC	This study
<i>P. polymyxa</i> DSM-365clu	DSM-365 Δ clu	This study
<i>P. polymyxa</i> DSM-365pgrac	DSM-365::pgrac	This study

2.1.4 Chemicals and reagents

Table 2.4. Chemicals and reagents used in this study.

Name	Manufacturer	Catalog number
1-Phenyl-3-Methyl-5-pyrazolone	Sigma-Aldrich	M70800
2-Propanol	VWR	20922.466
Acetic acid	Sigma-Aldrich	338826
Acetone	Carl-Roth	7328
Acetonitrile LC-MS grade	VWR	83040.320
Adenosine 5'-Triphosphate	New England Biolabs	P0756S
Agar-agar	Carl-Roth	5210.2
Agarose	Serva	11406
Ammonium solution 32%	Carl-Roth	P093.1
Ampicillin	Carl-Roth	HP62.1
Boric acid	Sigma-Aldrich	B7901
Bovine serum albumin	Sigma-Aldrich	A2153
Calcium chloride	Carl-Roth	5239.1
Carbenicillin	Applichem	A1491
Chloramphenicol	Sigma-Aldrich	C0378
Chloroform isoamylalcohol	Roti	X984.2
Cobalt (II) chloride hexahydrate	Alfa Aesar	A16346
Copper (II) sulfate pentahydrate	Sigma-Aldrich	61245
DA-64	Wako Chemicals	043-22351
Dimethyl sulfoxide	Carl-Roth	4720.1/ AE02.1
Dithiothreitol	Carl-Roth	6908.2
Ethanol absolute	VWR	20821.321
Glucose	Carl-Roth	6887.5
Glycerol	Roth (99.5% p.a.)	3783.2
HEPES	Carl-Roth	HN78.3
IPTG	Carl-Roth	CN08.3
Iron (II) sulfate heptahydrate	Sigma-Aldrich	31236
Isopropanol	Carl-Roth	7343.1
Kanamycin	Carl-Roth	T832.1
Lithium nitrate	Alfa	13405.30
Magnesium sulfate heptahydrate	Merck	1.05886.1000
Manganese (II) chloride tetrahydrate	Sigma-Aldrich	63535
Methanol LC-MS	VWR	83638.320
MOPS	Carl-Roth	6979.4
Neomycin sulfate	Carl-Roth	8668

Peptone from casein	Carl-Roth	8952.5
Phenol red	Alfa Aesar	B21710
Phosphoenol pyruvate	Sigma-Aldrich	860077
Polymyxin B sulfate (4 °C)	Carl-Roth	0235.1
<i>p</i> -nitrophenol	Sigma-Aldrich	425753
Potassium acetate	Carl-Roth	4986.1
Potassium phosphate dibasic	Carl-Roth	P749.3
Potassium phosphate monobasic	Merck	1.04873.1000
Potassium sulfate	Merck	221368
Pullulan standard	Sigma-Aldrich	53168
Rubidium chloride	Alfa Aesar	12892
Sodium, metallic	VWR	8222840250
Sodium-azide	Sigma-Aldrich	71290
Sodium chloride	Carl-Roth	P029.3
Sodium molybdate dehydrate	Carl-Roth	CN-62
Sodium nitrate	VWR	1065351000
Sucrose	Carl-Roth	4621.1
Tetracycline	Serva	35866.01
Trifluoroacetic acid	Sigma-Aldrich	T6508
TRIS	Carl-Roth	AE15.2
Vitamins solution RPMI 1640	Sigma-Aldrich	R7256
Yeast extract	Carl-Roth	2363
Zinc chloride	Merck	1.08816.0250

2.1.5 Kits, enzymes and special consumables

Table 2.5. Kits, enzymes and special consumables used in this study.

Name	Manufacturer
Accuzyme™ PCR Mastermix	Bioline
Cetrimonium chloride (VARIOSOFT 300)	Evonik Industries
Cocamidopropyl betaine (TEGO Betaine F50)	Evonik Industries
DNase	Applichem
GeneJET™ Plasmid Miniprep	Thermo Fischer Scientific
Glucose oxidase	Sigma-Aldrich
GoTaq DNA-polymerase	PROMEGA
Horseradish peroxidase	Sigma-Aldrich
Low acyl Gellan gum (Collstab G)	Colltect GmbH
Lysozyme	Carl-Roth

<i>Nucleospin</i> ® Gel and PCR Clean-up Kit	Macherey-Nagel
Lauryl glucoside (Plantacare 1200 UP)	BASF
Plasmid-Safe ATP-Dependent DNase kit	Epicentre
Phusion high-fidelity DNA-Polymerase	New England Biolabs
Polynucleotide kinase	New England Biolabs
Proteinase K	Thermo Scientific
Pyruvate oxidase	Sigma-Aldrich
Restriction endonucleases	
BbsI	New England Biolabs
BsaI	New England Biolabs
DpnI	New England Biolabs
NcoI	New England Biolabs
NdeI	New England Biolabs
NheI	New England Biolabs
SpeI	New England Biolabs
XbaI	New England Biolabs
XhoI	New England Biolabs
RNase A/T1 Mix	Thermo Scientific
Roti®-Nanoquant Kit for protein determination	Carl-Roth
Sodium lauryl ether sulfate (Texapon NSO)	BASF
T4 ligase	New England Biolabs
T7 ligase	New England Biolabs
Whatman Paper (Cat. No. 1001917)	GE Healthcare UK limited
Xanthan gum (Keltrol CG)	CP Kelco

2.1.6 Plasmids, primer and oligos

Plasmids utilized in this work are summarized in the table below. A detailed register of all used primers and oligonucleotides can be found in the supporting information of chapter 3.4. Primers utilized for bacterial strain identification are described in section 2.4.2. Primers were synthesized by biomers (Ulm) or Life Technologies (Darmstadt) and gBlocks were purchased from Integrated DNA Technologies (Coralville).

Table 2.6. Plasmids used in this study.

Plasmid	Description	Reference
pCRISPRomyces-2	Codon optimized Cas9 expression for <i>Streptomyces</i> carrying SpCas9, oriT and BbsI flanked lacZ cassette	(179)
pUBoriMC	Plasmid carrying Neo ^r , ori and repU gene, derivative of puB110 (ATCC 37015)	This study
pHT01	<i>E. coli</i> – <i>B. subtilis</i> shuttle vector enabling encoding pgrac expression system	MoBiTec GmbH
pCasPP	<i>P. polymyxa</i> genome editing vector	This study
pCasPP-pepFsg1	<i>pepF</i> targeting knockout plasmid not providing a repair template	This study
pCasPP-pepFsg1-harms	<i>pepF</i> targeting knockout plasmid providing a repair template	This study
pCasPP-pepFsg2-harms	<i>pepF</i> targeting knockout plasmid providing a repair template	This study
pCasPP-pepF-harms	Untargeted pCasPP derivative carrying <i>pepF</i> homologous regions	This study
pCasPP-pepCsg1-harms	<i>pepC</i> targeting knockout plasmid providing a repair template	This study
pCasPP-pepCsg2-harms	<i>pepC</i> targeting knockout plasmid providing a repair template	This study
pCasPP-pepJsg1-harms	<i>pepJ</i> targeting knockout plasmid providing a repair template	This study
pCasPP-pepJsg2-harms	<i>pepJ</i> targeting knockout plasmid providing a repair template	This study
pCasPP-ugdH1sg1-harms	<i>ugdH1</i> targeting knockout plasmid providing a repair template	This study
pCasPP-ugdH1sg2-harms	<i>ugdH1</i> targeting knockout plasmid providing a repair template	This study
pCasPP-manCsg1-harms	<i>manC</i> targeting knockout plasmid providing a repair template	This study
pCasPP-manCsg2-harms	<i>manC</i> targeting knockout plasmid providing a repair template	This study
pCasPP-clugBlock-harms	Multiplex pCasPP variant targeting two different sites at once for knockout of the 18 kb fragment; homologous regions are provided	This study
pCasPP-pgracsg2-harms	pCasPP derivative for pgrac integration upstream of <i>sacB</i>	This study

2.2 Media and Buffer

2.2.1 Media preparation

All growth media were sterilized by autoclaving at 121 °C for 20 min. To prevent maillard reactions, sugars and other media compounds were sterilized separately. Temperature instable compounds (vitamin solution) and trace element solution were filter-sterilized and added after temperature treatment. To prepare agar plates, 1.5% agar was added to liquid media prior to autoclaving.

2.2.2 Cultivation media

Lysogen-broth (LB) was prepared as 10 g·L⁻¹ sodium chloride, 10 g·L⁻¹ peptone, 5 g·L⁻¹ yeast extract. For the production of EPSs, bacterial strains were grown in MM1 P100, comprising 30 g·L⁻¹ glucose, 1.33 g·L⁻¹ magnesium sulfate heptahydrate, 1.67 g·L⁻¹ potassium dihydrogen phosphate, 0.05 g·L⁻¹ calcium chloride dihydrate, 2 mL·L⁻¹ RPMI 1640 vitamins solution and 1 mL·L⁻¹ trace elements solution. For testing of carbon source acceptance during initial strain selection, glucose was replaced with molar equivalents of sucrose, arabinose, xylose or glycerol.

2.2.3 Trace element solution

2.5 g·L⁻¹ iron-(II)-sulfate heptahydrate, 2.1 g·L⁻¹ sodium tartrate dihydrate, 1.8 g·L⁻¹ manganese-(II)-chloride dihydrate, 0.075 g·L⁻¹ cobalt-(II)-chloride hexahydrate, 0.031 g·L⁻¹ copper-(II)-sulfate pentahydrate, 0.258 g·L⁻¹ boric acid, 0.023 g·L⁻¹ sodium molybdate dihydrate and 0.021 g·L⁻¹ zinc chloride.

2.2.4 Buffers for chemical competent *E. coli* cells

TFBI contained 30 mM potassium acetate, 100 mM rubidium chloride, 10 mM calcium chloride dihydrate, 50 mM manganese (II) chloride tetrahydrate in 15% glycerol. TFBII contained 10 mM MOPS, 75 mM calcium chloride dehydrate, 10 mM rubidium chloride in 15% glycerol.

2.3 Microbiological methods

2.3.1 Bacterial strain storage

The strains were stored at -80 °C in cryo tubes containing 600 µL of the bacterial strain grown in corresponding media and 400 µL of a 60% glycerol solution.

2.3.2 Strain cultivation

For strain activation, bacterial suspensions were scratched from frozen cryo tubes using an inoculation loop, spread on corresponding agar plates and incubated overnight at 37 °C for *Escherichia coli* and 30 °C for *Paenibacillus*, *Rhodobacter*, *Rhizobium* and *Micrococcus* strains. Liquid cultures were inoculated with single colonies from the incubated agar plates. *E. coli* strains were grown in LB media at 37 °C and 300 rpm in single-use plastic tubes, sealed with a plastic lid. All other strains were grown in LB media for genetic manipulations and in MM1 P100 for EPS production. Slime-free culturing in LB was performed at 30 °C and 300 rpm in single-use plastic tubes, sealed with a plastic lid, or in 50 mL baffled culture flasks at 30 °C and 150 rpm. For polymer production, baffled 250 mL shake flasks sealed with aluminum caps were filled with 100 mL MM1 P100 media and inoculated with 1 mL of an overnight culture. Cultures were incubated at 30 °C and 170 rpm for 28 hours. If required, antibiotics were added at 50 µg·mL⁻¹ for neomycin and 20 µg·mL⁻¹ for polymyxin.

2.3.3 Antibiotic sensitivity tests

Antibiotic susceptibility of selected EPS producers was determined by a modified disk diffusion method. For this, 100 µL of a densely grown bacterial overnight cultures were plated on a LB agar plates. Afterwards, punched and autoclaved Whatman Paper (GE Healthcare) pads were placed on labeled spots on the agar using sterilized tweezers. Antibiotics were dissolved in ultra-pure water (ampicillin, kanamycin, polymyxin and neomycin) or 96% ethanol (chloramphenicol, tetracycline), diluted to various test concentrations and finally pipetted onto the paper pads (8 µL antibiotic solution on each pad). Subsequently, plates were incubated overnight at 30 °C and antibiotic sensitivities were determined by evaluating the area of “no growth”.

2.3.4 Fermentations

In-depth characterization of microbial growth and fermentative EPS production was conducted at 30 °C in a 30-L BIOSTAT®Cplus bioreactor, equipped with three propeller stirrers attached to one agitator shaft. A 20 L MM1 P100 medium containing 36 g·L⁻¹ glucose as carbon and 5 g·L⁻¹ peptone as nitrogen sources was used. The main culture was inoculated with an overnight seed culture (1 L MM1 P100 in a 5-L baffled shake-flask) at 5% of the final fermentation volume. Culture pH was kept constant at 6.8 with 42% H₃PO₄ and 8.4 M NaOH. The dissolved oxygen content was regulated via a cascade of stirrer speed and gas flow. Oxygen saturation was determined at maximal stirring (400 rpm) and gas flow (1.5 vvm) before inoculation. During the fermentation, 30% of the previously defined O₂ saturation value was initially maintained by increasing stirrer speed and by enhancing gas flow. CO₂ and O₂ concentrations in the exhaust gas were monitored using BCP-CO₂ and BCP-O₂ sensors, respectively. A further 10 g·L⁻¹ glucose was fed between hour 10 and 13 by adding a 360 g·L⁻¹ glucose solution at a rate of 3 mL·min⁻¹. The process was stopped after 20 h. Samples were obtained every 3 h to determine broth viscosity, optical density (OD) at 600 nm, glucose concentration, protein content, EPS titer, and EPS molecular weight. For titer measurements, 30 g culture broth was treated according to EPS purification scheme described for shake-flask experiments.

2.3.5 EPS extraction

To extract EPS from shake-flask experiments, the culture broth was diluted 1:5 with distilled water to decrease viscosity and centrifuged for 30 min at 17,600·g and 20 °C to separate cells. Subsequently, EPS was precipitated by slowly pouring the supernatant into two volumes of 2-propanol while stirring at 200 rpm with an overhead stirrer. The filtered polysaccharide was dried at 40 °C overnight in a VDL 53 vacuum drying oven and ground for 30 s at 30 revolutions per second in a mixer mill MM400. The fermentation broth from a 30-L bioreactor cultivation was treated slightly different. The culture broth was diluted in a ratio of 1:1 with distilled water and purified in a SartoJet crossflow filtration system (Sartorius AG) using three 100 kDa cutoff membranes to remove low molecular weight impurities and salts. The processed sample volume was kept constant during the process by replacing permeate with further fermentation broth or water, depending on the retentate pumpability. This allowed the simultaneous purification and concentration of large sample volumes. Purification was followed by measuring the retentate conductivity and stopped at <300 µS·cm⁻¹. Subsequent to the crossflow purification step, the retentate was centrifuged (30 min at 17,600·g and 20 °C) and further processed as described above.

2.3.6 Chemically competent *E. coli* cells

A single colony from a rich plate (LB agar) was inoculated into 5 mL of rich broth (LB) and shaken overnight at 37 °C. Then, the overnight culture was sub-cultured 1:100 in LB + 20 mM magnesium sulfate and grown to an OD₆₀₀ = 0.4 – 0.6. Subsequently, the culture was split into two conical tubes (50 mL) and centrifuge 800·g for 10 min at 4 °C. From this point, all steps were kept on ice in chilled tubes. The pellet was resuspended in 0.4x initial volume of TFBI, incubated on ice for 5 min and then centrifuged 800·g for 10 min at 4 °C.

Again, the pellet was resuspended gently in 0.08x initial volume of TFBII, fractions were pooled and incubate on ice for 60 min before aliquoting for storage. 100 μ L aliquots were quick-frozen in liquid N₂ and stored at -80 °C.

2.3.7 Conjugation

Plasmids were transferred to *E. coli* S17-1 for conjugation events. Plasmid transfer from *E. coli* S17-1 to *P. polymyxa* DSM 365 was performed as follows. Overnight cultures of recipient and donor strains were sub-cultured 1:100 in non-selective or selective LB media, respectively, and grown until early exponential phase (four hours). Afterwards, 900 μ L of the recipient culture were heat shocked for 15 min at 42 °C and mixed with 300 μ L of the donor strain culture. Cells were harvested by centrifugation for 3 min at 8,000·g and the pellet was gently resuspended and dropped on non-selective LB agar. After overnight incubation at 30 °C, cells were scraped from the agar, resuspended in 500 μ L 0.9% NaCl and plated on LB agar containing neomycin and polymyxin for counter selection. *P. polymyxa* conjugants were obtained after 48 h incubation at 30 °C

2.4 Molecular biological methods

2.4.1 Agarose gel electrophoresis

DNA samples were electrophoretically separated on 1% (w/v) agarose gels prepared with a 0.5x TAE buffer that was stored as a 50x TAE buffer (2 M TRIS, 0.05 M EDTA and 57.1 mL acetic acid, filled up with ddH₂O to 1 L and pH 8.0). Samples were mixed with a loading dye (0.075 mM TRIS pH 7.6; 0.05 mM EDTA; 50% glycerin (v/v); 0.025% (w/v) bromophenol blue and 0.025% (w/v) xylencyanol) in the ratio 5:1 and applied to a prepared agarose gel. Electrophoresis was performed at 110 V for approx. 30 min. By the application of ready-to-use DNA size standards (2log DNA Ladder, New England Biolabs GmbH) as molecular weight marker DNA size was determined. After staining with ethidium bromide (0.01 mg·mL⁻¹) in 1x TAE-buffer for 15 min, the gels were decolorized for a minimum of 30 min and banding profiles were visualized under UV light and digitalized by a gel documentation system from INTAS.

2.4.2 Bacterial strain identification

To identify the phylogenetic affiliation of isolated strains, genomic DNA was isolated from a pure culture according to the protocol described in 2.4.3 and 16S rDNA was amplified and sequenced using primers 27fn (5'-AGAGTTTGATCMTGGCTCAG-3') and 1525r (5'-AAGGAGGTGWTCCARCC-3'). Sequence data was aligned using Clone Manager 9 Professional software, and phylogenetic neighbors were identified using the BLASTN program against the curated EzTaxon-e database (180).

2.4.3 Isolation of genomic DNA from bacterial strains

For the isolation of genomic DNA from bacterial strains, 6 mL of a densely grown overnight culture were harvested in a single 2 mL reaction tube by centrifuging three times for 3 min at 12,000·g at room temperature. The supernatant was disposed after each centrifuge run.

The cell pellet was resuspended in 300 μL of the resuspension solution of the GeneJET™ Plasmid Miniprep kit, supplemented with 5 $\text{mg}\cdot\text{mL}^{-1}$ lysozyme and subsequently incubated for 1 h at 37 °C in a water bath. Then, 6 μL RNase A/T1 Mix were added and the suspension was again incubated for 1 h at 37 °C. Afterwards, 3 μL Proteinase K solution were added, followed by another 1 h incubation at 37 °C. Thereafter, 50 μL 10% SDS solution were pipetted into the tube, mixed gently and incubated for 10 min at room temperature. Cell debris was then precipitated by the addition of 300 μL acetate buffer (3 M sodium acetate, pH=4.8). After centrifugation for 10 min at 21,100·g and 4 °C, the clear supernatant was transferred to a new 2 mL reaction tube. Subsequently, 1x volume of a phenol - chloroform/isoamylalcohol mixture (1:1) was added and the tube was gently inverted 50 times. Phases were separated via centrifugation for 5 min at 21,100·g at 4 °C and the upper phase was transferred to a new reaction tube. The extraction with phenol – chloroform/isoamylalcohol was performed twice. Thereafter, the clear upper phase was transferred to a new 2 mL reaction tube and 1 mL cooled (-20 °C) 96% ethanol were added for DNA precipitation. After inverting gently, the sample was centrifuged for 1 h at 21,100·g and 4 °C. The supernatant was removed, and the DNA was washed twice with ice-cold 70%. For this, 1 mL 70% ethanol was added to the DNA, the pellet was gently resuspended and then centrifuged for 15 min at 21,100·g and 4 °C. After the second washing step, the DNA was allowed to dry for at least 1 h at ambient temperature and finally re-dissolved in 50 μL ultrapure, sterilized water. Genomic DNA samples were stored at 4 °C.

2.4.4 Genome editing in *P. polymyxa*

After spacer selection using Benchling, 24 bp oligos for guide annealing were designed phosphorylated and annealed:

- 1 μL fwd [100 μM]
- 1 μL rev [100 μM]
- 1 μL polynucleotide kinase
- 1 μL T4 ligase buffer
- 6 μL H_2O

The mix was incubated at 37 °C for 30 min, then heated up to 95 °C for 5 min. Thereafter, it was cooled down to 25 °C by decreasing the temperature by 0.5 °C every 6 seconds. After annealing, the mix was diluted 1:100 and 1 μL of this dilution was utilized for guide insertion via Golden Gate assembly:

- 0.75 μL BbsI
- 0.25 μL T7 ligase
- 1 μL 10x CutSmart Buffer
- 1 μL ATP (10 mM stock)
- 1 μL DTT (10 mM stock)
- 1 μL 100 $\text{ng}\cdot\mu\text{L}^{-1}$ backbone (circular destination vector)
- 1 μL annealed guide (100x diluted from above reaction)
- 4 μL H_2O

For assembly, the mixture was subjected to 20 cycles of heating to 37 °C for 5 min and afterwards incubating at 20 °C for 5 min. After heat inactivation for 20 min at 80 °C, the sample was cooled down to 12 °C. To reduce background by linearized (but not assembled) vector, linear DNA fragments were digested after Golden Gate annealing with help of Plasmid-Safe ATP-Dependent DNase, by adding:

1.5 µL Plasmid-Safe enzyme
 1.5 µL 10x Plasmid-Safe buffer
 1.5 µL ATP (10 mM stock)
 0.5 µL H₂O

After adding all reagents, the mixture was incubated for 30 min at 37 °C and finally inactivated at 70 °C for 30 min. After cooling, the whole mixture was used for transformation of chemically competent *E. coli* DH5α cells. Obtained clones were screened with colony PCR, and positive representatives were verified by sequencing. Subsequent to guide cloning, homologous regions were constructed by overlap extension PCR and inserted by restriction and ligation into the SpeI site. Specifically, approximately 1 kb flanks upstream and downstream of the target gene were amplified, purified by gel extraction and afterwards fused via the following overlap extension PCR protocol:

Step A:	
25 µL Accuzyme 2x mastermix (Bioline)	95 °C – 5 min
X µL upstream flank (100 – 200 ng)	95 °C – 30 s
X µL downstream flank (100 – 200 ng)	55 °C – 20 s
X µL H ₂ O to 50 µL	72 °C – 4 min
	72 °C – 10 min

Step B:	
25 µL Accuzyme 2x mastermix (Bioline)	95 °C – 5 min
2.5 µL forward primer upstream region	95 °C – 30 s
2.5 µL reverse primer downstream region	57 °C – 20 s
3 µL template from step A	72 °C – 4 min
17 µL H ₂ O	72 °C – 10 min

After assembly, DNA bands of appropriate length were excised from agarose gel and cloned after XbaI or SpeI digest into SpeI-linearized vector. After transformation in DH5α cells, clones were screened for inserted fragment with colony PCR, thereafter sequenced and finally transferred to *E. coli* S17-1 for conjugation events.

2.4.5 pCasPP plasmid construction

For construction of the pCasPP plasmid, the Cas9 gene was amplified alongside with the BbsI flanked lacZ cassette from pCRISPRomyces-2, which was purchased from Addgene (plasmid # 61737). The neomycin resistance and the repU gene were amplified from pUBoriMCS, which is a pUB110 derivate (181), containing an BbsI inserted origin of replication as well as a multiple cloning site from pUC18. A BsaI site within repU was removed by introducing a silent mutation with the utilized primers. The sgsE promotor⁵⁰ was obtained as artificial gBlock. A cytosine was replaced by a guanine to delete an interfering BbsI site. All five fragments were assembled via Golden Gate using BsaI. The oriT was amplified from pCRISPRomyces-2 and cloned into a XbaI restriction site afterwards. Subsequently, the unique SpeI site was added by introducing the desired sequence mutations while PCR-amplifying the pCasPP plasmid in two pieces with corresponding primers. To inactivate Cas9, the same procedure was deployed, and the two active sites were mutated to D10A and H840A, yielding pdCasPP. All cloning and mutation steps were verified by sequencing (Eurofins, Ebersberg, Germany).

2.4.6 Bioinformatics

In order to identify genes involved in EPS biosynthesis, the *P. polymyxa* DSM 365 genome was uploaded to RAST for automated genome annotation (178). Obtained data was screened manually and putatively identified genes involved in EPS-biosynthesis were annotated in detail using NCBI blastx (182) and UniProt blast (183). Intracellular protein localizations were predicted using CELLO v.2.5 (184). Biosynthetic pathways involved in nucleotide sugar production were identified using KEGG (185). Twenty base pair long spacers for Cas9 mediated edits were selected based on on- and off-target scores determined with benchling (<http://www.benchling.com>) using NGG as PAM motif and the uploaded *P. polymyxa* DSM 365 genome as reference. *In silico* cloning and sequence alignments were performed with SnapGene software.

2.5 Analytical methods

2.5.1 Sugar monomer composition

Simultaneous high resolution detection of carbohydrates which can be derivatized with 1-phenyl-3-methyl-5-pyrazolone (PMP) was performed via HT-PMP (186). For this, 1 g·L⁻¹ solutions of EPS were hydrolyzed in 2 M trifluoroacetic acid (TFA) for 90 min at 121 °C and subsequently neutralized with 3.2% (v/v) ammonium hydroxide. Thereafter, 25 µL neutralized sample were mixed with 75 µL derivatization reagent (0.1 M methanolic-PMP-solution: 0.4% ammonium hydroxide solution 2:1) and incubated for 100 min at 70 °C. Finally, 130 µL of 19.23 mM acetic acid were added to 20 µL cooled sample and HPLC separation was performed on a reverse phase column (Gravity C18) tempered to 50 °C. For gradient elution, mobile phase A (5 mM ammonium acetate buffer (pH 5.6) with 15% acetonitrile) and mobile phase B (pure acetonitrile) were pumped at a flow rate of 0.6 mL·min⁻¹. The HPLC system (Ultimate 3000RS, Dionex) was composed of a degasser (SRD 3400), a pump module (HPG 3400RS) auto sampler (WPS 3000TRS), a column compartment (TCC3000RS), a diode array detector (DAD 3000RS) and an ESI-ion-trap unit (HCT, Bruker).

Standards for each sugar (2, 3, 4, 5, 10, 20, 30, 40, 50 and 200 mg·L⁻¹) were processed as the samples, starting with the derivatization step. Data was collected and analyzed with BrukerHystar, QuantAnalysis and Dionex Chromelion software.

Ketose sugars were quantified using ion exclusion chromatography (IEC), wherein the HPLC system was coupled with a refractive index detector (RI 101, Shodex, Tokyo, Japan) and equipped with an Aminex ion exclusion column (HPX-87P; 300 × 7.8 mm, Biorad). The column temperature was set to 70 °C, and water was used for isocratic elution at a flow rate of 0.5 mL·min⁻¹. EPS (30 mg) was hydrolyzed in 10 mL 2.5% sulfuric acid for 1 h at 121 °C. After neutralization with barium carbonate, samples were filtered through 0.2 µm PVDF filters (Chromafil Xtra, Macherey-Nagel) and analyzed.

2.5.2 Molecular weight determinations

Gel permeation chromatography was performed using an Agilent 1260 Infinity system (Agilent Technologies, Waldbronn, Germany) equipped with a refractive index detector and a SECurity SLD7000 7-angle static light-scattering detector (PSS Polymer Standards Service GmbH, Mainz, Germany). Samples were analyzed using a Suprema guard column, one Suprema 100 Å (8 × 300 mm) and two Suprema 10,000 Å (8 × 300 mm) columns (PSS Polymer Standards Service). The eluent, 0.1 M LiNO₃, was pumped at a flow rate of 1 mL·min⁻¹ and the column compartment was kept at 50 °C. Samples were injected in 60 min intervals. Qualitative molecular weight results were obtained by comparing sample elution profiles with a 12-point pullulan standard curve.

2.5.3 Fourier transform infrared spectroscopy

For Fourier transform infrared (FTIR) analysis, 3 mg EPS was mixed with 100 mg potassium bromide and pressed at 7 t for 2 min (ATLAS Manual Hydraulic Press, Specac inc.). Pellets were inserted into a Nicolet 380 spectrometer (Thermo Scientific), and data were recorded at room temperature from 4000 to 500 cm⁻¹ by accumulating 32 scans with a resolution of 4 cm⁻¹.

2.5.4 Pyruvate assay

To determine the pyruvate content of the polymers, 1 g·L⁻¹ EPS solutions were hydrolyzed and neutralized as described for the sugar monomer analyses (187). To start the reaction, 10 µL neutralized sample + 90 µL of ddH₂O or standard were mixed with 100 µL assay mixture (50 µM N-(carboxymethylamino-carbonyl)-4,4'-bis(dimethylamino)-diphenylamine sodium salt (DA-64), 50 µM thiamine pyrophosphate, 100 µM MgCl₂·6H₂O, 0.05 U·mL⁻¹ pyruvate oxidase, 0.2 U·mL⁻¹ horseradish peroxidase, 20 mM KH₂PO₄ buffer pH 6) and incubated at 37 °C, 700 rpm for 30 min in a micro-plate shaker. The extinction was measured at 727 nm and subtracted with values measured at 540 nm to eliminate background signals. Nine standards in the range from 0.5 - 100 µM pyruvate were used for calibration.

2.5.5 Glucose assay

To determine the glucose content, 50 µL of sample or standard solution were placed in a 96-well plate. Reaction was started by adding 50 µL of assay mixture (40 mM potassium phosphate buffer (pH 6.0), 1.5 mM ABTS, 0.4 U glucose oxidase and 0.02 U horseradish peroxidase).

The plate was sealed with a 96-well silicon cap mat. After incubation on a microplate shaker at 400 rpm for 30 min at 30 °C the resulting extinction was measured at 418 nm. The absorption at 480 nm was subtracted to eliminate background signals in the UV. The calibration curve was compiled with eight points in the range of 2.5 to 500 μM ($n = 3$) of glucose.

2.5.6 Total sugar analysis

The phenol-sulfuric acid method (188) was used to determine the total sugar content of purified EPS samples. Since aldoses and ketoses show significantly different responses, standard calibrations were performed with glucose and fructose, at concentrations 0.05–2.5 $\text{g}\cdot\text{L}^{-1}$ sugars. To perform the analysis, 20 μL standard or dissolved polymer (3 $\text{g}\cdot\text{L}^{-1}$ in water) was placed into a 96-well plate, mixed with 180 μL phenol sulfuric acid (33 μL of 5% phenol (v/v) in water, 147 μL concentrated sulfuric acid), shaken for 5 min at 900 rpm in a microtiter plate shaker and incubated for 35 min at 80 °C. After cooling to room temperature, the absorbance at 480 nm was measured and the sugar content was calculated in either glucose or fructose equivalents.

2.5.7 Protein content

A modified Bradford assay (189) based on Coomassie Brilliant Blue-G250 was used to measure the protein concentration of fermentation broths and purified EPS samples. Standard calibration was performed with 20–100 $\mu\text{g}\cdot\text{mL}^{-1}$ bovine serum albumin. To analyze purified EPS, the polymer was dissolved overnight in water at a concentration of 3 $\text{g}\cdot\text{L}^{-1}$. Fermentation broth was immediately used after 1:3–1:6 dilution. For the analysis, 50 μL standard or sample ($n = 3$) was mixed with 200 μL 1x Roti®-Quant (CarlRoth) in each well of a 96-well plate. The absorbance at 595 nm was measured after 15 min incubation at room temperature.

2.6 Rheometry

Measurements were performed with an air-bearing MCR300 stress-controlled rheometer (Anton Paar Germany GmbH) with a cone plate geometry (50-mm diameter, 1° cone angle, 0.05-mm gap) at a constant, Peltier-controlled temperature of 20 °C. Data were collected and analyzed using Rheoplus V.3.61 software (Anton Paar). Samples were equilibrated at 20 ± 0.1 °C for 5 min before measurements were taken. All measurements were carried out in triplicate.

2.6.1 Sample preparation

For the determination of dynamic viscosities of aqueous EPS solutions during initial strain selection, polymers were dissolved at 1 wt% in ultra-pure water with stirring at 250 rpm overnight. For in-depth rheology, concentration series (wt%) of Paenan were prepared in aqueous solution by dissolving corresponding amounts of polymer in ultra-pure water (PURELAB classic system, ELGA LabWater) at 50 °C with stirring at 250 rpm overnight. To ensure the comparability of native Paenan solutions to subsequently prepared surfactant systems, the pH was set to 5.5 with a low concentration of HCl or NaOH, and the salt load of the samples was adjusted to a final concentration of 0.5% NaCl by adding concentrated NaCl solution. After pH adjustment and salt addition, Paenan solutions were stirred another 2 hours at 250 rpm and 50 °C. Samples then were allowed to rest for 24 h at room temperature (20 °C).

and analyzed. Xanthan solutions were prepared likewise, yielding properly dissolved solutions for both, Paenan and Xanthan.

The preparation of Gellan solutions resulted in broken gel systems, due to the destruction of the rigid, self-supporting Gellan gels upon continuous stirring. Since characteristics of broken gel systems largely depend on the preparation procedure, further details on this are explained in the following. For preparation of 0.6 wt% Gellan solutions, 300 mg Gellan were added to 50 g ultra-pure water in a 250-mL glass bulb, sealed with a plug and stirred for 15 hours at 250 rpm and 50 °C on a magnetic stirring plate using a triangular magnetic stirrer (40 x 14 mm) in a heating oven. Subsequently, the salt load was adjusted to a final concentration of 0.5% NaCl by adding 1 mL 25% NaCl. Excess-water was allowed to evaporate under stirring. Finally, the bulb was sealed again, and the sample was stirred another 2 hours at described conditions (250 rpm, 50 °C). Samples then were transferred to 50 mL conical tubes, allowed to rest for 24 h at room temperature (20 °C) and analyzed. Preparation of double-concentrated Gellan dispersions for Gellan/surfactant systems was performed likewise by using 600 mg Gellan.

EPS/surfactant mixtures were prepared at a final surfactant concentration of 5% active matter (AM), with one defined concentration for each EPS. Sodium lauryl ether sulfate (Texapon NSO) and lauryl glucoside (Plantacare 1200 UP) were purchased from BASF (Ludwigshafen). Cocamidopropyl betaine (TEGO Betaine F 50) and cetrimonium chloride (VARISOFT 300) were provided by Evonik Industries (Essen). Surfactant stock solutions at double the final concentration were prepared in ultra-pure water and adjusted to a pH of 5.5 with HCl or NaOH. EPSs were also dissolved in ultra-pure water alone at double the final concentrations (wt%) at 250 rpm, 50 °C overnight. Subsequently, surfactant stock solutions and EPS stock solutions were mixed at a ratio of 1:1 to obtain 5% AM surfactant and the desired EPS concentration. The pH of these mixtures was readjusted to 5.5 if necessary, stirred another 24 hours at 250 rpm, 50 °C, allowed to rest for 24 hours, and finally analyzed.

2.6.2 Dynamic viscosity

Dynamic viscosities were determined to assess the very basic rheological character of EPSs obtained during initial strain selection. For this, sample viscosities were measured for 10 min at a constant shear-rate of $\dot{\gamma} = 1 \text{ s}^{-1}$ with a measurement time of 3 s for each point. The mean of the last 10 measurement points was defined as the dynamic viscosity.

2.6.3 Viscosity curves

Viscosity curves were obtained during a logarithmic shear-rate ramp ($\dot{\gamma}$, 0.1–1000 s^{-1}) by measuring at 25 points with a gradually decreasing measurement time from 100–5 s.

2.6.4 Amplitude sweeps

The linear viscoelastic regimes, structural features, and yield stress values were determined using a shear stress amplitude sweep (logarithmic ramp from 0.1–1000 Pa) at a constant frequency of $f = 1 \text{ Hz}$ by measuring 20 points per decade. Yield stress values were determined as the stress value at which the elastic modulus decreased by $\geq 2\%$ as compared to previous measuring point.

2.6.5 Frequency sweeps

The time-dependent deformation behavior was tested at frequencies from 0.01 to 100 Hz at a constant strain within the linear viscoelastic region (usually 1 Pa). Samples were sealed with a thin film of low viscosity paraffin oil to avoid water evaporation during long measurements. Gel strengths were determined as G' values at the lowest measured frequency.

2.6.6 Thixotropy

Structure degradation at high shear and subsequent recovery was investigated using a three-segmented oscillation measurement by recording the elastic (G') and viscous (G'') modules.

A constant strain in the linear viscoelastic range at a frequency of 1 Hz was applied in segments one (reference) and three (recovery). High-shear conditions were simulated at a strain of 100 Pa for 60 seconds during segment two. The degree of recovery was determined by comparing G' values after defined time intervals in the recovery phase to the G' reference value before structure destruction.

3 Results

3.1 Selection of an EPS production strain

According to the Bacterial Carbohydrate Structure Data Base (190), approximately 400 different EPSs variants have been published up to now. Considering that < 1% of bacteria are culturable (191), most bacterial EPSs have probably not even been discovered yet. The fact that the majority of microbes are equipped with the genetic basis for EPS biosynthesis, but only use them under specific conditions, further emphasizes the huge potential in yet unexplored polymers.

To identify a potential EPS production strain for the present study, a recently published high throughput assisted screening platform was utilized as a first tool, to pre-select four promising bacterial EPS producers out of a collection of 192 EPS secreting strains. The method, developed by Rühmann *et al.*, allows for screening in 96-well format and covers visual observation of broth viscosity and EPS precipitation, as well as a screening of the carbohydrate fingerprint of the EPSs produced (192). Main selection criteria were versatile monomer compositions of produced EPSs, high glucose turnover rates during cultivation, and viscosities of the culture broth (data not shown). Based on the results of the pre-screening, four promising strains were selected and characterized in detail to evaluate the extent to which they meet the demanding requirements of the present study. Figure 3.1 summarizes the results of the in-depth strain characterization for the four candidates selected after pre-screening.

	EPS1.F2	EPS1.E6	EPS2.A7	EPS2.H2	
EPS formation [g EPS/kg broth]	0.76	6.75	1.06	3.41	
Slime free growth					
Antibiogramm [selectable with]	tet, kan	amp, kan	neo, kan	neo, kan	
Transformability					
Phylogeny	<i>Rhodobacter</i> sp.	<i>Mixed culture</i>	<i>Rhizobium</i> sp.	<i>Paenibacillus</i> sp.	
Viscosity [1s ⁻¹ , 1% in H ₂ O]	6.6 Pa·s	4.0 Pa·s	25.0 Pa·s	28.1 Pa·s	
Carbon source acceptance		Glc, Suc, Ara, Xyl, Glyc		Glc, Suc, Ara, Xyl, Glyc	




 positive
 no data
 failed

Figure 3.1. Basis for the strain selection. Relevant characteristics of the four strains selected after a pre-screening are given. EPS formation was determined in culture flasks using MM1 P100 media. Each strain exhibited a susceptibility against one or more antibiotics (tet, tetracyclin; kan, kanamycin; amp, ampicillin; neo, neomycin). The phylogenic affiliation is based on 16S rDNA sequencing. Carbon source acceptance was only tested for strains EPS1.E6 and EPS2.H2 (Glc, glucose; Suc, sucrose; Ara, arabinose; Glyc, glycerin).

Phylogenetic affiliations of the four selected strains were determined by 16S rDNA sequencing. EPS1.F2 was found to be a *Rhodobacter* sp. strain, EPS2.A7 a *Rhizobium* sp. strain and EPS2.H2 a *Paenibacillus* sp. strain. Initially, the closest relative to EPS1.E6 was found to be *Sphingomonas wittichii*. However, the follow up experiments revealed that EPS1.E6 was a mixed culture, comprising of *Micrococcus luteus* and another *Paenibacillus* sp. strain.

Since a main driver for the production costs of biopolymers is the yield of polymer as compared to the amount of the carbon source required (35), EPS titers were determined for each strain. EPS formation under standardized conditions was investigated by cultivating the corresponding bacterial strains in culture flasks using MM1 P100 media. Obtained EPS titers ranged from 0.76 g per kg broth for *Rhodobacter* sp. (EPS1.F2) up to 6.75 g EPS for the mixed culture EPS1.E6.

Furthermore, growth conditions preventing EPS formation were required to run molecular biological experiments, because polysaccharides strongly interfere with purification of e.g. genomic DNA (193). Cultivation conditions resulting in growth without EPS formation were implemented for all candidates, except for *Rhodobacter* sp.. Regardless of tested media composition or cultivation condition, polymer secretion by EPS1.F2 could not be stopped, which severely impaired molecular biological work.

Additionally, the susceptibility to at least one antibiotic allowing for selection and the accessibility to transformation with foreign DNA were fundamental strain properties for the scope of this work. Suitable antibiotics for bacterial selection were identified for all strains, however, a reliable and robust protocol for transformation with foreign DNA could only be implemented for *Paenibacillus* sp. (EPS2.H2). Concerning the rheological properties of the polymer, a high initial viscosity was preferred. Dynamic viscosities of purified polymers were determined at a shear rate of 1 s^{-1} after dissolution of EPSs in ultra-pure water at a final concentration of 1 wt%. The polysaccharide secreted by *Paenibacillus* sp. (EPS2.H2) exhibited the highest viscosity with 28.1 Pa·s.

Since no EPSs from *Paenibacilli* were commercialized until now and the strain met all pre-defined requirements, work on the other candidates was stopped and *Paenibacillus* sp. 2H2 was selected as production strain for this dissertation.

The following chapters describe the characterization of the fermentative EPS production by *Paenibacillus* sp. 2H2, investigations on structural and rheological features of the secreted polysaccharide Paenan, and the development of a CRISPR-Cas9 based genome editing tool in *P. polymyxa*.

3.2 Controlled production of polysaccharides – exploiting nutrient supply for levan and heteropolysaccharide production in *Paenibacillus* sp.

In this research article the high throughput assisted identification and in-depth characterization of a novel EPS producing bacterium is described. At first, a UHPLC-UV-ESI-MS assisted screening procedure was employed to identify a promising EPS producing bacterium based on growth characteristics and carbohydrate fingerprint of isolated polymer. The sugar profile of produced EPS, comprising mannose, glucose, galactose, and glucuronic acid, as well as a high conversion rate of glucose towards the biopolymer were decisive for the selection. A phylogenetic assignment based on 16S rDNA was performed, revealing that the organism belongs to the *Paenibacillaceae* genus with highest sequence similarities to *P. peoriae*, *P. jamilae* and *P. polymyxa*.

A detailed description of EPS biosynthesis in 30 L scale showed that polymer production by this strain primarily occurs during the stationary growth phase. After 17 h, the highest EPS titer of 4.54 g·L⁻¹ was reached, which corresponds to a volumetric productivity of 0.27 g·L⁻¹·h⁻¹. After 20 h fermentation, still 10 g·L⁻¹ glucose were available in the media, indicating that stagnation of EPS secretion was most likely induced by reduced mass and gas transfer rates due to the high broth viscosity of 20 Pa·s at $\dot{\gamma} = 1$. Furthermore, carbon and nitrogen were found to play a crucial role in the regulatory machinery of EPS biosynthesis. Quantitative sugar monomer analyses in combination with molecular weight determinations revealed that the choice of C and N source could be harnessed for the production of pure levan, pure heteropolysaccharide or mixtures of both. The identification and complete characterization of both EPSs required the combination of two independent UHPLC analyses, detecting different sugar profiles. These results highlight the importance of sophisticated analytical characterization of complex EPSs and help to interpret partially ambiguous reports on EPS synthesis (titers and structure) by various *Paenibacillus* species.

Finally, the rheological characterization of produced EPS showed impressive thickening properties of the isolated heteropolysaccharide rendering it interesting for application in commodity materials.

The author designed and conducted all experiments presented in this study together with Jochen Schmid. Technical support for the analytical characterization of EPSs was provided by Broder Rühmann. Volker Sieber and Martin Schilling provided scientific advice in several issues and all authors contributed to content and language of the manuscript.

Controlled production of polysaccharides – exploiting nutrient supply for levan and heteropolysaccharide production in *Paenibacillus* sp.

Marius Rütering, Jochen Schmid, Broder Rühmann, Martin Schilling and Volker Sieber

Carbohydrate Polymers
(2016)

DOI: 10.1016/j.carbpol.2016.04.074



Contents lists available at ScienceDirect

Carbohydrate Polymers

journal homepage: www.elsevier.com/locate/carbpol

Controlled production of polysaccharides—exploiting nutrient supply for levan and heteropolysaccharide formation in *Paenibacillus* sp.

Marius Rütering^a, Jochen Schmid^a, Broder Rühmann^a, Martin Schilling^b, Volker Sieber^{a,*}^a Chair of Chemistry of Biogenic Resources, Technical University of Munich, Schulgasse 16, 94315 Straubing, Germany^b Evonik Nutrition and Care GmbH, Goldschmidtstraße 100, 45127 Essen, Germany

ARTICLE INFO

Article history:

Received 19 January 2016

Received in revised form 15 April 2016

Accepted 16 April 2016

Available online 19 April 2016

Keywords:

Exopolysaccharide

Paenibacillus

Rheology

Levan

Carbon source

Nitrogen source

ABSTRACT

Bacterial exopolysaccharides (EPSs) are promising sustainable alternatives to synthetic polymers. Here we describe the production and characterization of different EPSs produced by the recently isolated *Paenibacillus* sp. 2H2. A final EPS titer of 4.54 g L⁻¹ was recovered after a 17-h fermentation, corresponding to a volumetric productivity of 0.27 g L⁻¹ h⁻¹. Remarkably, supplying the fermentation with specific carbon and nitrogen sources could be exploited for the production of different polymers. A pure heteropolysaccharide composed of glucose, mannose, galactose, and glucuronic acid (3.5:2:1:0.1) was obtained when using glucose/glycerol and peptone as substrates. A pure levan-type polymer or mixture of both polymers was observed with sucrose and NaNO₃ or peptone. To our knowledge, this is the first report that nutrients, particularly nitrogen sources, can be used to fine-tune EPS production in *Paenibacillaceae*. Rheological characterization of the heteropolysaccharide revealed impressive thickening properties, suggesting its potential application in commodity materials.

© 2016 Elsevier Ltd. All rights reserved.

1. Introduction

Polysaccharides are a very versatile class of natural, non-toxic, and biodegradable polymers, produced by every domain of life, and occur in a huge number of variations. In the natural environment, their versatility is reflected by the numerous tasks they fulfill. Polysaccharides serve, as structural elements, nutrient reservoirs, protection against external stressors, and virulence factors (Sutherland, 1998). This physicochemical variability is imparted by variations in molecular weight, sugar monomer composition, and side chains. Industry discovered the unique properties of polysaccharides years ago. Several products have already been brought to market for food, feed, or cosmetic applications; enhanced oil recovery; and drug delivery (Freitas, Alves, & Reis, 2014; García-Ochoa, Santos, Casas, & Gómez, 2000; Raveendran, Poulse, Yoshida, Maekawa, & Kumar, 2013; Suresh Kumar, Mody, & Jha, 2007). Polysaccharides are also used as rheological additives, stabilizers, emulsifiers and flocculants (Schmid, Sperl, & Sieber, 2014). Prominent examples of useful polysaccharides include plant- or algae-derived galactomannans and carrageenans; fungal schizo-

phyllan, scleroglucan, and pullulan; and bacterial xanthan and levan, as well as the class of sphingans. However, synthetic, petrochemical-based polymers still outperform natural polymers in terms of functionality and profitability in many applications (Rehm, 2010). Global megatrends, such as resource efficiency and corporate social responsibility, put pressure on the market and drive the search for novel natural polysaccharides to replace undesired petrochemical substances, like polyacrylates, polyvinyl polymers, and polyacrylamides, especially in consumer-oriented commodities.

Bacterial polysaccharides represent the most promising resource for natural alternatives to synthetic polymers. Over 400 bacterial polysaccharides have been structurally characterized (Rühmann et al., 2015b; Toukach, Joshi, Ranzinger, Knirel, & von der Lieth, 2007); more reports on other prokaryotic polysaccharides can be found in the literature. Considering that up to <1% of bacteria are culturable (Stewart, 2012), many bacterial polysaccharides have not yet been identified. Furthermore, bacterial polysaccharides can be produced independently of season and location. Exopolysaccharides (EPSs) are secreted into the extracellular space, facilitating downstream processing and reducing production costs. Recent advances in genome editing tools have significantly simplified bacterial genome targeted alteration, bringing tailored EPSs within researchers' grasps (Jiang, Bikard, Cox, Zhang, & Marraffini, 2013; Peters et al., 2015). Novel screening methodologies have been developed that enable high-throughput analyses of hundreds

* Corresponding author.

E-mail addresses: m.ruetering@tum.de (M. Rütering), j.schmid@tum.de (J. Schmid), broder.ruehmann@tum.de (B. Rühmann), martin.schilling@evonik.com (M. Schilling), sieber@tum.de (V. Sieber).

of strains per day and facilitate new, interesting EPS identification (Rühmann et al., 2015a).

The *Paenibacillus* genus provides one example of the intense research on new microbial EPSs. Several recent studies have identified novel EPSs produced by *Paenibacillus* isolates. A review article summarized the state of the art with respect to *Paenibacillus* EPSs (Liang & Wang, 2015). The habitats of this Gram-positive genus include soils, marine sediments, the rhizospheres of various crop plants, insect larvae, and forest trees (Raza, Yang, & Shen, 2008). Although 89 different *Paenibacillus* species are known so far, reports on EPS formation are limited to a very small number of strains, mainly those belonging to the plant growth-promoting species *Paenibacillus polymyxa* or phylogenetically closely related representatives, wherein EPSs were shown to be important for biofilm formation and plant root colonization (Haggag, 2007; Timmusk, Grantcharova, & Wagner, 2005). Structural differences among characterized *Paenibacillus* EPSs, however, are anything but small. Descriptions range from fructose-containing levan-type polysaccharides (Han & Clarke, 1990; Liu et al., 2009) to beta-glucans (Jung et al., 2007; Rafigh, Yazdi, Vossoughi, Safekordi, & Ardjmand, 2014) to complex heteropolysaccharides comprising different sugars and substituents, including glucose, galactose, mannose, rhamnose, xylose, sorbose, fucose, fructose, pyruvate, and uronic acids (Lee et al., 1997; Li et al., 2013; Madden, Dea, & Steer, 1986; Morillo, Guerra del Águila, Aguilera, Ramos-Cormenzana, & Monteoliva-Sánchez, 2007; Raza, Makeen, Wang, Xu, & Qirong, 2011; Tang et al., 2014; Yegorenkova, Tregubova, Matora, Burygin, & Ignatov, 2008). Some authors describe the existence of two/three polymer fractions of different molecular weights, charges, and monomer compositions. (Liu et al., 2009; Madden et al., 1986; Morillo et al., 2007; Tang et al., 2014).

Reasons for EPS versatility among strains may be found at the genomic level, in the EPS biosynthesis machinery, the demanding analytics of EPS characterization which potentially yield differing results, or the applied process parameters, such as the carbon and nitrogen sources used during fermentation. Polysaccharide formation is favored by high carbon to nitrogen ratios. Furthermore, levansucrases, which are frequently associated with *P. polymyxa*, catalyze a transfructosylation reaction when sucrose is present, resulting in microbial levan formation (Han & Clarke, 1990; Lee et al., 1997). Besides this, very little information is available on the impact of nutrient composition on EPS formation in *Paenibacillaceae*. Particularly, the influence of different nitrogen sources has not been described in detail, and variations in EPS structure, molecular weight, and product titer have been understood as strain specificities rather than the result of process parameters.

Here we describe the fermentative production of EPSs by a novel *Paenibacillus* sp. strain. The influence of different carbon and nitrogen sources on polymer biosynthesis and EPS composition is investigated, and two different analytical methods for the monomer analysis of purified EPSs are validated. Furthermore, rheological properties of isolated EPSs are described. The results suggest that the nitrogen source plays a key role in EPS regulation in *Paenibacillaceae* and emphasize the importance of sophisticated, in-depth analysis of purified EPSs for reliable product characterization.

2. Materials and methods

2.1. Chemicals and reagents

All chemicals were purchased in analytical or microbiological grade from Sigma-Aldrich, Carl Roth GmbH (Karlsruhe, Germany) or Merck KGaA (Darmstadt, Germany) unless otherwise stated.

Ultra-pure water was produced using a PURELAB classic system (ELGA LabWater) and used in all experiments.

2.2. Bacterial strain isolation and identification

Paenibacillus sp. 2H2 was identified as a promising EPS producer using a previously described screening technique, selecting for growth characteristics and carbohydrate fingerprint of the polysaccharide produced (Rühmann et al., 2015a). *Paenibacillus* sp. 2H2 was chosen due to its interesting carbohydrate profile and high broth viscosity.

To identify the phylogenetic affiliation of the strain, genomic DNA was isolated from a pure culture and 16S rDNA was amplified and sequenced using primers 27f (5'-AGAGTTTGATCMTGGCTCAG-3') and 1525r (5'-AAGGAGGTGWTCARCC-3'). Sequence data was aligned using Clone Manager 9 Professional software, and phylogenetic neighbors were identified using the BLASTN program against the curated EzTaxon-e database (Kim et al., 2012). Phylogenetic tree was constructed using MEGA version 6 software (Tamura, Stecher, Peterson, Filipski, & Kumar, 2013) applying the neighbor joining method.

2.3. Culture conditions and fed-batch fermentation

Flask cultures were prepared in baffled 500-mL shake flasks sealed with aluminum caps. The flasks contained 100 mL basal MM1 P100 medium carbon and nitrogen sources, 1.33 g L⁻¹ magnesium sulfate heptahydrate, 1.67 g L⁻¹ potassium dihydrogen phosphate, 0.05 g L⁻¹ calcium chloride dihydrate, 2 mL L⁻¹ RPMI 1640 vitamins solution (Sigma-Aldrich) and 1 mL L⁻¹ trace elements solution (2.5 g L⁻¹ iron(II) sulfate heptahydrate, 2.1 g L⁻¹ sodium tartrate dihydrate, 1.8 g L⁻¹ manganese(II) chloride tetrahydrate, 0.075 g L⁻¹ cobalt(II) chloride hexahydrate, 0.031 g L⁻¹ copper(II) sulfate heptahydrate, 0.258 g L⁻¹ boric acid, 0.023 g L⁻¹ sodium molybdate and 0.021 g L⁻¹ zinc chloride). The initial pH of the medium was adjusted to 7. Different carbon and nitrogen sources were tested (30 g L⁻¹ sucrose, glucose or glycerol; 0.05 mol L⁻¹ nitrogen from either peptone or NaNO₃). Cultures were inoculated with a single colony and incubated at 30 °C and 150 rpm for 48 h.

In-depth characterization of microbial growth and fermentative EPS production was conducted at 30 °C in a 30-L BIOSTAT® Cplus bioreactor (Sartorius AG, Göttingen, Germany), equipped with three propeller stirrers attached to one agitator shaft. A 20-L MM1 P100 medium containing 36 g L⁻¹ glucose as carbon and 5 g L⁻¹ peptone as nitrogen sources was used. The main culture was inoculated with an overnight seed culture (1 L MM1 P100 in a 5-L baffled shake-flask) at 5% of the final fermentation volume. Culture pH was kept constant at 6.8 with 42% H₃PO₄ and 8.4 M NaOH. The dissolved oxygen content was regulated via a cascade of stirrer speed and gas flow. Oxygen saturation was determined at maximal stirring (400 rpm) and gas flow (1.5 vvm) before inoculation. During the fermentation, 30% of the previously defined O₂ saturation value was initially maintained by increasing stirrer speed and by enhancing gas flow. CO₂ and O₂ concentrations in the exhaust gas were monitored using BCP-CO2 and BCP-O2 sensors, respectively (BlueSens gas sensor GmbH, Herten, Germany). A further 10 g L⁻¹ glucose was fed between hour 10 and 13 by adding a 360-g L⁻¹ glucose solution at a rate of 3 mL min⁻¹. The process was stopped after 20 h. Samples were obtained every 3 h to determine broth viscosity, optical density (OD) at 600 nm, glucose concentration, protein content, EPS titer, and EPS molecular weight. For titer measurements, 30-g culture broth was treated according to EPS purification scheme of the shake-flask experiments described below.

328

M. Rüttering et al. / Carbohydrate Polymers 148 (2016) 326–334

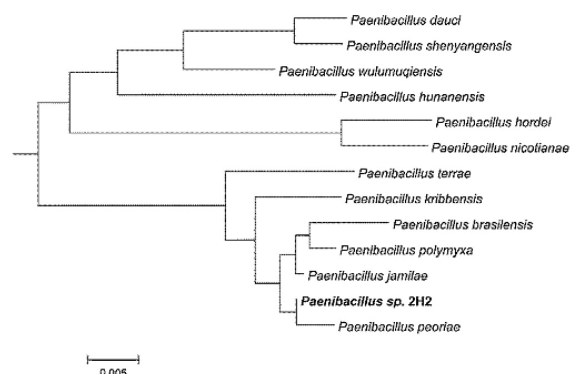


Fig. 1. Taxonomic characterization of the EPS-producing strain. Neighbor-joining tree based on 16S rDNA gene sequence showing the phylogenetic relationships of *Paenibacillus* sp. 2H2.

2.4. Error estimation

The coefficient of variation (CV) was used to estimate the error range of product titers from shake-flask experiments that were not repeated in triplicate. For this, fermentation in a particular fermentation set-up (100 mL MM1 P100 in 500-mL baffled shake flasks, using glucose as carbon and peptone as nitrogen source) was repeated five times. The arithmetic mean \bar{x} and standard deviation s of EPS titers were used to estimate the CV as follows (Häßler, Schieder, Pfaller, Faulstich, & Sieber, 2012):

$$CV = \frac{s}{\bar{x}} \times 100\% \quad (1)$$

2.5. EPS extraction

To extract EPS from shake-flask experiments, the culture broth was diluted 1:5 with distilled water to decrease viscosity and centrifuged for 30 min at 17,600g and 20 °C to separate cells. Subsequently, EPS was precipitated by slowly pouring the supernatant into two volumes of 2-propanol while stirring at 200 rpm with an overhead stirrer (Heidolph Instruments GmbH & Co. KG, Schwabach, Germany). The filtered polysaccharide was dried at 40 °C overnight in a VDL 53 vacuum drying oven (Binder, Tuttlin-

gen, Germany) and ground for 30 s at 30 revolutions per second in a mixer mill MM400 (Retsch, Haan, Germany).

The fermentation broth from a 30-L bioreactor cultivation was treated slightly different. The culture broth was diluted in a ratio of 1:1 and not 1:5 with distilled water and purified in a Sarto-Jet crossflow filtration system (Sartorius AG) using three 100 kDa cutoff membranes to remove low molecular weight impurities and salts. The processed sample volume was kept constant during the process by replacing the permeate with further fermentation broth or water, depending on the retentate pumpability. This allowed the simultaneous purification and concentration of large sample volumes. Purification was followed by measuring the retentate conductivity and stopped at $<300 \mu\text{S cm}^{-1}$. Subsequent to the crossflow purification step, the retentate was centrifuged (30 min at 17,600g and 20 °C) and further processed as described above. All analytical and rheological experiments comparing EPS produced on different C/N sources were conducted with EPS extracted from culture shake-flask cultivations via precipitation.

2.6. Glucose assay

The glucose concentration in the fermentation broth was determined as described previously (Rühmann et al., 2015a). All measurements were performed in triplicate.

2.7. Protein content

A modified Bradford assay (Bradford, 1976) based on Coomassie Brilliant Blue-G250 was used to measure the protein concentration of fermentation broths and purified EPS samples. Standard calibration was performed with 20–100 $\mu\text{g mL}^{-1}$ bovine serum albumin. To analyze purified EPS, the polymer was dissolved overnight in water at a concentration of 3 g L⁻¹. Fermentation broth was immediately used after 1:3–1:6 dilution. For the analysis, 50 μL standard or sample ($n=3$) was mixed with 200 μL 1 \times Roti®-Quant (Carl Roth) in each well of a 96-well plate. The absorbance at 595 nm was measured after 15 min incubation at room temperature.

2.8. Molecular weight determinations

Gel permeation chromatography was performed using an Agilent 1260 Infinity system (Agilent Technologies, Waldbronn,

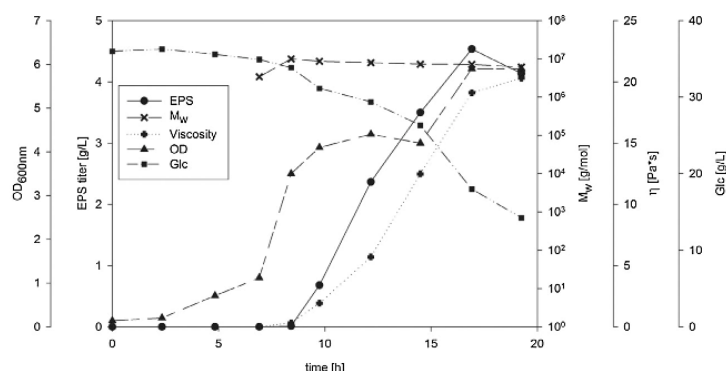


Fig. 2. Fermentative EPS production by *Paenibacillus* sp. 2H2.

To describe EPS production and growth characteristics, optical density (OD, ▲), broth viscosity (η , +), EPS titer (●), glucose concentration (Glc, ■), and EPS molecular weight (M_w , x) are plotted as a function of the process time. OD was measured at 600 nm; η was determined in triplicate at $\dot{\gamma} = 1$ directly after sampling; samples for M_w determinations were stored at -20°C until measurement; EPS titer was obtained by precipitating a 30 g aliquot of cell-free fermentation broth and weighing the vacuum-dried polymer.

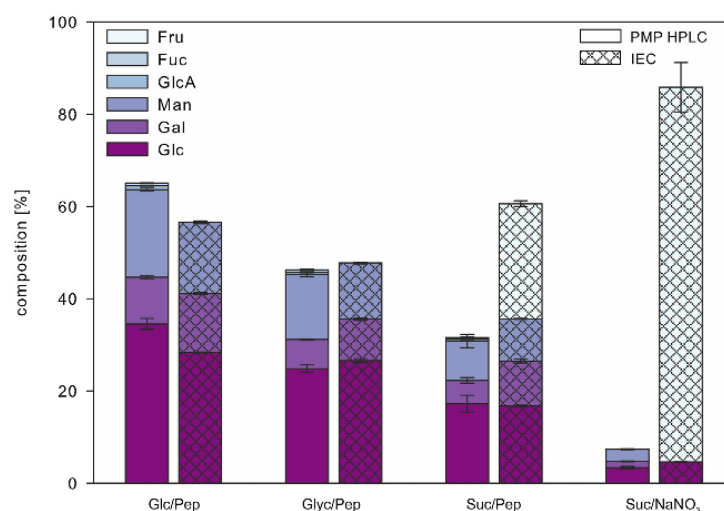


Fig. 3. Influence of nutrient supply on the monomer composition of EPSs.

Monomer compositions of EPSs produced on different carbon and nitrogen sources. Plain bars represent data obtained from UHPLC-UV-ESI-MS measurements. Patterned bars depict the results of ion exclusion chromatography (IEC) analysis. Glucose, Glc; galactose, Gal; mannose, Man; glucuronic acid, GlcA; fucose, Fuc; fructose, Fru; peptone, Pep; glycerol, Glyc; and sucrose, Suc.

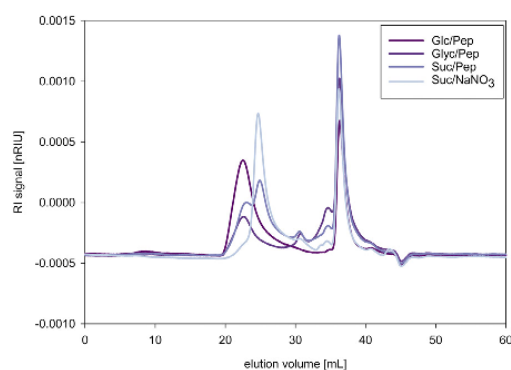


Fig. 4. Gel permeation chromatography elution profiles of *Paenibacillus* sp. 2H2 EPSs.

Polymer molecular weight distributions of EPSs were determined by comparison with pullulan standards. Weight average molecular weights (M_w) were $(1.3 \pm 0.2) \times 10^7 \text{ g mol}^{-1}$ for EPS produced on glucose and peptone (Glc/Pep), $(1.5 \pm 0.3) \times 10^7 \text{ g mol}^{-1}$ for those produced on glycerol and peptone (Glyc/Pep), $(1.5 \pm 0.3) \times 10^7 \text{ g mol}^{-1}$ and $(9.8 \pm 0.8) \times 10^5 \text{ g mol}^{-1}$ for the bimodal distribution of those produced on sucrose and peptone (Suc/Pep) and $(1.3 \pm 0.1) \times 10^6 \text{ g mol}^{-1}$ for sucrose and NaNO_3 .

Germany) equipped with a refractive index detector and a SECcurity SLD7000 7-angle static light-scattering detector (PSS Polymer Standards Service GmbH, Mainz, Germany). Samples from bacterial cultures were diluted to approximately 1 g L^{-1} EPS (according to values obtained from titer determinations). The diluted samples were incubated in a heating block at 900 rpm and 60°C for 1 h for homogenization and viscosity reduction. Thereafter, samples were centrifuged for 20 min at 21,100g and 20°C to pellet the cells. The supernatant was filtered through a $0.45 \mu\text{m}$ regenerated cellulose filter (VWR, Radnor, PA, USA), adjusted to 0.1 M LiNO_3 for water signal silencing and analyzed using a Suprema guard column, one Suprema 100 Å ($8 \times 300 \text{ mm}$) and two Suprema 10,000 Å ($8 \times 300 \text{ mm}$) columns (PSS Polymer Standards Service). The eluent 0.1 M LiNO_3 was pumped at a flow rate of 1 mL min^{-1} and samples ($100 \mu\text{L}$) were injected at 60-min intervals. Column temperature

was kept constant at 50°C . Purified polymers were dissolved in 0.1 M LiNO_3 at a concentration of $0.5\text{--}2 \text{ g L}^{-1}$ and analyzed using the same setup. Qualitative molecular weight results were obtained by comparing sample elution profiles with a 12-point pullulan standard curve.

2.9. Total sugar analysis

The phenol-sulfuric acid method (DuBois, Gilles, Hamilton, Rebers, & Smith, 1956) was used to determine the total sugar content of purified EPS samples. Since aldoses and ketoses show significantly different responses, standard calibrations were performed with glucose and fructose, at concentrations $0.05\text{--}2.5 \text{ g L}^{-1}$ sugars. To perform the analysis, $20\text{--}200 \mu\text{L}$ standard or dissolved polymer (3 g L^{-1} in water) was placed into a 96-well plate, mixed with $180 \mu\text{L}$ phenol-sulfuric acid ($33 \mu\text{L}$ of 5% phenol (v/v) in water, $147 \mu\text{L}$ concentrated sulfuric acid), shaken for 5 min at 900 rpm in a microtiter plate shaker and incubated for 35 min at 80°C . After cooling to room temperature, the absorbance at 480 nm was measured and the sugar content was calculated in either glucose or fructose equivalents.

2.10. Sugar monomer composition

To perform simultaneous high-resolution detection of carbohydrates that can be derivatized with 1-phenyl-3-methyl-5-pyrazolone (PMP) via HPLC-UV-ESI-MS, 1 g L^{-1} EPS was dissolved in water and subjected to hydrolysis, neutralization, and PMP derivatization as described before (Rühmann, Schmid, & Sieber, 2014).

Ketose sugars were quantified using ion exclusion chromatography (IEC), wherein the HPLC system was coupled with a refractive index detector (RI 101, Shodex, Tokyo, Japan) and equipped with an Aminex ion exclusion column (HPX-87P; $300 \times 7.8 \text{ mm}$, Biorad). The column temperature was set to 70°C , and water was used for isocratic elution at a flow rate of 0.5 mL min^{-1} . EPS (30 mg) was hydrolyzed in 10 mL 2.5% sulfuric acid for 1 h at 121°C . After neutralization with barium carbonate, samples were filtered through $0.2\text{--}0.45 \mu\text{m}$ PVDF filters (Chromafil Xtra, Macherey-Nagel) and analyzed.

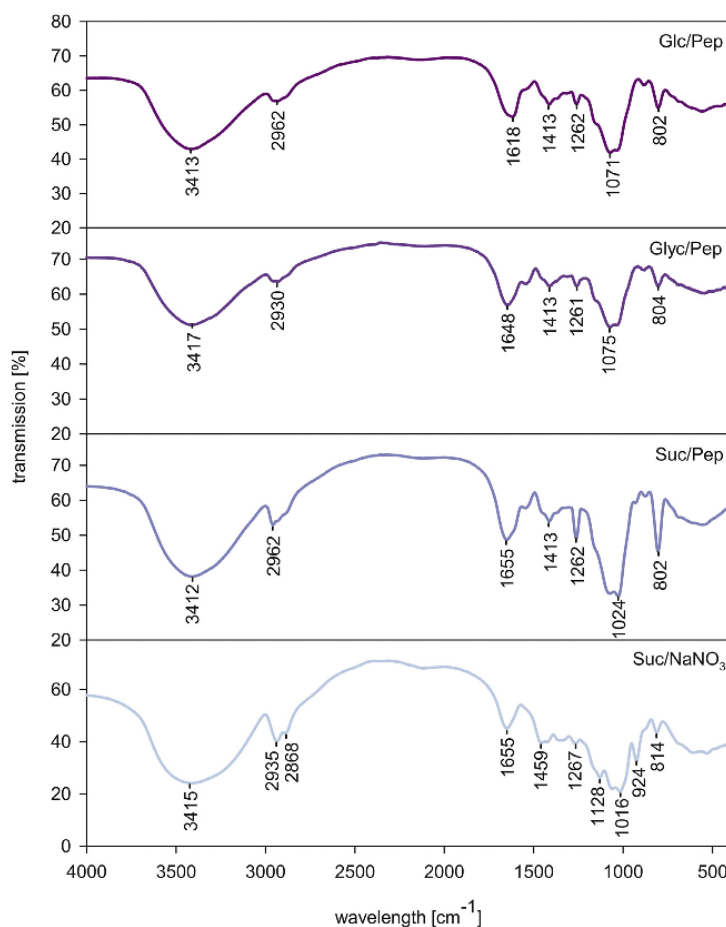


Fig. 5. FTIR spectra of *Paenibacillus* sp. 2H2 EPSs.

Spectra of EPSs produced using different carbon and nitrogen sources (glucose (Glc), glycerol (Glyc), sucrose (Suc), and peptone (Pep)) were recorded at room temperature over the range of 4000 to 500 cm⁻¹.

2.11. Fourier transform infrared spectroscopy

For Fourier transform infrared (FTIR) analysis, 3 mg EPS was mixed with 100 mg potassium bromide and pressed at 7 t for 2 min. Pellets were inserted into a Nicolet 380 spectrometer (Thermo Scientific), and data were recorded at room temperature from 4000 to 500 cm⁻¹ by accumulating 32 scans with a resolution of 4 cm⁻¹.

2.12. Rheological measurements

To determine the rheological properties of purified EPSs in aqueous solution, 0.5 wt% polymer solutions were prepared at 50 °C and 250 rpm overnight in a water bath. Subsequently, samples were allowed to rest a further 24 h at room temperature and analyzed. Measurements were performed with an air-bearing MCR300 controlled-stress rheometer (Anton Paar Germany GmbH) using a cone plate geometry (50 mm diameter, 1 ° cone angle, 0.05 mm gap) at a constant, Peltier-controlled temperature of 20 °C. Data were collected and analyzed with Rheoplus V.3.61 software (Anton Paar). Samples were equilibrated at 20 ± 0.1 °C for 5 min before measurements. Viscosity curves were obtained during a logarithmic shear-rate ramp ($\dot{\gamma}$ = 0.1–1000 s⁻¹) by recording the viscosity at 25 points with a gradually decreasing measurement time from 100

to 5 s. The linear viscoelastic regimes, structural features and yield points were determined with a shear stress amplitude sweep (logarithmic ramp from 0.1–1000 Pa) at a constant frequency of 1 Hz by recording measurements at 20 points per decade. All measurements were performed in triplicate.

3. Results and discussion

3.1. Strain selection and phylogenetic analysis

A high-throughput screening approach was used to identify EPS-producing strains from a collection of several hundred bacteria (Rühmann et al., 2015a). The strain described herein was chosen because of its outstanding characteristics identified during the screening procedure. Within 48 h of growth in a 96-well plate, the entire carbon source was depleted and high EPS production was detected via precipitation of the culture supernatant, indicating rapid carbohydrate metabolism and a high conversion rate of glucose towards the biopolymer. Additionally, the culture broth had very high viscosity. The carbohydrate fingerprint, obtained using a UHPLC-UV-ESI-MS assessment of the precipitated and PMP-derivatized polymer, indicated the presence of a heteropolysaccharide composed of glucose, mannose, galactose,

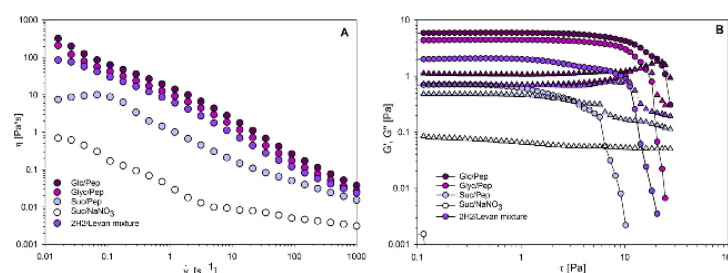


Fig. 6. Rheological properties of *Paenibacillus* sp. 2H2 EPSs.

All measurements were performed on a controlled-stress rheometer using a cone-plate geometry and a constant temperature of 20 °C. (A) Viscosity curves of 0.5 wt% EPS solutions in water. (B) Shear stress amplitude sweeps of 0.5 wt% EPS solutions at a frequency of 1 Hz. Storage moduli are illustrated by circles, loss moduli by triangles.

and uronic acids. To determine the phylogenetic affiliation of the strain, genomic DNA was isolated from a pure culture and the 16S rDNA was amplified and sequenced. Sequence data were compared with entries in the curated EzTaxon database (Kim et al., 2012), and a phylogenetic tree was constructed based on sequence similarity (Fig. 1). The strain was assigned to the *Paenibacillus* genus with highest pairwise sequence similarities to *Paenibacillus peoriae* DSM8320^T (99.77%), *Paenibacillus jamilae* CECT 5266^T (99.77%), and *P. polymyxa* ATCC 842^T (99.47%) (Aguilera et al., 2001; Ash, Priest, & Collins, 1993; Heyndrickx et al., 1996; Montefusco, Nakamura, & Labeda, 1993). Since unambiguous assignment on the species level was not possible based on 16S rDNA, the novel strain was named *Paenibacillus* sp. 2H2.

3.2. Fermentative EPS production

Microbial biopolymer production by *Paenibacillus* sp. 2H2 was characterized in a 30-L fed-batch process. As in the previous screening procedure, glucose was provided as the carbon source and casein peptone as the nitrogen source. The 30-L fermentation system was chosen to minimize effects of volume reduction due to sampling. However, it is worth mentioning that the process was comparable when performed on 2 L and 10 L scale (data not shown). Fermentation parameters related to EPS production are summarized in Fig. 2. Bacterial growth monitored based on OD measurement was characterized by a short, 2-h lag phase, followed by 10 h of exponential growth. The increase in OD after approximately 15 h during the stationary growth phase can be explained by EPS accumulation, which also causes turbidity. The end of the process was reached after <20 h, as evidenced by the plateaus of fermentation parameters that were being monitored. This is by far the fastest microbial EPS formation process reported for *Paenibacillaceae* in the scientific literature. Most processes are completed in a 48-h to 5-day time frame (Lee et al., 1997; Liang & Wang, 2015; Sukplang & Vela, 2000). The highest EPS titer during the fermentation (4.54 g L⁻¹) was reached after 17 h, which corresponds to a volumetric productivity of 0.27 g L⁻¹ h⁻¹ and a specific yield of 0.16 g EPS per g glucose. The observation that glucose consumption did not correlate with OD during exponential growth can be explained by the initial consumption of 5 g L⁻¹ peptone as the carbon source. The glucose decline at constant OD and EPS titer observed toward the process end was probably due to a shift toward alcoholic fermentation, indicated by CO₂ exhaust gas analytics and ethanol and butanediol detection in the culture broth via GC-MS (see Supplementary information Figs. S1 and S2). Since 10 g L⁻¹ glucose were still available in the medium after 20 h, the reason for stagnated EPS production is the high viscosity of the cultivation broth, rather than nutrient limitation. At approximately 20 Pa s ($\gamma = 1$) viscosity, mixing of the entire fermentation volume is significantly impeded, and molecule diffusion is substantially limited

(Seviour, McNeil, Fazenda, & Harvey, 2011). Therefore, the bacterial cells lack nutrients, and metabolism is slowed (Moraine & Rogovin, 1973). A comparison of titer, viscosity, and molecular weight measurements with OD values suggests that EPS biosynthesis starts in late exponential phase but primarily occurs during the stationary growth phase. Since EPSs can be considered secondary metabolites, this production profile is typical for this kind of production process (Degeest, Vaningelgem, & De Vuyst, 2001).

3.3. Nutrient impact on EPS production

To investigate the influence of different carbon and nitrogen sources on EPS production by *Paenibacillus* sp. 2H2, the strain was grown on several carbon and nitrogen sources, including the combinations glucose and peptone (Glc/Pep), glycerol and peptone (Glyc/Pep), sucrose and peptone (Suc/Pep), and sucrose and NaNO₃ (Suc/NaNO₃). Subsequent to fermentative production in 500-mL shake flasks, EPS was extracted and characterized in terms of monomer composition, molecular weight, and rheological behavior. Default EPS extraction was compared to crossflow purification in terms of EPS recovery in HPLC-MS measurements (Supplementary data Fig. 3). Crossflow treatment resulted in a 5% recovery increase, suggesting, that the procedure is superior to default extraction, especially for the standardized purification of large sample volumes. Monomer composition, however, did not change in dependency of the purification method and default extraction yielded EPS of decent purities, too. Hence, this procedure was considered appropriate for EPS recovery from culture flasks. EPS titers on sucrose were remarkably higher than titers on glycerol or glucose (Table 1). Up to 11.3 g L⁻¹ EPS could be recovered using Suc/NaNO₃, whereas less than half that amount was produced using Glc/Pep (5.2 g L⁻¹). This finding is consistent with those of other reports, where high EPS titers of *Paenibacillaceae* producing either levan-type polymers or heteropolysaccharides were described when sucrose was used as the carbon source. For levan-producing strains, titers of up to 36 g L⁻¹ have been described, and for heteropolysaccharide production on sucrose, even 54 g L⁻¹ could be achieved (Han & Clarke, 1990; Lee et al., 1997; Liu et al., 2010).

Interestingly, the lowest recoveries in HPLC-MS analyses were obtained for Suc/NaNO₃ (<8%), the sample with highest product titer, and highest recoveries were obtained for Glc/Pep (65%) (Fig. 3). However, total sugar content, determined using the phenol-sulfuric acid method, and protein contaminations were in the same range (Table 1). Since calibration with glucose rather overestimates the total sugar content of EPS due to varying responses of different sugars, an additional calibration with fructose was performed. A possible explanation for low analytical recoveries in LC analyses is that the HPLC-MS method used detects only carbohydrates with an aldehyde group, which is necessary for

Table 1

Data on titers, protein content, fructose (Fru) content, total sugar content and analytical recoveries in ion exclusion chromatography (IEC) and HPLC–MS (PMP) of EPS produced on different carbon/nitrogen combinations.

C/N	Titer	Protein	Fru content ^a	Total sugar [%]		HPLC recoveries [%]	
	[g L ⁻¹]	[%]		Fru calibration	Glc calibration	IEC	PMP
Glc/Pep	5.2 ± 0.5	2.4 ± 0.2	0	87.1 ± 2.0	110.0 ± 2.5	56.6 ± 0.5	65.1 ± 2.0
Glyc/Pep	6.7 ± 0.7	1.6 ± 0.0	0	67.8 ± 1.9	86.3 ± 2.3	47.8 ± 0.5	46.2 ± 1.5
Suc/Pep	8.9 ± 0.9	1.5 ± 0.3	41.2 ± 1.0	82.1 ± 1.5	103.8 ± 1.8	60.6 ± 0.7	31.6 ± 3.3
Suc/NaNO ₃	11.3 ± 1.1	1.0 ± 0.1	94.6 ± 6.2	87.6 ± 2.0	110.5 ± 2.4	85.9 ± 5.3	7.4 ± 0.7

^a Results from IEC.

derivatization with PMP. To identify ketoses, we performed an IEC analysis. As suspected, the missing sugar was found to be fructose, which accounted for a large proportion of EPS produced on sucrose (Fig. 3). The entire polymer produced on Suc/NaNO₃ was literally composed of fructose (95%), suggesting that this sample is a pure levan-type EPS. In contrast, the use of glycerol and glucose as carbon sources led to pure heteropolysaccharide biosynthesis, whereas that of Suc/Pep resulted in a mixture of both. GPC measurements of the different polysaccharides supported these results. A single polymer fraction was observed for the pure heteropolysaccharides (Glc/Pep, Glyc/Pep) and for pure levan-type polymer (Suc/NaNO₃), respectively. EPS containing both polymers (Suc/Pep) showed a bimodal distribution with two distinct peaks (Fig. 4). To our knowledge, this is the first report that culture medium composition can be harnessed to produce either pure levan or pure heteropolysaccharide with the same *Paenibacillus* strain. Furthermore, it was shown that carbon and nitrogen sources are key players in the regulatory machinery of EPS synthesis. EPS produced on Suc/Pep comprised levan-type polymer and heteropolysaccharide whereas growth on Suc/NaNO₃ solely yielded levan. The first hypothesis that a constituent of peptone is necessary for heteropolysaccharide production was disproven by the result that EPS formation on Glc/NaNO₃ produced pure heteropolysaccharide (see Supplementary information Fig. S4). Polysaccharide biosynthesis generally involves a complex regulatory network driven by various factors (Schmid, Sieber, & Rehm, 2015). One of these factors is the metabolic burden that arises when microbes encounter different nutrient conditions. The fact that nitrogen plays an important role in *Paenibacillaceae* metabolism is obvious, since they are nitrogen-fixing symbionts in their natural environment (Lal & Tabacchioni, 2009). The polymerization activity of levansucrase relies on the presence of sucrose, since it provides the fructosyl group that is added to the growing polyfructose chain (Li, Yu, Zhang, Jiang, & Mu, 2015). Consequently, levan formation can only be observed when sucrose is used as a carbon source. The influence of the nitrogen source is more ambiguous. A plausible explanation is that NaNO₃ requires complete de-novo amino acid synthesis, which puts pressure on the bacterial cells. Hence, only sucrose-induced levan formation occurs (Schmid et al., 2015) and heteropolysaccharide is not produced. However, peptone provides several amino acids that can be directly incorporated. This allows the redirection of carbon flux from catabolism to heteropolysaccharide production.

3.4. Analytical characterization of EPS

The recently established carbohydrate fingerprint method was used to obtain information on the monomer composition of purified EPS. Molecular weight distribution was determined using gel permeation chromatography, and FTIR was employed to investigate structural differences between EPSs. Results from an HPLC–MS analysis of *Paenibacillus* sp. 2H2 heteropolysaccharide revealed that it is composed of glucose, mannose, galactose, and glucuronic acid in the ratio 3.5:2:1:0.1 (Fig. 3). As uronic acids are prone to degradation during acid hydrolysis (Tait, Sutherland, & Clarke-

Sturman, 1990), glucuronic acid is underrepresented in the data in Fig. 3. It is probably present in every repeating unit of the polymer, which would correspond to a monomer composition of 3.5:2:1:1. Detected fucose traces are negligible, since amounts are too small to account for a reasonable proportion of a repeating unit. Remarkably, the heteropolysaccharide composition was found to be independent of the production scale and remained the same in 96-well plates, shake-flasks, and 2-L, 10-L, and 30-L bioreactors. The same sugar monomers have been identified in *Paenibacillus* heteropolysaccharides analyzed in other studies (Ahn et al., 1998; Ninomiya & Kizaki, 1969; Raza et al., 2011). However, sugar ratios vary and the presence of pyruvate substituents is also often reported, which is not true for *Paenibacillus* sp. 2H2 heteropolysaccharides. The levan-type polymer showed the expected monomer composition, comprising fructose and glucose, which is consistent with existing studies (Liu et al., 2010).

Gel permeation chromatography was used to identify the relative polymer molecular weight distributions of isolated polysaccharides in comparison to a pullulan standard calibration. Heteropolysaccharides produced on glucose or glycerol, as well as levan-type polymers produced from sucrose, featured a single peak elution profile corresponding to weight average molecular weights of $(1.3 \pm 0.2) \times 10^7$ g mol⁻¹ for glucose, $(1.5 \pm 0.3) \times 10^7$ g mol⁻¹ for glycerol and $(1.3 \pm 0.1) \times 10^6$ g mol⁻¹ for sucrose, respectively (Fig. 4). The bimodal molecular weight distribution of the EPS mixture from Suc/Pep fermentations were assigned to $(1.5 \pm 0.3) \times 10^7$ g mol⁻¹ for the early peak and to $(9.8 \pm 0.8) \times 10^5$ g mol⁻¹ for the second peak. All substances eluting after 30 mL have molecular weights $< 5 \times 10^4$ g mol⁻¹ were not taken into consideration. Molecular weight averages obtained from comparison with a standard calibration have to be critically evaluated, as the hydrodynamic radii of structurally different polymers may vary significantly (Morris, Adams, & Harding, 2014). Furthermore, physicochemical network formation in concentrated polysaccharide solutions, due to hydrogen bonding, can cause non-size exclusion effects that impede absolute measurements (Kostanski, Keller, & Hamielec, 2004). Nevertheless, a qualitative comparison among different samples is valid, and values obtained for *Paenibacillus* sp. 2H2 polymers are in the range of molecular weights found in other studies. Literature values of the molecular weights of levan-type polymers from *Paenibacillaceae* range from 8.7×10^5 g mol⁻¹ to 2.0×10^6 g mol⁻¹ (Han & Clarke, 1990; Liu et al., 2009) and heteropolysaccharides of up to 3.2×10^7 g mol⁻¹ have been described (Weon-Taek et al., 1999).

FTIR spectra of EPSs produced on different carbon and nitrogen sources were recorded to investigate their structural features and their differences (Fig. 5). Strong bands between 3380 and 3390 cm⁻¹ were assigned to hydroxyl stretching vibrations (Tang et al., 2014). The band at 2962 cm⁻¹ for heteropolysaccharide samples and the two distinct bands at 2935 cm⁻¹ and 2868 cm⁻¹ for the Suc/NaNO₃ sample result from C–H stretching vibration of aliphatic CH₂ groups and indicate the presence of fructose residues in case of the levan-type polymer (Küçükşakık et al., 2011; Liu et al., 2010). Bands around 1650 cm⁻¹ were attributed to bound water;

signals between 1400 and 1460 cm⁻¹ were related to C=O symmetric stretching vibrations, which are characteristic absorptions of carboxyl groups (Pooja & Chandra, 2009). The C–C–O absorption bands at 1261–1267 cm⁻¹ are followed by signals resulting from symmetric vibrations of fructofuranose rings and glycosidic linkages at wavelengths of 924–1128 cm⁻¹ (Kačuráková & Mathlouthi, 1996). Bands at 802, 804, and 811 cm⁻¹ were assigned to out-of-plane C–H wagging vibrations (Baranska, Schulz, Krüger, & Quilitzsch, 2005). Differences between samples obtained during this study can especially be observed in the fingerprint region: <1500 cm⁻¹. The spectra of Glc/Pep and Glyc/Pep heteropolysaccharides are nearly identical, whereas the Suc/NaNO₃ polymer exhibits absorption bands typical for levan polysaccharides. The spectrum of Suc/Pep EPS is more similar to pure heteropolysaccharide samples; however, some deviations in glycosidic bond absorption bands can be observed, indicating the existence of another polymer.

3.5. Rheological properties

The rheological behavior of isolated *Paenibacillus* sp. 2H2 EPS was characterized under rotating and oscillating measurement conditions by recording viscosity curves and stress sweeps, respectively (Fig. 6). The differences between the pure heteropolysaccharides (obtained using Glc/Pep and Glyc/Pep) and levan-containing samples are striking. Although all polymers display shear thinning, the viscosities of heteropolysaccharide solutions are much higher than those of levan-containing samples. Furthermore, viscosity curves of Glc/Pep and Glyc/Pep suggest that a pronounced physicochemical network exists in these samples, as viscosities do not approach a plateau value at low shear rates; they increase exponentially. This η plateau, however, can be observed in the sample obtained using Suc/Pep, indicating a solution of solely entangled molecules simultaneously unraveling and unraveling when applied to low shear stress (Graessley, 1967). Pure levan-type EPS behaves similarly, however, with significantly lower viscosities. Results of the amplitude sweep (Fig. 6(B)) strengthen the hypothesis of polymer network behavior. The sample structure degeneration, usually visible through a decrease of the storage modulus G' , is initiated by an increase in the loss modulus G'' for the pure heteropolysaccharide samples. The loss modulus overshoot is not yet fully understood, but a possible explanation is based on increased friction, induced by micro cracks or flexible side chains within the cross-linked network (Hyun et al., 2011; Mezger, 2006). Neither the Suc/Pep polymer mixture, nor the pure levan show this G'' peak. The gel strength of approximately 6 Pa for EPS derived from Glc/Pep and Glyc/Pep demonstrates the strong elastic character of this polymer, whereas almost no elasticity can be observed for the pure levan-type EPS. The findings suggest that physicochemical network formation in mixtures of levan and heteropolysaccharide may be hindered because heteropolysaccharide concentration is too low or because levan incorporation disturbs network construction. The latter assumption is supported by results obtained from rheological measurements of an EPS solution containing levan-type polymer and heteropolysaccharide at a ratio of 1:1. This sample was prepared by mixing purified polymer powders and dissolving them together in water. Similar to the pure heteropolysaccharide, a clear network structure was observed (Fig. 6). This finding suggests that fine-tuning the rheology of heteropolysaccharide/levan blends is not possible by simply mixing both products. An elaborated fermentation strategy, however, may be employed to induce polymer formation at desired ratios.

4. Conclusions

Bacterial EPSs represent a promising class of sustainable biopolymers to replace commonly used petrochemical substances for thickening, emulsifying, or flocculating applications in everyday items. Although several EPSs have already been commercialized, low-cost synthetic polymers still dominate the commodity materials market. The launch of additional EPSs requires the discovery of new polymers with superior properties, identification of applications that perfectly match the respective EPS's strengths, and a better understanding of EPS biosynthesis and downstream processing for a more profitable process.

Here, a high-throughput screening approach was employed to isolate the auspicious EPS producer *Paenibacillus* sp. 2H2 from a large number of bacterial strains based on growth characteristics and EPS carbohydrate fingerprint. The fermentative EPS production was characterized in detail in a 30-L bioreactor. Furthermore, it was found that fermentation with certain carbon and nitrogen sources leads to the biosynthesis of different EPSs, namely pure heteropolysaccharides, pure levan-type polymers, or mixtures of both. This finding could only be obtained by combining sophisticated analytical tools to describe the entire EPS sample, emphasizing the importance of analytics for reliable product and process characterization. Finally, the isolated polymers' fundamental rheological characterization revealed highly promising thickening properties of the *Paenibacillus* sp. 2H2 heteropolysaccharide. Future work will focus on in-depth investigation of this new EPS to assess its potential for commercial exploitation.

Acknowledgements

The authors acknowledge the financial and technical support of Evonik Industries and the scientific advice of Jochen Kleinen regarding rheological issues.

Appendix A. Supplementary data

Supplementary data associated with this article can be found, in the online version, at <http://dx.doi.org/10.1016/j.carbpol.2016.04.074>.

References

- Aguilera, M., Monteoliva-Sanchez, M., Suarez, A., Guerra, V., Lizama, C., Bennisar, A., et al. (2001). *Paenibacillus jamilae* sp. nov.: an exopolysaccharide-producing bacterium able to grow in olive-mill wastewater. *International Journal of Systematic and Evolutionary Microbiology*, 51(Pt. 5), 1687–1692.
- Ahn, S., Suh, H.-H., Lee, C.-H., Moon, S.-H., Kim, H.-S., Ahn, K.-H., et al. (1998). Isolation and characterization of a novel polysaccharide producing *Bacillus polymyxa* A49 KCTC 4648P. *Journal of Microbiology and Biotechnology*, 8(2), 171–177.
- Ash, C., Priest, F., & Collins, M. D. (1993). Molecular identification of rRNA group 3 bacilli (Ash, Farrow, Wallbanks and Collins) using a PCR probe test. *Antonie Van Leeuwenhoek*, 64(3–4), 253–260.
- Baranska, M., Schulz, H., Krüger, H., & Quilitzsch, R. (2005). Chemotaxonomy of aromatic plants of the genus *Origanum* via vibrational spectroscopy. *Analytical and Bioanalytical Chemistry*, 381(6), 1241–1247.
- Bradford, M. M. (1976). A rapid and sensitive method for the quantitation of microgram quantities of protein utilizing the principle of protein-dye binding. *Analytical Biochemistry*, 72(1), 248–254.
- Degeest, B., Vaningelgem, F., & De Vuyst, L. (2001). Microbial physiology, fermentation kinetics, and process engineering of heteropolysaccharide production by lactic acid bacteria. *International Dairy Journal*, 11(9), 747–757.
- DuBois, M., Gilles, K. A., Hamilton, J. K., Rebers, P. A., & Smith, F. (1956). Colorimetric method for determination of sugars and related substances. *Analytical Chemistry*, 28(3), 350–356.
- Freitas, F., Alves, V., & Reis, M. M. (2014). Bacterial polysaccharides: production and applications in cosmetic industry. In K. G. Ramawat, & J.-M. Mérillon (Eds.), *Polysaccharides* (pp. 1–24). Springer International Publishing.
- García-Ochoa, F., Santos, V. E., Casas, J. A., & Gómez, E. (2000). Xanthan gum: production, recovery, and properties. *Biotechnology Advances*, 18(7), 549–579.
- Graessley, W. W. (1967). Viscosity of entangling polydisperse polymers. *The Journal of Chemical Physics*, 47(6), 1942–1953.

- Häfler, T., Schieder, D., Pfäler, R., Faulstich, M., & Sieber, V. (2012). Enhanced fed-batch fermentation of 2,3-butanediol by *Paenibacillus polymyxa* DSM 365. *Bioresource Technology*, 124, 237–244.
- Haggag, W. M. (2007). Colonization of exopolysaccharide-producing *Paenibacillus polymyxa* on peanut roots for enhancing resistance against crown rot disease. *African Journal of Biotechnology*, 6(13).
- Han, Y. W., & Clarke, M. A. (1990). Production and characterization of microbial levan. *Journal of Agricultural and Food Chemistry*, 38(2), 393–396.
- Heyndrickx, M., Vandemeulebroeck, K., Scheldeman, P., Kersters, K., De Vos, P., Logan, N., et al. (1996). A polyphasic reassessment of the genus *Paenibacillus*, reclassification of *Bacillus lautus* (Nakamura, 1984) as *Paenibacillus lautus* comb. nov. and of *Bacillus peoriae* (Montefusco et al., 1993) as *Paenibacillus peoriae* comb. nov., and emended descriptions of *P. lautus* and of *P. peoriae*. *International Journal of Systematic Bacteriology*, 46(4), 988–1003.
- Hyun, K., Wilhelm, M., Klein, C. O., Cho, K. S., Nam, J. G., Ahn, K. H., et al. (2011). A review of nonlinear oscillatory shear tests: analysis and application of large amplitude oscillatory shear (LAOS). *Progress in Polymer Science*, 36(12), 1697–1753.
- Jiang, W., Bikard, D., Cox, D., Zhang, F., & Marraffini, L. A. (2013). CRISPR-assisted editing of bacterial genomes. *Nature Biotechnology*, 31(3), 233–239.
- Jung, H.-K., Hong, J.-H., Park, S.-C., Park, B.-K., Nam, D.-H., & Kim, S.-D. (2007). Production and physicochemical characterization of β -glucan produced by *Paenibacillus polymyxa* JB115. *Biotechnology and Bioengineering*, 12(6), 713–719.
- Küçükaşık, F., Kazak, H., Güney, D., Finore, L., Poli, A., Yenigün, O., et al. (2011). Molasses as fermentation substrate for levan production by *Halomonas* sp. *Applied Microbiology and Biotechnology*, 89(6), 1729–1740.
- Kačuráková, M., & Mathlouthi, M. (1996). FTIR and laser-Raman spectra of oligosaccharides in water: characterization of the glycosidic bond. *Carbohydrate Research*, 284(2), 145–157.
- Kim, O.-S., Cho, Y.-J., Lee, K., Yoon, S.-H., Kim, M., Na, H., et al. (2012). Introducing EzTaxon-e: a prokaryotic 16S rRNA gene sequence database with phylogenies that represent uncultured species. *International Journal of Systematic and Evolutionary Microbiology*, 62(3), 716–721.
- Kostanski, L. K., Keller, D. M., & Hamielec, A. E. (2004). Size-exclusion chromatography—a review of calibration methodologies. *Journal of Biochemical and Biophysical Methods*, 58(2), 159–186.
- Lal, S., & Tabacchioni, S. (2009). Ecology and biotechnological potential of *Paenibacillus polymyxa*: a minireview. *Indian Journal of Microbiology*, 49(1), 2–10.
- Lee, I. Y., Seo, W. T., Kim, G. J., Kim, M. K., Ahn, S. G., Kwon, G. S., et al. (1997). Optimization of fermentation conditions for production of exopolysaccharide by *Bacillus polymyxa*. *Bioprocess Engineering*, 16(2), 71–75.
- Li, O., Lu, C., Liu, A., Zhu, L., Wang, P.-M., Qian, C.-D., et al. (2013). Optimization and characterization of polysaccharide-based biofloculant produced by *Paenibacillus elgii* B69 and its application in wastewater treatment. *Bioresource Technology*, 134, 87–93.
- Li, W., Yu, S., Zhang, T., Jiang, B., & Mu, W. (2015). Recent novel applications of levansucrases. *Applied Microbiology and Biotechnology*, 99(17), 6959–6969.
- Liang, T.-W., & Wang, S.-L. (2015). Recent advances in exopolysaccharides from *Paenibacillus* spp.: production, isolation, structure, and bioactivities. *Marine Drugs*, 13(4), 1847–1863.
- Liu, J., Luo, J., Ye, H., Sun, Y., Lu, Z., & Zeng, X. (2009). Production, characterization and antioxidant activities in vitro of exopolysaccharides from endophytic bacterium *Paenibacillus polymyxa* EJS-3. *Carbohydrate Polymers*, 78(2), 275–281.
- Liu, J., Luo, J., Ye, H., Sun, Y., Lu, Z., & Zeng, X. (2010). Medium optimization and structural characterization of exopolysaccharides from endophytic bacterium *Paenibacillus polymyxa* EJS-3. *Carbohydrate Polymers*, 79(1), 206–213.
- Madden, J. K., Dea, I. C. M., & Steer, D. C. (1986). Structural and rheological properties of the extracellular polysaccharides from *Bacillus polymyxa*. *Carbohydrate Polymers*, 6(1), 51–73.
- Mezger, T. G. (2006). *The rheology handbook: for users of rotational and oscillatory rheometers*. Vincentz Network GmbH & Co. KG.
- Montefusco, A., Nakamura, L. K., & Labeda, D. P. (1993). *Bacillus peoriae* sp. nov. *International Journal of Systematic and Evolutionary Microbiology*, 43(2), 388–390.
- Moraine, R. A., & Rogovin, P. (1973). Kinetics of the xanthan fermentation. *Biotechnology and Bioengineering*, 15(2), 225–237.
- Morillo, J., Guerra del Águila, V., Aguilera, M., Ramos-Cormenzana, A., & Monteoliva-Sánchez, M. (2007). Production and characterization of the exopolysaccharide produced by *Paenibacillus jamilae* grown on olive mill-waste waters. *World Journal of Microbiology and Biotechnology*, 23(12), 1705–1710.
- Morris, G. A., Adams, G. G., & Harding, S. E. (2014). On hydrodynamic methods for the analysis of the sizes and shapes of polysaccharides in dilute solution: a short review. *Food Hydrocolloids*, 42(Pt. 3), 318–334.
- Ninomiya, E., & Kizaki, T. (1969). Bacterial polysaccharide from *Bacillus polymyxa* No. 271. *Die Angewandte Makromolekulare Chemie*, 6(1), 179–185.
- Peters, J. M., Silvius, M. R., Zhao, D., Hawkins, J. S., Gross, C. A., & Qi, L. S. (2015). Bacterial CRISPR: accomplishments and prospects. *Current Opinion in Microbiology*, 27, 121–126.
- Pooja, K. P., & Chandra, T. S. (2009). Production and partial characterization of a novel capsular polysaccharide KP-EPS produced by *Paenibacillus pabuli* strain ATSKP. *World Journal of Microbiology and Biotechnology*, 25(5), 835–841.
- Rühmann, B., Schmid, J., & Sieber, V. (2014). Fast carbohydrate analysis via liquid chromatography coupled with ultra violet and electrospray ionization ion trap detection in 96-well format. *Journal of Chromatography A*, 1350, 44–50.
- Rühmann, B., Schmid, J., & Sieber, V. (2015a). High throughput exopolysaccharide screening platform: from strain cultivation to monosaccharide composition and carbohydrate fingerprinting in one day. *Carbohydrate Polymers*, 122, 212–220.
- Rühmann, B., Schmid, J., & Sieber, V. (2015b). Methods to identify the unexplored diversity of microbial exopolysaccharides. *Frontiers in Microbiology*, 6.
- Rafigh, S. M., Yazdi, A. V., Vossoughi, M., Safekordi, A. A., & Ardjmand, M. (2014). Optimization of culture medium and modeling of curdlan production from *Paenibacillus polymyxa* by RSM and ANN. *International Journal of Biological Macromolecules*, 70, 463–473.
- Raveendran, S., Poullose, A. C., Yoshida, Y., Maekawa, T., & Kumar, D. S. (2013). Bacterial exopolysaccharide based nanoparticles for sustained drug delivery, cancer chemotherapy and bioimaging. *Carbohydrate Polymers*, 91(1), 22–32.
- Raza, W., Makeen, K., Wang, Y., Xu, Y., & Qirong, S. (2011). Optimization, purification, characterization and antioxidant activity of an extracellular polysaccharide produced by *Paenibacillus polymyxa* SQR-21. *Bioresource Technology*, 102(10), 6095–6103.
- Raza, W., Yang, W., & Shen, Q. (2008). *Paenibacillus polymyxa*: antibiotics, hydrolytic enzymes and hazard assessment. *Journal of Plant Pathology*, 90(3), 419–430.
- Rehm, B. H. (2010). Bacterial polymers: biosynthesis, modifications and applications. *Nature Reviews Microbiology*, 8(8), 578–592.
- Schmid, J., Sieber, V., & Rehm, B. (2015). Bacterial exopolysaccharides: biosynthesis pathways and engineering strategies. *Frontiers in Microbiology*, 6.
- Schmid, J., Sperl, N., & Sieber, V. (2014). A comparison of genes involved in sphingian biosynthesis brought up to date. *Applied Microbiology and Biotechnology*, 98(18), 7719–7733.
- Seviour, R. J., McNeil, B., Fazenda, M. L., & Harvey, L. M. (2011). Operating bioreactors for microbial exopolysaccharide production. *Critical Reviews in Biotechnology*, 31(2), 170–185.
- Stewart, E. J. (2012). Growing unculturable bacteria. *Journal of Bacteriology*, 194(16), 4151–4160.
- Sukplang, P., & Vela, G. R. (2000). *Production and characterization of a novel extracellular polysaccharide produced by Paenibacillus velaei*, sp. nov. University of North Texas.
- Suresh Kumar, A., Mody, K., & Jha, B. (2007). Bacterial exopolysaccharides—a perception. *Journal of Basic Microbiology*, 47(2), 103–117.
- Sutherland, I. W. (1998). Novel and established applications of microbial polysaccharides. *Trends in Biotechnology*, 16(1), 41–46.
- Tait, M. I., Sutherland, I. W., & Clarke-Sturman, A. J. (1990). Acid hydrolysis and high-performance liquid chromatography of xanthan. *Carbohydrate Polymers*, 13(2), 133–148.
- Tamura, K., Stecher, G., Peterson, D., Filipowski, A., & Kumar, S. (2013). MEGA6: molecular evolutionary genetics analysis version 6.0. *Molecular Biology and Evolution*, 30(12), 2725–2729.
- Tang, J., Qi, S., Li, Z., An, Q., Xie, M., Yang, B., et al. (2014). Production: purification and application of polysaccharide-based biofloculant by *Paenibacillus mucilaginosus*. *Carbohydrate Polymers*, 113, 463–470.
- Timmusk, S., Grantcharova, N., & Wagner, E. G. H. (2005). *Paenibacillus polymyxa* invades plant roots and forms biofilms. *Applied and Environmental Microbiology*, 71(11), 7292–7300.
- Toukach, P., Joshi, H. J., Ranzinger, R., Knirel, Y., & von der Lieth, C.-W. (2007). Sharing of worldwide distributed carbohydrate-related digital resources: online connection of the Bacterial Carbohydrate Structure DataBase and GLYCOSCIENCES de. *Nucleic Acids Research*, 35(Suppl. 1), D280–D286.
- Weon-Taek, S., Kahng, G.-G., Nam, S.-H., Choi, S.-D., Suh, H.-H., Kim, S.-W., et al. (1999). Isolation and characterization of a novel exopolysaccharide-producing *Paenibacillus* sp. WN9 KCTC 8951P. *Journal of Microbiology and Biotechnology*, 9(6), 820–825.
- Yegorenkova, I. V., Tregubova, K. V., Matora, L. Y., Burygin, G. L., & Ignatov, V. V. (2008). Composition and immunochemical characteristics of exopolysaccharides from the rhizobacterium *Paenibacillus polymyxa* 1465. *Microbiology*, 77(5), 553–558.

Appendix A: Supplementary Data

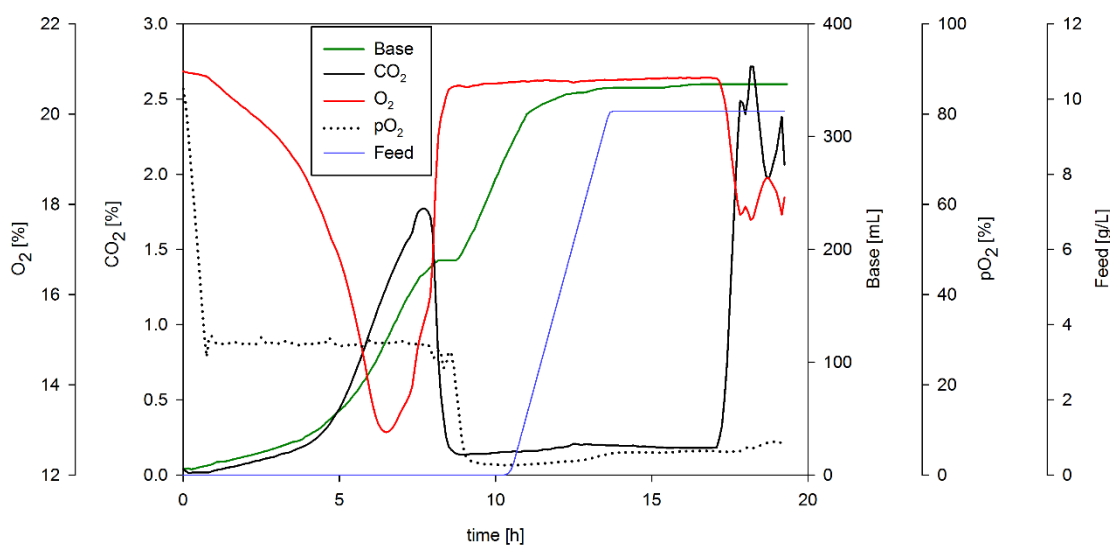


Fig. S1. Process parameter of the fermentative EPS production by *Paenibacillus* sp. 2H2 in 30 L scale.

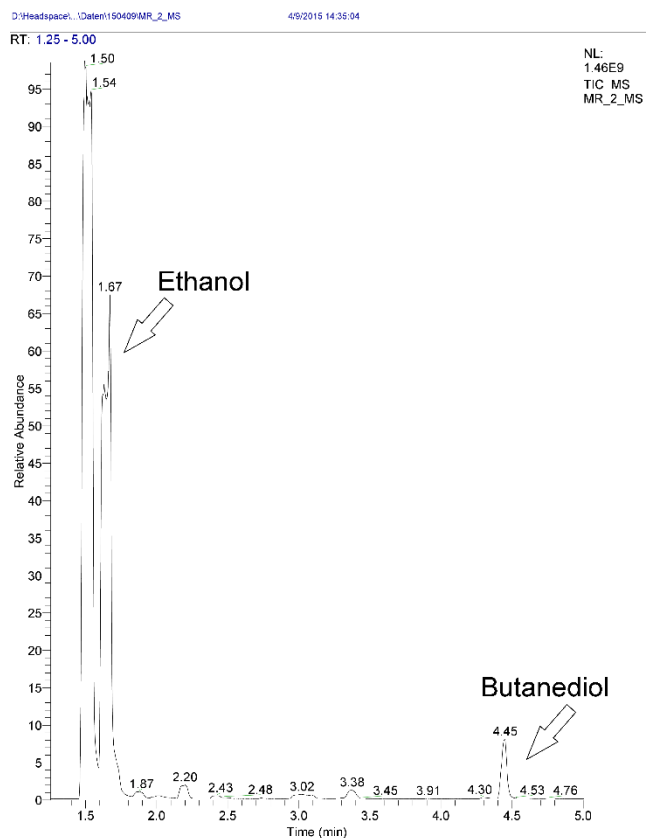


Fig. S2. GC-FID profile of the culture broth from the 30 L fermentation at the end of the process.

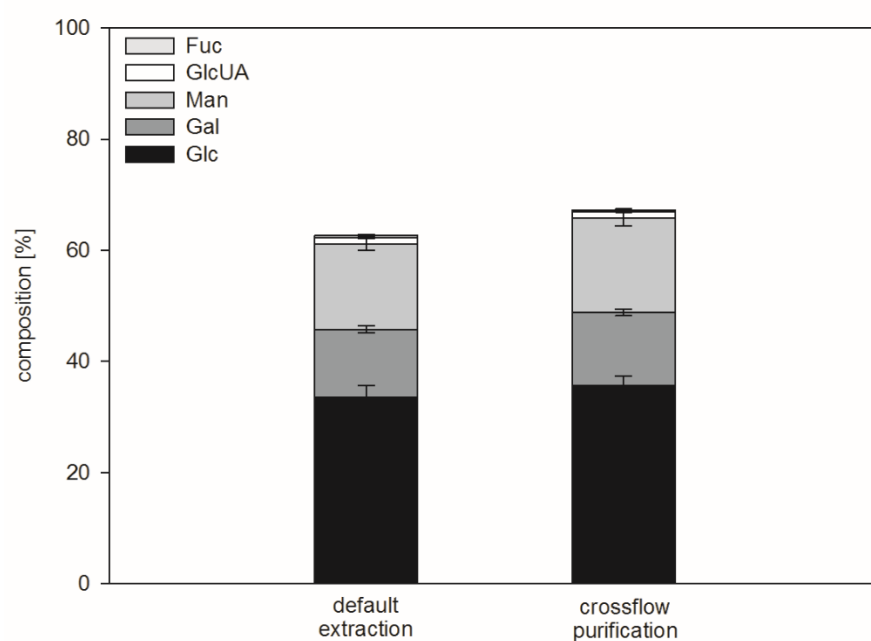


Fig. S3. Comparison of EPS's monomer composition and recovery in UHPLC-UV-ESI-MS measurements after default extraction or purification via crossflow.

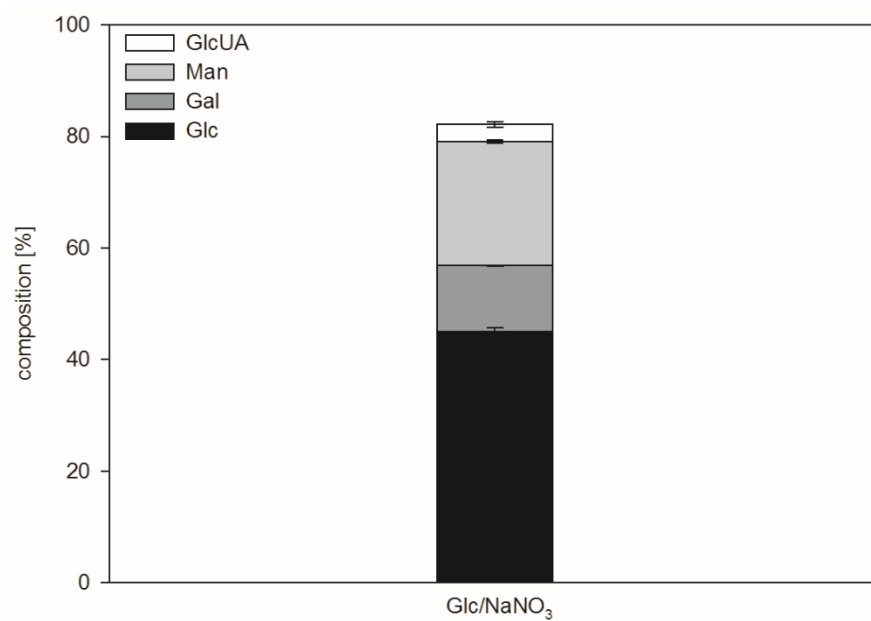


Fig. S4. Monomer composition of EPS produced on glucose as carbon source and NaNO₃ as nitrogen source.

3.3 Rheological characterization of the exopolysaccharide Paenan in surfactant systems

This publication deals with the thorough rheological characterization of Paenan - the heteropolysaccharide secreted by the *Paenibacillus* sp. strain described in chapter 3.2. Main subjects are the rheology of aqueous Paenan solutions and the applicability of Paenan in surfactant containing systems. Aim of this work was to gain a fundamental understanding of Paenan's rheology and to evaluate its performance in comparison to the commercial benchmark polymers Gellan and Xanthan.

Aqueous Paenan solutions in 0.5% NaCl exhibited high viscosities and a pronounced shear-thinning character, already at polymer concentrations $\geq 0.1\text{wt}\%$. A flow behavior, relevant to industrial applications, was obtained with 60-65% less polymer as compared to Xanthan and Gellan. Amplitude sweep tests, frequency tests and thixotropy measurements revealed that Paenan forms stable, weak-gel systems with distinct intermolecular interactions, delivering elasticity as well as thixotropy. Thereby, Paenan occupies a novel application profile that lies between rigid Gellan gels and Xanthan fluids.

Furthermore, Paenan's applicability in surfactant containing systems was evaluated. For this, mixtures with commonly used surfactants of each class were prepared, analyzed and compared to the commercial benchmarks. Remarkably, Paenan was compatible with every class of surfactant, even with cationic cetrimonium chloride, which resulted in the formation of insoluble complexes in combination with Xanthan and Gellan. The rheology of the Paenan/surfactant systems largely remained dominated by the polysaccharide, hence qualifying Paenan as a rheological additive for surfactant containing formulations. Solely mixtures with neutral sugar glucoside, showed an altered flow behavior, similar to that of pure surfactant, indicating a strong interference of lauryl glucoside worm-like micelles with the polymer network. In Xanthan and Gellan solutions, the neutral surfactant had a similar effect. Especially the loss moduli significantly increased in presence of lauryl glucoside, suggesting the considerable contribution of micellar superstructures to the rheology of the mixtures. All other compatible surfactants only showed marginal impact on Xanthan systems. For Gellan, however, the impact of surfactant molecules on the rigid, strong network was more distinct and the rheological behavior changed considerably as compared to the pure system. Especially the anionic surfactant showed a pronounced interaction with Gellan, resulting in a decreased gel strength.

The comparison of Paenan to commercial benchmark polymers emphasized that the unique surfactant compatibility and the weak-gel rheology render Paenan interesting for industrial application, especially in surfactant containing formulations.

Designed and execution of all experiments presented in this study was performed by the author in close collaboration with Jochen Schmid, Andre Braun and Moritz Gansbiller. Scientific support for rheological measurements and data interpretation was provided by Jochen Kleinen and Andre Braun. All co-authors contributed to content and language of the manuscript and gave scientific or technical advice in certain issues.

Rheological characterization of the exopolysaccharide Paenan in surfactant systems

Marius Rütering, Jochen Schmid, Moritz Gansbiller, Andre Braun, Jochen Kleinen, Martin Schilling
and Volker Sieber

Carbohydrate Polymers
(2017)

DOI: 10.1016/j.carbpol.2017.11.086



Contents lists available at ScienceDirect

Carbohydrate Polymers

journal homepage: www.elsevier.com/locate/carbpol

Rheological characterization of the exopolysaccharide Paenan in surfactant systems

Marius Rütering^a, Jochen Schmid^a, Moritz Gansbiller^a, Andre Braun^b, Jochen Kleinen^c, Martin Schilling^d, Volker Sieber^{a,e,f,g,*}^a Chair of Chemistry of Biogenic Resources, Technical University of Munich, Schulgasse 16, 94315, Straubing, Germany^b Anton Paar Germany GmbH, Hellmuth-Hirth-Str. 6, 73760, Ostfildern, Scharnhausen, Germany^c Evonik Nutrition and Care GmbH, Goldschmidtstraße 100, 45127, Essen, Germany^d Evonik Nutrition and Care GmbH, Kirschenallee, 64293, Darmstadt, Germany^e Fraunhofer IGB, Straubing Branch Bio, Electro, and Chemocatalysis BioCat, 94315, Straubing, Germany^f Catalysis Research Center, Technical University of Munich, 85748, Garching, Germany^g The University of Queensland, School of Chemistry and Molecular Biosciences, 68 Cooper Road, St. Lucia 4072, Australia

ARTICLE INFO

Keywords:

Paenan
Gellan
Xanthan
Rheology
Surfactant

ABSTRACT

Rheology-controlling agents are of importance for numerous products in a variety of industries. Replacement of synthetic chemicals with natural additives is desired in light of current environmental awareness and limited fossil resources. This study investigates the rheological features of Paenan, an exopolysaccharide produced by *Paenibacillus polymyxa*. Paenan exhibits highly shear-thinning flow behavior at concentrations $\geq 0.1\%$ in 0.5% NaCl. Because of its pronounced intermolecular network, it forms stable, weak gels, thereby delivering elasticity as well as thixotropy. Application-relevant flow behavior is obtained with 60–65% less polymer as compared to the benchmark commercial products Xanthan and Gellan. In mixtures with surfactants (sodium lauryl ether sulfate, cetrimonium chloride, cocamidopropyl betaine, or lauryl glucoside), Paenan displays outstanding compatibility with every class of surfactant, making it superior to the partially incompatible Xanthan and Gellan. The weak-gel character of Paenan/surfactant systems is retained with three out of four surfactants, rendering Paenan highly interesting for various applications.

1. Introduction

The propensity to flow or deform is a fundamental property of all materials and ultimately determines their physical appearance. In industries involving food, personal care products, pharmaceuticals, oil drilling, construction, and paints, the rheology of a product is of utmost importance to its functionality in specific applications. Viscosity, pseudoplasticity, thixotropy or gel structures are product characteristics that can be adjusted by the use of certain rheological additives (Laba, 1993). Commonly, these additives are polymeric materials that deliver the desired functional properties via thickening, gelling, stabilizing, or emulsifying mechanisms (Glass, Schulz, & Zukoski, 1991).

The market of polymeric rheology modifiers is still dominated by synthetic or semi-synthetic chemicals such as polyacrylates, polyvinyl polymers, polyacrylamides, and cellulose derivatives (Gutowski, Lee, de Bruyn, & Frisken, 2012; Llamas et al., 2015; Wang, Kislalioglu, &

Breuer, 1999), although social and environmental awareness have triggered a high demand for “all-natural” products. These synthetic compounds still outperform many natural products in terms of functionality and profitability, and only a few “green” rheological agents produced from renewable resources are competitive today (Rehm, 2010). Therefore, consumer-oriented industries seek novel, natural rheological additives with superior properties. Best-known representatives from natural sources are Xanthan, Gellan, alginates, carrageenans, and hyaluronic acid, all of which are polysaccharides (Freitas, Alves, & Reis, 2014; Schmid, Sperl, & Sieber, 2014). The enormous potential of polysaccharides lies in their biocompatibility, biodegradability, low toxicity, and structural variability (Schmid, Sieber, & Rehm, 2015; Sutherland, 1998). Polysaccharides secreted by microorganisms, termed “exopolysaccharides” (EPS), represent a seemingly inexhaustible source of new compounds that can be produced independent of season and location in reliable quality and quantity by

Abbreviations: s, sodium lauryl ether sulfate; n, lauryl glucoside; b, cocamidopropyl betaine; c, cetrimonium chloride; P, Paenan; X, Xanthan; G, Gellan

* Corresponding author at: Chair of Chemistry of Biogenic Resources, Technical University of Munich, Schulgasse 16, 94315, Straubing, Germany.

E-mail addresses: m.ruetering@gmail.com (M. Rütering), j.schmid@tum.de (J. Schmid), m.gansbiller@tum.de (M. Gansbiller), andre.braun@anton-paar.com (A. Braun), jochen.kleinen@evonik.com (J. Kleinen), martin.schilling@evonik.com (M. Schilling), sieber@tum.de (V. Sieber).<https://doi.org/10.1016/j.carbpol.2017.11.086>

Received 12 September 2017; Received in revised form 8 November 2017; Accepted 23 November 2017

Available online 26 November 2017

0144-8617/ © 2017 Elsevier Ltd. All rights reserved.

fermentation. While over 400 different EPSs have been structurally described (Toukach, Joshi, Ranzinger, Knirel, & von der Lieth, 2007), and only a handful of these have been commercialized (Ates, 2015; Rühmann, Schmid, & Sieber, 2015). As reviewed recently, EPSs secreted by the Gram-positive genus *Paenibacilli* have been the subject of numerous studies. Because they vary widely in structure (levans, glucans, heteropolysaccharides), numerous potential applications have been suggested, including use as antioxidants, animal feed additives, and biofloculants (Liang & Wang, 2015).

Publications focusing on the rheology of EPSs have primarily focused on *P. polymyxa* heteropolysaccharides, composed of glucose, galactose, mannose, glucuronic acid, and occasionally fucose and pyruvate (Ahn et al., 1998; Kim, Ahn, Seo, Kwon, & Park, 1998; Madden, Dea, & Steer, 1986; Ninomiya & Kizaki, 1969). Because these studies differ with respect to the production strains used, monomer ratios, and detected polymer fractions, no uniform nomenclature has been established for *P. polymyxa* heteropolysaccharides. These EPSs form stable hydrogels in up to 40% ethanol (Ninomiya & Kizaki, 1969), exhibit a broad tolerance toward different salts (Ahn et al., 1998; Madden et al., 1986), and retain high viscosity in the presence of surfactants (Kim et al., 1998). Detailed analyses of concentration-dependent rheology employing state-of-the-art rheometry and investigations of application-relevant matrices have not been conducted. In a previous work, we introduced the fermentative production, structural features, and fundamental rheology of a heteropolysaccharide secreted by *P. polymyxa*, which we have named “Paenan” (Rüttering, Schmid, Rühmann, Schilling, & Sieber, 2016). Paenan is composed of glucose, mannose, galactose, and glucuronic acid (3.5:2.1:0.1) and has a molecular weight of approximately 1.3×10^7 g mol⁻¹. Paenan production is characterized by a process requiring 17 h fermentation time (30-L bioreactor scale) and a volumetric productivity of 0.27 g L⁻¹ h⁻¹ (Rüttering et al., 2016). Basic studies of its rheology have already revealed its impressive thickening potential and provided impetus for this work, which evaluates the applicability of Paenan as a rheological additive.

The implementation of EPSs as rheological agents requires a fundamental understanding of their rheology in aqueous solution as well as in the matrix of the final formulation. In particular, the interaction between EPSs and surfactants is crucial, because surfactants are important ingredients of several industrial formulations and can drastically influence the rheology imparted by the polysaccharide (Bais, Trevisan, Lapasin, Partal, & Gallegos, 2005; Fijan, Šostar-Turk, & Lapasin, 2007). Incompatibilities between certain surfactant classes and EPSs result in coacervation (Piculell, 2013; Wilde, 2000), and several other interactions can alter the physicochemistry delivered by the polymers (Bao, Li, Gan, & Zhang, 2008; Bonnaud, Weiss, & McClements, 2010; Mukherjee, Sarkar, & Moulik, 2010). The main factors influencing polysaccharide/surfactant interactions include the charges, polymer characteristics (functional groups, backbone, and chain stiffness), and relative concentrations of both constituents (Aust & Zugenmaier, 1993; Guzmán et al., 2016). In addition to the numerous optical and electrochemical techniques required to investigate the interactions in polymer/surfactant systems, rheological measurements can provide initial application-relevant insights into the fundamental characteristics and interaction properties of a material.

This study focuses on the concentration-dependent rheology of Paenan in aqueous solution as well as its performance in surfactant-containing systems in comparison to benchmark polymers. Unique compatibilities and outstanding rheology make this polymer interesting for several applications.

2. Materials and methods

2.1. Materials and sample preparation

Paenan EPS was obtained by fermentative production and purification as described previously (Rüttering et al., 2016). Low acyl

Gellan gum (Collstab G) was a kind gift by Colltec GmbH (Bielefeld), and Xanthan gum (Keltrol CG) was provided by CP Kelco (Atlanta). Sodium lauryl ether sulfate (Texapon NSO) and lauryl glucoside (Plantacare 1200 UP) were purchased from BASF (Ludwigshafen). Cocamidopropyl betaine (TEGO Betaine F 50) and cetrimonium chloride (VARISOFT 300) were provided by Evonik Industries (Essen). Concentration series (wt%) of Paenan in aqueous solution were prepared by dissolving corresponding amounts of polymer in ultra-pure water (PURELAB classic system, ELGA LabWater) at 50 °C with stirring at 250 rpm overnight. To ensure the comparability of native Paenan solutions to subsequently prepared surfactant systems, the pH was set to 5.5 with a low concentration of HCl or NaOH, and the salt load of the samples was adjusted to a final concentration of 0.5% NaCl by adding concentrated NaCl solution. After pH adjustment and salt addition, Paenan solutions were stirred another 2 h at 250 rpm and 50 °C. Samples then were allowed to rest for 24 h at room temperature (20 °C) and analyzed. Xanthan solutions were prepared likewise, yielding properly dissolved solutions for both, Paenan and Xanthan. The preparation of Gellan solutions resulted in broken gel systems, due to the destruction of the rigid, self-supporting Gellan gels upon continuous stirring. Since characteristics of broken gel systems largely depend on the preparation procedure, details on this can be found in the supplements.

All EPS/surfactant mixtures were prepared at a final surfactant concentration of 5% active matter (AM), with one defined concentration for each EPS. To this end, surfactant stock solutions at double the final concentration were prepared in ultra-pure water and adjusted to a pH of 5.5 with HCl or NaOH. EPSs were also dissolved in ultra-pure water alone at double the final concentrations (wt%) at 250 rpm, 50 °C overnight. Subsequently, surfactant stock solutions and EPS stock solutions were mixed at a ratio of 1:1 to obtain 5% AM surfactant and the desired EPS concentration. The pH of these mixtures was readjusted to 5.5 if necessary, stirred another 24 h at 250 rpm, 50 °C, allowed to rest for 24 h, and finally analyzed.

2.2. Rheological measurements

Measurements were performed with an air-bearing MCR300 stress-controlled rheometer (Anton Paar Germany GmbH) with a cone plate geometry (50-mm diameter, 1° cone angle, 0.05-mm gap) at a constant, Peltier-controlled temperature of 20 °C. Data were collected and analyzed using Rheoplus V.3.61 software (Anton Paar). Samples were equilibrated at 20 ± 0.1 °C for 5 min before measurements were taken. All measurements were carried out in triplicate.

2.2.1. Viscosity curves

Viscosity curves were obtained during a logarithmic shear-rate ramp ($\dot{\gamma}$, 0.1–1000 s⁻¹) by measuring at 25 points with a gradually decreasing measurement time from 100 to 5 s.

2.2.2. Amplitude sweeps

The linear viscoelastic regimes, structural features, and yield stress values were determined using a shear stress amplitude sweep (logarithmic ramp from 0.1–1000 Pa) at a constant frequency of $f = 1$ Hz by measuring 20 points per decade. Yield stress values were determined as the stress value at which the elastic modulus decreased by $\geq 2\%$ as compared to previous measuring point.

2.2.3. Frequency sweeps

The time-dependent deformation behavior was tested at frequencies from 0.01 to 100 Hz at a constant strain within the linear viscoelastic region (usually 1 Pa). Samples were sealed with a thin film of low viscosity paraffin oil to avoid water evaporation during long measurements. Gel strengths were determined as G' values at the lowest measured frequency.

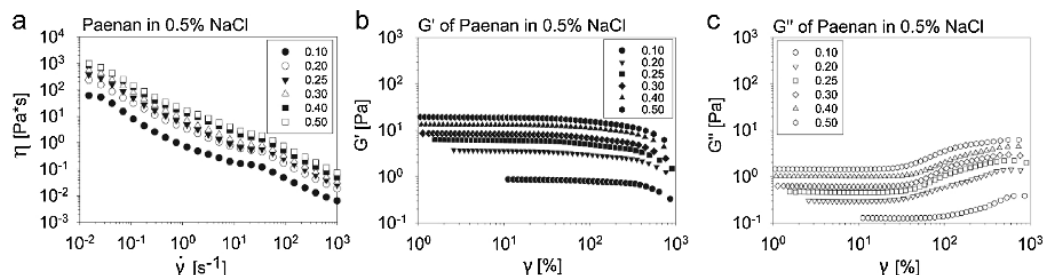


Fig. 1. Viscosity curves (a) and amplitude sweeps (b and c) of Paenan concentration series in 0.5% NaCl. Storage moduli (G' , middle), and loss moduli (G'' , right) of amplitude sweep tests are shown as a function of shear strain.

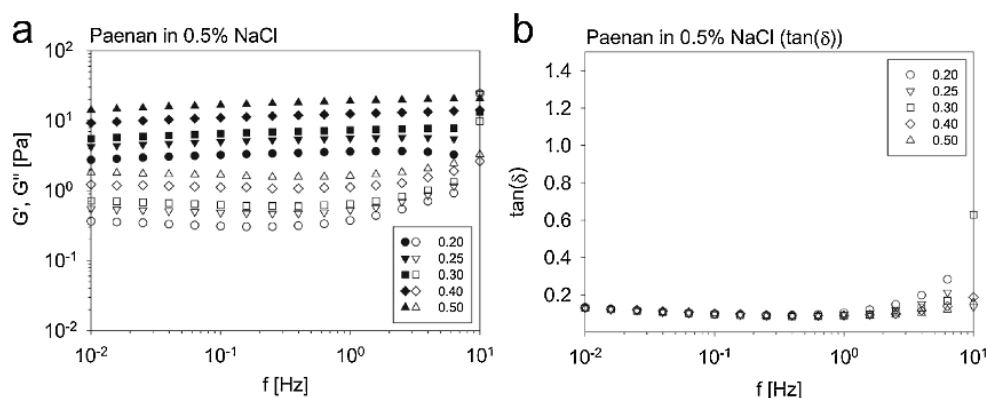


Fig. 2. Frequency sweeps of selected Paenan concentrations. Storage moduli are shown as filled symbols, loss moduli as empty symbols (a). The loss factor of all systems is depicted on the right (b).

2.2.4. Thixotropy

Structure degradation at high shear and subsequent recovery was investigated using a three-segmented oscillation measurement by recording the elastic (G') and viscous (G'') modules. A constant strain in the linear viscoelastic range at a frequency of 1 Hz was applied in segments one (reference) and three (recovery). High-shear conditions were simulated at a strain of 100 Pa for 60 s during segment two. The degree of recovery was determined by comparing G' values after defined time intervals in the recovery phase to the G' reference value before structure destruction.

3. Results and discussion

3.1. Paenan rheology

The rheological behavior of polymer solutions under shear stress is an important metric that gives information on the sample properties under relevant shear conditions. The low-shear region (10^{-3} – 1 s $^{-1}$) is equivalent to storage, transport, and post-application conditions, whereas the mid- to high-shear range (1 – 10^3 s $^{-1}$) mirrors the shear stress during application. Fig. 1a shows the viscosity curves of a Paenan concentration series. The distinct shear-thinning character of tested Paenan solutions is clearly observable at all concentrations (Fig. 1a). At low shear, intertwined polysaccharide molecules show high resistance to flow and thereby deliver high viscosity. Upon shear increase, the macromolecules align along the streamline of the flow, resulting in a viscosity decrease (Chagas, Machado, Haag, De Souza, & Lucas, 2004). The viscosity at 0.01 s $^{-1}$ is as high as 380 Pa s for 0.25% Paenan. To obtain a similar viscosity at low shear required 1.0% for Xanthan and 0.6% for Gellan (Fig. S1). Notably, the apparent viscosities of all three EPSs in the high-shear range were comparable at these concentrations, suggesting that far less Paenan is needed to obtain a satisfactory

pseudoplasticity in a formulation as compared to Xanthan and Gellan.

Amplitude sweep tests were carried out to determine the linear viscoelastic regimes of polymer solutions (Fig. 1b–c). Within this strain range, the sample can be deformed without degeneration of the structure. The linear viscoelastic region is reflected by strain-independent G' and G'' plateaus and is a fundamental sample characteristic that is important for subsequent oscillatory measurements. Furthermore, the yield stress can be deduced from amplitude sweeps, and general intermolecular interactions become obvious. For all Paenan concentrations, the storage modulus G' dominates over the loss modulus G'' in the linear viscoelastic region (Fig. 1b–c). Interestingly, upon increase of the applied strain, G'' values first leave their plateau, while G' remains constant. This property is typical of polymer solutions with distinct intermolecular interactions such as ionic bonding, hydrogen bonding, and van der Waals forces, which result in the formation of a strong physicochemical network (Mezger, 2006; Sun et al., 2011). In a study of a comparable *P. polymyxa* EPS, Madden and Dea proposed that the polymer adopts a rigid, ordered conformation stabilized by both specific ionic interactions and other non-covalent forces, resulting in the observed weak-gel character (Madden et al., 1986).

The time-dependent sample behavior was investigated at constant low strain with frequency sweeps from 0.01–100 Hz (Fig. 2). Low frequencies correspond to long time scales, for example, during storage and transport. High frequencies simulate short time scales. Paenan shows the mentioned weak-gel character over all tested concentrations.

The polymer solutions exhibit an elastic character even at the lowest frequencies, and absolute gel strengths (G' values at $f = 0.01$ Hz) are between 3 and 14 Pa (0.2–0.5%). A creep test, which was performed to extend data on the long time behavior, underlines the elastic character of Paenan (Fig. S2). This behavior suggests that Paenan could readily be applied for the stabilization of suspensions, as Paenan solutions do not start flowing in the long term but rather maintain their elastic gel

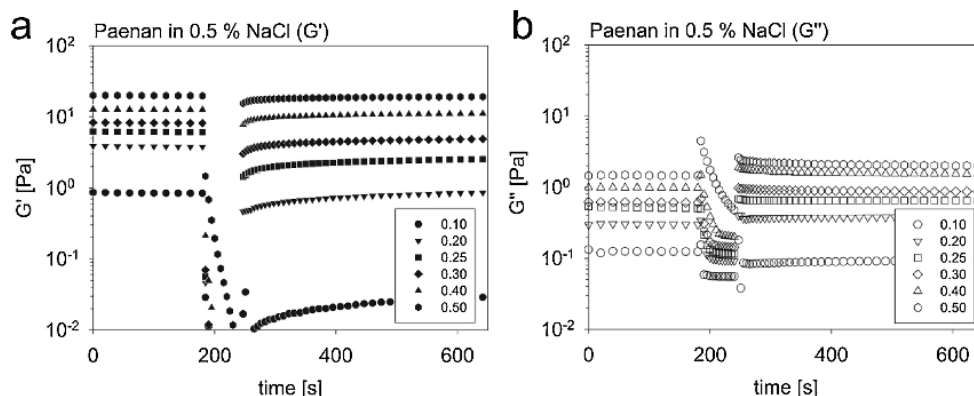


Fig. 3. Thixotropic behavior of a Paenan concentration series. Storage moduli (G') are shown in a, loss moduli (G'') in b. Low oscillatory strain within the linear viscoelastic region was applied in sections one (0–200 s) and three 260–650 s). High-shear conditions were simulated with an oscillation at 100 Pa in section two (200–260 s).

character. Gelling agents are known to prevent suspended particles, from settling or coagulating, as for example oil droplets in cosmetic oil/water emulsions (Saha & Bhattacharya, 2010). The loss factor ($\tan \delta$) of Paenan solutions is concentration-independent (Fig. 2b), indicating that although gel strength increases, the proportion of viscous and elastic behavior ($\tan \delta = G''/G'$) stays constant.

Another important feature of shear-thinning rheological additives is their ability to regenerate solution structure after high-shear events. In practice, high-shear stress occurs during product application and manufacturing or unintended shaking. Rapid sample structure regeneration is desirable to prevent uncontrolled running and dripping of the product after application and to guarantee product homogeneity. Fig. 3 shows the results of thixotropy tests of Paenan solutions.

Structure regeneration after destruction occurs completely or partially, depending on the EPS concentration. Down to 0.3%, the storage modulus recovers almost completely within the third interval (Fig. 3a). Below this concentration, only partial regeneration is observed. However, G' values are still increasing at the end of the segment, and complete recovery is probably a matter of time. Importantly, even low-concentration solutions immediately exhibit an elastic character ($G' > G''$) after stress removal, indicating that the basic gel character is restored.

When comparing the fundamental rheology of Paenan to industrially important EPSs such as Gellan and Xanthan, it becomes clear that Paenan occupies a niche between those representatives. Native Xanthan is a highly viscous thickener with a clear, concentration-independent thixotropy (Benmouffok-Benbelkacem, Caton, Baravian, & Skali-Lami, 2010), but it does not form gels and shows less long-term stability at concentrations < 0.7% (Fig. S5). In contrast, low-acetylated Gellan also forms hydrogels. However, the difference between Paenan and Gellan is the rigidity of the gels. The storage moduli of Gellan gels are much higher than those of Paenan gels. This stiffness of Gellan results in poor performance in thixotropy tests (García, Alfaro, & Muñoz, 2016). A commercial rheological additive exhibiting similar rheological traits as Paenan is the polyacrylic-acid based Carbopol. This synthetic polymer shows a comparable, shear-thinning, weak-gel character at the same concentrations (Bonacucina, Martelli, & Palmieri, 2004; Kim, Song, Lee, & Park, 2003).

3.2. Polysaccharide/surfactant systems

Surfactants are grouped according to the hydrophilic moiety of the molecule (cationic, anionic, amphoteric, and nonionic), and they are important ingredients of several industrial formulations, such as paintings, agrochemicals and especially cosmetics (Llamas et al., 2015). Surfactants are crucial to product performance, and their compatibility

with other components of the formulation must be ensured. One surfactant of each class was selected, and mixtures with Paenan, Gellan, and Xanthan were prepared for evaluation of surfactant applicability to these anionic EPSs. The surfactants tested are as follows: anionic, sodium lauryl ether sulfate (s); cation, cetrimonium chloride (c); amphoteric, cocamidopropyl betaine (b); and nonionic, lauryl glucoside (n). These particular surfactants were chosen because they are frequently used representatives of their classes. Furthermore, they all possess comparatively long hydrophobic tails (s, C_{12} ; b, C_{8-18} ; n, C_{12-16} ; c, C_{16}), allowing for better comparability between the different compounds.

For each EPS, a polymer concentration was chosen that resulted in flow curves representative of a real application. It is worth mentioning that Paenan and Xanthan existed as homogeneous polymer solutions, whereas Gellan appeared as broken gel system. The continuous stirring during sample preparation destroys the rigid, self-supporting Gellan gel, yielding a fluid gel structure. Fig. S3 shows an overlay of the viscosity curves of 0.25% Paenan (P), 0.7% Xanthan (X), and 0.6% Gellan (G) — the effect-concentrations that were selected for subsequent analyses in surfactant systems. Mixtures of surfactants in corresponding effect-concentrations with 5% AM surfactants were prepared as described in Section 2.1. As expected, not all EPSs were compatible with every surfactant (Table 1).

Complex coacervation and precipitation occurred in mixtures of all oppositely charged polyanionic and cationic surfactants, as well as in the combination of Gellan with amphoteric surfactant. Previous studies describe similar effects for several gums (Bao et al., 2008; Goddard, 1994; Mukherjee et al., 2010). Coacervation was reversible in the case of Paenan by adjusting the salt load of the sample to 1% NaCl. As described for other polyanions, sodium cations probably shield exposed anionic groups, thereby preventing complex formation with surfactant molecules (Holmberg, Jönsson, Kronberg, & Lindman, 2003; Thalberg & Lindman, 1991). The positive effect of NaCl addition was not

Table 1
Compatibility matrix of Paenan (0.25%), Xanthan (0.7%), and Gellan (0.6%) with 5% active matter surfactant of each class. Immiscible systems are marked with “-” and miscible systems as “+”.

	nonionic ^a	anionic ^b	amphoteric ^c	cationic ^d
Paenan	+	+	+	+
Xanthan	+	+	+	-
Gellan	+	+	-	-

^a plantacare lauryl glucoside.

^b sodium lauryl ether sulfate.

^c cocamidopropyl betaine.

^d cetrimonium chloride.

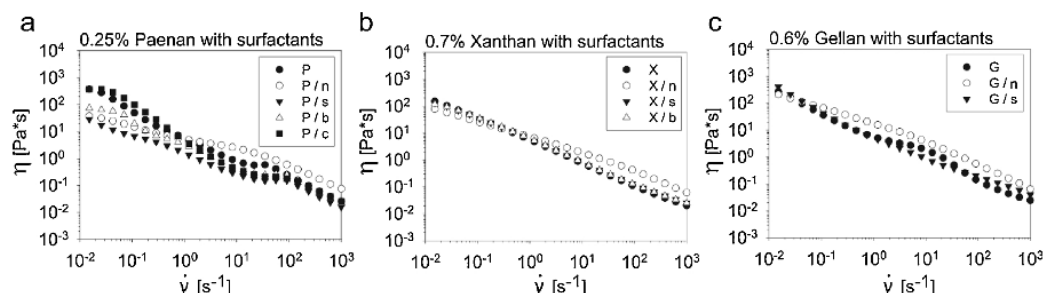


Fig. 4. Viscosity curves of EPS/surfactant systems. The curve of the pure polymer in 0.5% NaCl is shown as a reference in each graph. EPSs are abbreviated with capital letters (P, Paenan; X, Xanthan; G, Gellan), surfactants with lowercase letters (n, lauryl glucoside; s, sodium lauryl ether sulfate; b, cocamidopropyl betaine; c, cetrimonium chloride).

observable for Xanthan or Gellan. Rheological measurements were solely performed for homogeneous, one-phase systems. Fig. 4 shows the viscosity curves of all compatible EPS/surfactant systems.

The sugar-based, nonionic lauryl glucoside had the greatest effect on the rheological behavior of the systems analyzed. Upon addition of this nonionic surfactant, the viscosities of all EPSs were decreased at low shear and increased at high shear. This effect can be attributed to micellar superstructures formed at elevated concentrations of long-alkyl-chain glucosides (Platz et al., 1995). Surfactant molecules aggregate to form rod-shaped micelles, which behave like short chain polymers and disturb the EPS network. Hence, the viscosity decreases at low-shear result from reduced polymer-polymer interactions due to incorporated micelles (Fijan et al., 2007), and high viscosities at high shear indicate that the system's rheology is dominated by lauryl glucoside, which exhibits Newtonian flow behavior at a considerable viscosity from 0.01 to 30 s⁻¹ (Fig. S4). The influence of the other surfactants on Xanthan and Gellan was negligible (Fig. 4b–c). The systems were still dominated by the polymers, and deviations from the pure EPSs were only minor. In the case of Paenan, the addition of surfactants showed a stronger influence (Fig. 4a). Particularly in the low-shear region, anionic sodium lauryl ether sulfate and amphoteric betaine noticeably reduced the viscosity. Similar to lauryl glucoside, this observation can be explained by the interference of surfactant molecules or micelles with the physicochemical polymer network. However, the fundamental shear-thinning character and behavior under high shear were unchanged. Viscosity curves of pure surfactant solutions and additional rheological data on lauryl glucoside can be found in the supplements (Fig. S4). These results are in accordance with literature and support the assumption that lauryl glucoside forms micellar superstructures, whereas pure solutions of the other surfactants do not assemble into worm-like micelles (Abdel-Rahem, Reger, Hloucha, & Hoffmann, 2014; Róžańska, 2015).

Under non-destructive, oscillatory conditions, lauryl glucoside was found to have the strongest effect on EPS/surfactant rheology (Fig. 5). In amplitude sweep tests, loss moduli (G'') increased markedly for every polymer and even dominated over G' for Paenan (Fig. 5a). For Xanthan and Gellan, G' was still higher than G'' , but the viscous proportion of both systems was dramatically increased (Fig. 5b–c). This finding can also be explained by the incorporation of rod-like lauryl glucoside micelles, which significantly contribute to the loss moduli of the systems (increase of G'') because of their own structure and additionally reduce polymer-polymer interactions (reduction of G') (Platz et al., 1995). Amplitude sweep tests of aqueous lauryl glucoside solutions without EPS support this assumption (Fig. S4). Accordingly, nonionic surfactants are reported as useful for decreasing the viscosity of fermentation broth during Gellan production (Arockiasamy & Banik, 2008).

The other surfactants only had marginal effects on the amplitude sweeps of Paenan and Xanthan. Storage moduli were slightly reduced in P/s and P/b mixtures and remained unchanged in P/c. The rheology of Xanthan was influenced by neither sodium lauryl ether sulfate nor betaine. The effect of all surfactants on Gellan again underscores the

susceptibility of strong networks to structure weakening upon incorporation of surfactant. Similar to lauryl glucoside, anionic sodium lauryl ether sulfate also caused a decrease in both G' and G'' , yielding a weaker structure. Furthermore, the distinct G'' overshoot, observable for the pure Gellan solution, was remarkably attenuated, suggesting that the three-dimensional network was disturbed. Interestingly, the yield stress value of Gellan was significantly increased in the G/s system (Table S1). A previous study described the effect of sodium dodecyl sulfate (SDS) on Gellan conformation and hypothesized that SDS micelles form long ionic bridges between separated Gellan helices (Chizhik, Khripov, & Nishinari, 2003). A similar mechanism could explain the decreased rigidity and increased flexibility of the G/s system.

The profiles of mechanical spectra did not change substantially for Paenan in combination with any surfactant, and the weak-gel character was maintained in every system over the whole frequency range (Fig. 6). Hence, the specific property of Paenan, a weak but stable gel character, is not influenced by the addition of anionic sodium lauryl ether sulfate, amphoteric betaine, or cationic cetrimonium chloride. Only the gel strengths slightly decreased in surfactant-containing systems (Table S2). The P/n mixture was not assessed in frequency sweeps, since this system was governed by viscous behavior throughout the entire stress range in strain sweeps. Xanthan systems also remained dominated by polymer rheology, and only X/n exhibited a slight decrease in the storage modulus (Fig. 6b). Although G' is higher than G'' over all measured frequencies in Xanthan systems, the increase in the loss factor toward low frequencies clearly indicates that the solutions behave like structured fluids rather than weak gels. Of note, weak-gel rheology can indeed be promoted in Xanthan systems by adding defined amounts of Ca²⁺ ions (Mohammed, Haque, Richardson, & Morris, 2007). In accordance with the other experiments, Gellan solutions were most affected by anionic surfactant (Fig. 6c). The gel strength was reduced by more than 80% with anionic sodium lauryl ether sulfate (Table S2). Nevertheless, the strong-gel character, with gel strengths > 100 Pa, did not change in any Gellan/surfactant system.

The results of time-dependent structure regeneration in thixotropy measurements are consistent with data obtained from already discussed protocols (Fig. 7). Xanthan exhibited a perfect thixotropy, independent of added surfactant. Only lauryl glucoside addition caused the previously mentioned increase in loss modulus. Structure regeneration however, was unaffected. Both moduli reached their reference values (G' , G'' before shear disruption) instantly in the recovery section (Fig. 7b). Hence, entanglement of individual Xanthan helices was obviously not impaired by the presence of surfactant. The same tendencies were observed for P/n and G/n. As previously speculated, micelles or single molecules of nonionic lauryl glucoside probably interfere with intermolecular polymer/polymer adherence. This interference leads to a behavior similar to that imparted by entangled polymers, without a physicochemical network. Similar effects were described for the interaction of nonionic surfactants with Carbopol gels (Barreiro-Iglesias, Alvarez-Lorenzo, & Concheiro, 2001). Thixotropy tests of pure lauryl glucoside solutions underline the contribution of the nonionic

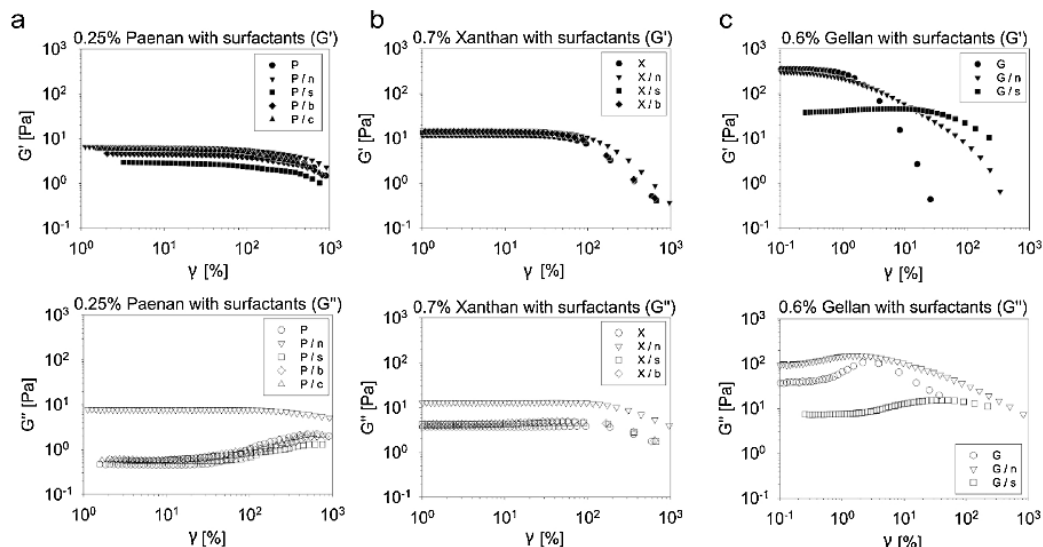


Fig. 5. Amplitude sweep tests of EPS/surfactant systems. Storage moduli (filled symbols) are shown on top, loss moduli (empty symbols) at the bottom. Paenan frequency sweeps are depicted on the left (a), Xanthan in the middle (b), and Gellan on the right (c). EPSs are abbreviated with capital letters (P, Paenan; X, Xanthan; G, Gellan), surfactants with lowercase letters (n, lauryl glucoside; s, sodium lauryl ether sulfate; b, cocamidopropyl betaine; c, cetrimonium chloride).

surfactant, especially to the loss modulus.

When examining the effect of the other surfactants on Paenan structure regeneration, surfactant-dependent differences can be observed (Fig. 7a). The pure Paenan system regenerated the fastest, followed by P/c, P/b, and finally P/s. Since the surfactant-free system recovered the fastest, we assume that the speed of recovery of surfactant-containing systems mirrors the degree of surfactant interference with rebuilding of the polymer network. Although it is known that surfactants can have supporting effects on polymer/polymer interactions (e.g., via a bridging mechanism (Holmberg et al., 2003)), all investigated Paenan systems were negatively influenced by the addition of surfactant. Their consistency was weakened, as shown by gel strengths in frequency sweeps, and their structural recovery after

destruction was slowed. These observations probably result from the high concentration of surfactants used. Synergistic effects are usually reported for low surfactant concentrations (Goddard, 1994; Noskov, 2010). Nevertheless, except for P/n, the fundamental weak-gel character of Paenan was retained in combination with all other surfactants.

In case of Gellan, surfactant addition also induced remarkable changes in the thixotropy of the system (Fig. 7c). In addition to the previously described effect of nonionic lauryl glucoside, anionic sodium lauryl ether sulfate also influenced the structural recovery after high shear. Interestingly, regeneration was significantly supported in the presence of anionic surfactant, as compared to the pure Gellan solution. Both moduli nearly reached their reference values in the measured timeframe, whereas pure Gellan further degenerated after stress

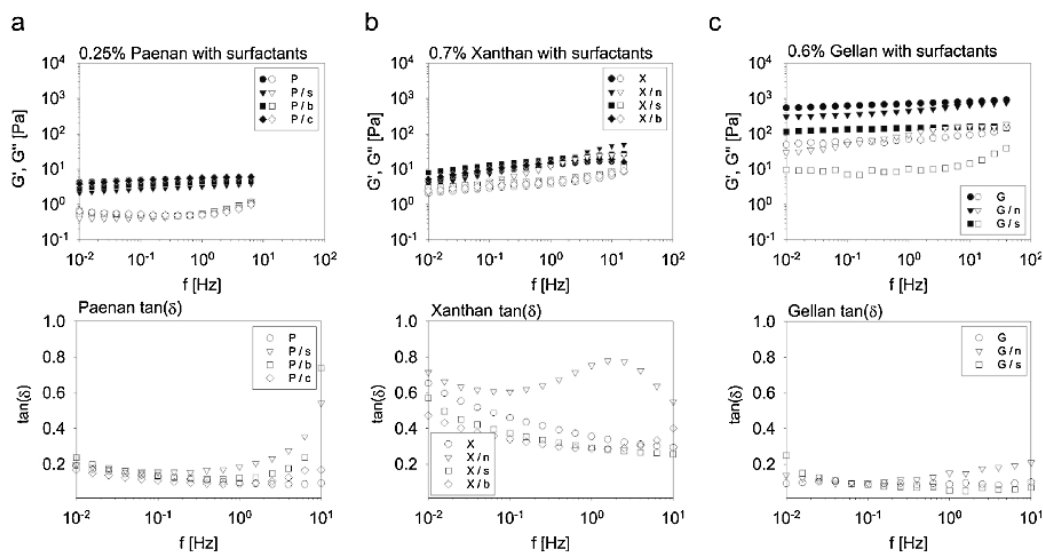


Fig. 6. Frequency sweeps of EPS/surfactant systems. Paenan is depicted on the left (a), Xanthan in the middle (b), and Gellan on the right (c). G' is shown as filled symbols, G'' as empty symbols (graphs on the top). Loss factors are depicted for each system at the bottom. EPSs are abbreviated with capital letters (P, Paenan; X, Xanthan; G, Gellan), surfactants with lowercase letters (n, lauryl glucoside; s, sodium lauryl ether sulfate; b, cocamidopropyl betaine; c, cetrimonium chloride).

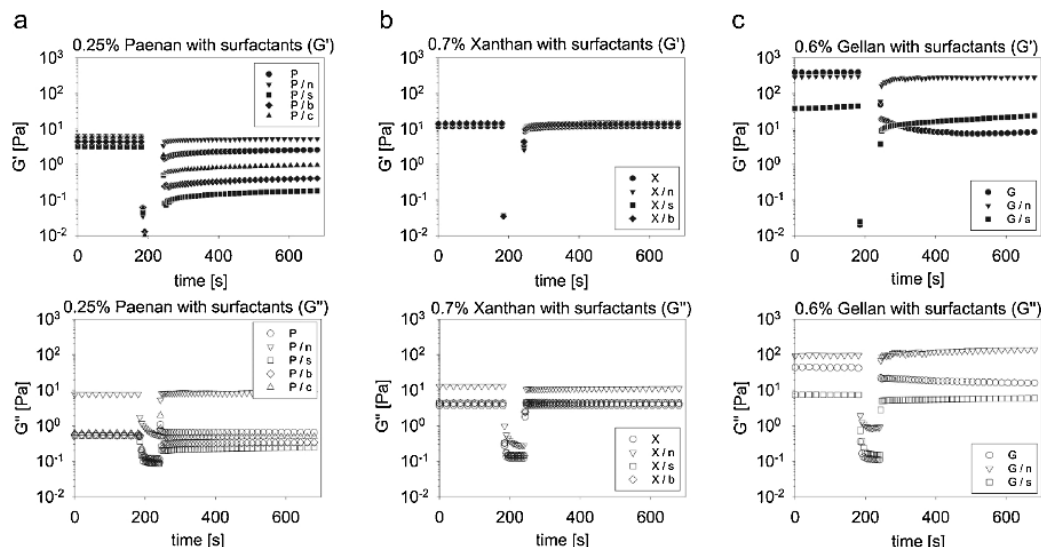


Fig. 7. Thixotropic behavior of EPS/surfactant systems. Paenan is shown left (a), Xanthan in the middle (b), and Gellan right (c). Storage moduli (G') are depicted at the top and loss moduli at the bottom (G''). Low oscillatory strain within the linear viscoelastic region was applied in sections one (0–200 s) and three (260–650 s). High-shear conditions were simulated with an oscillation at 100 Pa in section two (200–260 s). EPSs are abbreviated with capital letters (P, Paenan; X, Xanthan; G, Gellan), surfactants with lowercase letters (n, lauryl glucoside; s, sodium lauryl ether sulfate; b, cocamidopropyl betaine; c, cetrimonium chloride).

removal. This beneficial influence was already perceptible during amplitude sweeps, in which the yield point of Gellan was increased almost fourfold by the addition of sodium lauryl ether sulfate. The theory that micelles of anionic surfactants function as sodium-bridged linkers between individual Gellan helices is consistent with this finding (Chizhik et al., 2003). Another study reporting SDS-induced separation of Gellan aggregates is also consistent with the observed structural changes (Ikeda, Nitta, Tamsiripong, Pongsawatmanit, & Nishinari, 2004).

4. Conclusions

The present study thoroughly characterizes the rheological behavior of Paenan polysaccharide and evaluates its applicability to surfactant-containing systems. Aqueous Paenan solutions exhibited an apparent shear-thinning character with outstanding viscosities in the low-shear range. Flow behavior relevant to industrial applications was obtained with significantly less polymer as compared to the commercial benchmarks Xanthan and Gellan. The distinct weak-gel character of Paenan solutions represents a novel application profile that lies between the rigid Gellan gels and Xanthan fluids. Paenan gels deliver stability over time, while retaining an evident thixotropy. Furthermore, Paenan exhibits a unique compatibility with every class of surfactant. This property makes it superior to Gellan and Xanthan, which display incompatibilities, especially with a cationic surfactant. The rheology of all compatible EPS/surfactant systems largely remained dominated by the polymer. Only the nonionic, sugar-based surfactant significantly altered the physicochemical properties of all EPSs. Future work should aim at gaining a fundamental understanding of Paenan/surfactant interactions by complete elucidation of the polymer structure using conductometry, tensiometry, microcalorimetry, and microscopy.

Acknowledgements

This work was financially supported by Evonik Industries. Special thanks go to Steven Koenig for technical and scientific support in rheological measurements.

Appendix A. Supplementary data

Supplementary data associated with this article can be found, in the online version, at <http://dx.doi.org/10.1016/j.carbpol.2017.11.086>.

References

- Abdel-Rahem, R. A., Reger, M., Hloucha, M., & Hoffmann, H. (2014). Rheology of aqueous solutions containing SLES, CAPB, and microemulsion: Influence of cosurfactant and salt. *Journal of Dispersion Science and Technology*, 35(1), 64–75.
- Ahn, S., Suh, H.-H., Lee, C.-H., Moon, S.-H., Kim, H.-S., Ahn, K.-H., et al. (1998). Isolation and characterization of a novel polysaccharide producing *Bacillus polymyxa* A49 KCTC 4648P. *Journal of Microbiology and Biotechnology*, 8, 171–177.
- Arockiasamy, S., & Banik, R. M. (2008). Optimization of gellan gum production by *Sphingomonas paucimobilis* ATCC 31461 with nonionic surfactants using central composite design. *Journal of Bioscience and Bioengineering*, 105, 204–210.
- Ates, O. (2015). Systems biology of microbial exopolysaccharides production. *Frontiers in Bioengineering and Biotechnology*, 3, 200.
- Aust, N., & Zugenmaier, P. (1993). Formation of supermolecular structures of polysaccharide-surfactant complexes in aqueous solutions. Influence of the polymer backbone. *Die Makromolekulare Chemie*, 194, 1583–1593.
- Bais, D., Trevisan, A., Lapasin, R., Partal, P., & Gallegos, C. (2005). Rheological characterization of polysaccharide-surfactant matrices for cosmetic O/W emulsions. *Journal of Colloid and Interface Science*, 290, 546–556.
- Bao, H., Li, L., Gan, L. H., & Zhang, H. (2008). Interactions between ionic surfactants and polysaccharides in aqueous solutions. *Macromolecules*, 41, 9406–9412.
- Barreiro-Iglesias, R., Alvarez-Lorenzo, C., & Concheiro, A. (2001). Incorporation of small quantities of surfactants as a way to improve the rheological and diffusional behavior of carbopol gels. *Journal of Controlled Release*, 77, 59–75.
- Benmouffok-Benbelkacem, G., Caton, F., Baravian, C., & Skali-Lami, S. (2010). Non-linear viscoelasticity and temporal behavior of typical yield stress fluids: Carbopol, Xanthan and Ketchup. *Rheologica Acta*, 49, 305–314.
- Bonacucina, G., Martelli, S., & Palmieri, G. F. (2004). Rheological: mucoadhesive and release properties of Carbopol gels in hydrophilic cosolvents. *International Journal of Pharmaceutics*, 282, 115–130.
- Bonnaud, M., Weiss, J., & McClements, D. J. (2010). Interaction of a food-grade cationic surfactant (lauric arginate) with food-grade biopolymers (Pectin, Carrageenan, Xanthan, Alginate, Dextran, and Chitosan). *Journal of Agricultural and Food Chemistry*, 58, 9770–9777.
- Chagas, B. S., Machado, D. L. P., Haag, R. B., De Souza, C. R., & Lucas, E. F. (2004). Evaluation of hydrophobically associated polyacrylamide-containing aqueous fluids and their potential use in petroleum recovery. *Journal of Applied Polymer Science*, 91, 3686–3692.
- Chizhik, V. I., Khripov, A. A., & Nishinari, K. (2003). Phase state of the gellan gum-SDS-water system. *Journal of Molecular Liquids*, 106, 249–255.
- Fijan, R., Šostar-Turk, S., & Lapasin, R. (2007). Rheological study of interactions between non-ionic surfactants and polysaccharide thickeners used in textile printing. *Carbohydrate Polymers*, 68, 708–717.

- Freitas, F., Alves, V., & Reis, M. M. (2014). Bacterial polysaccharides: production and applications in cosmetic industry. In K. G. Ramawat, & J.-M. Mérillon (Eds.). *Production and applications in cosmetic industry*. 1–24: Springer International Publishing.
- García, M. C., Alfaro, M. C., & Muñoz, J. (2016). Creep-recovery-creep tests to determine the yield stress of fluid gels containing gellan gum and Na⁺. *Biochemical Engineering Journal*, 114, 257–261.
- Glass, J. E., Schulz, D. N., & Zukoski, C. F. (1991). *Polymers as rheology modifiers*. Polymers as rheology modifiers. 2–17: American Chemical Society.
- Goddard, E. D. (1994). Polymer/surfactant interaction—Its relevance to detergent systems. *Journal of the American Oil Chemists' Society*, 71, 1–16.
- Gutowski, I. A., Lee, D., de Bruyn, J. R., & Frisken, B. J. (2012). Scaling and mesostructure of Carbopol dispersions. *Rheologica Acta*, 51, 441–450.
- Guzmán, E., Llamas, S., Maestro, A., Fernández-Peña, L., Akanno, A., Miller, R., et al. (2016). Polymer–surfactant systems in bulk and at fluid interfaces. *Advances in Colloid and Interface Science*, 233, 38–64.
- Holmberg, K., Jönsson, B., Kronberg, B., & Lindman, B. (2003). Surfactant–polymer systems. In K. Holmberg, B. Jönsson, B. Kronberg, & B. Lindman (Eds.). *Surfactants and polymers in aqueous solution* (pp. 277–303). John Wiley Sons, Ltd.
- Ikeda, S., Nitta, Y., Temsiripong, T., Pongsawatmanit, R., & Nishinari, K. (2004). Atomic force microscopy studies on cation-induced network formation of gellan. *Food Hydrocolloids*, 18, 727–735.
- Kim, S.-W., Ahn, S.-G., Seo, W.-T., Kwon, G.-S., & Park, Y.-H. (1998). Rheological properties of a novel high viscosity polysaccharide, A49-Pol: produced by *Bacillus polymyxa*. *Journal of Microbiology and Biotechnology*, 8, 178–181.
- Kim, J.-Y., Song, J.-Y., Lee, E.-J., & Park, S.-K. (2003). Rheological properties and microstructures of Carbopol gel network system. *Colloid and Polymer Science*, 281, 614–623.
- Laba, D. (1993). *Rheological properties of cosmetics and toiletries*. CRC Press.
- Liang, T.-W., & Wang, S.-L. (2015). Recent Advances in exopolysaccharides from *Paenibacillus* spp.: Production, isolation, structure and bioactivities. *Marine Drugs*, 13, 1847–1863.
- Llamas, S., Guzmán, E., Ortega, F., Baghdadli, N., Cazeneuve, C., Rubio, R. G., et al. (2015). Adsorption of polyelectrolytes and polyelectrolytes-surfactant mixtures at surfaces: A physico-chemical approach to a cosmetic challenge. *Advances in Colloid and Interface Science*, 222, 461–487.
- Madden, J. K., Dea, I. C. M., & Steer, D. C. (1986). Structural and rheological properties of the extracellular polysaccharides from *Bacillus polymyxa*. *Carbohydrate Polymers*, 6, 51–73.
- Mezger, T. G. (2006). *The rheology handbook: For users of rotational and oscillatory rheometers*. Vincentz Network GmbH & Co KG.
- Mohammed, Z. H., Haque, A., Richardson, R. K., & Morris, E. R. (2007). Promotion and inhibition of xanthan weak-gel rheology by calcium ions. *Carbohydrate Polymers*, 70, 38–45.
- Mukherjee, I., Sarkar, D., & Moulik, S. P. (2010). Interaction of gums (Guar, Carboxymethylhydroxypropyl Guar, Diutan, and Xanthan) with surfactants (DTAB, CTAB and TX-100) in aqueous medium. *Langmuir*, 26, 17906–17912.
- Ninomiya, E., & Kizaki, T. (1969). Bacterial polysaccharide from *Bacillus polymyxa* No: 271. *Die Angewandte Makromolekulare Chemie*, 6, 179–185.
- Noskov, B. A. (2010). Dilational surface rheology of polymer and polymer/surfactant solutions. *Current Opinion in Colloid & Interface Science*, 15, 229–236.
- Piculell, L. (2013). Understanding and exploiting the phase behavior of mixtures of oppositely charged polymers and surfactants in water. *Langmuir*, 29, 10313–10329.
- Platz, G., Poelike, J., Thunig, C., Hofmann, R., Nickel, D., & von Rybinski, W. (1995). Phase behavior, lyotropic phases: and flow properties of alkyl glycosides in aqueous solution. *Langmuir*, 11, 4250–4255.
- Rózańska, S. (2015). Rheology of wormlike micelles in mixed solutions of cocoamidopropyl betaine and sodium dodecylbenzenesulfonate. *Colloids and Surfaces A: Physicochemical and Engineering Aspects*, 482(Suppl. C), 394–402.
- Rühmann, B., Schmid, J., & Sieber, V. (2015). Methods to identify the unexplored diversity of microbial exopolysaccharides. *Frontiers in Microbiology*, 6, 565.
- Rüterring, M., Schmid, J., Rühmann, B., Schilling, M., & Sieber, V. (2016). Controlled production of polysaccharides—exploiting nutrient supply for levan and heteropolysaccharide formation in *Paenibacillus* sp. *Carbohydrate Polymers*, 148, 326–334.
- Rehm, B. H. (2010). Bacterial polymers: Biosynthesis: Modifications and applications. *Nature Reviews Microbiology*, 8, 578–592.
- Saha, D., & Bhattacharya, S. (2010). Hydrocolloids as thickening and gelling agents in food: A critical review. *Journal of Food Science and Technology*, 47, 587–597.
- Schmid, J., Sperl, N., & Sieber, V. (2014). A comparison of genes involved in sphingane biosynthesis brought up to date. *Applied Microbiology and Biotechnology*, 98, 1–15.
- Schmid, J., Sieber, V., & Rehm, B. (2015). Bacterial exopolysaccharides: Biosynthesis pathways and engineering strategies. *Frontiers in Microbiology*, 6, 6.
- Sun, W., Yang, Y., Wang, T., Liu, X., Wang, C., & Tong, Z. (2011). Large amplitude oscillatory shear rheology for nonlinear viscoelasticity in hectorite suspensions containing poly(ethylene glycol). *Polymer*, 52, 1402–1409.
- Sutherland, I. W. (1998). Novel and established applications of microbial polysaccharides. *Trends in Biotechnology*, 16, 41–46.
- Thalberg, K., & Lindman, B. (1991). Polyelectrolyte—Ionic surfactant systems: Phase behavior and interactions. In K. L. Mittal, & D. O. Shah (Eds.). *Surfactants in solution: volume 11* (pp. 243–260). Boston, MA: Springer US.
- Toukach, P., Joshi, H. J., Ranzinger, R., Knirel, Y., & von der Lieth, C.-W. (2007). Sharing of worldwide distributed carbohydrate-related digital resources: Online connection of the Bacterial Carbohydrate Structure DataBase and GLYCOSCIENCES. de. *Nucleic Acids Research*, 35, 280–286.
- Wang, S., Kislalioglu, M. S., & Breuer, M. (1999). The effect of rheological properties of experimental moisturizing creams/lotions on their efficacy and perceptual attributes. *International Journal of Cosmetic Science*, 21, 167–188.
- Wilde, P. J. (2000). Interfaces: Their role in foam and emulsion behaviour. *Current Opinion in Colloid & Interface Science*, 5, 176–181.

Appendix A: Supplementary Data

Preparation of Gellan solutions

For preparation of 0.6 wt% Gellan solutions, 300 mg Gellan were added to 50 g ultra-pure water in a 250 mL glass bulb, sealed with a plug and stirred for 15 hours at 250 rpm and 50 °C on a magnetic stirring plate using a triangular magnetic stirrer (40 x 14 mm) in a heating oven. Subsequently, the salt load was adjusted to a final concentration of 0.5% NaCl by adding 1 mL 25% NaCl. Excess-water was allowed to evaporate under stirring. Finally, the bulb was sealed again, and the sample was stirred another 2 hours at described conditions (250 rpm, 50 °C). Samples then were transferred to 50 mL conical tubes, allowed to rest for 24 h at room temperature (20 °C) and analyzed. Preparation of double-concentrated Gellan dispersions for Gellan/surfactant systems was performed likewise by using 600 mg Gellan. Adjustment of the salt load was not performed for EPS/surfactant systems, since the utilized surfactant solutions already contained comparable amounts of salt. Following EPS dissolution, surfactant stock solutions were added to the Gellan dispersion and proceeded as described in the manuscript.

Fig. S1. Viscosity curves of Xanthan and Gellan concentration series in 0.5% NaCl.

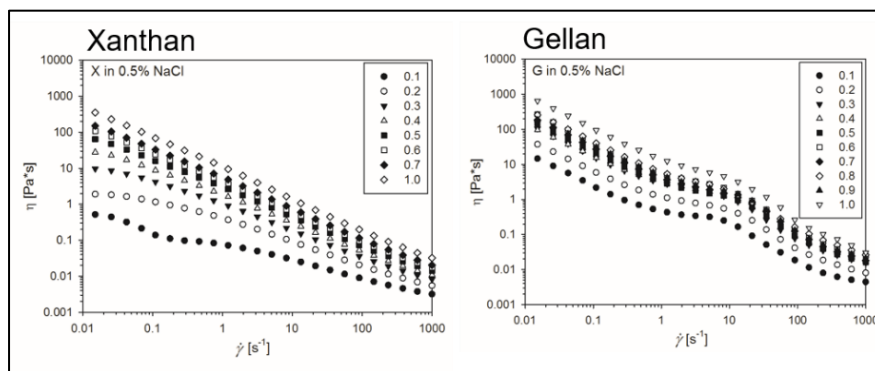


Fig. S2. Creep recovery test of a 0.25% Paenan solution in 0.5% NaCl. A constant stress within the linear viscoelastic range ($\tau = 1$ Pa) was applied for 650 s before release.

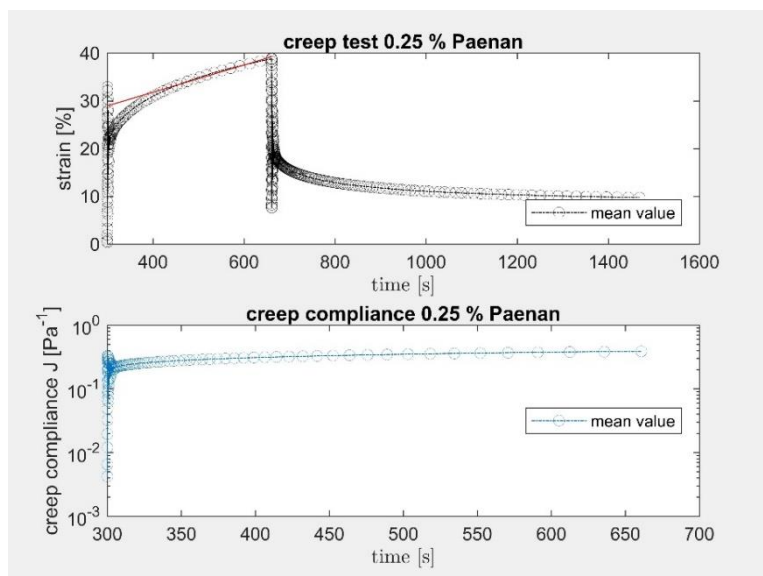


Fig. S3. Viscosity curves of 0.25% Paenan, 0.7% Xanthan, and 0.6% Gellan. Shown effect-concentrations were selected for EPS/surfactant systems, as imparted viscosities are relevant to potential applications.

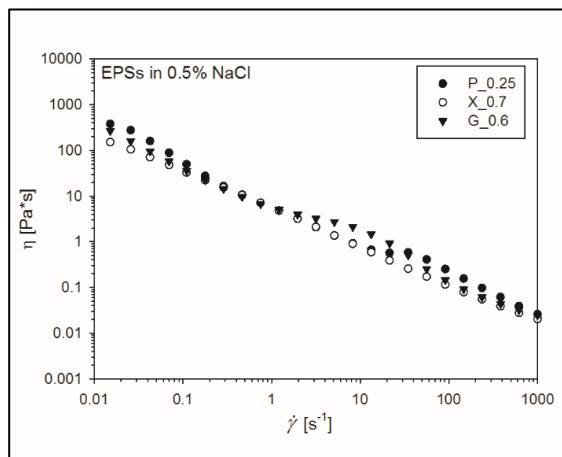
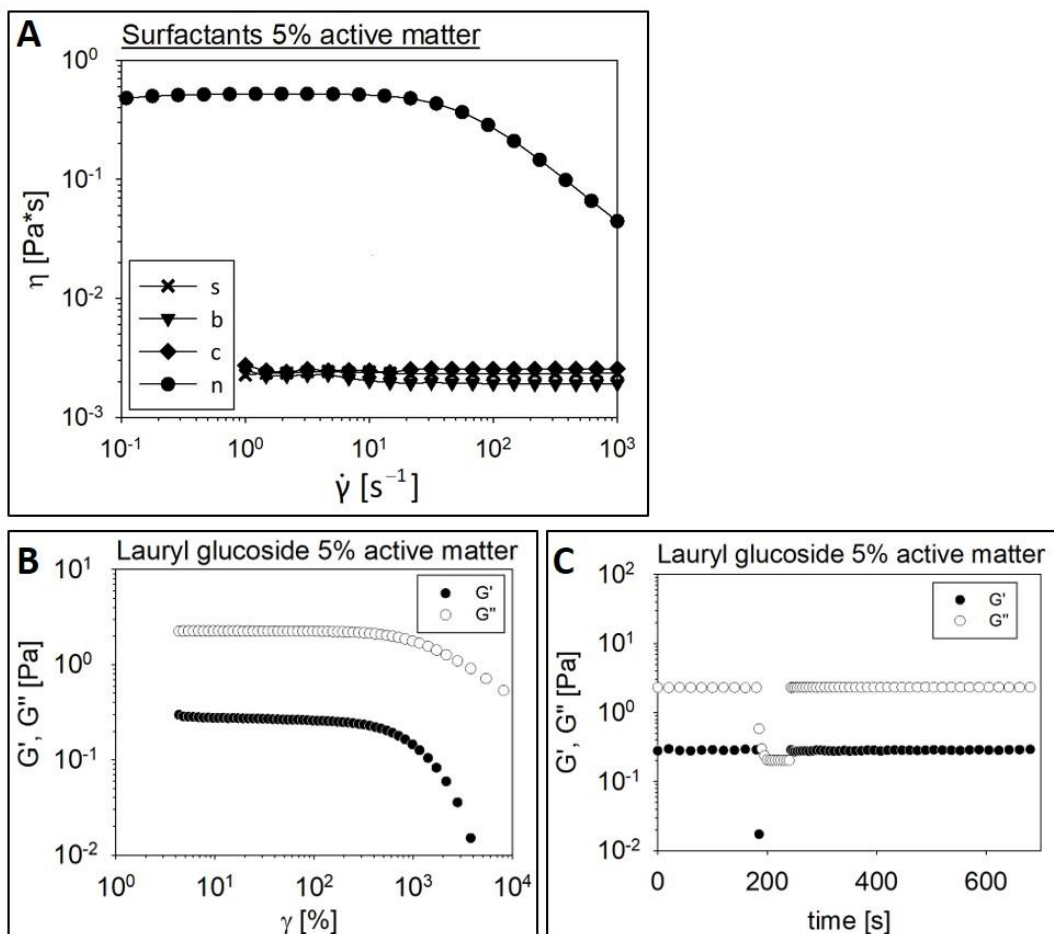


Fig. S4. Rheological measurements of surfactant solutions. (A) Viscosity curves of investigated surfactants at 5% active matter concentration. Sodium lauryl ether sulfate (s), cetrimonium chloride (c), and cocamidopropyl betaine (b) show Newtonian flow behavior at low viscosity, indicating the absence of a superstructure. Lauryl glucoside (n) exhibits a distinct self-viscosity, which has to be considered



when assessing the rheology of EPS/surfactant mixtures. **(B)** Amplitude sweep test of lauryl glucoside. **(C)** Thixotropy test of lauryl glucoside.

Fig. S5. Frequency sweeps of selected Xanthan concentrations in 0.5% NaCl. The G'/G'' crossover point moves to lower frequencies if EPS concentration increases. However, the fundamental character of a Maxwell fluid remains.

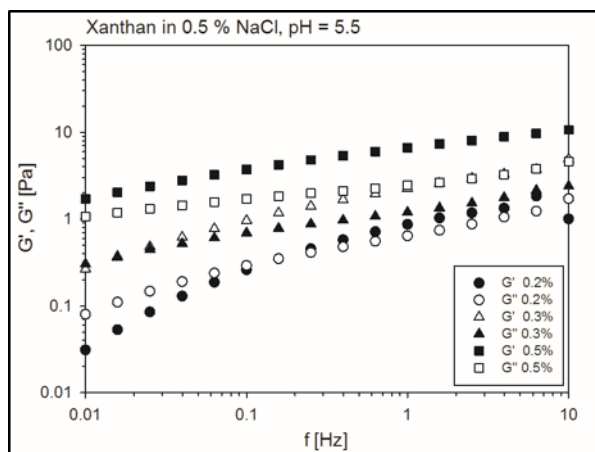


Table S1. Yield stress values of Paenan (0.25%), Xanthan (0.7%), and Gellan (0.6%) in combination with 5% active matter surfactant of each class.

Surfactant	Yield stress values [Pa], limit of LVR		
	Paenan	Xanthan	Gellan
none	3.2 ± 0.0	5.1 ± 0.0	1.8 ± 0.4
n	11.1 ± 0.6	7.5 ± 0.4	0.8 ± 0.2
s	2.0 ± 0.1	5.1 ± 0.5	5.8 ± 0.7
b	3.9 ± 0.2	5.1 ± 0.5	n.d.*
c	4.1 ± 0.4	n.d.*	n.d.*

*not determined

Table S2. Gel strengths for Paenan (0.25%), Xanthan (0.7%), and Gellan (0.6%) in combination with 5% active matter surfactants of each class.

Surfactant	Gel strength [Pa], G' at 0.01 Hz		
	Paenan	Xanthan	Gellan
none	4.3 ± 0.2	4.5 ± 0.1	551.0 ± 100.6
n	n.d.*	3.1 ± 0.1	308.5 ± 9.5
s	2.1 ± 0.2	7.9 ± 0.4	109.0 ± 0.0
b	2.8 ± 0.1	5.2 ± 0.0	n.d.*
c	3.8 ± 0.0	n.d.*	n.d.*

*not determined

3.4 Genome sequencing – *Paenibacillus* sp. 2H2

To evaluate the molecular basis for the production of EPSs in *Paenibacillus* sp. 2H2 (strain assessed in 3.2 and producer of Paenan), the whole genome of the organism was sequenced. For this, genomic DNA was isolated as described in section 2.4.3 and the whole-genome shotgun sequence was obtained by an Illumina MiSeq run. DNA library preparation and sequencing was performed by Christopher Huptas at the Chair of Microbial Ecology (Zentralinstitut für Ernährungs- und Lebensmittelforschung, ZIEL). Obtained reads were trimmed and quality filtered using TrimmingReads.pl (194), cutadapt (195), and DynamicTrim.pl (196). Quality assessment was done using FastQC (<http://www.bioinformatics.babraham.ac.uk/projects/fastqc/>) and SolexaQA (196). Assemblies were carried out using Velvet 1.2.08 (197).

In total 8,208,390 reads were generated, reaching a depth of 171-fold genome coverage. For assembly, all *k-mer* values from 17 to 185 were examined. The assembly using a *k-mer* length of 57 yielded the longest contig (3,305,932 bp) with a total sequence length of 6,057,843 bp. This data set was used for further analyses. The draft genome is made up of 212 contigs with a GC content of 45.3% (Figure 3.2). Annotation was carried out by uploading the generated scaffolds to RAST (198), which found 5,709 coding sequences, comprising 1,891 genes in several subsystems. Furthermore, RAST analysis detected 89 RNA genes. In total, 72 features could be attributed to EPS and CPS synthesis. The putative EPS biosynthesis cluster of *Paenibacillus* sp. 2H2 was determined by detailed analysis of the identified coding sequences. Thorough manual annotation of clustered, EPS related genes yielded a locus comprising 28 non-regulatory genes, which are probably involved in the production and secretion of EPSs via the Wzx/Wzy biosynthesis pathway (Figure 3.2).

The phylogenetic assignment based on 16S rDNA analyses (see chapter 3.2) had revealed that *P. jamilae*, *P. peoriae* and *P. polymyxa* are the closest relatives of *Paenibacillus* sp. 2H2 (199). Analyses of DNA sequence similarities of the entire EPS cluster to available genomes of the afore-mentioned *Paenibacillus* species revealed that the assigned locus exhibits a 97% DNA sequence similarity to the putative EPS cluster of *P. polymyxa* DSM 365 and a 90% similarity to that of *P. peoriae* KCTC3763. A genome sequence of a *P. jamilae* strain was not available at the time of this study.

The experimental proof of the functionality of the EPS cluster was subject to a follow up study (see chapter 3.5). As part of this, a genome-editing tool had to be developed. In order to provide a system, amenable to several research groups, this work was conducted in the type strain *P. polymyxa* DSM 365.

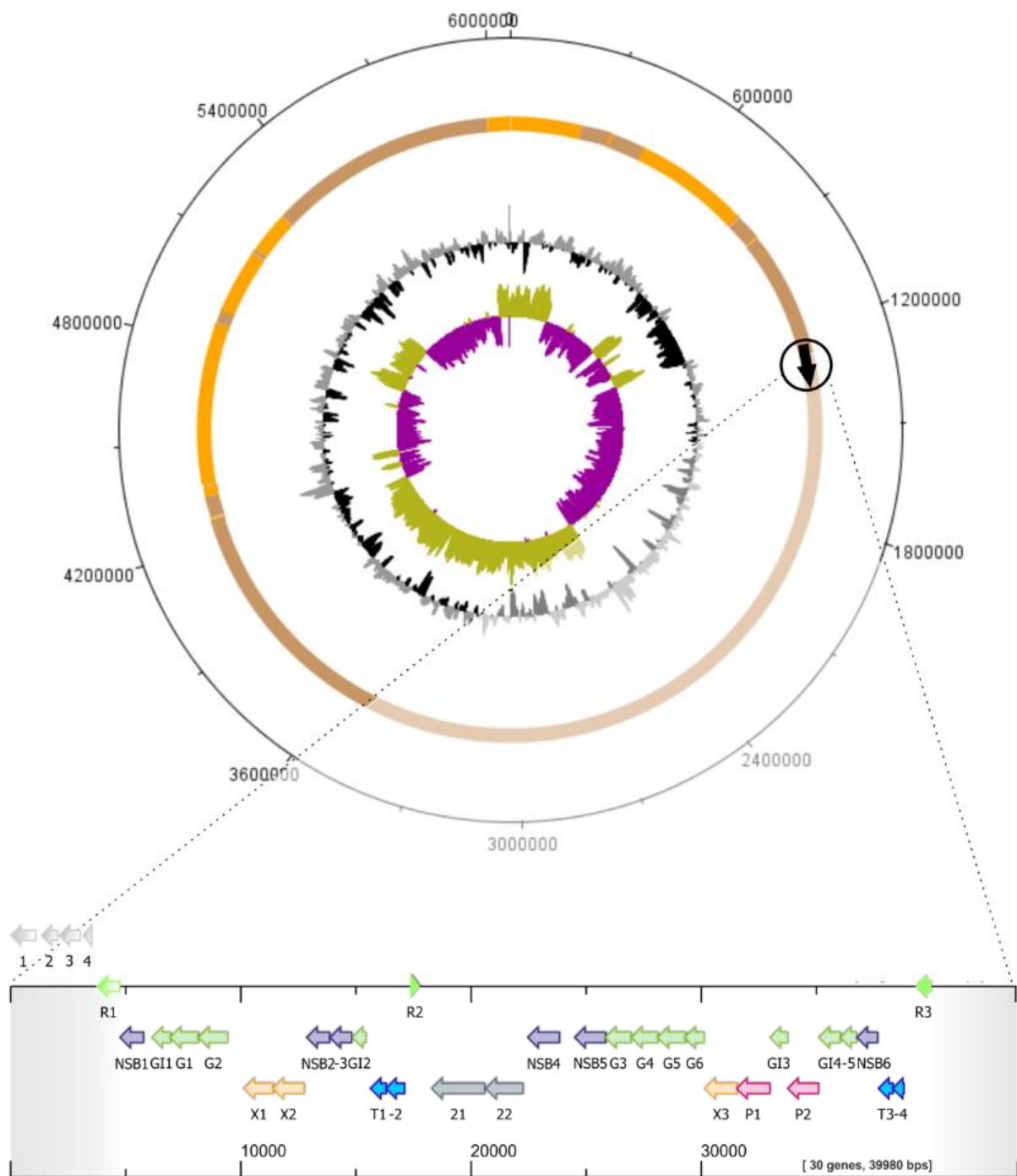


Figure 3.2. Genome map and putative EPS cluster of *Paenibacillus* sp. 2H2.

The different circles of the genome map (top) represent (from inside): GC-skew to identify origin and terminus of the chromosome; GC content to map gene-rich regions within the genome; string together of sequenced contigs (the locus of the found EPS cluster is indicated by a black arrow); Scale.

The putative EPS cluster is depicted at the bottom. Blue arrows represent genes that are putatively involved in chain length determination. Purple arrows represent genes for nucleotide sugar synthesis. Pink arrows indicate genes encoding polymerases. Green arrows on top are regulatory genes and light green arrows show genes that are annotated glycosyl transferases. Orange arrows represent genes encoding flippases and grey arrows show genes that could not be annotated unambiguously.

3.5 Tailor-made Exopolysaccharides – CRISPR-Cas9 mediated genome editing in *Paenibacillus polymyxa*

This research article describes the implementation and application of a CRISPR-Cas9 based vector system (pCasPP) in a *P. polymyxa* type strain, enabling fast and reliable genome edits in this host. The design of the pCasPP plasmid was inspired by a CRISPR-Cas9 vector system, which was successfully used in *Streptomyces* (pCRISPRomyces-2.) The combination of pCRISPRomyces-2 with essential elements of a plasmid that was readily taken up by the utilized *Paenibacillus* strain (pUB110) yielded a system allowing for highly efficient deletions of single genes and larger regions, as well as insertions. Single gene deletions via homology directed repair resulted in several hundred *P. polymyxa* conjugants per experiment with all tested clones showing the desired mutation. A robust curing procedure was also established, enabling the removal of pCasPP plasmids from edited strains and thereby facilitating sequential edits in a single strain.

Furthermore, the putative gene cluster, responsible for EPS biosynthesis in *P. polymyxa*, was thoroughly annotated by mining a published *P. polymyxa* genome. The size of the locus is at the high end of known bacterial EPS gene clusters, spanning almost 35 kb and comprising 28 coding sequences that could be assigned to polysaccharide production or hydrolysis. The encoded proteins suggest that EPS assembly and secretion in *P. polymyxa* follows the Wzx/Wzy dependent pathway.

Subsequently, the implemented pCasPP vector system was utilized to proof the functionality of the EPS gene cluster experimentally and to generate tailored polymer variants. For this, five genes, probably involved in monomer assembly and precursor synthesis, were deleted individually and mutant EPSs were produced and analytically characterized. In addition, an 18 kb fragment of the EPS locus was deleted, to generate an EPS deficient mutant. Analysis of the sugar monomer compositions of generated EPS variants and investigations on protein sequence similarities to already annotated enzyme functionalities, suggested putative biochemical functions of several key genes of the biosynthetic pathway for EPS production. This gives a first basic understanding of the yet undescribed EPS biosynthesis in *P. polymyxa*. Furthermore, some of the generated mutant EPSs showed a significantly altered monomer composition and the rheological characterization of one of these mutants revealed that also physicochemical properties were changed fundamentally. Hence, these results exemplify the possibility of EPS tailoring through genetic recoding to generate custom-made polymers for various applications.

The design and planning of this study, was performed by the author and Jochen Schmid. All experiments were conducted by the author. Construction of the pCasPP plasmid was performed in collaboration with Brady F. Cress. Scientific support for analytical measurements was provided by Broder Rühmann. The co-authors contributed to content and language of the manuscript and gave scientific or technical advice in certain issues.

Tailor-made Exopolysaccharides – CRISPR-Cas9 mediated genome editing in *Paenibacillus polymyxa*

Marius Rütering, Brady F. Cress, Martin Schilling, Broder Rühmann, Mattheos A. G. Koffas, Volker Sieber and Jochen Schmid

Synthetic Biology
(2017)

DOI: 10.1093/synbio/ysx007



Synthetic Biology, 2017, 2(1): ysx007

doi: 10.1093/synbio/ysx007

Research article

Tailor-made exopolysaccharides—CRISPR-Cas9 mediated genome editing in *Paenibacillus polymyxa*

Marius Rütering^{1,2}, Brady F. Cress^{2,3}, Martin Schilling⁴, Broder Rühmann¹, Mattheos A. G. Koffas^{2,3}, Volker Sieber^{1,5,6}, and Jochen Schmid^{1,*}

¹Chair of Chemistry of Biogenic Resources, Technical University of Munich, Straubing, Germany, ²Center for Biotechnology and Interdisciplinary Studies, Rensselaer Polytechnic Institute, Troy, NY, USA, ³Department of Chemical and Biological Engineering, Rensselaer Polytechnic Institute, Troy, NY, USA, ⁴Evonik Nutrition and Care GmbH, Kirschenallee, Darmstadt, Germany, ⁵Fraunhofer IGB, Straubing Branch Bio, Electro, and Chemocatalysis BioCat, Straubing, Germany and ⁶Catalysis Research Center, Technical University of Munich, Garching, Germany

*Corresponding author. E-mail: j.schmid@tum.de

Abstract

Application of state-of-the-art genome editing tools like CRISPR-Cas9 drastically increase the number of undomesticated micro-organisms amenable to highly efficient and rapid genetic engineering. Adaptation of these tools to new bacterial families can open up entirely new possibilities for these organisms to accelerate as biotechnologically relevant microbial factories, also making new products economically competitive. Here, we report the implementation of a CRISPR-Cas9 based vector system in *Paenibacillus polymyxa*, enabling fast and reliable genome editing in this host. Homology directed repair allows for highly efficient deletions of single genes and large regions as well as insertions. We used the system to investigate the yet undescribed biosynthesis machinery for exopolysaccharide (EPS) production in *P. polymyxa* DSM 365, enabling assignment of putative roles to several genes involved in EPS biosynthesis. Using this simple gene deletion strategy, we generated EPS variants that differ from the wild-type polymer not only in terms of monomer composition, but also in terms of their rheological behavior. The developed CRISPR-Cas9 mediated engineering approach will significantly contribute to the understanding and utilization of socially and economically relevant *Paenibacillus* species and extend the polymer portfolio.

Key words: exopolysaccharides; CRISPR-Cas9; genome editing; *Paenibacillus polymyxa*

1. Introduction

Value-added compounds synthesized by microorganisms, such as alkaloids, flavonoids, terpenoids, polyketides, lipopeptides, biofuels and exopolysaccharides (EPSs), are of huge interest for a variety of applications in the food, medicine, agriculture and consumer goods industries (1–3). Although advances in synthetic biology and metabolic engineering have significantly contributed to the design of improved microbial factories, robust heterologous expression of complex pathways is often hampered by

product toxicity, low yields and the absence or insufficient availability of biosynthetic precursors (4, 5). State-of-the-art genome editing tools like CRISPR-Cas9 rapidly increase the accessibility of undomesticated strains to genetic engineering, and therefore pave the way for taming wild-type (WT) species in order to construct new, biotechnologically relevant production strains (6). Thorough implementation of such tools in a species of interest is of fundamental importance for efficient rewiring of metabolic circuits and optimization or alteration of the produced

Submitted: 26 August 2017; Received (in revised form): 24 October 2017. Accepted: 16 November 2017

© The Author 2017. Published by Oxford University Press.

This is an Open Access article distributed under the terms of the Creative Commons Attribution Non-Commercial License (<http://creativecommons.org/licenses/by-nc/4.0/>), which permits non-commercial re-use, distribution, and reproduction in any medium, provided the original work is properly cited. For commercial re-use, please contact journals.permissions@oup.com

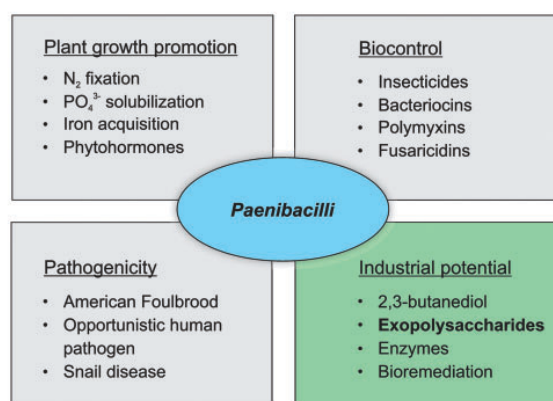


Figure 1. Relevance of *Paenibacilli* for agriculture, society and industry. The main subject of this study, exopolysaccharides, are highlighted. A detailed review on all aspects can be found in reference (36).

metabolites. Gram-positive bacteria of the phylum firmicutes are promising candidates for this endeavor. Their robustness toward environmental stress in combination with their promiscuity toward different carbon sources, the huge variety in gene clusters dedicated to secondary metabolite production and their well-established cultivability exemplify their potential as customizable microbial factories (7–11). Several genera of this phylum, like *Lactobacillus* and *Clostridium*, have been used in biotechnology for centuries, both consciously and unconsciously (12,13). Numerous recent studies demonstrated the successful application of CRISPR-Cas9 in a variety of firmicute families including *Bacillaceae*, *Lactobacillaceae*, *Clostridiaceae* and *Staphylococcaceae* (14–19). However, no reports on CRISPR-Cas9 based genome editing tools for *Paenibacillaceae* are available yet, and existing genetic engineering approaches are limited due to low efficiencies or the dependence on integration of selectable markers (20,21). Nevertheless, this family comprises several species of economic and social relevance (Figure 1). *Paenibacillus larvae*, for example, is the causative agent of American Foulbrood, a lethal disease of honeybee larvae (22), posing grave concern for the future of agriculture, and some *Paenibacilli* are known to be opportunistic human pathogens (23,24). Easily deployable vectors facilitating rapid elucidation of the genetic basis for pathogenicity, immunogenicity and toxicity would hold tremendous scientific value. On the constructive side, numerous studies describe the beneficial use of *Paenibacilli* in miscellaneous fields. In agriculture, they are critical because of their intrinsic capacity for nitrogen fixation (25) and phosphate solubilization (26), thereby directly promoting plant growth. Furthermore, they produce a variety of insecticides (27) and antimicrobials like polymyxins (28) and fusaricidins (29), which protect plants from phytopathogens and have potential use in medical applications. Their extensive enzymatic capabilities to degrade complex carbohydrates and to produce and tolerate high levels of commercially relevant chemicals like 2,3-butanediol, for example, make *Paenibacilli* an interesting genus for the fermentative production of this and other platform chemicals from renewable resources (30). Critically, they produce a class of still underappreciated but highly promising EPSs possessing antioxidant activity and outstanding rheological properties, qualifying them for applications in therapeutics or as thickeners (31–35). Grady *et al.* (36) recently reviewed the potential of *Paenibacilli* in agriculture and industrial biotechnology in detail.

EPSs are linear or branched, high-molecular weight polymers composed of sugars molecules, which are secreted into the extracellular environment during microbial growth. Due to variations in monomer composition, molecular weight and decoration with functional groups, these polymers exhibit an immense physicochemical versatility making them interesting for various applications (37). This structural variability is highlighted by the existence of over 350 annotated EPSs from prokaryotes (38). EPSs have been primarily used as rheological additives for food, agricultural feed, oil recovery and cosmetic applications (39). Prominent representatives of commercialized EPSs are sphinganes, xanthan, pullulan, dextran and levan (40–42). Although these compounds hold big shares of the markets for bio-based viscosifiers and gelling agents, they are only narrowly suited for specialized applications matching their imparted rheologies. Especially high-value niche applications like tissue engineering, cell encapsulation or drug delivery require explicitly defined physicochemical characteristics, which are not covered by the existing EPSs (43) without further, post-biosynthetic chemical or enzymatic modification.

Using synthetic biology for design and synthesis of tailor-made EPSs is a highly promising approach to fill these gaps. The aforementioned structural diversity of existing EPSs makes their associate biosynthetic pathways ideal templates for generating polymers with tunable properties through the rational engineering of novel structures (44). Typical targets for EPS engineering are functional groups like pyruvyl groups, which contribute to polymer charge density and thereby influence the rheological traits (45). However, the adjustment of substituent patterns only allows for alterations in the degree of superficial decorations while leaving the core, underlying glycan structure and sequence unchanged. Other engineering targets are the glycosyltransferases (GTs), which transfer defined sugar moieties to the nascent, pre-assembled repeating units and thereby determine the composition and linkage pattern of the mature EPS (46,47). Complementation experiments have shown that exchange of GTs with distinct monosaccharide preferences is feasible, indicating that the EPS polymerization and secretion machinery of one organism can potentially be harnessed for the production of various polymers with disparate structures and properties (37). The combination of in-depth characterizations of known and to-be-discovered GTs with protein-engineering will eventually yield a catalog of enzymes, which can be used for the directed incorporation of user-specified sugars imparting desired properties (48). Polymer variants produced in this fashion will successively contribute to the still superficial understanding of EPS structure–function relationships and thereby ultimately allow for the rational design of application-defined properties (43). Modern synthetic biology tools, such as CRISPR-Cas9, will not only facilitate engineering of structural features but will also drastically accelerate strain improvements, spurring the rise of robust and economical production processes for competitive, custom-made EPSs.

In this study, we describe the development of a CRISPR-Cas9 based genome-editing tool for *Paenibacillus polymyxa*. The single plasmid system was employed for highly efficient, homology directed deletions as well as integrations. The developed CRISPR method was subsequently used to annotate and provide the first experimental evidence of the gene cluster responsible for EPS biosynthesis in *P. polymyxa* DSM 365. Besides shutting down and significantly attenuating EPS biosynthesis, we were also able to produce structurally altered EPSs exhibiting fundamentally distinct rheological properties. On the basis of these findings, putative substrate specificities of two GTs were assigned.

We envision that this system will be used to further decipher and harness the EPS biosynthesis machinery of *P. polymyxa* in order to construct a generic host, capable of producing polymers with disparate structures. Furthermore, the CRISPR method developed here should expedite investigation of several other important fields related to *Paenibacilli*, including production of value-added chemicals or answering fundamental questions about host-pathogen interactions for socially important diseases caused by *Paenibacilli*, like the American Foulbrood.

2. Materials and methods

2.1 Plasmids, bacterial strains, primers and growth conditions

The bacterial strains, plasmids and oligonucleotides used in this study are listed in [Supplementary Tables S1–S3](#). *Escherichia coli* strains were grown in Lysogen-broth (LB; 10 g l⁻¹ sodium chloride, 10 g l⁻¹ peptone and 5 g l⁻¹ yeast extract) at 37 °C. *Paenibacillus polymyxa* DSM365 (DSMZ, Braunschweig, Germany) was cultured at 30 °C in LB for genetic manipulations and in MM1 P100 for EPS production and phenotype evaluations [30 g l⁻¹ glucose, 1.33 g l⁻¹ magnesium sulfate heptahydrate, 1.67 g l⁻¹ potassium dihydrogen phosphate, 0.05 g l⁻¹ calcium chloride dihydrate, 2 ml l⁻¹ RPMI 1640 vitamins solution (Sigma-Aldrich) and 1 ml l⁻¹ trace elements solution containing 2.5 g l⁻¹ iron (II) sulfate heptahydrate, 2.1 g l⁻¹ sodium tartrate dihydrate, 1.8 g l⁻¹ manganese (II) chloride tetrahydrate, 0.075 g l⁻¹ cobalt (II) chloride hexahydrate, 0.031 g l⁻¹ copper (II) sulfate heptahydrate, 0.258 g l⁻¹ boric acid, 0.023 g l⁻¹ sodium molybdate and 0.021 g l⁻¹ zinc chloride] (32). Antibiotics were added at 50 µg ml⁻¹ for neomycin and 20 µg ml⁻¹ for polymyxin.

2.2 Construction of pCasPP

For construction of the pCasPP plasmid, the Cas9 gene was amplified alongside with the BbsI flanked lacZ cassette from pCRISPRomyces-2, which was a gift from Huimin Zhao (Addgene plasmid # 61737). The neomycin resistance and the repU gene were amplified from pUBorIMCS, which is a pUB110 derivative (49), containing a BbsI inserted origin of replication as well as a multiple cloning site from pUC18. A BsaI site within repU was removed by introducing a silent mutation with the utilized primers. The *sgsE* promoter (50) was obtained as artificial gBlock (Integrated DNA Technologies). A cytosine was replaced by a guanine to delete an interfering BbsI site. All five fragments were assembled via Golden Gate using BsaI. The oriT was amplified from pCRISPRomyces-2 and cloned into a XbaI restriction site afterwards. Subsequently, the unique SpeI site was added by introducing the desired sequence mutations while PCR-amplifying the pCasPP plasmid in two pieces with corresponding primers. To inactivate Cas9, the same procedure was deployed and the two active sites were mutated to D10A and H840A, yielding pdCasPP. All cloning and mutation steps were verified by sequencing (Eurofins, Ebersberg, Germany).

2.3 Bioinformatics

In order to identify genes involved in EPS biosynthesis, the *P. polymyxa* DSM 365 genome was uploaded to RAST for automated genome annotation (51). Obtained data was screened manually and putatively identified genes involved in EPS-biosynthesis were annotated in detail using NCBI blastx (52) and UniProt blast (53). Intracellular protein localizations were predicted using CELLO v.2.5 (54). Biosynthetic pathways

involved in nucleotide sugar production were identified using KEGG (55). Twenty base pair long spacers for Cas9 mediated edits were selected based on on- and off-target scores determined with benchling (<http://www.benchling.com>) using NGG as PAM motif and the uploaded *P. polymyxa* DSM 365 genome as reference. In silico cloning and sequence alignments were performed with SnapGene software (GSL Biotech, Chicago, IL, USA).

2.4 Genome editing in *Paenibacillus polymyxa* DSM 365

CRISPR-Cas9 mediated genome editing in *P. polymyxa* DSM 365 was performed as follows. Subsequent to spacer selection using benchling (<http://www.benchling.com>), 24 bp oligos for guide annealing were designed as described in the supplemental material of Cobb et al. (56). Oligonucleotides were phosphorylated, annealed and finally inserted into the pCasPP backbone via Golden Gate assembly. Subsequent to guide cloning, homologous regions were constructed by overlap extension PCR and inserted by restriction and ligation into the SpeI site. A detailed description of the entire cloning procedure can be found in the [supplementary information](#). Constructed plasmids were sequenced and then transferred to *E. coli* S17-1 for conjugation events. Plasmid transfer from *E. coli* S17-1 to *P. polymyxa* DSM 365 was performed as follows. Overnight cultures of recipient and donor strains were subcultured 1:100 in non-selective or selective LB media, respectively, and grown until early exponential phase (4 h). Afterwards, 900 µl of the recipient culture were heat shocked for 15 min at 42 °C and mixed with 300 µl of the donor strain culture. Cells were harvested by centrifugation for 3 min at 8000 × g and the pellet was gently resuspended and dropped on non-selective LB agar. After overnight incubation at 30 °C, cells were scraped from the agar, resuspended in 500 µl 0.9% NaCl and plated on LB agar containing neomycin and polymyxin for counter selection. *Paenibacillus polymyxa* conjugants were obtained after 48 h incubation at 30 °C and screened for editing events using colony PCR. Sequence verification of genome edits was performed by amplifying edited regions from isolated genomic *P. polymyxa* DNA using suitable primers. Obtained PCR products were purified, adjusted to a concentration of 10 ng µl⁻¹, mixed with corresponding primers, and sent for sequencing.

2.5 EPS production and purification

For polymer production, baffled 250 ml shake flasks sealed with aluminum caps were filled with 100 ml MM1 P100 media and inoculated with 1 ml of a *P. polymyxa* overnight culture. Cultures were incubated at 30 °C and 170 rpm for 28 h. To extract EPS from shake-flask experiments, the culture broth was diluted 1:3 with distilled water to decrease viscosity and centrifuged for 30 min at 17 600 × g and 20 °C to separate cells. Subsequently, EPS was precipitated by slowly pouring the supernatant into two volumes of 2-propanol. The precipitated polymer was collected using a spatula and dried overnight at 45 °C in a VDL 53 vacuum drying oven (Binder, Tuttlingen, Germany).

2.6 Molecular weight determinations

Gel permeation chromatography was performed using an Agilent 1260 Infinity system (Agilent Technologies, Waldbronn, Germany) equipped with a refractive index detector and a SECurity SLD7000 7-angle static light-scattering detector (PSS Polymer Standards Service GmbH, Mainz, Germany). Samples were analyzed using a Suprema guard column, one Suprema 100 Å (8 × 300 mm) and two

Suprema 10 000 Å (8×300 mm) columns (PSS Polymer Standards Service). The eluent, 0.1 M LiNO₃, was pumped at a flow rate of $1 \text{ ml} \cdot \text{min}^{-1}$ and the column compartment was kept at 50°C . Samples were injected in 60 min intervals. Qualitative molecular weight results were obtained by comparing sample elution profiles with a 12-point pullulan standard curve.

2.7 Carbohydrate fingerprint

Simultaneous high resolution detection of carbohydrates which can be derivatized with 1-phenyl-3-methyl-5-pyrazolone (PMP) was performed via HT-PMP as described before (57). Briefly, $1 \text{ g} \cdot \text{l}^{-1}$ solutions of EPS were hydrolyzed in 2 M trifluoroacetic acid (TFA) for 90 min at 121°C and subsequently neutralized with 3.2% (v/v) ammonium hydroxide. Thereafter, $25 \mu\text{l}$ neutralized sample were mixed with $75 \mu\text{l}$ derivatization reagent (0.1 M methanolic-PMP-solution:0.4% ammonium hydroxide solution 2:1) and incubated for 100 min at 70°C . Finally, $130 \mu\text{l}$ of 19.23 mM acetic acid were added to $20 \mu\text{l}$ cooled sample and HPLC separation was performed on a reverse phase column (Gravity C18, 100 mm length, 2 mm i.d.; $1.8 \mu\text{m}$ particle size; Macherey-Nagel) tempered to 50°C . For gradient elution, mobile phase A [5 mM ammonium acetate buffer (pH 5.6) with 15% acetonitrile] and mobile phase B (pure acetonitrile) were pumped at a flow rate of $0.6 \text{ ml} \cdot \text{min}^{-1}$. The HPLC system (Ultimate 3000RS, Dionex) was composed of a degasser (SRD 3400), a pump module (HPG 3400RS) auto sampler (WPS 3000TRS), a column compartment (TCC3000RS), a diode array detector (DAD 3000RS) and an ESI-ion-trap unit (HCT, Bruker). Standards for each sugar (2, 3, 4, 5, 10, 20, 30, 40, 50 and $200 \text{ mg} \cdot \text{l}^{-1}$) were processed as the samples, starting with the derivatization step. Data were collected and analyzed with BrukerHystar, QuantAnalysis and Dionex Chromelion software.

2.8 Pyruvate assay

To determine the pyruvate content of the polymers, $1 \text{ g} \cdot \text{l}^{-1}$ EPS solutions were hydrolyzed and neutralized as described for the sugar monomer analyses (58). To start the reaction, $10 \mu\text{l}$ neutralized sample + $90 \mu\text{l}$ of ddH₂O or standard were mixed with $100 \mu\text{l}$ assay mixture [50 μM N-(carboxymethylamino-carbonyl)-4,4'-bis(dimethylamino)-diphenylamine sodium salt (DA-64), 50 μM thiamine pyrophosphate, 100 μM MgCl₂ $\times 6\text{H}_2\text{O}$, 0.05 U $\cdot \text{ml}^{-1}$ pyruvate oxidase, 0.2 U $\cdot \text{ml}^{-1}$ horseradish peroxidase, 20 mM K₂PO₄ buffer pH 6] and incubated at 37°C , 700 rpm for 30 min in a micro-plate shaker. The extinction was measured at 727 nm and subtracted with values measured at 540 nm to eliminate background signals. Nine standards in the range from 0.5 to 100 μM pyruvate were used for calibration.

2.9 Rheological measurements

Rheological measurements were performed with an air-bearing MCR300 controlled-stress rheometer (Anton Paar Germany GmbH) using a cone plate geometry (50 mm diameter, 1° cone angle, 0.05 mm gap) at a constant, Peltier-controlled temperature of 20°C . Data was collected and analyzed with Rheoplus V.3.61 software (Anton Paar). Viscosity curves were obtained during a logarithmic shear-rate ramp ($\dot{\gamma} = 0.1\text{--}1000 \text{ s}^{-1}$). The linear viscoelastic range and further structural features of polymer solutions were determined with a shear stress amplitude sweep from 0.1 to 1000 Pa at a constant frequency of $f = 1 \text{ Hz}$. Time dependent flow behavior at non-destructive stress was assessed during frequency sweeps

from 0.01 to 100 Hz. All measurements were carried out in triplicates.

3. Results and discussion

3.1 CRISPR-Cas9 vector system

Design and construction of the pCasPP CRISPR-Cas9 expression plasmid (Figure 2) was inspired by a vector system which was efficiently used for genome editing in *Streptomyces* (56). *Streptococcus pyogenes* Cas9 (SpCas9) and synthetic guide RNA (sgRNA) region, including the BbsI flanked lacZ selection cassette and origin of transfer (oriT), were amplified from pCRISPRomyces-2 plasmid. The Cas9-encoding gene was set under transcriptional control of the broad-host-range S-layer gene promoter sgsE from *Geobacillus stearothermophilus*, which was previously shown to be functional in *Paenibacillus alvei* (21,50). Since the transcription start for guide expression is crucial for guide length and thereby targeting efficiency, the constitutive *gapdh* promoter for sgRNA expression was not changed. To the best of our knowledge, this is the first report on *gapdh* promoter functionality in *Paenibacilli*. Origin of replication (ori), neomycin resistance gene and the *repU* gene, involved in plasmid replication (59), were amplified from pUBori, a pUB110-derived plasmid which is readily taken up and propagated by *P. polymyxa* (unpublished data). All DNA parts were assembled using Golden Gate cloning (60). A unique SpeI site was utilized for insertion of homologous arms (1 kb upstream and 1 kb downstream, fused by overlap extension PCR), necessary for homology directed repair (HDR) after successful double strand break by the activity of Cas9.

Insertion of 20 bp long single guide spacers was performed via BbsI based Golden Gate cloning of annealed and phosphorylated primers. For multiplexing, gBlocks comprising two copies of the sgRNA region were utilized as described for the pCRISPRomyces-2 system (56). Plasmid transfer to *P. polymyxa* DSM 365 was conducted via conjugation using the *E. coli* S17-1 donor strain and counter-selection on polymyxin-containing media. The functionality of the designed system was first tested on a putative glycosyltransferase (*pepF*) of the hypothetical EPS cluster. Using this target, different variants of the pCasPP plasmid were assembled, and transformation efficiencies were evaluated (Table 1, Supplementary Figure S1).

Guided Cas9 resulted in high lethality in the absence of a repair template, yielding less than 0.2% colonies compared to the dummy plasmid pCasPP. Although not examined further, it is likely that these colonies resulted from escape mutation as reported by others (61). When a HDR template was included, the survival rate increased significantly, and >200 clones were obtained, independently of the chosen spacer. A plasmid containing a non-targeting gRNA and homologous arms resulted in less conjugants than the dummy, which is probably due to reduced conjugation efficiency of the larger vector, but in noticeably more colonies than the guided variants. Colony PCR confirmed that all tested colonies transformed with the guided plasmid containing a repair template were successful knockout events (eight individual conjugants), whereas tested colonies from all other plasmid transformations showed to be the unedited WT (Supplementary Figure S2). Sequencing of at least three clones from pCasPP, pCasPP-pepFsg1 and pCasPP-pepFsg1-harms corroborated this finding. These results suggest that the non-homologous end-joining (NHEJ) DNA repair based on the Ku and LigD enzymes is not functional or insufficient to introduce indels in *P. polymyxa*, although the required genes for NHEJ are encoded within the organism's genome (62). To more

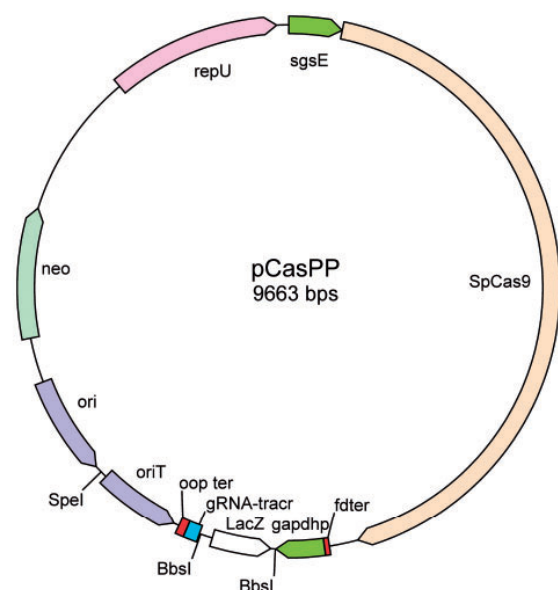


Figure 2. CRISPR-Cas9 vector system. Promoter *sgsE* controls *SpCas9* expression, *gapdh* promoter regulates guide RNA levels. Spacer insertion is performed via Golden gate using *BbsI*. The unique *SpeI* site allows for insertion of homologous regions for HDR.

Table 1. Conjugation efficiency of different pCasPP derivatives

Plasmid	Colonies/ conjugation	Description
pCasPP	>10 000	Non-targeting plasmid; no repair template
pCasPP-pepFsg1	<20	Targeting <i>pepF</i> at Site 1; no repair template
pCasPP-pepFsg1-harms	>200	Targeting <i>pepF</i> at Site 1; repair template provided
pCasPP-pepFsg2-harms	>200	Targeting <i>pepF</i> at Site 2; repair template provided
pCasPP-harms	>1000	Non-targeting plasmid; repair template provided

thoroughly assess the efficiency of the system, another knockout (*UgdH1*, found to result in phenotypically distinguishable colonies as a consequence of reduced EPS production) was investigated. Due to the ease of screening this knockout by colony morphology, a much larger sample of 50 colonies for each of two distinct spacers within the *ugdH1* ORF were analyzed for their phenotypic appearance. Edited conjugants appeared as irregular, flat, opaque colonies with a brittle, dry consistency. WT colonies in contrast were loosely attached, circular and convex with a highly mucoid consistency. All conjugants for both spacers showed the phenotype consistent with an edited strain (Supplementary Figure S3). For all other edits described in this study, at least eight isolated colonies were analyzed using colony PCR, and each successful knockout was verified via sequencing.

In order to perform deletions in series, it is critical that the CRISPR-Cas9 plasmid is curable, so that the vector can be recursively transformed with new sgRNA inserts. Toward this end,

we found that curing of the plasmid after editing was readily achieved by incubating liquid cultures of the knockout mutant for 72 h at elevated temperatures (37°C) in absence of antibiotic with a single 1:100 sub-culturing after 36 h. Curing efficiency was assessed for the WT strain and six knockout strains. Specifically, eight colonies obtained from a culture of each knockout strain (by plating dilution series on non-selective agar) were picked and streaked on neomycin plates to test for neomycin sensitivity and to thus determine the curing efficiency. Out of the eight colonies obtained from subculture of each knockout strain, a cured colony sensitive to neomycin was readily found in each case (typically approximately 75% of tested colonies), confirming that the vector can be cured easily (Supplementary Figure S4). To investigate the possibility of performing genome-integration of heterologous DNA with the constructed system, a 300bp *pgrac* promoter region was cloned between the 1 kb homologous regions of *sacB*, a gene encoding for a levansucrase in the *P. polymyxa* genome, and the editing experiments were performed as described above. All eight tested clones were colony PCR positive and sequencing verified the successful integration of the artificial *pgrac* promoter sequence, proving the functionality of pCasPP for genome integration (Supplementary Figure S5).

3.2 Exopolysaccharide biosynthesis in *Paenibacillus polymyxa* DSM 365

Fundamental mechanisms of polysaccharide synthesis in bacteria have been extensively investigated in organisms such as *E. coli*, *X. campestris* and *S. pneumoniae* (63–65). While research on polysaccharide gene clusters in Gram-negatives started as early as the 1980s, the first studies on EPS genetics in Gram-positive bacteria were published approximately 20 years later (66). The best-characterized clusters of Gram-positive representatives are those of *Lactobacillaceae* and *Streptococcaceae*. EPS production by *Paenibacillaceae* is also described by several reports (34). However, except for the levansucrase catalyzed production of levan in the presence of sucrose as carbon source (67), the genetic basis for the biosynthesis of heteropolysaccharides in this genus is unknown territory. To use the implemented genome editing tool for elucidation and engineering of EPS synthesis, the published *P. polymyxa* DSM 365 genome (62) was mined, and putative EPS-related genes were annotated thoroughly (accession number: BK010330).

The majority of coding sequences putatively involved in EPS synthesis were found clustered together, as is typical for most heteropolysaccharides (37) (Figure 3, Table 2).

The size of the locus is at the high end of known bacterial EPS gene clusters, spanning almost 35 kb and comprising 28 coding sequences that could be assigned to polysaccharide production or hydrolysis. EPS gene clusters from *Lactobacilli* typically comprise 14 to 18 kb (68,69), whereas clusters from *S. thermophilus* can be up to 35 kb in size (70). Interestingly, several functional elements within the *P. polymyxa* DSM 365 EPS-cluster appear to be encoded twice. This could indicate an evolutionary development of the strains towards reliable EPS production. Another explanation could be that the strain is capable of producing two different polymers, with some genes being involved in both pathways (e.g. polymerases and precursors) and some being unique for each polymer (GTs). Some genes associated with precursor supply are encoded one (*ugdH*) or two more times (*manC*, *galU*) at different loci of the genome. *Fcl* and *gmd* are exclusively found within the cluster.

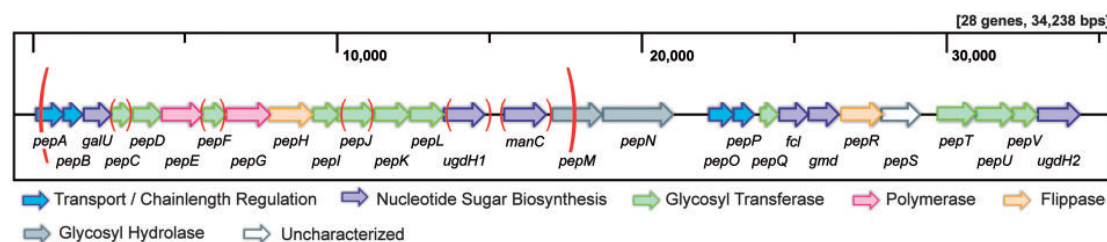


Figure 3. Gene cluster of *P. polymyxa* DSM 365 encoding for exopolysaccharide biosynthesis (accession number: BK010330). Blue arrows represent genes that are putatively involved in chain length determination. Purple arrows represent genes responsible for nucleotide sugar synthesis, pink arrows stand for genes, which encode membrane-spanning polymerases, light green arrows show genes that are annotated glycosyl transferases and orange arrows represent genes encoding flippases. Grey arrows represent genes encoding glycosyl hydrolases. The regions highlighted with red brackets were deleted during knockout experiments.

Table 2. Hypothetical annotation of clustered genes involved in exopolysaccharide biosynthesis

Gene	Length [aa]	Localization ^a	Protein family ^b	Function ^b	Accession number
<i>pepA</i>	302	Membrane	Wzz	Chain length determination	E0RL99
<i>pepB</i>	212	Cytoplasmic, membrane	Wzc	Regulation	A0A074M2H7
<i>galU</i>	300	Cytoplasmic	galU	Precursor	E0RLA1
<i>pepC</i>	232	Cytoplasmic	GT	Priming transferase ^c	E0RLA2
<i>pepD</i>	311	Cytoplasmic	GT2	Transferase, assembly	A0A074LI20
<i>pepE</i>	445	Membrane	Wzy_C	Polymerase	A0A074LD40
<i>pepF</i>	256	Cytoplasmic	WecB (GT26)	Galactosyltransferase ^c , assembly	E0RLA5
<i>pepG</i>	480	Membrane	Wzy_C	Polymerisation	A0A074LK02
<i>pepH</i>	472	Membrane	Wzx	Flippase	A0A074LG88
<i>pepI</i>	279	Cytoplasmic	GT2	Transferase, assembly	A0A074LI22
<i>pepJ</i>	407	Cytoplasmic	GT4	Mannosyltransferase ^c , assembly	A0A074LD42
<i>pepK</i>	382	Cytoplasmic	GT1	Transferase, assembly	A0A074M2I1
<i>pepL</i>	366	Cytoplasmic	GT4	Transferase, assembly	A0A074LK07
<i>ugdH1</i>	445	Cytoplasmic	UDPG_MGDP_dh	Precursor	A0A074LG92
<i>manC</i>	458	Cytoplasmic	PMI	Precursor	E0RLB3
<i>pepM</i>	535	Extracellular	GH26	Hydrolysis	A0A074LD47
<i>pepN</i>	765	Extracellular	Glycoside_hydrolase_SF	Hydrolysis	A0A074M2I4
<i>pepO</i>	270	Membrane	Wzz	Chain length determination	E0RLB8
<i>pepP</i>	228	Membrane	Wzc	Regulation	A0A074LD53
<i>pepQ</i>	192	Membrane	GT	Priming transferase ^c	E0RLC0
<i>fcl</i>	312	Cytoplasmic	Epimerase	GDP-fucose-synthase	A0A074LK14
<i>gmd</i>	329	Cytoplasmic	gmd	Precursor	E0RLC2
<i>pepR</i>	447	Membrane	Wzx	Flippase	A0A074LI33
<i>pepS</i>	420	Cytoplasmic	uncharacterized	unknown	A0A074LD55
<i>pepT</i>	416	Cytoplasmic	GT1	Transferase, assembly	A0A074M2J0
<i>pepU</i>	405	Cytoplasmic	GT1	Transferase, assembly	A0A074LK16
<i>pepV</i>	269	Cytoplasmic	WecB (GT26)	Transferase, assembly	A0A074LGA5
<i>ugdH2</i>	456	Cytoplasmic	UDPG_MGDP_dh	Precursor	E0RLC8

Uncharacterized genes were named alphabetically from *pepA* though *pepV*. Confidently annotated enzymes involved in nucleotide sugar synthesis are named according to standards used in literature.

^aProtein localizations were predicted using CELLO v.2.5.

^bFamily and putative function assignment is based on domain comparisons in the Pfam database.

^cPutative function assignment based on results obtained in this study.

The encoded proteins suggest that EPS assembly and secretion in *P. polymyxa* follows the Wzx/Wzy dependent pathway, which is common in Gram-positive and Gram-negative bacteria and is also utilized for EPS formation in *Lactococci* and *Streptococci* (64). Through this pathway, the repeating units of the polymer are assembled on the inner side of the cytoplasmic membrane by GTs, starting with the transfer of the first sugar to a membrane bound lipid undecaprenyl carrier via the so-called priming GT. Thereafter, the nascent polysaccharide repeating unit is elongated through successive addition of distinct sugars by the other GTs. The fully assembled repeating units are then transferred over the membrane by a Wzx flippase and finally

polymerized by the Wzy protein in reducing-end growth via a block transfer mechanism. A schematic representation of the hypothetical Wzx/Wzy dependent biosynthesis machinery of *P. polymyxa* is presented in Figure 4.

3.3 Exopolysaccharide engineering

The ultimate objective of the presented EPS engineering approach was to alter the chemical structure of the produced EPS in order to influence the physicochemical characteristics of the secreted polymer, yielding EPSs with new or superior material properties.

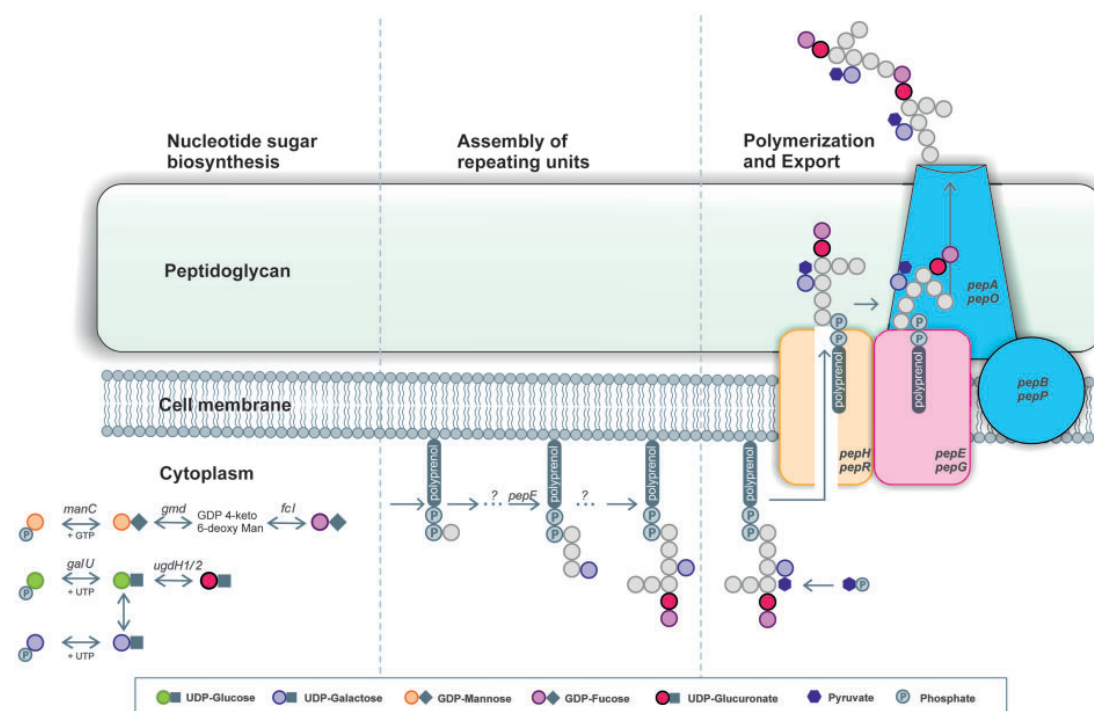


Figure 4. Schematic overview of the putative EPS biosynthesis machinery of *P. polymyxa*. Labeled proteins are encoded in the described gene cluster. Synthesis and interconversion of the different precursors occurs in the cytoplasm. Activated nucleotide sugars are then transferred to the membrane anchored lipid carrier by glycosyl transferases. Colored sugar monomers of the repeating unit are annotations as concluded from mass spectrometry analyses. After assembly, repeating units are transported across the membrane by a flippase (encoded by *pepH* and *pepR*) and then polymerized by *Wzy* (encoded by *pepE* and *pepG*). Chain length determination is probably controlled by *Wzz* (*pepA* and *pepO*) and *Wzc* (encoded by *pepB* and *pepP*) analogs.

To achieve this goal, the developed CRISPR-Cas9 system was deployed for gene disruption studies targeting different genes within the identified EPS cluster. Five different genes were deleted individually, three of which are putative GTs (*pepF*, *pepJ*, *pepC*), and two of which are probably involved in precursor synthesis (*ugdH1*, *manC*). Additionally, an 18 kb fragment was deleted (*clu*), to generate an EPS deficient mutant (Figure 5). Details on the deletion sites can be found in Supplementary Table S4. After successful verification of deletions, strains were cured of the plasmid, and EPS of each mutant and WT strain was produced and purified under standardized conditions in biological triplicates (Table 3). To prevent falsification of EPS data by levan production, the utilized fermentation media contained glucose as sole carbon source. In a previous study, we showed that this media composition results in heteropolysaccharide production only (31).

All mutant strains produced less EPS than the WT, with $\Delta pepF$ and $\Delta pepJ$ still producing relatively high quantities, $\Delta pepC$ and $\Delta ugdH1$ secreting considerably less and with $\Delta manC$ and Δclu not producing any precipitable polymer. Diminished EPS titers after deletions of GTs are in accordance with studies in *Lactobacilli*, *Xanthomonas* and *Streptococci* reporting similar effects upon inactivation of transferases (71–73). In particular, priming GTs are known to be essential for EPS formation, resulting in EPS deficient mutants if deleted. The importance of enzymes involved in biosynthesis of nucleotide sugars is also described in literature. It has been shown many times that levels of key intermediates for nucleotide sugar biosynthesis directly correlate with obtained EPS titers (74). Li et al. (75) described the crucial role of two UDP-xylose synthases (*uxs*) for EPS formation in a related *Paenibacillus* strain,

secreting a xylose containing EPS. Inactivation of the first *uxs* gene reduced EPS titers by 50% and deletion of the second copy abrogated EPS biosynthesis completely. By disruption of the 18 kb fragment (Δclu) in *P. polymyxa*, all genes involved in polymerization (*pepE*, *pepG*) of the glycan were removed, logically resulting in an EPS deficient mutant. Knockout of *manC* creates a mutant that is not capable of producing GDP-Mannose and GDP-Fucose (Figure 6). At least one of these nucleotide sugars is probably an essential building block of the repeating unit, because deletion results in non-polymerizable or non-precipitable carbohydrates.

To characterize the EPSs produced by the *P. polymyxa* mutants and WT strain, molecular weights and monomer compositions of obtained polymers were analyzed. Molecular weights of all polymers were found to be in the same range (Table 3) and comparable to values found for *Paenibacillus* heteropolysaccharides in literature (76).

Of note, the $\Delta manC$ mutant still showed a small but non-negligible polymer peak in GPC analyses, which was in the same order of magnitude in MW as all other polymers, indicating that still some full-length polymer was formed, but too little to allow for processing (Supplementary Figure S6). A possible explanation for this observation is that basal expression of the two other *manC* copies encoded in the genome compensates the deletion to a very little extent. Since regulation of cluster expression is presumably decoupled from the regulation of the other *manC* versions, this compensation is only marginal.

Similar findings were reported for capsule biogenesis in *Streptococci* (77). No polymer peak was observable by GPC for the Δclu mutant, experimentally proving that EPS biosynthesis was eliminated.

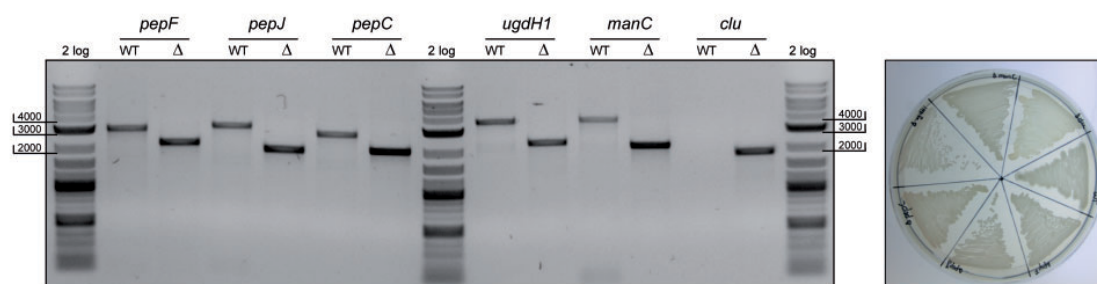


Figure 5. CRISPR-Cas9 mediated knockout studies in *P. polymyxa*. The agarose gel shows PCR analyses from purified genomic DNA of WT and knockout mutants (Δ) for each target. Repair templates were provided by fusing 1 kb upstream and 1 kb downstream regions of the gene of interest, and PCR amplification of this region in the modified strain resulted in an ~ 2 kb band, indicating successful disruptions. The WT PCR for the 18 kb fragment (*cll*) does not yield a PCR product with the chosen polymerase due to its large size. Phenotype analysis of the generated mutants revealed that all strains were viable under standard growth conditions.

Table 3. Data on EPSs produced by the WT strain and the generated deletion mutants

Strain	Titer (g l^{-1})	Mw (g mol^{-1}) ^a	HPLC-MS recovery (%) ^b
WT	2.91 ± 0.09	$(8.93 \pm 1.56) \times 10^6$	55.1 ± 2.2
ΔpepF	1.74 ± 0.02	$(1.95 \pm 0.09) \times 10^7$	50.5 ± 2.5
ΔpepJ	1.31 ± 0.01	$(7.87 \pm 0.36) \times 10^6$	47.6 ± 2.8
ΔpepC	0.53 ± 0.06	$(1.70 \pm 0.05) \times 10^7$	46.2 ± 2.8
ΔugdH1	0.53 ± 0.05	$(1.85 \pm 0.14) \times 10^7$	34.9 ± 1.7
ΔmanC	No precipitate	$(1.56 \pm 0.15) \times 10^7$	Not measured

^aPeak integration of the refractive index (RI) signal for molecular weight determinations was performed if the light scattering signal indicated presence of a polymer.

^bRecoveries in HPLC-MS are reported as the sum of all quantifiable sugars relative to titer.

To compare sugar monomer compositions of produced WT and mutant EPSs, dried and ground polymer was re-dissolved, hydrolyzed and analyzed via HT-PMP analysis. The HPLC-MS data shows that all obtained polymers were composed of the same sugar monomers: glucose (Glc), mannose (Man), galactose (Gal), fucose (Fuc) and glucuronic acid (GlcA) (Figure 7). We assume that traces of glucosamine (GlcN) found in the samples are probably impurities from cell debris since its low amount does not suggest a stoichiometrically plausible participation in a conserved repeating unit. Sugar recoveries of about 50% during HPLC-MS (Table 3) are in the expected range for crude EPS batches (78). Since different sugars show different susceptibilities to release and degradation during hydrolysis, some are underrepresented in the final data.

Uronic acids, for example, are prone to degradation and can only be recovered partially (79). In contrast to this, dimers of uronic acids and hexoses are fairly stable, resulting in a reduced release and thereby reduced detection of attached hexose (78). Salts, co-precipitated protein and water, attracted by the hygroscopic EPS powders also contribute to recoveries below 100%. The compositions of ΔpepC and ΔugdH1 EPSs only displayed minor differences compared to the WT polymer, indicating that the produced EPSs are highly similar in monomer pattern. We assume that the enzymes encoded by *pepC* and *ugdH1* are crucial for EPS production, but that their functions are present twice in the clusters. Deletion of one copy might partially be taken over by its paralog, resulting in lower amounts but structurally identical EPS. *UgdH1* has a 64% protein sequence identity to *ugdH2*, and both genes were confidently annotated to catalyze the oxidation of UDP-Glc to UDP-GlcA. Hence, it is likely that knockout of only one *ugdH* gene does not completely eliminate synthesis of this component. A similar explanation accounts for the results of *pepC*, which exhibits a protein

sequence identity of 60% with *pepQ* (Supplementary Figure S7). Multiple sequence alignment of all *P. polymyxa* GTs with priming GTs of *Streptococcus agalactiae* (CpsE) and *Lactobacillus helveticus* (EpsE) revealed that protein similarities of *PepC* and *PepQ* with *EpsE* and *CpsE* are above 40%, whereas the homologies of all other GTs with the annotated, priming GTs are below 22%. We therefore assume that *pepC* and *pepQ* encode two redundant priming glycosyl transferases.

The most interesting deletion mutants in terms of EPS structure are ΔpepF and ΔpepJ . These variants produced polymers with a significantly altered monomer distribution compared to the WT. In the case of ΔpepJ , the amount of mannose in the polymer was reduced by 15% and the amount of glucose by 7.5%, making galactose and fucose fill a correspondingly larger proportion of the overall composition.

In the case of the ΔpepF mutant, the galactose content is reduced to 50% of its WT content, accompanied by a near complete loss of pyruvate. This data suggests that 50% of the contained galactose molecules, are being pyruvylated, and that the pyruvate-substituted galactose monomer is transferred by *pepF*. The pyruvate group is typically added before secretion (80).

Since colony morphology and viscosity of liquid cultures indicated that the polymer produced by the ΔpepF mutant exhibited considerably different physicochemical characteristics than the WT, a comparison of the rheological behavior of WT and ΔpepF mutant EPS was performed. The results obtained by recording viscosity curves, amplitude sweeps and frequency sweeps clearly underscore the fundamental physicochemical differences between WT and ΔpepF polymer (Figure 8).

Although both EPSs create highly viscous, shear-thinning solutions when dissolved in water, their behavior upon stress and time is substantially different, making each interesting for entirely different applications. The WT EPS forms a gel-like

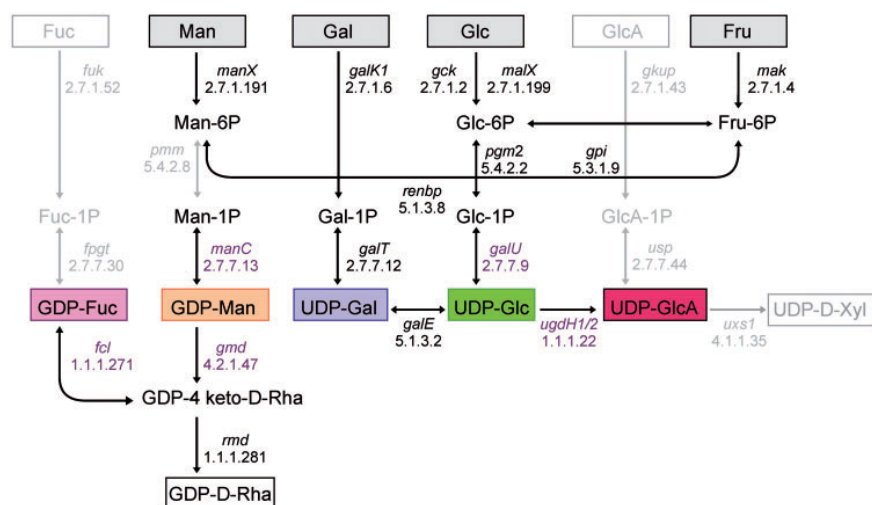


Figure 6. Biosynthetic pathways dedicated to the production of activated nucleotide sugars in *P. polymyxa*. The map was constructed based on a metabolic network model of a *P. polymyxa* strain annotated on KEGG database. All pathways present in the *P. polymyxa* genome are shown in black. Grey routes are not annotated. Enzymes written in purple are located within the EPS cluster, black ones somewhere else in the genome. Nucleotide sugars highlighted with color are constituents of the WT polymer.

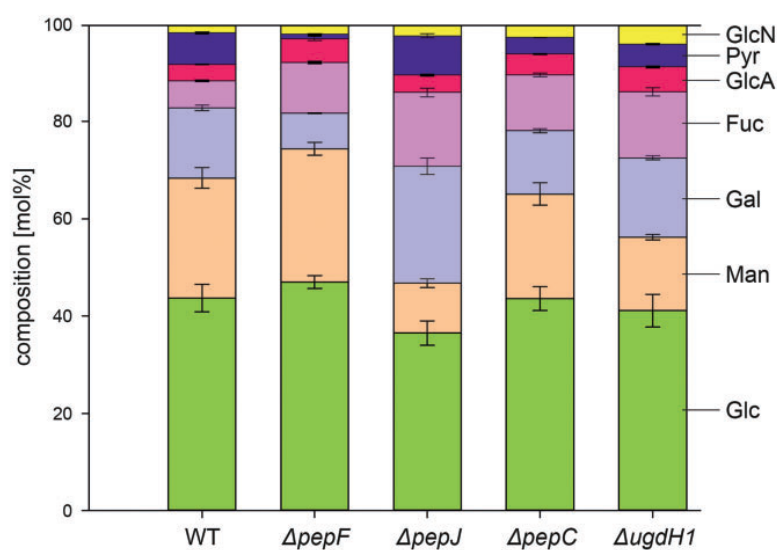


Figure 7. Sugar monomer compositions of EPSs from mutants and WT *P. polymyxa*. Pyruvate content was determined with a pyruvate oxidase assay. All other components were analyzed and quantified via HPLC-ESI-MS/MS.

structure with a pronounced network, delivering high viscosity and stability to mechanical stress. No viscosity plateau at low shear rates can be observed in the viscosity curves of the WT EPS, indicating that polymer strands are linked with each other via inter-molecular forces. The remarkable difference between G' and G'' in amplitude sweeps describes the elastic character of the WT solution. Upon increase of applied strain, the degeneration of the sample network begins with a G'' overshoot, which probably occurs due to micro crack formation within the structured gel (81). The depicted frequency test points out the stability of the sample over time. Even at low frequencies, simulating long-term stress, the sample character remains dominated by

the elastic modulus and does not show any tendencies to start flowing. The WT EPS could potentially be applied as stabilizer for suspensions or as hydrogel for biomedical, cosmetic or food applications. The generated mutant EPS, however, reveals remarkably different attributes. A distinct viscosity plateau can be observed in the flow curves, assigning this sample to the group of entangled polymers without a strong physicochemical network. At low shearing, polymer strands simultaneously ravel and unravel, resulting in constant friction (82). Similar contributions of elasticity and viscosity to the sample structure and the lack of a G'' overshoot in strain sweeps emphasize the viscous but not gel-like character of the mutant EPS. In frequency

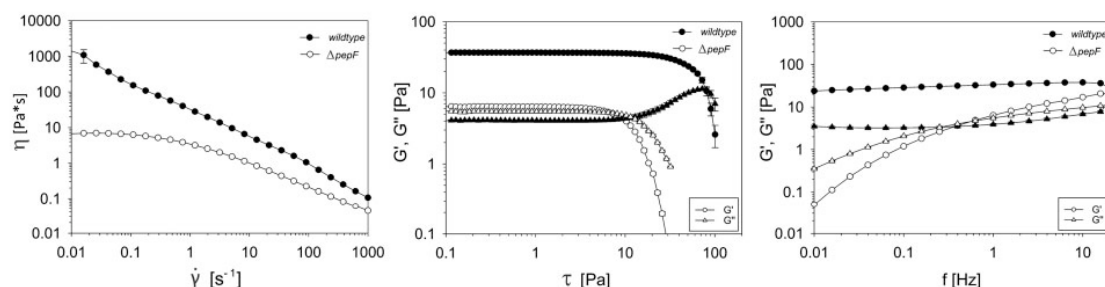


Figure 8. Rheological characterization of polymer produced by the WT and ΔpepF mutant. Viscosity curves (left), strain sweeps (middle) and frequency sweeps (right) of 1% EPS solutions in ultra-pure water were recorded on a controlled shear stress rheometer using a cone-plate geometry.

sweeps, this solution behaves like a typical Maxwell material. Sudden deformations, simulated by high frequencies, result in a rather elastic response of the material, whereas long-term stress induces viscous flowing of the solution. This polymer is suited for any application in which a shear thinning, viscous thickener is needed. Examples are cosmetic lotions, oil drilling fluids or paints and lacquers.

4. Conclusion

In the present study, we designed and adapted a CRISPR-Cas9 based genome-editing tool for *P. polymyxa* for the first time. We proved its functionality in knockout studies of single genes and large regions via sgRNA multiplexing and harnessed it for genome integration experiments. After implementation, we utilized the system to study the yet undescribed EPS biosynthesis machinery of *P. polymyxa*. Results obtained here yield the first insights into basic principles of this Wzx/Wzy pathway, and putative roles of selected key genes were assigned. Furthermore, we exemplified EPS tailoring through genetic recoding. Specifically, we generated mutant EPSs with significantly altered monomer compositions. Rheological characterization revealed that one of these polymer variants exhibits fundamentally different physicochemical properties than the WT, making it suitable for an entirely different set of applications. Future work will focus on the in-depth characterization of all genes involved in biosynthesis of *P. polymyxa* EPS in order to construct a biotechnologically relevant production strain for tailor-made EPS. Thorough chemical structure analysis via NMR will enhance our understanding of structure–function relationships of generated EPS variants. Furthermore, an already constructed, inactivated variant of the pCasPP plasmid (pdCasPP) will be used for CRISPRi-mediated repression studies in *P. polymyxa*. We also anticipate that the vector system will expedite research in distinct fields related to *Paenibacilli*, including the production of other value-added products like 2,3-butanediol and health related issues like *P. larvae* pathogenesis in honeybee larvae.

Supplementary data

Supplementary Data are available at SYNBIO Online.

Acknowledgements

Special thanks go to José Guillermo Ortiz Tena for technical and scientific support in analytical measurements.

Funding

Evonik Industries; DECHEMA (in part).

Conflict of interest statement. None declared.

References

- Du, J., Shao, Z. and Zhao, H. (2011) Engineering microbial factories for synthesis of value-added products. *J. Ind. Microbiol. Biotechnol.*, 38, 873–890.
- Rehm, B.H. (2010) Bacterial polymers: biosynthesis, modifications and applications. *Nat. Rev. Microbiol.*, 8, 578–592.
- Bhan, N., Xu, P. and Koffas, M.A.G. (2013) Pathway and protein engineering approaches to produce novel and commodity small molecules. *Curr. Opin. Biotechnol.*, 24, 1137–1143.
- Wenzel, S.C. and Müller, R. (2005) Recent developments towards the heterologous expression of complex bacterial natural product biosynthetic pathways. *Curr. Opin. Biotechnol.*, 16, 594–606.
- Cress, B.F., Trantas, E.A., Ververidis, F., Linhardt, R.J. and Koffas, M.A.G. (2015) Sensitive cells: enabling tools for static and dynamic control of microbial metabolic pathways. *Curr. Opin. Biotechnol.*, 36, 205–214.
- Mougiakos, I., Bosma, E.F., de Vos, W.M., van Kranenburg, R. and van der Oost, J. (2016) Next generation prokaryotic engineering: the CRISPR-Cas toolkit. *Trends Biotechnol.*, 34, 575–587.
- Chow, V., Kim, Y.S., Rhee, M.S., Sawhney, N., St John, F.J., Nong, G., Rice, J.D. and Preston, J.F. (2016) A 1, 3-1, 4- β -glucan utilization regulon in *Paenibacillus* sp. strain JDR-2. *Appl. Environ. Microbiol.*, 82, 1789–1798.
- Sharmin, F., Wakelin, S., Huygens, F. and Hargreaves, M. (2013) Firmicutes dominate the bacterial taxa within sugar-cane processing plants. *Sci. Rep.*, 3, 3107.
- Devaraj, S., Hemarajata, P. and Versalovic, J. (2013) The human gut microbiome and body metabolism: implications for obesity and diabetes. *Clin. Chem.*, 59, 617–628.
- Aleti, G., Sessitsch, A. and Brader, G. (2015) Genome mining: prediction of lipopeptides and polyketides from *Bacillus* and related Firmicutes. *Comp. Struct. Biotechnol. J.*, 13, 192–203.
- Ju, F., Guo, F., Ye, L., Xia, Y. and Zhang, T. (2014) Metagenomic analysis on seasonal microbial variations of activated sludge from a full-scale wastewater treatment plant over 4 years. *Environ. Microbiol. Rep.*, 6, 80–89.
- Giraffa, G., Chanishvili, N. and Widyastuti, Y. (2010) Importance of lactobacilli in food and feed biotechnology. *Res. Microbiol.*, 161, 480–487.
- Jones, D.T. and Woods, D.R. (1986) Acetone-butanol fermentation revisited. *Microbiol. Rev.*, 50, 484–524.

14. Altenbuchner, J. (2016) Editing of the *Bacillus subtilis* genome by the CRISPR-Cas9 system. *Appl. Environ. Microbiol.*, 82, 5421–5427.
15. Zhang, K., Duan, X. and Wu, J. (2016) Multigene disruption in undomesticated *Bacillus subtilis* ATCC 6051a using the CRISPR/Cas9 system. *Sci. Rep.*, 6, 27943.
16. Westbrook, A.W., Moo-Young, M. and Chou, C.P. (2016) Development of a CRISPR-Cas9 toolkit for comprehensive engineering of *Bacillus subtilis*. *Appl. Environ. Microbiol.*, 82, 4876–4895.
17. Oh, J.-H. and van Pijkeren, J.-P. (2014) CRISPR–Cas9-assisted recombineering in *Lactobacillus reuteri*. *Nucleic Acids Res.*, 42, e131.
18. Pyne, M.E., Bruder, M.R., Moo-Young, M., Chung, D.A. and Chou, C.P. (2016) Harnessing heterologous and endogenous CRISPR-Cas machineries for efficient markerless genome editing in *Clostridium*. *Sci. Rep.*, 6, 25666.
19. Chen, W., Zhang, Y., Yeo, W.-S., Bae, T. and Ji, Q. (2017) Rapid and efficient genome editing in *Staphylococcus aureus* by using an engineered CRISPR/Cas9 system. *J. Am. Chem. Soc.*, 139, 3790–3795.
20. Kim, S.-B. and Timmusk, S. (2013) A simplified method for gene knockout and direct screening of recombinant clones for application in *Paenibacillus polymyxa*. *PLoS One*, 8, e68092.
21. Zarschler, K., Janesch, B., Zayni, S., Schäffer, C. and Messner, P. (2009) Construction of a gene knockout system for application in *Paenibacillus alvei* CCM 2051T, exemplified by the S-layer glycan biosynthesis initiation enzyme WsfP. *Appl. Environ. Microbiol.*, 75, 3077–3085.
22. Genersch, E. (2010) American Foulbrood in honeybees and its causative agent, *Paenibacillus larvae*. *J. Invertebr. Pathol.*, 103(Suppl.1), S10–S19.
23. Padhi, S., Dash, M., Sahu, R. and Panda, P. (2013) Urinary tract infection due to *Paenibacillus alvei* in a chronic kidney disease: a rare case report. *J. Lab. Physicians*, 5, 133–135.
24. Roux, V., Fenner, L. and Raoult, D. (2008) *Paenibacillus provencensis* sp. nov., isolated from human cerebrospinal fluid, and *Paenibacillus urinalis* sp. nov., isolated from human urine. *Int. J. Syst. Evol. Microbiol.*, 58, 682–687.
25. Xie, J.-B., Du, Z., Bai, L., Tian, C., Zhang, Y., Xie, J.-Y., Wang, T., Liu, X., Chen, X. and Cheng, Q. (2014) Comparative genomic analysis of N₂ fixing and non-N₂-fixing *Paenibacillus* spp.: organization, evolution and expression of the nitrogen fixation genes. *PLoS Genet.*, 10, e1004231.
26. Xie, J., Shi, H., Du, Z., Wang, T., Liu, X. and Chen, S. (2016) Comparative genomic and functional analysis reveal conservation of plant growth promoting traits in *Paenibacillus polymyxa* and its closely related species. *Sci. Rep.*, 6, 21329.
27. Klein, M.G. (1988) Pest management of soil-inhabiting insects with microorganisms. *Agric. Ecosyst. Environ.*, 24, 337–349.
28. Storm, D.R., Rosenthal, K.S. and Swanson, P.E. (1977) Polymyxin and related peptide antibiotics. *Annu. Rev. Biochem.*, 46, 723–763.
29. Kajimura, Y., Kaneda, M. and Fusaricidin, A. (1996) a New depsipeptide antibiotic produced by *Bacillus polymyxa* KT-8. *J. Antibiot.*, 49, 129–135.
30. Häfslér, T., Schieder, D., Pfaller, R., Faulstich, M. and Sieber, V. (2012) Enhanced fed-batch fermentation of 2,3-butanediol by *Paenibacillus polymyxa* DSM 365. *Bioresour. Technol.*, 124, 237–244.
31. Rütering, M., Schmid, J., Rühmann, B., Schilling, M. and Sieber, V. (2016) Controlled production of polysaccharides—exploiting nutrient supply for levan and heteropolysaccharide formation in *Paenibacillus* sp. *Carbohydr. Polym.*, 148, 326–334.
32. Raza, W., Makeen, K., Wang, Y., Xu, Y. and Qirong, S. (2011) Optimization, purification, characterization and antioxidant activity of an extracellular polysaccharide produced by *Paenibacillus polymyxa* SQR-21. *Bioresour. Technol.*, 102, 6095–6103.
33. Kim, S.-W., Ahn, S.-G., Seo, W.-T., Kwon, G.-S. and Park, Y.-H. (1998) Rheological properties of a novel high viscosity polysaccharide, A49-Pol, produced by *Bacillus polymyxa*. *J. Microbiol. Biotechnol.*, 8, 178–181.
34. Liang, T.-W. and Wang, S.-L. (2015) Recent advances in exopolysaccharides from *Paenibacillus* spp.: production, isolation, structure, and bioactivities. *Mar. Drugs*, 13, 1847–1863.
35. Kahng, G.-G., Lim, S.-H., Yun, H.-D. and Seo, W.-T. (2001) Production of extracellular polysaccharide, EPS WN9, from *Paenibacillus* sp. WN9 KCTC 8951P and its usefulness as a cement mortar admixture. *Biotechnol. Bioprocess Eng.*, 6, 112–116.
36. Grady, E.N., MacDonald, J., Liu, L., Richman, A. and Yuan, Z.-C. (2016) Current knowledge and perspectives of *Paenibacillus*: a review. *Microb. Cell Fact.*, 15, 203.
37. Schmid, J., Sieber, V. and Rehm, B. (2015) Bacterial exopolysaccharides: biosynthesis pathways and engineering strategies. *Front. Microbiol.*, 6, 496.
38. Toukach, P.V. (2011) Bacterial carbohydrate structure database 3: principles and realization. *J. Chem. Inf. Model*, 51, 159–170.
39. Freitas, F., Alves, V.D. and Reis, M.A. (2011) Advances in bacterial exopolysaccharides: from production to biotechnological applications. *Trends Biotechnol.*, 29, 388–398.
40. Schmid, J., Sperl, N. and Sieber, V. (2014) A comparison of genes involved in sphingane biosynthesis brought up to date. *Appl. Microbiol. Biotechnol.*, 98, 7719–7733.
41. Freitas, F., Alves, V. and Reis, M.M. (2014) Bacterial polysaccharides: production and applications in cosmetic industry. In: R Kishan Gopal and M Jean-Michel (eds) *Polysaccharides*. Springer International Publishing, Cham, pp. 1–24.
42. Ates, O. (2015) Systems biology of microbial exopolysaccharides production. *Front. Bioeng. Biotechnol.*, 3, 200.
43. Rehm, B.H.A. (2015) Synthetic biology towards the synthesis of custom-made polysaccharides. *Microb. Biotechnol.*, 8, 19–20.
44. Becker, A. (2015) Challenges and perspectives in combinatorial assembly of novel exopolysaccharide biosynthesis pathways. *Front. Microbiol.*, 6, 687.
45. Hassler, R.A. and Doherty, D.H. (1990) Genetic engineering of polysaccharide structure: production of variants of xanthan gum in *Xanthomonas campestris*. *Biotechnol. Prog.*, 6, 182–187.
46. Welman, A.D. and Maddox, I.S. (2003) Exopolysaccharides from lactic acid bacteria: perspectives and challenges. *Trends Biotechnol.*, 21, 269–274.
47. Schmid, J. and Sieber, V. (2015) Enzymatic transformations involved in the biosynthesis of microbial exo-polysaccharides based on the assembly of repeat units. *ChemBioChem*, 16, 1141–1147.
48. —, Heider, D., Wendel, N.J., Sperl, N. and Sieber, V. (2016) Bacterial glycosyltransferases: challenges and opportunities of a highly diverse enzyme class toward tailoring natural products. *Front. Microbiol.*, 7, 182.
49. Boe, L., Gros, M.F., Te Riele, H., Ehrlich, S.D. and Gruss, A. (1989) Replication origins of single-stranded-DNA plasmid pUB110. *J. Bacteriol.*, 171, 3366–3372.
50. Novotny, R., Novotny, R., Berger, H., Schinko, T., Messner, P., Schäffer, C. and Strauss, J. (2008) A temperature-sensitive expression system based on the *Geobacillus stearothermophilus* NRS 2004/3a *sgsE* surface-layer gene promoter. *Biotechnol. Appl. Biochem.*, 49, 35–40.
51. Aziz, R.K., Bartels, D., Best, A.A., DeJongh, M., Disz, T., Edwards, R.A., Formsma, K., Gerdes, S., Glass, E.M., Kubal, M.

- et al. (2008) The RAST server: rapid annotations using subsystems technology. *BMC Genomics*, 9, 75.
52. Altschul, S.F., Gish, W., Miller, W., Myers, E.W. and Lipman, D.J. (1990) Basic local alignment search tool. *J. Mol. Biol.*, 215, 403–410.
 53. Apweiler, R., Bairoch, A., Wu, C.H., Barker, W.C., Boeckmann, B., Ferro, S., Gasteiger, E., Huang, H., Lopez, R. and Magrane, M. et al. (2004) UniProt: the Universal Protein knowledgebase. *Nucleic Acids Res.*, 32(suppl_1), D115–D119.
 54. Yu, C.-S., Lin, C.-J. and Hwang, J.-K. (2004) Predicting subcellular localization of proteins for Gram-negative bacteria by support vector machines based on n-peptide compositions. *Protein Sci.*, 13, 1402–1406.
 55. Kanehisa, M. and Goto, S. (2000) KEGG: Kyoto encyclopedia of genes and genomes. *Nucleic Acids Res.*, 28, 27–30.
 56. Cobb, R.E., Wang, Y. and Zhao, H. (2015) High-efficiency multiplex genome editing of streptomyces species using an engineered CRISPR/Cas system. *ACS Synth. Biol.*, 4, 723–728.
 57. Rühmann, B., Schmid, J. and Sieber, V. (2014) Fast carbohydrate analysis via liquid chromatography coupled with ultra violet and electrospray ionization ion trap detection in 96-well format. *J. Chrom. A*, 1350, 44–50.
 58. —, — and — (2016) Automated modular high throughput exopolysaccharide screening platform coupled with highly sensitive carbohydrate fingerprint analysis. *J. Vis. Exp.* doi:10.3791/53249.
 59. Müller, A.K., Rojo, F. and Alonso, J.C. (1995) The level of the pUB110 replication initiator protein is autoregulated, which provides an additional control for plasmid copy number. *Nucleic Acids Res.*, 23, 1894–1900.
 60. Engler, C., Kandzia, R. and Marillonnet, S. (2008) A one pot, one step, precision cloning method with high throughput capability. *PLoS One*, 3, e3647.
 61. Jiang, W., Bikard, D., Cox, D., Zhang, F. and Marraffini, L.A. (2013) RNA-guided editing of bacterial genomes using CRISPR-Cas systems. *Nat. Biotechnol.*, 31, 233–239.
 62. Xie, N.-Z., Li, J.-X., Song, L.-F., Hou, J.-F., Guo, L., Du, Q.-S., Yu, B. and Huang, R.-B. (2015) Genome sequence of type strain *Paenibacillus polymyxa* DSM 365, a highly efficient producer of optically active (R, R)-2, 3-butanediol. *J. Biotechnol.*, 195, 72–73.
 63. Whitfield, C. (2006) Biosynthesis and assembly of capsular polysaccharides in *Escherichia coli*. *Annu. Rev. Biochem.*, 75, 39–68.
 64. Yother, J. (2011) Capsules of *Streptococcus pneumoniae* and other bacteria: paradigms for polysaccharide biosynthesis and regulation. *Annu. Rev. Microbiol.*, 65, 563–581.
 65. Becker, A., Katzen, F., Pühler, A. and Ielpi, L. (1998) Xanthan gum biosynthesis and application: a biochemical/genetic perspective. *Appl. Microbiol. Biotechnol.*, 50, 145–152.
 66. Jolly, L. and Stingle, F. (2001) Molecular organization and functionality of exopolysaccharide gene clusters in lactic acid bacteria. *Int. Dairy J.*, 11, 733–745.
 67. Bezzate, S., Aymerich, S., Chambert, R., Czarnes, S., Berge, O. and Heulin, T. (2000) Disruption of the *Paenibacillus polymyxa* levansucrase gene impairs its ability to aggregate soil in the wheat rhizosphere. *Environ. Microbiol.*, 2, 333–342.
 68. Jolly, L., Newell, J., Porcelli, I., Vincent, S.J.F. and Stingle, F. (2002) *Lactobacillus helveticus* glycosyltransferases: from genes to carbohydrate synthesis. *Glycobiology*, 12, 319–327.
 69. Péant, B., LaPointe, G., Gilbert, C., Atlan, D., Ward, P. and Roy, D. (2005) Comparative analysis of the exopolysaccharide biosynthesis gene clusters from four strains of *Lactobacillus rhamnosus*. *Microbiology*, 151, 1839–1851.
 70. Wu, Q., Tun, H.M., Leung, F.C.-C. and Shah, N. P. (2014) Genomic insights into high exopolysaccharide-producing dairy starter bacterium *Streptococcus thermophilus* ASCC 1275. *Sci. Rep.*, 4, 4974.
 71. Kim, S.-Y., Kim, J.-G., Lee, B.-M. and Cho, J.-Y. (2008) Mutational analysis of the gum gene cluster required for xanthan biosynthesis in *Xanthomonas oryzae* pv *oryzae*. *Biotechnol. Lett.*, 31, 265.
 72. Cieslewicz, M.J., Kasper, D.L., Wang, Y. and Wessels, M.R. (2001) Functional analysis in type Ia Group B *Streptococcus* of a cluster of genes involved in extracellular polysaccharide production by diverse species of *Streptococci*. *J. Biol. Chem.*, 276, 139–146.
 73. Lamothe, G., Jolly, L., Mollet, B. and Stingle, F. (2002) Genetic and biochemical characterization of exopolysaccharide biosynthesis by *Lactobacillus delbrueckii* subsp. *bulgaricus*. *Arch. Microbiol.*, 178, 218–228.
 74. Boels, I.C., Kranenburg, R. v., Hugenholtz, J., Kleerebezem, M. and de Vos, W.M. (2001) Sugar catabolism and its impact on the biosynthesis and engineering of exopolysaccharide production in lactic acid bacteria. *Int. Dairy J.*, 11, 723–732.
 75. Li, O., Qian, C.-D., Zheng, D.-Q., Wang, P.-M., Liu, Y., Jiang, X.-H. and Wu, X.-C. (2015) Two UDP-glucuronic acid decarboxylases involved in the biosynthesis of a bacterial exopolysaccharide in *Paenibacillus elgii*. *Appl. Microbiol. Biotechnol.*, 99, 3127–3139.
 76. Weon-Taek, S., Kahng, G.-G., Nam, S.-H., Choi, S.-D., Suh, H.-H., Kim, S.-W. and Park, Y.-H. (1999) Isolation and characterization of a novel exopolysaccharide-producing *Paenibacillus* sp. WN9 KCTC 8951P. *J. Microbiol. Biotechnol.*, 9, 820–825.
 77. Cole, J.N., Aziz, R.K., Kuipers, K., Timmer, A.M., Nizet, V. and van Sorge, N.M. (2012) A conserved UDP-glucose dehydrogenase encoded outside the hasABC operon contributes to capsule biogenesis in Group A *Streptococcus*. *J. Bacteriol.*, 194, 6154–6161.
 78. Rühmann, B., Schmid, J. and Sieber, V. (2015) High throughput exopolysaccharide screening platform: from strain cultivation to monosaccharide composition and carbohydrate fingerprinting in one day. *Carbohydr. Polym.*, 122, 212–220.
 79. Tait, M.I., Sutherland, I.W. and Clarke-Sturman, A.J. (1990) Acid hydrolysis and high-performance liquid chromatography of xanthan. *Carbohydr. Polym.*, 13, 133–148.
 80. Katzen, F., Ferreiro, D.U., Oddo, C.G., Ielmini, M.V., Becker, A., Pühler, A. and Ielpi, L. (1998) *Xanthomonas campestris* pv. *campestris* gum mutants: effects on xanthan biosynthesis and plant virulence. *J. Bacteriol.*, 180, 1607–1617.
 81. Hyun, K., Wilhelm, M., Klein, C.O., Cho, K.-S., Nam, J.-G., Ahn, K.-H., Lee, S.-J., Ewoldt, R.H. and McKinley, G.H. (2011) A review of nonlinear oscillatory shear tests: analysis and application of large amplitude oscillatory shear (LAOS). *Prog. Polym. Sci.*, 36, 1697–1753.
 82. Graessley, W.W. (1967) Viscosity of entangling polydisperse polymers. *J. Chem. Phys.*, 47, 1942–1953.

Supporting Information

EXPERIMENTAL SECTION

Genome editing in *Paenibacillus polymyxa* DSM 365

After spacer selection using Benchling, 24 bp oligos for guide annealing were designed phosphorylated and annealed:

1 μ L fwd [100 μ M]
1 μ L rev [100 μ M]
1 μ L polynucleotide kinase (NEB)
1 μ L T4 ligase buffer (NEB)
6 μ L H₂O

The mix was incubated at 37 °C for 30 min, then heated up to 95 °C for 5 min. Thereafter, it was cooled down to 25 °C by decreasing the temperature by 0.5 °C every 6 seconds. After annealing, the mix was diluted 1:100 and 1 μ L of this dilution was utilized for guide insertion via Golden Gate assembly:

0.75 μ L BbsI (NEB)
0.25 μ L T7 ligase (NEB)
1 μ L 10x CutSmart Buffer (NEB)
1 μ L ATP (10 mM stock)
1 μ L DTT (10 mM stock)
1 μ L 100 ng· μ L⁻¹ backbone (circular destination vector)
1 μ L annealed guide (100x diluted from above reaction)
4 μ L H₂O

For assembly, the mixture was subjected to 20 cycles of heating to 37 °C for 5 min and afterwards incubating at 20 °C for 5 min. After heat inactivation for 20 min at 80 °C, the sample was cooled down to 12 °C. To reduce background by linearized (but not assembled) vector, linear DNA fragments were digested after Golden Gate annealing with help of Plasmid-Safe ATP-Dependent DNase (Epicentre), by adding:

1.5 μ L Plasmid-Safe enzyme
1.5 μ L 10x Plasmid-Safe buffer
1.5 μ L ATP (10 mM stock)
0.5 μ L H₂O

After adding all reagents, the mixture was incubated for 30 min at 37 °C and finally inactivated at 70 °C for 30 min. After cooling, the whole mixture was used for transformation of chemically competent *E. coli* DH5 α cells. Obtained clones were screened with colony PCR, and positive representatives were verified by sequencing. Subsequent to guide cloning, homologous regions were constructed by overlap extension PCR and inserted by restriction and ligation into the SpeI site. Specifically, approximately 1 kb flanks upstream and downstream of the target gene were amplified, purified by gel extraction and afterwards fused via the following overlap extension PCR protocol:

Step A:

25 μ L Accuzyme 2x mastermix (Bioline)	95 $^{\circ}$ C – 5 min	
X μ L upstream flank (100 – 200 ng)	95 $^{\circ}$ C – 30 s	} 30 x
X μ L downstream flank (100 – 200 ng)	55 $^{\circ}$ C – 20 s	
X μ L H ₂ O to 50 μ L	72 $^{\circ}$ C – 4 min	
	72 $^{\circ}$ C – 10 min	

Step B:

25 μ L Accuzyme 2x mastermix (Bioline)	95 $^{\circ}$ C – 5 min	
2.5 μ L forward primer upstream region	95 $^{\circ}$ C – 30 s	} 30 x
2.5 μ L reverse primer downstream region	57 $^{\circ}$ C – 20 s	
3 μ L template from step A	72 $^{\circ}$ C – 4 min	
17 μ L H ₂ O	72 $^{\circ}$ C – 10 min	

Subsequent to assembly, DNA bands of appropriate length were excised from agarose gel and cloned after XbaI or SpeI digest into SpeI-linearized vector. After transformation in DH5 α cells, clones were screened for inserted fragment with colony PCR, thereafter sequenced and finally transferred to *E. coli* S17-1 for conjugation events.

SUPPORTING RESULTS

Figure S1. Conjugation efficiencies of different pCasPP variants in *P. polymyxa*.

- (A) Plasmid targeting site 1 of *pepF* and providing a template for HDR (pCasPP-*pepF*_sg1-harms), >200 clones.
 (B) Plasmid targeting site 2 of *pepF* and providing a template for HDR (pCasPP-*pepF*_sg2-harms), >200 clones.
 (C) Empty, non-targeting vector without an inserted repair template (pCasPP), >10,000 clones.
 (D) Plasmid targeting site 1 of *pepF*; no template for HDR is provided (pCasPP-*pepF*-sg1), <20 clones.
 (E) Non-targeting vector containing the homologous arms of *pepF* (pCasPP-harms), >1,000 clones.

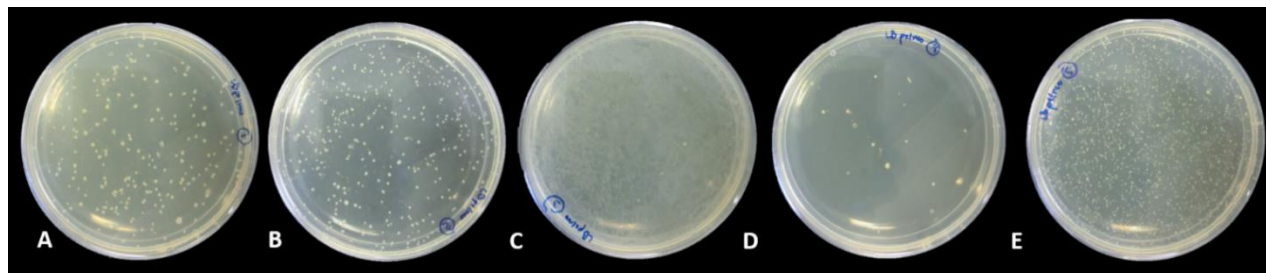
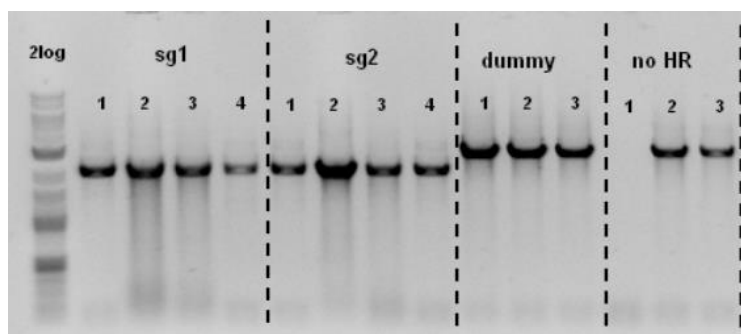
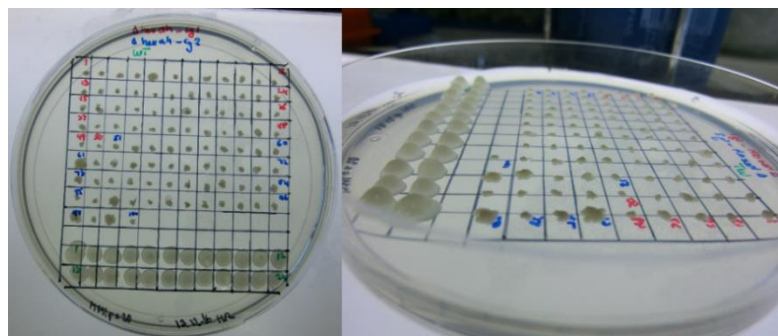
**Figure S2.** Colony PCR results on *P. polymyxa* clones obtained after conjugation with various pCasPP constructs. Control primers lying upstream (forward) and downstream (reverse) of the homologous regions were used, yielding a 3 kb band for unedited loci and a 2 kb band for knockout events. First eight lanes represent clones contain plasmids targeted to different sites (sg1 and sg2) and a repair template. Bands 9 – 11 are unedited genes from clones containing a dummy version of the plasmid. Last three bands show clones containing a targeted plasmid without providing a repair template.**Figure S3.** Colony morphologies of *P. polymyxa* wild type strain and Δ *ugdH1* mutant. Colonies 1 – 50 are clones obtained after conjugation with pCasPP-*ugdH1*-sg1-harms. Clones 51 – 100 were conjugated with pCasPP-*ugdH1*-sg2-harms. Rows 11 and 12 (mucooid colonies) are 24 individually picked wild type colonies.

Figure S4. Curing of plasmids from *P. polymyxa* after editing. Plates A1 and A2 show eight clones of each deletion mutant transferred to LB agar without selection pressure (left) and to neomycin containing media (right).

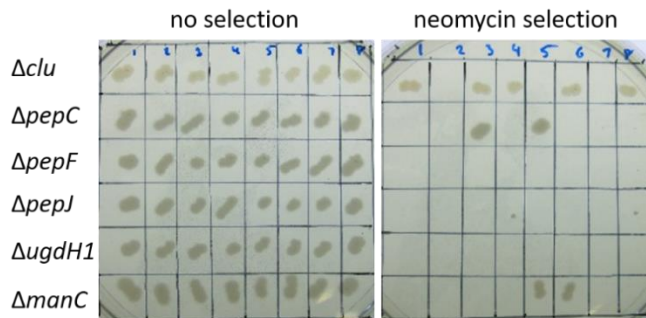


Figure S5. Colony PCR on eight *P. polymyxa* clones after conjugation with pCasPP-pgrac-sg2-harms plasmid. Primers were chosen to bind within the integrated pgrac site (forward) and downstream of the region used for homology directed repair (reverse). A band at 1.7 kb shows a successful insertion. Colonies containing a non-targeting version of the plasmid served as negative control.

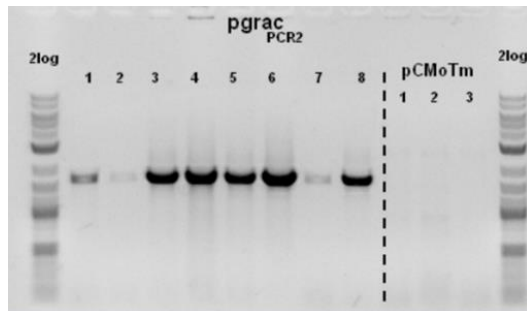


Figure S6. Elution profiles of analyzed polymers by gel permeation chromatography. All graphs are averaged values from triplicates. (A) Complete chromatogram of the wild type sample (left) and a zoom-in on the actual polymer peak (right). RI signal is shown in blue, light scattering in green. (B) Overlay of RI signals of all measured samples. (C) Overlay of light scattering signals of all measured samples.

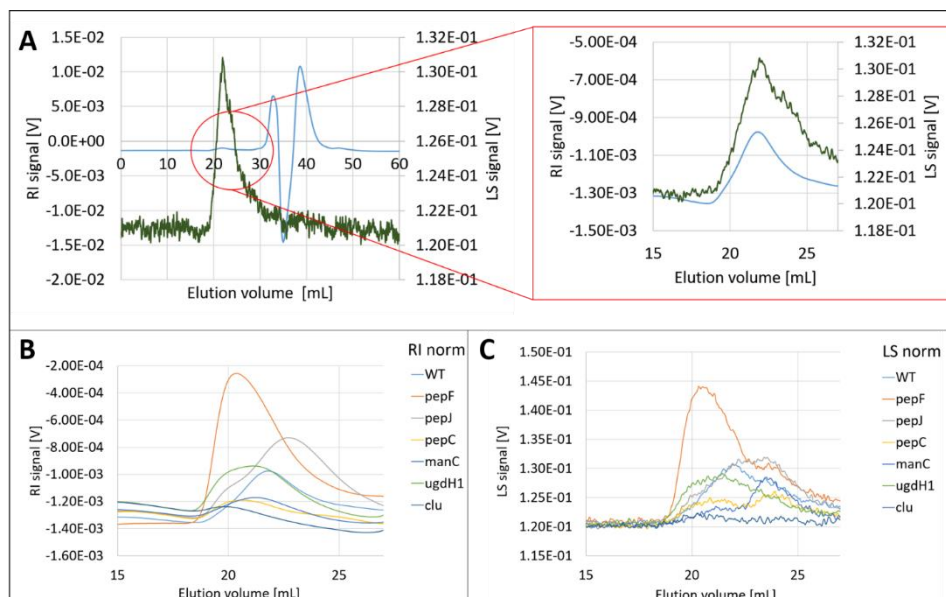


Figure S7. Percent identity matrix of all putative glycosyl transferases encoded in the EPS cluster of *P. polymyxa* and priming GTs of *S. agalactiae* (CpsE; Q04664) and *L. helveticus* (EpsE; Q0ZR64). Sequence alignment was performed with Clustal 2.1.

	pepD	pepT	pepI	CpsE	EpsE	pepC	pepQ	pepF	pepV	pepJ	pepK	pepL	pepU
1: pepD	100.00	20.71	17.92	17.35	10.92	13.82	16.51	11.02	9.70	17.90	13.25	12.90	10.06
2: pepT	20.71	100.00	15.13	17.23	14.20	15.34	14.07	12.44	11.46	16.84	15.38	16.73	15.60
3: pepI	17.92	15.13	100.00	22.11	18.44	19.44	21.82	8.53	10.29	11.85	13.49	12.41	13.19
4: CpsE	17.35	17.23	22.11	100.00	44.09	43.17	47.89	9.04	5.76	12.69	11.86	16.13	12.45
5: EpsE	10.92	14.20	18.44	44.09	100.00	53.33	53.93	8.90	9.40	8.63	10.87	10.57	12.14
6: pepC	13.82	15.34	19.44	43.17	53.33	100.00	59.90	9.40	7.24	14.69	10.64	11.02	12.50
7: pepQ	16.51	14.07	21.82	47.89	53.93	59.90	100.00	7.83	5.93	12.93	12.50	9.09	13.91
8: pepF	11.02	12.44	8.53	9.04	8.90	9.40	7.83	100.00	28.35	11.57	12.84	13.40	11.59
9: pepV	9.70	11.46	10.29	5.76	9.40	7.24	5.93	28.35	100.00	13.97	19.00	15.35	15.45
10: pepJ	17.90	16.84	11.85	12.69	8.63	14.69	12.93	11.57	13.97	100.00	24.44	19.08	22.48
11: pepK	13.25	15.38	13.49	11.86	10.87	10.64	12.50	12.84	19.00	24.44	100.00	21.89	23.03
12: pepL	12.90	16.73	12.41	16.13	10.57	11.02	9.09	13.40	15.35	19.08	21.89	100.00	23.10
13: pepU	10.06	15.60	13.19	12.45	12.14	12.50	13.91	11.59	15.45	22.48	23.03	23.10	100.00

SUPPORTING MATERIALS

Table S1. Bacterial strains

Strain	Description	Reference
<i>E. coli</i> DH5 α	F– Φ 80lacZ Δ M15 Δ (lacZYA-argF) 169 recA1 endA1 hsd R17 (rK–, K+) phoA supE44 λ – thi-1 gyrA96 relA1	NEB
<i>E. coli</i> S17-1	Conjugation strain; recA pro hsdR RP42Tc::MuKm::Tn7 integrated into the chromosome	ATCC 47055
<i>P. polymyxa</i> DSM-365	Wild type	DSMZ
<i>P. polymyxa</i> DSM-365pepC	DSM-365 Δ pepC	This study
<i>P. polymyxa</i> DSM-365pepF	DSM-365 Δ pepF	This study
<i>P. polymyxa</i> DSM-365pepJ	DSM-365 Δ pepJ	This study
<i>P. polymyxa</i> DSM-365ugdH1	DSM-365 Δ ugdH1	This study
<i>P. polymyxa</i> DSM-365manC	DSM-365 Δ manC	This study
<i>P. polymyxa</i> DSM-365clu	DSM-365 Δ clu	This study
<i>P. polymyxa</i> DSM-365pgrac	DSM-365::pgrac	This study

Table S2. Plasmids

Plasmid	Description	Reference
pCRISPRomyces-2	Codon optimized Cas9 expression for <i>Streptomyces</i> carrying SpCas9, oriT and BbsI flanked lacZ cassette	Cobb et al. (2015)
pUBoriMC	Plasmid carrying Neo ^r , ori and repU gene, derivative of puB110 (ATCC 37015)	This study
pHT01	<i>E. coli</i> – <i>B. subtilis</i> shuttle vector enabling encoding pgrac expression system	MoBiTec GmbH
pCasPP	<i>P. polymyxa</i> genome editing vector	This study
pCasPP-pepFsg1	<i>pepF</i> targeting knockout plasmid not providing a repair template	This study
pCasPP-pepFsg1-harms	<i>pepF</i> targeting knockout plasmid providing a repair template	This study

pCasPP-pepFsg2-harms	<i>pepF</i> targeting knockout plasmid providing a repair template	This study
pCasPP-pepF-harms	Untargeted pCasPP derivative carrying <i>pepF</i> homologous regions	This study
pCasPP-pepCsg1-harms	<i>pepC</i> targeting knockout plasmid providing a repair template	This study
pCasPP-pepCsg2-harms	<i>pepC</i> targeting knockout plasmid providing a repair template	This study
pCasPP-pepJsg1-harms	<i>pepJ</i> targeting knockout plasmid providing a repair template	This study
pCasPP-pepJsg2-harms	<i>pepJ</i> targeting knockout plasmid providing a repair template	This study
pCasPP-ugdH1sg1-harms	<i>ugdH1</i> targeting knockout plasmid providing a repair template	This study
pCasPP-ugdH1sg2-harms	<i>ugdH1</i> targeting knockout plasmid providing a repair template	This study
pCasPP-manCsg1-harms	<i>manC</i> targeting knockout plasmid providing a repair template	This study
pCasPP-manCsg2-harms	<i>manC</i> targeting knockout plasmid providing a repair template	This study
pCasPP-clugBlock-harms	Multiplex pCasPP variant targeting two different sites at once for knockout of the 18 kb fragment; homologous regions are provided	This study
pCasPP-pgracsg2-harms	pCasPP derivative for pgrac integration upstream of <i>sacB</i>	This study

Table S3. Primers and gBlocks

Name	Sequence (5'-3')	Description
pCasPP and pdCasPP construction		
GG_neo.FOR	ggccggtctcaaatggttattaatagctgaataagaacggtgctc	Amplification of Neo ^r from pUBoriMCS
GG_neo.REV	ggccggtctcaaccttcgtatctttattcagcaatcgcg	Amplification of Neo ^r from pUBoriMCS
GG_bsaI.FOR	ggccggtctcaagggtgatggtttgaactgttctttatc	Removal of a BsaI site from pUBoriMCS
GG_bsaI.REV	ggccggtctcatctccatggcctcactttccacttttgc	Removal of a BsaI site from pUBoriMCS
GG_repU.FOR	ggccggtctcagagagaaaagaaatcgctaattgtgattac	Amplification of repU from pUBoriMCS
GG_repU.REV	ggccggtctcactcccatcctcaatcctttaataacaattatagc	Amplification of repU from pUBoriMCS
GG_PsgsE.FOR	ggccggtctcaggagctgttacaggcatattcatatcaatgtcgc	Amplification of PsgeE promotor from gBlock
GG_PsgsE.REV	ggccggtctcaagtaaaagcctaaaatccccctcggtttatga	Amplification of PsgeE promotor from gBlock
oriT_XbaI.FOR	ctgatctagaggctacggcggttgatgc	Amplification of oriT from pCRISPRomyces-2
oriT_XbaI.REV	ctgatctagacctgactccgcctgcagg	Amplification of oriT from pCRISPRomyces-2

GG_Cas9Com2.FOR	ggcc ggtctc ataactaatggacaagaagtacagcatcg	Amplification of SpCas9 and lacZ cassette from pCRISPRomyces-2
GG_Cas9Com2.REV	ggcc ggtctc acattaacggcactgttgcaaatagtcg	Amplification of SpCas9 and lacZ cassette from pCRISPRomyces-2
dCas9_D10A_F	ggcc ggtctc acctggccatcggcaccaacagcgtgg	Amplification of pCasPP backbone and inactivation of Cas9 active regions
dCas9_D10A_R	ggcc ggtctc acagggcgtgctgtactcttctcc	Amplification of pCasPP backbone and inactivation of Cas9 active regions
dCas9_H840A_F	ggcc ggtctc acgtcgacccatcgtccgcagtccttc	Amplification of pCasPP backbone and inactivation of Cas9 active regions
dCas9_H840A_R	ggcc ggtctc agacgtcgtagtcgctcagccgg	Amplification of pCasPP backbone and inactivation of Cas9 active regions
GG_oriT_F	ggcc ggtctc aactagtgccaggaaccgtaaaaaggccg	Amplification of pCasPP backbone for the insertion of a unique SpeI site
GG_oriT_R	gcg cggtctc atagtcggcgggcttgatgcgccggttcggg	Amplification of pCasPP backbone for the insertion of a unique SpeI site
GG_oriT2_F	ggcc ggtctc aggtcaacaccgagatcaccaaggcc	Amplification of pCasPP backbone for the insertion of a unique SpeI site
GG_oriT2_R	ggcc ggtctc agaccgcaggatgctgctgagcagg	Amplification of pCasPP backbone for the insertion of a unique SpeI site
<i>pepC</i> deletion		
pepC_sg1_F	acgc gagcatg gaaaatttaccgg	spacer 1 for gene knockout
pepC_sg1_R	aaacc ggtaaat ttccatgctc	spacer 1 for gene knockout
pepC_sg2_R	aaacc cttgat gctgctgctgct	spacer 2 for gene knockout
pepC_sg2_F	acgcac gacagc agcatatcaagg	spacer 2 for gene knockout
pepC_usHR_XbaI_F	ggc ctctag acaaaaatcgatgaagcaaggagaatgagtgcg	Amplification of 1 kb upstream of deletion target
pepC_usHR_R	cgcttgaatgcatccatcaataagcatcccgta ccctctca acctgccgtgg	Amplification of 1 kb upstream of deletion target
pepC_dsHR_F	ccacggcaggttgagagggggtacgggatgcttattgatggatgattcaagcg	Amplification of 1 kb downstream of deletion target
pepC_dsHR_XbaI_R	ggc ctctag accatctttcacccgcagctgactcg	Amplification of 1 kb downstream of deletion target
pepC_KOproof_F	gcaactcatggagcaggccagtgcgacg	Control primers for gene deletions
pepC_KOproof_R	gctgtatggtgtttattctagtagtccaagg	Control primers for gene deletions
<i>pepF</i> deletion		
pepF_sg1_R	aaacc aaggtg tattcagatgccg	spacer 1 for gene knockout
pepF_sg1_F	acgc ggcatct gaatacaccttg	spacer 1 for gene knockout
pepF_sg2_R	aaacat gggatgc ctatcatatgg	spacer 2 for gene knockout

pepF_sg2_F	<u>acgcccataatgataggcatcccat</u>	spacer 2 for gene knockout
pepF_usHR_XbaI_F	<u>ggcctctagagggtctgggcattggtgatcatgctgg</u>	Amplification of 1 kb upstream of deletion target
pepF_usHR_R	<u>gccaaccgactcatgtttctaccggtatcacttctcttgcgaaaatcgg</u>	Amplification of 1 kb upstream of deletion target
pepF_dsHR_F	<u>ccgatttgcgaaagagaagtgtacgggtgagaacatgagtcggtggc</u>	Amplification of 1 kb downstream of deletion target
pepF_dsHR_XbaI_R	<u>ggcctctagagcatacagaccaccaaaccctctgcc</u>	Amplification of 1 kb downstream of deletion target
pepF_KOproof_F	<u>ggctctgctggtgccgtgcatgc</u>	Control primers for gene deletions
pepF_KOproof_R	<u>gcatcgtatgcagtaaatccaaacgc</u>	Control primers for gene deletions
<i>pepJ</i> deletion		
pepJ_sg2_R	<u>aaaccaacacatatattccaatcga</u>	spacer 1 for gene knockout
pepJ_sg2_F	<u>acgctcgattggaaatatgtgtt</u>	spacer 1 for gene knockout
pepJ_sg3_F	<u>acgcaggttctggtctgatcacgg</u>	spacer 2 for gene knockout
pepJ_sg3_R	<u>aaaccctgtatcagaccgaaacct</u>	spacer 2 for gene knockout
pepJ_usHR_XbaI_F	<u>ggcctctagaggaggcaccgcctaatgaacc</u>	Amplification of 1 kb upstream of deletion target
pepJ_usHR_R	<u>cgcgcgcgcctttctgtcaaggcccggtgcccgaatacgaatcc</u>	Amplification of 1 kb upstream of deletion target
pepJ_dsHR_F	<u>ggatttcgattgcggcaacggggccttgacagaaaggcggcg</u>	Amplification of 1 kb downstream of deletion target
pepJ_dsHR_XbaI_R	<u>ggcctctagaccctgaccgaatggttctggtgtaataagg</u>	Amplification of 1 kb downstream of deletion target
pepJ_KOproof_F	<u>ccaacaagattttcaatggctccgatcaacg</u>	Control primers for gene deletions
pepJ_KOproof_R	<u>ggtttcattgggtaccaccgtttcc</u>	Control primers for gene deletions
<i>ugdH1</i> deletion		
ugdH1_sg1_F	<u>acgctggcgccgatgtaacctgtg</u>	spacer 1 for gene knockout
ugdH1_sg1_R	<u>aaaccacaggttacatcggcgcca</u>	spacer 1 for gene knockout
ugdH1_sg2_F	<u>acgccttgcctacattgaacagg</u>	spacer 2 for gene knockout
ugdH1_sg2_R	<u>aaaccctgttcaatgtaggacaag</u>	spacer 2 for gene knockout
ugdH1_usHR_XbaI_F	<u>ggcctctagacctgtcgcgtaactgaaagatgcgg</u>	Amplification of 1 kb upstream of deletion target
ugdH1_usHR_R	<u>ggaagaacaatctgcacgtgtagcgtctcccaattacagccagcttcattccg</u>	Amplification of 1 kb upstream of deletion target
ugdH1_dsHR_F	<u>cggaatgaagctggctgtaattggggagacgctacacgtgcagattgtcttcc</u>	Amplification of 1 kb downstream of deletion target
ugdH1_dsHR_XbaI_R	<u>ggcctctagagggtctacggaagcgaagaaagcatcc</u>	Amplification of 1 kb downstream of deletion target

ugdH1_KOproof_F	cgattacttaatccaaatggcgagcg	Control primers for gene deletions
ugdH1_KOproof_R	gcgtagccagtgtaccttg	Control primers for gene deletions
<i>manC</i> deletion		
manC_sg1_F	acgcgggcagaggttagtaacgg	spacer 1 for gene knockout
manC_sg1_R	aaaccggttactacacctgccc	spacer 1 for gene knockout
manC_sg2_F	acgcgaaggtactggagagcccg	spacer 2 for gene knockout
manC_sg2_R	aaaccgggctctccagtaccttc	spacer 2 for gene knockout
manC_usHR_XbaI_F	ggcctctagagccaaatacacgacatccg	Amplification of 1 kb upstream of deletion target
manC_usHR_R	cgcgaatttcgacagttcgggcggttgatgatcgatgggc	Amplification of 1 kb upstream of deletion target
manC_dsHR_F	gccccatccgatcatcaaccgccgaactgtcgaattggcg	Amplification of 1 kb downstream of deletion target
manC_dsHR_XbaI_R	ggcctctagacgcattcgactccataccacagc	Amplification of 1 kb downstream of deletion target
manC_KOproof_F	ccaagctgctgaatcgctgg	Control primers for gene deletions
manC_KOproof_R	ccgagcagaccttcgtaatgacttgc	Control primers for gene deletions
<i>clu</i> deletion		
clu1_usHR_XbaI_F	ggcctctagagcaatacaaaatctgcgtaacaatcg	Amplification of 1 kb upstream of deletion target
clu1_usHR_R	ccgagcagaccttcgtaatgacttgcgggagggaaatgtatacttccgat acgg	Amplification of 1 kb upstream of deletion target
clu1_dsHR_F	ccgtatccgaaagtatacttccctccgcaaaagtcattacgaaggtctgc tcgg	Amplification of 1 kb downstream of deletion target
clu1_dsHR_XbaI_R	ggcctctagaccctctctctcatatttttagaccgg	Amplification of 1 kb downstream of deletion target
clu1_KOproof_F	ccattccggaatgcttatgaatgagg	Control primers for deletion of the 18 kb region
clu1_KOproof_R	gctacgaccgctaatagtccagataaaacg	Control primers for deletion of the 18 kb region
<i>pgrac</i> integration		
pgrac_sg3_F	acgcggacctttgaataaaagtc	spacer 1 for gene knockout
pgrac_sg3_R	aaacggacttttattcaaaagtc	spacer 1 for gene knockout
pgrac_sg2_F	acgcaaaattactaggaataatg	spacer 2 for gene knockout
pgrac_sg2_R	aaacatatcttctagtaattt	spacer 2 for gene knockout
pgrac_usHR_SpeI_F	ggccactagtggctgccgtagccatttgttc	Amplification of 1 kb upstream of deletion target
pgrac_usHR_R	ccgattatgtacaatagctggtacattatgctgttcttctgtgtgtcttac g	Amplification of 1 kb upstream of deletion target

pgrac_dsHR_F	cctaccatcaccatggcatggccctatcaacaaaaagttgg	Amplification of 1 kb downstream of deletion target
pgrac_dsHR_SpeI_R	ggccactagtcgcttgctgtacatttgataggtttccc	Amplification of 1 kb downstream of deletion target
pgrac_msHR1_F	cgtaaagacaccacaaagagaacacgcataaggtaccagctattgaaca taatcgg	Amplification of pgrac from pHT01
pgrac_msHR2_R	ggtgatggtgatggtgatggatccttctcttaattggg	Annealing of a His tag and GSG linker cloned after pgrac
pgrac_msHR3_F	atgcaccatcaccatcaccatcaccatcaccatggctctggc	Annealing of a His tag and GSG linker cloned after pgrac and control primer for successful integration
pgrac_msHR4_R	ccaacttttggatagggccatgccagagccatggtgatggtgatgg	Amplification of pgrac from pHT01
seq3_levsuc_R	gcacgttatgtaccgccc	control primer for successful integration
Promoters gBlock (including sgsE)		
ggagtctgagaattggtatgccttataagtccaattaacagtgaaaacctgcataggagagctatcggggtttttattttacataatgatacataatttaccgaaactgcggaacataat tgaggaatcatagaattttgtcaaaataattttatgacaacgcttataacgttgatataatttaattttttgacaaaaatgggctcgtgtgtacaataaatgtagtctgttacagccat tcataatcatgctccatcgtaggaaataatttcaatggcatattctctaaaaattgtatttagggctagaatttagaaagaaaatgtattattatagaagaggtagaacattaaggaatga tgtgaaagtctagcactgaatgatagccttgcttaataagtcctatcctggacacacaggatgatctggttcattgtagcaccttttaggcaatgaatctactaaacggcagccgttag gatcattgtctaaagtccataaaaaagaagggggttttaggcttcaaaaatcagaccagacaaaagcggcaaatgaataagcgaacggggaagatttgcggtcaagtcctc cctccgcacgtatcaattcgcaagcttttctttataatagaatgaatga		
gBlock for clu deletion		
gagacatctttgaagacaaacgaattggctctgtgaacgacagtttagagctagaatagcaagttaaaataaggctagtccgttatcaactgaaaaagtgaccagtcgggtgc tttttagcataacccttggggcctctaaacgggtcttgagggtttttggctgctccttcggcggacgtgctacgggcacctaccgcagccgctggctgtgcgacacggacg gatcggcgcaactggccgatgctgggagaagcgctgctgtacggcgccgacgggtgagccctcggcgagcgggtgtgaaacttctgtgaatggcctgtcgggtgctttt tttatagcgtgccagataagcgttgacgatctggcggtaccgctatgatcggggcttctgcaattcttagtcgagtatctgaaaggggatacgcgtataccccgaaatacc gggtttaagtcttcttcacgtggc		

Table S4. Details on deletion experiments within the EPS cluster (BK010330).

Target	Deletion Site (bp)	Length (bps)
<i>pepC</i>	2476 - 3166	691
<i>pepF</i>	5467 - 6232	766
<i>pepJ</i>	9958 - 11078	1121
<i>ugdH1</i>	13406 - 14734	1329
<i>manC</i>	15330 - 16777	1448
<i>clu</i>	54 - 17801	17748

4 Discussion

The overall goal of the presented work was to identify, characterize and establish a bacterial strain, capable of producing a novel EPS that can replace or compete with the existing benchmark polymers due to unique properties, such as rheological behavior and compatibilities in relevant matrices.

Ideally, the identified organism is non-pathogenic and even meets the generally regarded as safe (GRAS) standard, exhibits a high growth-rate and a good polymer productivity, is promiscuous towards cheap carbon sources, and features a robust fermentation and straightforward downstreaming process, enabling the cost-efficient and reliable supply of the desired product. Once established, it is desired that certain polymer features could be tailored via genetic engineering to meet the requirements of highly specific applications. Researchers all around the globe already dedicated decades of work to this endeavor. Considering the proportion of described versus commercialized EPSs, the objectives of this work are, of course, ambitious. The successful establishment of an organism allowing for the custom-made production of certain polymer variants is a highly complex goal, since ultimately, this would not only require a capable chassis-organism, but also the encompassing understanding of EPS structure function relationship in relevant industrial formulations. However, our knowledge on the relationship between structure and function of polysaccharides is still superficial and rational genome editing towards tailor-made EPS is also still in its infancy. Nonetheless, the aim of this dissertation was to contribute to the challenging objective of custom-made polysaccharides.

4.1 Strain selection

All results presented in this work were obtained with *Paenibacillus* strains and their EPSs. Reasons for the selection of this production host are discussed below.

As described above, a high throughput assisted screening approach was employed to pre-select promising EPS producers from a large strain collection (192). Besides the high number of organisms that can be screened at once, a strength of this method is the variety of strain and polymer characteristics recorded in a single run. Information on growth characteristics, carbon source turnover rates, broth viscosities, and monomer compositions of produced polymers allow for an encompassing view on the assessed production systems and substantiate the decision for one or another EPS producer. Commonly applied strategies for the identification of novel EPS producers from environmental isolates usually focus on a single polymer or strain property, including the detection of EPS production by phenotype analysis (200), staining secreted polymers with dyes on agar-plates (201), or screening liquid cultures for viscosity (202) or EPS precipitation (203). Nevertheless, high throughput based approaches have the drawback of standardizing conditions, which helps in comparing strains, but also holds the risk of underrating certain strains due to potentially providing suboptimal conditions for specific candidates. Therefore a detailed analysis of pre-selected EPS producers was conducted following high throughput screening. The reasons for eliminating three of the four candidates from the pool of promising producers varied and is described in the following.

In case of EPS1.E6 the impurity of the environmental isolate was decisive for sorting out this candidate. The two strains in the mixed culture, *Micrococcus luteus* and *Paenibacillus* sp., were closely associated and therefore not distinguishable based on phenotypical appearance. Only genome sequencing identified two independent genomes within the extracted DNA sample, allowing for the subsequent separation of both strains by adjusted culture conditions. The separated strains did not exhibit superior EPS formation capacities than the other three candidates and work on EPS1.E6 was not investigated further. This finding highlights the drawback of the applied screening method. “*You get what you screen for*” - Frances Arnold. The selected cultivation conditions will always favor one organism or the other, or even mixed cultures, and it is likely that many promising candidates fall behind in screenings, because the parameters chosen are simply unfavorable.

This could also explain the comparatively low EPS titer that was determined for EPS2.A7. *Rhizobiaceae* are well known for their ability to produce EPSs, with succinoglycan being the most prominent and best studied EPS from this family (204), and studies utilizing optimized media and suitable fermentation processes report EPS titers up to 40 g·L⁻¹ (205). Although the assessed properties qualified EPS2.A7 as an interesting candidate for further investigations, work on this strain was stopped, because all experiments aiming at the transformation with foreign DNA failed. However, publications describe the successful delivery of plasmids to several *Rhizobia* species (206), and the optimization of the transformation procedures applied would eventually have led to success for EPS2.A7 at some point.

In case of the strain EPS1.F2, no culture conditions were found that favored slime-free growth. Furthermore, *Rhodobacter* strains are known to produce CPSs (207), which stay attached to the cell, thereby complicating the separation of cells and polymer further. Due to this, molecular biological experiments with EPS1.F2 were severely impaired and work on this strain was not continued as well. The strain EPS2.H2 produced a highly viscous polymer with a versatile carbohydrate fingerprint, grew without EPS formation on LB media and was transformable with test vectors. Furthermore, no EPSs from *Paenibacilli* have been commercialized until now and the strain converted all carbon sources tested, rendering it the most promising candidate for this project.

4.2 The potential of Paenan

In-depth literature research elucidated that Paenan, the *Paenibacillus* sp. polymer covered in this thesis, is by far not the first discovered EPS from *Paenibacilli*. As summarized in table 1.2, at least seven other *Paenibacillus* polymers comprising the same main building blocks as Paenan (Man, Glc, Gal, GlcA) have already been described. Although this does not automatically imply that these studies deal with the exact same EPS, certain structural similarities are obvious. However, even though all these studies proposed potential applications for the described polymers, or at least highlighted certain polymer characteristics relevant to industrial applications, no *Paenibacillus* polymer has been commercialized yet. This of course raises the questions: “What makes Paenan superior or unique as compared to the other heteropolysaccharides from *Paenibacilli*?”, and “why should Paenan be successful as rheological additive?” Although this will not be fully answered in the present work, some considerations will still be made, underlining the potential of Paenan.

First, approximately half of the studies did not even consider the extracted EPSs as rheological additives, but rather focused on different applications such as antioxidant (165) or biosorption (171) properties. From the studies focusing on rheology, only the two earliest reports, dating from 1969 and 1986, mentioned the impressive gelling capacity of extracted EPSs (153, 167). Others frequently mentioned high viscosities and shear thinning behavior (166, 176), but did not report the capability to form viscoelastic gels. However, the weak gel character is the most unique property of Paenan, which opens up new application profiles between rigid gels (e.g. Gellan) and viscous fluids (e.g. Xanthan). At the time of the first two studies, the replacement of petro-based gelling agents with sustainable alternatives was not a pressing issue as it is at the moment, which could explain the lack of a commercialization initiative for these EPSs. The possible reasons for the lack in gelling capacity of other described heteropolysaccharides from *Paenibacilli* are that either structurally different polymers were extracted, which simply do not exhibit gel formation potential, or that the utilized production processes resulted in non-gelling polymer. The latter argument is valid especially, as in the course of this study changes to the established fermentative production, such as nutrient supply, resulted in the production of thickening, but not gelling polymer (data not shown). Even the type of baffled culture flasks affected the rheological behavior of the polymer secreted. The explanation for this is probably an altered, sub-optimal physical or chemical environment (e.g. O₂ or nutrient transfer), which was also reported to reduce molecular weight and hence the viscosity in Xanthan fermentations (208). Another argument redefining the potential of Paenan and EPSs from *Paenibacilli* in general is the developed genetic engineering tool, which is discussed in chapter 4.3. The CRISPR-Cas9 based system will not only facilitate rewiring of metabolic circuits to improve intracellular fluxes towards EPS production but will probably also allow for the design of polymer variants with the same organism. Similar approaches were already applied for other EPSs successfully (78, 79) and an increased understanding of the underlying molecular mechanisms will provide further adjustment screws to tweak EPS yields. Finally, an adaptable EPS production system could abolish the necessity of optimizing the fermentation and downstream operations for each product, thereby streamlining the development of novel polymers.

To conclude, one can say that the recent global developments resulted in an increased demand for all-natural products and that bacterial EPSs, including Paenan, might get a chance to claim certain commercial markets. However, lots of work is to be done to make novel polymers competitive. Some crucial steps in the exploitation of Paenan are discussed below.

4.2.1 Production and purification

Economically viable polymer production means that the market value of the prospective product exceeds the production costs, thereby generating profit. In capitalism, monetary profit is the most necessary element for the success of any product. In case of biopolymers, two major matters of expense drive the overall costs of a process. The polymer yield, relative to the amount of C-source supplied, and the costs for downstream processing (35). To give an estimation on where the current Paenan production process ranks in comparison to well-established processes, relevant parameters concerning EPS production and purification are summarized in table 4.1. Since only detailed studies were considered, this data collection does not mean to be exhaustive. In terms of obtained EPS titers, Paenan fermentations range at the lower end of the processes listed in table 4.1. Even highly viscous fermentations, such as Xanthan and Gellan, reach titers of up to 30 and 35 g·L⁻¹, respectively.

Other reports even describe Xanthan titers of up to $50 \text{ g}\cdot\text{L}^{-1}$ (63). If less viscous polymers like Dextran were to be considered, titers above $100 \text{ g}\cdot\text{L}^{-1}$ can be obtained. This comparison highlights the limitations of fermentative EPS production, as already mentioned in the introduction. Due to high broth viscosity, oxygen and nutrient transport collapses, pH and temperature regulations become difficult and product formation levels off (57, 58). This also explains the low yields (g polymer per g carbon source) in Paenan production. As mentioned in section 3.2, the C-source glucose was not entirely depleted by *Paenibacillus* sp. 2H2 in the described 30 L fed-batch fermentation, but EPS formation and cell growth stagnated, indicating that the transport of O_2 (required for metabolism) was the limiting factor (see Fig. S1, Appendix A, chapter 3.2). Oxygen transfer rates are frequently reported to be limiting in highly viscous fermentation processes (42). The yields of Paenan fermentations could probably be optimized easily by fine-tuning the process.

Table 4.1. Process characteristics of selected bacterial exopolysaccharides taken from detailed studies.

Polymer	Titer [g·L ⁻¹]	Yield [%]	Productivity [g·L ⁻¹ ·h ⁻¹]	Downstream Processing	Comments	Reference
Paenan	4.5	16	0.27	<ul style="list-style-type: none"> Dilution to reduce viscosity Centrifugation to remove cells Crossflow filtration Precipitation in alcohol 	<ul style="list-style-type: none"> Titer limitations due to high viscosity 	This study
Curdlan	45 - 93	48 - 66	0.12 - 0.55	<ul style="list-style-type: none"> NaOH addition to broth Incubation Cell separation via centrifugation Precipitation of product by acidification 	<ul style="list-style-type: none"> Dissolved O₂ concentration important variable Various complex and synthetic nutrient sources usable 	(58, 209-212)
Dextran	135	45	2.81	<ul style="list-style-type: none"> Dilution of broth Centrifugation to separate cells Precipitation in methanol 	<ul style="list-style-type: none"> Only on sucrose Also cell free synthesis possible 	(213, 214)
Hyaluronan	0.9 - 7	1 - 17.35	≤ 0.59	<ul style="list-style-type: none"> Cell separation Ultrafiltration Spray drying 	<ul style="list-style-type: none"> Highly viscous fermentations Industrial production with engineered <i>B. subtilis</i> strains 	(215)
Gellan	6.6 - 35.7	25 - 50	≤ 0.2	<ul style="list-style-type: none"> Heating to 95 °C Precipitation in alcohol Filtration or Centrifugation 	<ul style="list-style-type: none"> Dissolved O₂ can be limiting 	(43, 216, 217)
Xanthan	10.5 - 30	34 - 81	0.13 - 0.43	<ul style="list-style-type: none"> Pasteurization Cell removal Precipitation Separation 	<ul style="list-style-type: none"> Highly viscous process Dissolved O₂ can become limiting 	(218)

As for Gellan and Xanthan, a batch fermentation with initial C-source concentrations of < 4% (43, 218) would most likely yield similar EPS titers as the published fed-batch process (199), but exhibit better conversion rates of glucose to the polymer. Thereby, the cost-determining factor of fermentative EPS production, the yield, could be improved. However, these measures would not increase overall Paenan titers, since mass and gas transfer limitations depend on EPS titers and not on the yield. This problem could be tackled by an adjusted reactor or propeller design or altered fermentation strategies, such as solid state fermentations, which were successfully applied to increase titers in succinoglycan production (205). Furthermore, the fermentation media for Paenan production could be optimized by employing the statistical experiment design method as in the case of Xanthan (219), Gellan (220), and several other biopolymers. The two existing studies that also describe the fermentative production of gel-forming EPSs by *Paenibacilli* report titers of 10 g·L⁻¹ (167) and 14 g·L⁻¹ (153), respectively. This suggests that there is space for improvement in Paenan production.

Interestingly, the productivity of the Paenan process described is comparable to some of the commercialized processes listed in table 4.1. Since this was not the focus of this work, no effort was put into optimizing the production process to reach commercialization standards. However, the metabolic potential of *Paenibacillus* sp. 2H2 is highly competitive and probably, an optimized production process could compete with already marketed products.

The downstream processing employed for Paenan purification is similar to the processes used for commercial representatives (table 4.1). As for Paenan, these procedures typically start with a cell-disruption or –removal step, followed by polymer washing, concentration, and finally precipitation in organic solvents, such as alcohols, mostly. Scaling-up the process would of course require recovery of the solvent by distillation, and an optimization of the final drying process by spray drying, for instance. An important parameter in polymer purification is the actual ratio of polymer that is recovered from the fermentation broth. Studies on the recovery of Gellan report that up to 45% of native product gets lost during the purification (43) step. Monitoring and improving this parameter would certainly be required for the optimization of Paenan downstream processing.

Ultimately, not only the costs of production and purification, but also the price of the product will determine, whether a process is economically feasible. As seen for hyaluronan, even low titers and yields can be profitable, if the corresponding polymer fits a high value application. Hence, Paenan will only become commercially interesting if a suitable application, which matches the unique properties can be found.

4.2.2 Polymer characterization

Another aspect that needs to be discussed when it comes to the evaluation of Paenans' potential, is the characterization of the polymer. This topic can be subdivided into the physicochemical - primarily rheological in this case - and the analytical characterization.

The rheological behavior of pure Paenan solutions was described extensively during this study (see chapter 3.3). Rotational and oscillatory measurements of aqueous concentration series revealed that Paenan exhibits an apparent shear-thinning character with outstanding viscosities in the low-shear range. Flow behavior relevant to industrial applications was obtained with significantly less polymer as compared to the commercial benchmarks Xanthan and Gellan (221). Furthermore, Paenan forms stable

weak-gels due to a pronounced intermolecular network, thereby delivering elasticity and thixotropy. These properties represent a novel application profile for bio-based polymers that lies between the rigid Gellan gels and Xanthan fluids. Currently, the polyacrylic-acid based, synthetic polymer Carbopol is mainly used in personal care applications, when a shear-thinning, weak-gel character is required (222, 223). Paenan might represent a green alternative to this petro-based product.

The compatibility and rheology of Paenan in surfactant containing systems was also evaluated in this work. The most important results of these experiments were that the weak-gel character remained with three out of four different surfactants and that Paenan is compatible with all the assessed surfactants, even with cationic cetrimonium chloride. This is another interesting property of Paenan, since many gums, including Xanthan and Gellan, are incompatible with cationic surfactants due to complex coacervation and precipitation (224-226).

Although the rheology of Paenan was characterized fundamentally, further investigations on the physicochemical behavior should be conducted. Assessing the rheological characteristics over a wide pH range and in the presence of different salts could yield a better understanding of intermolecular interactions and could help to anticipate functional properties of Paenan in certain matrices.

On the analytical side, the experiments that were performed solely focused on the chemical polymer composition via HPLC-MS and photometric assays, molecular mass determinations employing GPC, and superficial analyses of functional groups by using FTIR (199). Considering the fact that molecular mass determinations from comparisons to pullulan standards are rather qualitative than absolute (due to variations in hydrodynamic radii of different polymers (227) and potential non-size exclusion effect of gel forming polymers (228)), structural data on Paenan is actually limited to the monomeric sugar composition. In fact, results obtained by generating *P. polymyxa* EPS variants suggest that the pyruvate substitutions that are present are probably linked to a branched galactose unit (see 3.5). However, this assumption is only hypothetical and conclusive experiments are necessary to prove this. The type of glycosidic bonds, backbone sequence, amount and type of side chains or type and location of the functional substituents (pyruvate, acetate, glycerate etc.) are not elucidated yet. Furthermore, indications on conformational arrangements of the secondary, tertiary or quaternary structure are still not investigated. However, in order to fully understand and describe the behavior of the polysaccharide in aqueous solutions, complete data on the structural features of each conformational level is indispensable (229).

A sophisticated analytical technique to characterize the primary structure of polysaccharides, including nature and linkage of sugar units and the type and degree of substituent pattern, is NMR (230). NMR was used to determine the location and ratio of pyruvate and acetate substituents in Xanthan for instance (231) and was employed to describe the structure of Gellan (232). NMR can also be used to study the secondary structure of EPSs, as proven by identifying the helical conformations for Xanthan and Gellan in solid state (233, 234). Although first attempts to characterize Paenan via NMR failed due to the high viscosity of the solutions, further effort should be made to develop a suitable NMR method for elucidating the structure of Paenan.

Combining the advanced rheological data with the results of detailed structure elucidations will ease the identification of potential structural elements that could be rationally targeted to generate polymer variants with altered physicochemical properties. Nevertheless, lots of effort has to be put into the structural characterization of Paenan in order to obtain tailor-made variants of the polymer.

4.3 Genome editing in *P. polymyxa*

Advances in synthetic biology and metabolic engineering have significantly contributed to the design of microbial factories. State-of-the-art genome editing tools like CRISPR-Cas9 rapidly increased the accessibility of undomesticated strains to genetic engineering. Owing to their robustness toward environmental stress, their promiscuity to various C-sources, and their variety in gene clusters dedicated to secondary metabolite production, many bacterial families of the phylum firmicutes are promising candidates for the genetic-engineering assisted generation of biotechnologically relevant production strains (235, 236). Thanks to its superior efficiency, CRISPR-Cas9 represents a key technology in this endeavor. In contrast to many other families such as *Lactobacillaceae* (237), *Bacillaceae* (238), *Clostridiaceae* (239) and *Staphylococcaceae* (240), no reports on establishing the CRISPR-Cas9 in *Paenibacillaceae* were available before.

However, numerous studies reported the successful deletion of genomic elements in various *Paenibacillus* strains using classical methods, such as homologous recombination of suicide plasmids (241), or more advanced techniques like bacterial mobile group II introns (242). In the course of this work, several knockout procedures, including the cited ones, were tested for their success in different *Paenibacillus* strains. Unfortunately, none of those procedures resulted in satisfactory results due to low efficiencies (mobile group II introns) or problems in plasmid transfer (integrative vectors). Therefore, the CRISPR-Cas9 based genome-editing tool was developed for *Paenibacillus* strains used in this work (see chapter 3.5). The tool turned out to be highly efficient in the deletion of single genes and larger genome regions and supported genomic integrations. Furthermore, it does not require the integration of selectable markers, and allows for sequential edits thanks to an established curing procedure. Additionally, multiplexing is feasible, enabling multiple edits at a time. Hence, the system exhibits major advantages over already published strategies and could potentially revolutionize genome editing in several *Paenibacillus* species. However, this system also features some drawbacks. As for all CRISPR-Cas9 based systems, off targeting effects are a concern that have to be taken into account. Although no limitations due to random DNA splicing occurred in the present study, several reports raise attention to the potential side effects that can alter the edited genome unpredictably (243, 244). Furthermore, the functionality of pCasPP in other *Paenibacillus* species remains to be proven. Minor optimizations, such as Cas9 codon optimization or tight expression control to avoid Cas9 toxicity are potentially required (115). Nevertheless, if the transfer of this system to other *Paenibacillus* species turns out to be successful, several fields of research could harness the system. EPS tailoring through genetic recoding is only one potential application. Further fields related to *Paenibacilli* that might profit from the system include research on the production of value-added products like 2,3-butanediol (245) and health related issues like *P. larvae* pathogenesis in honeybee larvae (246). In addition, the development of *Paenibacilli* as novel or improved production systems for medically relevant substances like antibiotics can be foreseen. Finally, yet importantly, employing the tool to better understand and potentially develop plant growth-promoting *Paenibacillus* strains as biocontrol agents could contribute to a more sustainable agriculture and a reduction of chemical pesticides.

5 Conclusions

The main goal of this dissertation was to establish a bacterial strain, capable of producing a novel EPS with unique, industrially relevant properties to replace petro-based rheological additives in certain fields of applications where no sustainable, bio-based alternatives are available up to now.

As a first step, *Paenibacillus* sp. 2H2 was identified as a promising candidate for this project by an in-depth strain characterization. *Paenibacillus* sp. 2H2 surpassed other pre-selected strains due to superior growth and polymer characteristics.

A detailed investigation of EPS production by *Paenibacillus* sp. 2H2 in 30 L scale revealed that the strain exhibits volumetric EPS productivities, comparable to commercially used strains, such as *S. paucimobilis*. However, due to viscosity induced process limitations, EPS titers did not exceed $4.5 \text{ g} \cdot \text{L}^{-1}$, which is at the lower end of established processes and the yield of 16% requires improvement to make the process industrially relevant. On a further note, the supply with different carbon and nitrogen sources could be harnessed to produce two different polymers, a levan-type homopolysaccharide and a highly viscous heteropolysaccharide, named Paenan.

Due to the impressive rheological behavior, Paenan was subjected to further investigation. Analytical investigations using UHPLC-ESI-MS/MS suggested a monomeric sugar composition comprising Glc, Man, Gal, and GlcA sub-units in the ratio of approximately 3.5:2:1:0.1 and photometrical enzyme assays identified pyruvate as a functional group, which is probably attached to a branched galactose unit. Furthermore, SEC-MALLS experiments indicated a high molecular weight of $1.3 \cdot 10^7 \text{ g} \cdot \text{mol}^{-1}$. Since unambiguous data on the backbone sequence, type and degree of substituent decoration, and information on glycosidic linkages is missing, thorough NMR assisted structural analyses of Paenan will be indispensable in the future.

The rheological behavior of Paenan was characterized in aqueous solution and in surfactant containing systems by rotational and oscillatory rheometry. Thanks to a pronounced intermolecular network, Paenan forms stable weak-gels, thereby delivering elasticity and thixotropy. This represents a novel application profile that lies between rigid Gellan gels and Xanthan fluids. In addition, Paenan exhibited superior compatibilities with every class of surfactant, even cationic, and retained its weak-gel character in three out of four systems, indicating its suitability for surfactant containing formulations.

To unravel the genetic basis for EPS production in *Paenibacillus* sp. 2H2, the genome was sequenced, and the putative EPS biosynthesis cluster was annotated based on sequence similarities to already characterized EPS machineries. The functionality of the locus was subsequently proven in a closely related *Paenibacillus* type strain (*P. polymyxa* DSM 365) by deleting a large proportion and single genes of the assigned cluster, thereby abrogating or significantly reducing EPS synthesis. These deletions were made possible with a newly developed, CRISPR-Cas9 based, genome-editing tool. The vector system is the first of its kind for *Paenibacillus* species and allows for highly efficient knockouts, as well as genomic integrations. By deleting certain genes within the EPS cluster, biochemical functions of some glycosyl transferases involved in the Wzx/Wzy-mediated biosynthesis could be proposed. These results are the first published indications on the genetic basis for EPS biosynthesis in *Paenibacilli*. Furthermore, EPS variants with altered physicochemical properties, as compared to the wild type polymer, were generated via genetic recoding of the production strain, underlining the possibility of providing custom-made polysaccharides by harnessing chassis organisms, amenable to genetic engineering.

Future work on *Paenibacillus* sp. 2H2 as a biotechnologically relevant EPS producer should focus on the optimization of the fermentative polymer production and on the in-depth characterization of Paenan. Adaption of process parameters and fermentation media could probably improve EPS yields and titers significantly, thereby making the overall process economically viable.

Identification of the exact chemical structure of Paenan will not only enhance the fundamental understanding of the physicochemical behavior of Paenan, but also help to uncover the relationship between genetic basis and resulting polymer structure. Ultimately, the precise knowledge on the functionality of each enzyme involved in EPS biosynthesis is essential to target the engineering of EPS variants. For this, a sophisticated and reliable analytical procedure to determine detailed structural features is key and is of major importance for future work on Paenan.

The established CRISPR-Cas9 based genome-editing tool represents a powerful instrument for several genetic studies in *Paenibacilli*. In case of EPSs, this of course includes the thorough investigation of biochemical functionalities of endogenous GTs, and the supply with exogenous or artificial enzymes to expand the producers' enzyme portfolio to generate novel EPS variants. In addition, the vector system could also be valuable to several other fields of *Paenibacillus* associated research. Once adapted to the corresponding strains, it could expedite studies on the production of value-added products by *Paenibacilli*, such as 2,3-butanediol or biocontrol agents, and it could be used to answer health related issues like *P. larvae* pathogenesis in honeybee larvae.

It is the increasing awareness of the society towards limitations of our natural resources that made this study possible and hopefully relevant to the future. Replacing petro-based products with bio-based alternatives, reducing chemical pesticides and protecting bees from extinction are only some examples related to this work and to *Paenibacilli* in general. The fact that the strains of this family affect humans in several beneficial as well as detrimental ways suggests that *Paenibacilli* will be subject to several studies in the near future. Desirably, the results presented here will help to answer some of the questions that may arise.

6 References

1. Hall S & Roome N (1996) Strategic choices and sustainable strategies. In: Groenewegen P (Ed.) *The Greening of Industry: Resource Guide and Bibliography*. Island Press, Washington.
2. Gavrilescu M & Chisti Y (2005) Biotechnology - a sustainable alternative for chemical industry. *Biotechnol. Adv.* 23(7):471-499.
3. Alban S & Blaschek W (2007) Kohlenhydrate II: Polysaccharide und Polysacchariddrogen. In: Hänsel R & Sticher O (Eds.) *Pharmakognosie - Phytopharmazie*. Springer Berlin Heidelberg, Berlin, Heidelberg, pp 515-653.
4. Busuioc M, Mackiewicz K, Buttaro BA, & Piggot PJ (2009) Role of intracellular polysaccharide in persistence of *Streptococcus mutans*. *J. Bacteriol.* 191(23):7315-7322.
5. Wilson WA, Roach PJ, Montero M, Baroja-Fernández E, Muñoz FJ, Eydallin G, Viale AM, & Pozueta-Romero J (2010) Regulation of glycogen metabolism in yeast and bacteria. *FEMS Microbiol. Rev.* 34(6):952-985.
6. Nwodo U, Green E, & Okoh A (2012) Bacterial exopolysaccharides: functionality and prospects. *Int. J. Mol. Sci.* 13(11):14002-14015.
7. Robyt JF (1998) Polysaccharides I. In: Robyt JF (Ed.) *Essentials of carbohydrate chemistry*. Springer New York, New York, NY, pp 157-227.
8. Selbmann L, Onofri S, Fenice M, Federici F, & Petruccioli M (2002) Production and structural characterization of the exopolysaccharide of the Antarctic fungus *Phoma herbarum* CCFEE 5080. *Res. Microbiol.* 153(9):585-592.
9. Roberson EB & Firestone MK (1992) Relationship between desiccation and exopolysaccharide production in a soil *Pseudomonas* sp. *Appl. Environ. Microbiol.* 58(4):1284-1291.
10. Ates O (2015) Systems biology of microbial exopolysaccharides production. *Front. Bioeng. Biotechnol.* 3:200.
11. Costerton JW, Stewart PS, & Greenberg EP (1999) Bacterial biofilms: A common cause of persistent infections. *Science* 284(5418):1318.
12. Cress BF, Englaender JA, He W, Kasper D, Linhardt RJ, & Koffas MAG (2014) Masquerading microbial pathogens: capsular polysaccharides mimic host-tissue molecules. *FEMS Microbiol. Rev.* 38(4):660-697.
13. Decho AW, Norman RS, & Visscher PT (2009) Quorum sensing in natural environments: emerging views from microbial mats. *Trends Microbiol.* 18(2):73-80.
14. Flemming H-C & Wingender J (2010) The biofilm matrix. *Nat. Rev. Microbiol.* 8:623.
15. Sutherland IW (1994) Structure-function relationships in microbial exopolysaccharides. *Biotechnol. Adv.* 12(2):393-448.
16. Dimitriu S (Ed.) (2005) *Polysaccharides: structural diversity and functional versatility*. Marcel Dekker, New York.
17. Larm O & Lindberg B (1976) The pneumococcal polysaccharides: a re-examination. In: Tipson RS & Horton D (Eds.) *Advances in Carbohydrate Chemistry and Biochemistry*. Academic Press, Washington, Vol 33, pp 295-322.
18. Becker A, Katzen F, Pühler A, & Ielpi L (1998) Xanthan gum biosynthesis and application: a biochemical/genetic perspective. *Appl. Microbiol. Biotechnol.* 50(2):145-152.
19. Wang Q & Cui SW (2005) Understanding the conformation of polysaccharides. In: Cui SW (Ed.) *Food Carbohydrates: Chemistry, Physical Properties, and Applications*. CRC Press, Boca Raton, pp 220-219.
20. Rees DA & Welsh EJ (1977) Secondary and tertiary structure of polysaccharides in solutions and gels. *Angew. Chem. Int. Ed.* 16(4):214-224.

21. Doraiswamy D (2002) The origins of rheology: a short historical excursion. *Rheology Bulletin* 71(1):1-9.
22. Williams PA & Phillips GO (2009) Introduction to food hydrocolloids. In: Williams PA & Phillips GO (Eds.) *Handbook of Hydrocolloids* (Second edition), Woodhead Publishing, Sawston, pp 1-22.
23. Chagas BS, Machado DLP, Haag RB, De Souza CR, & Lucas EF (2004) Evaluation of hydrophobically associated polyacrylamide-containing aqueous fluids and their potential use in petroleum recovery. *J. Appl. Poly. Sci.* 91(6):3686-3692.
24. Lapasin R & Priel S (1995) Rheology of polysaccharide systems. In: Lapasin R (Ed.) *Rheology of industrial polysaccharides: theory and applications*, Springer US, Boston, pp 250-494.
25. Becker A (2015) Challenges and perspectives in combinatorial assembly of novel exopolysaccharide biosynthesis pathways. *Front. Microbiol.* 6(687).
26. Islam ST, Taylor VL, Qi M, & Lam JS (2010) Membrane topology mapping of the O-antigen flippase (Wzx), polymerase (Wzy), and ligase (WaaL) from *Pseudomonas aeruginosa* PAO1 reveals novel domain architectures. *mBio* 1(3).
27. Willis LM & Whitfield C (2013) Structure, biosynthesis, and function of bacterial capsular polysaccharides synthesized by ABC transporter-dependent pathways. *Carbohydr. Res.* 378(Supplement C):35-44.
28. Whitney JC & Howell PL (2013) Synthase-dependent exopolysaccharide secretion in Gram-negative bacteria. *Trends Microbiol.* 21(2):63-72.
29. Schmid J, Sieber V, & Rehm B (2015) Bacterial exopolysaccharides: Biosynthesis pathways and engineering strategies. *Front. Microbiol.* 6.
30. Yother J (2011) Capsules of *Streptococcus pneumoniae* and other bacteria: paradigms for polysaccharide biosynthesis and regulation. *Annu. Rev. Microbiol.* 65(1):563-581.
31. Jolly L & Stingle F (2001) Molecular organization and functionality of exopolysaccharide gene clusters in lactic acid bacteria. *Int. Dairy J.* 11(9):733-745.
32. Whitfield C (2006) Biosynthesis and assembly of capsular polysaccharides in *Escherichia coli*. *Annu. Rev. Biochem.* 75(1):39-68.
33. Cuthbertson L, Mainprize IL, Naismith JH, & Whitfield C (2009) Pivotal roles of the outer membrane polysaccharide export and polysaccharide copolymerase protein families in export of extracellular polysaccharides in Gram-negative bacteria. *Microbiol. Mol. Biol. Rev.* 73(1):155-177.
34. Morona R, Purins L, Tocilj A, Matte A, & Cygler M (2009) Sequence-structure relationships in polysaccharide copolymerase (PCP) proteins. *Trends Biochem. Sci.* 34(2):78-84.
35. Rehm BH (2010) Bacterial polymers: biosynthesis, modifications and applications. *Nat. Rev. Microbiol.* 8(8):578-592.
36. Rehm BH & Valla S (1997) Bacterial alginates: biosynthesis and applications. *Appl. Microbiol. Biotechnol.* 48(3):281-288.
37. Chong BF, Blank LM, McLaughlin R, & Nielsen LK (2005) Microbial hyaluronic acid production. *Appl. Microbiol. Biotechnol.* 66(4):341-351.
38. Dols M, Remaud-Simeon M, Willemot RM, Vignon M, & Monsan P (1998) Characterization of the different dextransucrase activities excreted in glucose, fructose, or sucrose medium by *Leuconostoc mesenteroides* NRRL B-1299. *Appl. Environ. Microbiol.* 64(4):1298-1302.

39. Ceska M (1971) Biosynthesis of levan and a new method for the assay of levansucrase activity. *Biochem. J.* 125(1):209-211.
40. Finan TM, Kunkel B, De Vos GF, & Signer ER (1986) Second symbiotic megaplasmid in *Rhizobium meliloti* carrying exopolysaccharide and thiamine synthesis genes. *J. Bacteriol.* 167(1):66-72.
41. Schmid J, Heider D, Wendel NJ, Sperl N, & Sieber V (2016) Bacterial glycosyltransferases: Challenges and opportunities of a highly diverse enzyme class toward tailoring natural products. *Front. Microbiol.* 7:182.
42. Seviour RJ, McNeil B, Fazenda ML, & Harvey LM (2011) Operating bioreactors for microbial exopolysaccharide production. *Crit. Rev. Biotechnol.* 31(2):170-185.
43. Giavasis I, Harvey LM, & McNeil B (2000) Gellan gum. *Crit. Rev. Biotechnol.* 20(3):177-211.
44. Fazenda ML, Seviour R, McNeil B, & Harvey LM (2008) Submerged culture fermentation of “higher fungi”: the macrofungi. *Adv. Appl. Microbiol.* 63(1):33-103.
45. Gibbs PA & Seviour RJ (1996) Does the agitation rate and/or oxygen saturation influence exopolysaccharide production by *Aureobasidium pullulans* in batch culture? *Appl. Microbiol. Biotechnol.* 46(5):503-510.
46. Göksungur Y, Dağbaşı S, Uçan A, & Güvenç U (2005) Optimization of pullulan production from synthetic medium by *Aureobasidium pullulans* in a stirred tank reactor by response surface methodology. *J. Chem. Technol. Biotechnol.* 80(7):819-827.
47. Ürküt Z, Dağbaşı S, & Göksungur Y (2007) Optimization of pullulan production using Ca-alginate-immobilized *Aureobasidium pullulans* by response surface methodology. *J. Chem. Technol. Biotechnol.* 82(9):837-846.
48. Survase SA, Saudagar PS, Bajaj IB, & Singhal RS (2007) Scleroglucan: fermentative production, downstream processing and applications. *Food Technol. Biotechnol.* 45(2):107-118.
49. Singh RS, Saini GK, & Kennedy JF (2008) Pullulan: microbial sources, production and applications. *Carbohydr. Polym.* 73(4):515-531.
50. Freitas F, Alves VD, & Reis MA (2011) Advances in bacterial exopolysaccharides: from production to biotechnological applications. *Trends Biotechnol.* 29(8):388-398.
51. de Oliveira MR, da Silva RSSF, Buzato JB, & Celligoi MAPC (2007) Study of levan production by *Zymomonas mobilis* using regional low-cost carbohydrate sources. *Biochem. Eng. J.* 37(2):177-183.
52. Premjet S, Premjet D, & Ohtani Y (2007) The Effect of Ingredients of Sugar Cane Molasses on Bacterial Cellulose Production by *Acetobacter xylinum* ATCC 10245. *Sen'i Gakkaishi* 63(8):193-199.
53. Garcia-Ochoa F & Gomez E (2009) Bioreactor scale-up and oxygen transfer rate in microbial processes: An overview. *Biotechnol. Adv.* 27(2):153-176.
54. Gibbs PA, Seviour RJ, & Schmid F (2000) Growth of filamentous fungi in submerged culture: problems and possible solutions. *Crit. Rev. Biotechnol.* 20(1):17-48.
55. McNeil B & Harvey LM (1993) Viscous fermentation products. *Crit. Rev. Biotechnol.* 13(4):275-304.
56. McNeil B & Harvey LM (2008) Fermentation equipment selection: laboratory scale bioreactor design considerations. In: Matthews G (Ed.) *Practical Fermentation Technology*, John Wiley & Sons, Hoboken, pp 3-36.
57. Fialho A, Moreira L, Granja A, Popescu A, Hoffmann K, & Sá-Correia I (2008) Occurrence, production, and applications of gellan: current state and perspectives. *Appl. Microbiol. Biotechnol.* 79(6):889-900.

58. McIntosh M, Stone BA, & Stanisich VA (2005) Curdlan and other bacterial (1→3)-β-d-glucans. *Appl. Microbiol. Biotechnol.* 68(2):163-173.
59. Nienow AW (1990) Agitators for mycelial fermentations. *Trends Biotechnol.* 8:224-233.
60. Rosalam S & England R (2006) Review of xanthan gum production from unmodified starches by *Xanthomonas campestris* sp. *Enzyme Microb. Technol.* 39(2):197-207.
61. Giavasis I, Robertson I, McNeil B, & Harvey LM (2003) Simultaneous and rapid monitoring of biomass and biopolymer production by *Sphingomonas paucimobilis* using Fourier transform-near infrared spectroscopy. *Biotechnol Lett* 25(12):975-979.
62. Bajaj IB, Survase SA, Saudagar PS, & Singhal RS (2007) Gellan gum: fermentative production, downstream processing and applications. *Food Technol. Biotechnol.* 45(4).
63. Hublik G (2012) Xanthan. In: Matyjaszewski K & Möller M (Eds.). *Polymer Science: A Comprehensive Reference*, Elsevier, Amsterdam, pp 221-229.
64. Freitas F, Alves V, & Reis MM (2014) Bacterial polysaccharides: production and applications in cosmetic industry. In: Ramawat KG & Mérillon J-M (Eds.) *Polysaccharides*, Springer International Publishing, Cham, pp 1-24.
65. Becker A & Vorhölter F-J (2009) Xanthan biosynthesis by *Xanthomonas* bacteria: an overview of the current biochemical and genomic data. In: Rehm BH (Ed.) *Microbial production of biopolymers and polymer precursors: Applications and perspectives*. Caister Academic Press, Poole, pp 1-11.
66. Imeson A (Ed.) (2011) *Food stabilizers, thickeners and gelling agents*. John Wiley & Sons, Hoboken.
67. Rehm BH (Ed.) (2009) *Microbial production of biopolymers and polymer precursors: applications and perspectives*. Caister Academic Press, Poole.
68. Rehm BH (Ed.) (2009) *Alginates: biology and applications*. Springer, New York.
69. Chawla PR, Bajaj IB, Survase SA, & Singhal RS (2009) Microbial cellulose: fermentative production and applications. *Food Technol. Biotechnol.* 47(2):107-124.
70. Yang S-T (Ed.) (2011) *Bioprocessing for value-added products from renewable resources: new technologies and applications*. Elsevier, Amsterdam.
71. Simsek S, Mert B, Campanella OH, & Reuhs B (2009) Chemical and rheological properties of bacterial succinoglycan with distinct structural characteristics. *Carbohydr. Polym.* 76(2):320-324.
72. Ullrich M (Ed.) (2009) *Bacterial polysaccharides: current innovations and future trends*, Caister Academic Press, Poole.
73. Glass JE, Schulz DN, & Zukoski CF (1991) Polymers as rheology modifiers. *ACS Symposium Series*, Vol 462, pp 2-17.
74. Alves VD, Ferreira AR, Costa N, Freitas F, Reis MAM, & Coelho IM (2011) Characterization of biodegradable films from the extracellular polysaccharide produced by *Pseudomonas oleovorans* grown on glycerol byproduct. *Carbohydr. Polym.* 83(4):1582-1590.
75. Aguilera JM, Aguilera JM, Lillford P, & Peter JL (Eds.) (2008) *Food materials science: principles and practice*. Springer, New York.
76. Nguyen VT, Gidley MJ, & Dykes GA (2008) Potential of a nisin-containing bacterial cellulose film to inhibit *Listeria monocytogenes* on processed meats. *Food Microbiol.* 25(3):471-478.
77. Rodríguez-Carmona E & Villaverde A (2010) Nanostructured bacterial materials for innovative medicines. *Trends Microbiol.* 18(9):423-430.

78. Thorne L, Mikolajczak MJ, Armentrout RW, & Pollock TJ (2000) Increasing the yield and viscosity of exopolysaccharides secreted by *Sphingomonas* by augmentation of chromosomal genes with multiple copies of cloned biosynthetic genes. *J. Ind. Microbiol. Biotechnol.* 25(1):49-57.
79. Schatschneider S, Persicke M, Watt SA, Hublik G, Pühler A, Niehaus K, & Vorhölter F-J (2013) Establishment, in silico analysis, and experimental verification of a large-scale metabolic network of the xanthan producing *Xanthomonas campestris* pv. *campestris* strain B100. *J. Biotechnol.* 167(2):123-134.
80. van Kranenburg R, Boels IC, Kleerebezem M, & de Vos WM (1999) Genetics and engineering of microbial exopolysaccharides for food: approaches for the production of existing and novel polysaccharides. *Curr. Opin. Biotechnol.* 10(5):498-504.
81. Pollock TJ, Yamazaki M, Thorne L, Mikolajczak M, & Armentrout RW (2001) DNA segments and methods for increasing polysaccharide production. Patent: US6284516 B1.
82. Harding NE, Patel YN, Coleman R, & Matzke S (2011) High viscosity diutan gums. Patent: US7868167 B2.
83. Jones KM (2012) Increased production of the exopolysaccharide succinoglycan enhances *Sinorhizobium meliloti* 1021 symbiosis with the host plant *Medicago truncatula*. *J. Bacteriol.* 194(16):4322-4331.
84. Peña C, Miranda L, Segura D, Núñez C, Espín G, & Galindo E (2002) Alginate production by *Azotobacter vinelandii* mutants altered in poly- β -hydroxybutyrate and alginate biosynthesis. *J. Ind. Microbiol. Biotechnol.* 29(5):209-213.
85. Galindo E, Peña C, Núñez C, Segura D, & Espín G (2007) Molecular and bioengineering strategies to improve alginate and polydihydroxyalkanoate production by *Azotobacter vinelandii*. *Microb. Cell Fact.* 6(1):7.
86. Díaz-Barrera A, Silva P, Berrios J, & Acevedo F (2010) Manipulating the molecular weight of alginate produced by *Azotobacter vinelandii* in continuous cultures. *Bioresour. Technol.* 101(23):9405-9408.
87. Galván EM, Ielmini MV, Patel YN, Bianco MI, Franceschini EA, Schneider JC, & Ielpi L (2013) Xanthan chain length is modulated by increasing the availability of the polysaccharide copolymerase protein GumC and the outer membrane polysaccharide export protein GumB. *Glycobiology* 23(2):259-272.
88. Hassler RA & Doherty DH (1990) Genetic engineering of polysaccharide structure: production of variants of xanthan gum in *Xanthomonas campestris*. *Biotechnol. Progr.* 6(3):182-187.
89. Morris ER, Rees DA, Young G, Walkinshaw MD, & Darke A (1977) Order-disorder transition for a bacterial polysaccharide in solution. A role for polysaccharide conformation in recognition between *Xanthomonas* pathogen and its plant host. *J. Mol. Biol.* 110(1):1-16.
90. Lecourtier J, Chauveteau G, & Muller G (1986) Salt-induced extension and dissociation of a native double-stranded xanthan. *Int. J. Biol. Macromol.* 8(5):306-310.
91. Muller G, Aurhourrache M, Lecourtier J, & Chauveteau G (1986) Salt dependence of the conformation of a single-stranded xanthan. *Int. J. Biol. Macromol.* 8(3):167-172.
92. Welman AD & Maddox IS (2003) Exopolysaccharides from lactic acid bacteria: perspectives and challenges. *Trends Biotechnol.* 21(6):269-274.
93. Schmid J & Sieber V (2015) Enzymatic transformations involved in the biosynthesis of microbial exopolysaccharides based on the assembly of repeat units. *ChemBioChem.* 16(8):1141-1147.
94. Rehm BHA (2015) Synthetic biology towards the synthesis of custom-made polysaccharides. *Microb. Biotechnol.* 8(1):19-20.

95. Scherer S & Davis RW (1979) Replacement of chromosome segments with altered DNA sequences constructed in vitro. *PNAS* 76(10):4951-4955.
96. Rudin N, Sugarman E, & Haber JE (1989) Genetic and physical analysis of double-strand break repair and recombination in *Saccharomyces cerevisiae*. *Genetics* 122(3):519.
97. Strobel SA, Doucette-Stamm LA, Riba L, Housman DE, & Dervan PB (1991) Site-specific cleavage of human chromosome 4 mediated by triple-helix formation. *Science* 254(5038):1639.
98. Strobel SA & Dervan PB (1991) Single-site enzymatic cleavage of yeast genomic DNA mediated by triple helix formation. *Nature* 350:172.
99. Sandor Z & Bredberg A (1995) Deficient DNA repair of triple helix-directed double psoralen damage in human cells. *FEBS Lett.* 374(2):287-291.
100. Bibikova M, Beumer K, Trautman JK, & Carroll D (2003) Enhancing gene targeting with designed zinc finger nucleases. *Science* 300(5620):764.
101. Boch J, Scholze H, Schornack S, Landgraf A, Hahn S, Kay S, Lahaye T, Nickstadt A, & Bonas U (2009) Breaking the code of DNA binding specificity of TAL-type III effectors. *Science* 326(5959):1509.
102. Enyeart PJ, Chirieleison SM, Dao MN, Perutka J, Quandt EM, Yao J, Whitt JT, Keatinge-Clay AT, Lambowitz AM, & Ellington AD (2013) Generalized bacterial genome editing using mobile group II introns and Cre-lox. *Mol. Syst. Biol.* 9:685.
103. Doudna JA & Charpentier E (2014) The new frontier of genome engineering with CRISPR-Cas9. *Science* 346(6213).
104. Bhaya D, Davison M, & Barrangou R (2011) CRISPR-Cas systems in bacteria and archaea: versatile small RNAs for adaptive defense and regulation. *Annu. Rev. Genet.* 45(1):273-297.
105. Wiedenheft B, Sternberg SH, & Doudna JA (2012) RNA-guided genetic silencing systems in bacteria and archaea. *Nature* 482:331.
106. Horvath P & Barrangou R (2010) CRISPR-Cas, the immune system of bacteria and archaea. *Science* 327(5962):167.
107. Brouns SJJ, Jore MM, Lundgren M, Westra ER, Slijkhuis RJH, Snijders APL, Dickman MJ, Makarova KS, Koonin EV, & van der Oost J (2008) Small CRISPR RNAs guide antiviral defense in prokaryotes. *Science* 321(5891):960.
108. Mali P, Esvelt KM, & Church GM (2013) Cas9 as a versatile tool for engineering biology. *Nat. Meth.* 10(10):957-963.
109. Jinek M, Jiang F, Taylor DW, Sternberg SH, Kaya E, Ma E, Anders C, Hauer M, Zhou K, Lin S, Kaplan M, Iavarone AT, Charpentier E, Nogales E, & Doudna JA (2014) Structures of Cas9 endonucleases reveal RNA-mediated conformational activation. *Science* 343(6176).
110. Jinek M, Chylinski K, Fonfara I, Hauer M, Doudna JA, & Charpentier E (2012) A programmable dual-RNA - guided DNA endonuclease in adaptive bacterial immunity. *Science* 337(6096):816.
111. Deltcheva E, Chylinski K, Sharma CM, Gonzales K, Chao Y, Pirzada ZA, Eckert MR, Vogel J, & Charpentier E (2011) CRISPR RNA maturation by trans-encoded small RNA and host factor RNase III. *Nature* 471(7340):602-607.
112. Barrangou R & Marraffini Luciano A (2014) CRISPR-Cas systems: prokaryotes upgrade to adaptive immunity. *Mol. Cell* 54(2):234-244.
113. van der Oost J, Westra ER, Jackson RN, & Wiedenheft B (2014) Unravelling the structural and mechanistic basis of CRISPR-Cas systems. *Nat. Rev. Microbiol.* 12:479.

114. Bondy-Denomy J & Davidson AR (2013) To acquire or resist: the complex biological effects of CRISPR-Cas systems. *Trends Microbiol.* 22(4):218-225.
115. Peters JM, Silvis MR, Zhao D, Hawkins JS, Gross CA, & Qi LS (2015) Bacterial CRISPR: accomplishments and prospects. *Curr. Opin. Microbiol.* 27:121-126.
116. Selle K & Barrangou R (2013) Harnessing CRISPR-Cas systems for bacterial genome editing. *Trends Microbiol.* 23(4):225-232.
117. Gasiunas G, Barrangou R, Horvath P, & Siksnyš V (2012) Cas9–crRNA ribonucleoprotein complex mediates specific DNA cleavage for adaptive immunity in bacteria. *PNAS* 109(39):E2579–E2586.
118. Fu Y, Sander JD, Reyon D, Cascio VM, & Joung JK (2014) Improving CRISPR-Cas nuclease specificity using truncated guide RNAs. *Nat. Biotechnol.* 32:279.
119. Grady EN, MacDonald J, Liu L, Richman A, & Yuan Z-C (2016) Current knowledge and perspectives of *Paenibacillus*: a review. *Microb. Cell Fact.* 15(1):203.
120. Ash C, Priest F, & Collins MD (1993) Molecular identification of rRNA group 3 *bacilli* using a PCR probe test. *Antonie Leeuwenhoek* 64(3-4):253-260.
121. Priest FG, Goodfellow M, & Todd C (1988) A numerical classification of the genus *Bacillus*. *Microbiology* 134(7):1847-1882.
122. Ash C, Farrow JAE, Wallbanks S, & Collins MD (1991) Phylogenetic heterogeneity of the genus *Bacillus* revealed by comparative analysis of small-subunit-ribosomal RNA sequences. *Lett. Appl. Microbiol.* 13(4):202-206.
123. Shida O, Takagi H, Kadowaki K, Nakamura Lk, & Komagata K (1997) Transfer of *Bacillus alginolyticus*, *Bacillus chondroitinus*, *Bacillus curdulanolyticus*, *Bacillus glucanolyticus*, *Bacillus kobensis*, and *Bacillus thiaminolyticus* to the genus *Paenibacillus* and emended description of the genus *Paenibacillus*. *Int. J. Syst. Evol. Microbiol.* 47(2):289-298.
124. Zeigler D (2013) The family *Paenibacillaceae*. Strain catalog and reference. Columbus: Bacillus Genetic Stock Center:1-32.
125. Fürnkranz M, Adam E, Müller H, Grube M, Huss H, Winkler J, & Berg G (2012) Promotion of growth, health and stress tolerance of Styrian oil pumpkins by bacterial endophytes. *Euro. J. Plant Pathol.* 134(3):509-519.
126. de Souza R, Meyer J, Schoenfeld R, da Costa PB, & Passaglia LMP (2015) Characterization of plant growth-promoting bacteria associated with rice cropped in iron-stressed soils. *Ann. Microbiol.* 65(2):951-964.
127. Xie J-B, Du Z, Bai L, Tian C, Zhang Y, Xie J-Y, Wang T, Liu X, Chen X, Cheng Q, Chen S, & Li J (2014) Comparative genomic analysis of N₂-fixing and non-N₂-fixing *Paenibacillus* spp.: organization, evolution and expression of the nitrogen fixation genes. *PLoS Genet.* 10(3):e1004231.
128. Xie J, Shi H, Du Z, Wang T, Liu X, & Chen S (2016) Comparative genomic and functional analysis reveal conservation of plant growth promoting traits in *Paenibacillus polymyxa* and its closely related species. *Sci. Rep.* 6:21329.
129. Das SN, Dutta S, Kondreddy A, Chilukoti N, Pullabhotla SVSRN, Vadlamudi S, & Podile AR (2010) Plant growth-promoting chitinolytic *Paenibacillus elgii* responds positively to tobacco root exudates. *J. Plant Growth Regul.* 29(4):409-418.
130. Wang Y, Shi Y, Li B, Shan C, Ibrahim M, Jabeen A, Xie G, & Sun G (2012) Phosphate solubilization of *Paenibacillus polymyxa* and *Paenibacillus macerans* from mycorrhizal and non-mycorrhizal cucumber plants. *Afr. J. Microbiol. Res.* 6(21):4567-4573.

131. Delker C, Raschke A, & Quint M (2008) Auxin dynamics: the dazzling complexity of a small molecule's message. *Planta* 227(5):929-941.
132. Duca D, Lorv J, Patten CL, Rose D, & Glick BR (2014) Indole-3-acetic acid in plant-microbe interactions. *Antonie Leeuwenhoek* 106(1):85-125.
133. Yang J, Kharbanda P, & Mirza M (2002) Evaluation of *Paenibacillus polymyxa* pkb1 for biocontrol of Pythium disease of cucumber in a hydroponic system. XXVI International Horticultural Congress: Managing Soil-Borne Pathogens: A Sound Rhizosphere to Improve Productivity in Intensive Horticultural Systems 635, pp 59-66.
134. Akhtar MS & Siddiqui ZA (2007) Biocontrol of a chickpea root-rot disease complex with *Glomus intraradices*, *Pseudomonas putida* and *Paenibacillus polymyxa*. *Australas. Plant Pathol.* 36(2):175-180.
135. Haggag WM (2007) Colonization of exopolysaccharide-producing *Paenibacillus polymyxa* on peanut roots for enhancing resistance against crown rot disease. *Afr. J. Biotechnol.* 6(13).
136. Zhou K, Yamagishi M, & Osaki M (2008) *Paenibacillus* BRF-1 has biocontrol ability against *Phialophora gregata* disease and promotes soybean growth. *J. Soil Sci. Plant Nutr.* 54(6):870-875.
137. Phi Q-T, Park Y-M, Seul K-J, Ryu C-M, Park S-H, Kim J-G, & Ghim S-Y (2010) Assessment of root-associated *Paenibacillus polymyxa* groups on growth promotion and induced systemic resistance in pepper. *J. Microbiol. Biotechnol.* 20(12):1605-1613.
138. Pieterse CMJ, Zamioudis C, Berendsen RL, Weller DM, Van Wees SCM, & Bakker PAHM (2014) Induced systemic resistance by beneficial microbes. *Annu. Rev. Phytopathol.* 52(1):347-375.
139. Lee B, Farag MA, Park HB, Kloepper JW, Lee SH, & Ryu C-M (2012) Induced resistance by a long-chain bacterial volatile: elicitation of plant systemic defense by a C13 volatile produced by *Paenibacillus polymyxa*. *PLoS ONE* 7(11):e48744.
140. Sharma A, Thakur DR, Kanwar S, & Chandla VK (2013) Diversity of entomopathogenic bacteria associated with the white grub, *Brahmina coriacea*. *J. Pest Sci.* 86(2):261-273.
141. Neung S, Nguyen XH, Naing KW, Lee YS, & Kim KY (2014) Insecticidal potential of *Paenibacillus elgii* HOA73 and its combination with organic sulfur pesticide on diamondback moth, *Plutella xylostella*. *J. Korean Soc. Appl. Biol. Chem.* 57(2):181-186.
142. Cochrane SA & Vederas JC (2016) Lipopeptides from *Bacillus* and *Paenibacillus* spp.: a gold mine of antibiotic candidates. *Med. Res. Rev.* 36(1):4-31.
143. Velkov T, Roberts KD, Nation RL, Wang J, Thompson PE, & Li J (2014) Teaching 'old' polymyxins new tricks: new-generation lipopeptides targeting gram-negative 'superbugs'. *ACS Chem. Biol.* 9(5):1172-1177.
144. He Z, Kisla D, Zhang L, Yuan C, Green-Church KB, & Yousef AE (2007) Isolation and identification of a *Paenibacillus polymyxa* strain that coproduces a novel lantibiotic and polymyxin. *Appl. Environ. Microbiol.* 73(1):168-178.
145. Abriouel H, Franz CMAP, Omar NB, & Gálvez A (2011) Diversity and applications of *Bacillus* bacteriocins. *FEMS Microbiol. Rev.* 35(1):201-232.
146. Kajimura Y & Kaneda M (1996) Fusaricidin A, a new depsipeptide antibiotic produced by *Bacillus polymyxa* KT-8. *J. Antibiot.* 49(2):129-135.
147. Abbasian F, Lockington R, Mallavarapu M, & Naidu R (2015) A comprehensive review of aliphatic hydrocarbon biodegradation by bacteria. *Appl. Biochem. Biotechnol.* 176(3):670-699.

148. Haritash AK & Kaushik CP (2009) Biodegradation aspects of polycyclic aromatic hydrocarbons (PAHs): a review. *J. Hazard. Mater.* 169(1):1-15.
149. Häßler T, Schieder D, Pfaller R, Faulstich M, & Sieber V (2012) Enhanced fed-batch fermentation of 2,3-butanediol by *Paenibacillus polymyxa* DSM 365. *Bioresour. Technol.* 124:237-244.
150. Genersch E (2010) American Foulbrood in honeybees and its causative agent, *Paenibacillus larvae*. *J. Invertebr. Pathol.* 103, Supplement:S10-S19.
151. Djukic M, Brzuszkiewicz E, Fünfhaus A, Voss J, Gollnow K, Poppinga L, Liesegang H, Garcia-Gonzalez E, Genersch E, & Daniel R (2014) How to kill the honey bee larva: genomic potential and virulence mechanisms of *Paenibacillus larvae*. *PLoS ONE* 9(3):e90914.
152. Jatulan EO, Rabajante JF, Banaay CGB, Fajardo AC, Jr., & Jose EC (2015) A mathematical model of intra-colony spread of American Foulbrood in European honeybees (*Apis mellifera* L.). *PLoS ONE* 10(12):e0143805.
153. Ninomiya E & Kizaki T (1969) Bacterial polysaccharide from *Bacillus polymyxa* No. 271. *Angew. Makromol. Chem.* 6(1):179-185.
154. Jung H-K, Hong J-H, Park S-C, Park B-K, Nam D-H, & Kim S-D (2007) Production and physicochemical characterization of β -glucan produced by *Paenibacillus polymyxa* JB115. *Biotechnol. Bioprocess Eng.* 12(6):713-719.
155. Han YW & Clarke MA (1990) Production and characterization of microbial levan. *J. Agr. Food Chem.* 38(2):393-396.
156. Li O, Lu C, Liu A, Zhu L, Wang P-M, Qian C-D, Jiang X-H, & Wu X-C (2013) Optimization and characterization of polysaccharide-based bioflocculant produced by *Paenibacillus elgii* B69 and its application in wastewater treatment. *Bioresour. Technol.* 134(0):87-93.
157. Morillo J, Guerra del Águila V, Aguilera M, Ramos-Cormenzana A, & Monteoliva-Sánchez M (2007) Production and characterization of the exopolysaccharide produced by *Paenibacillus jamilae* grown on olive mill-waste waters. *World J. Microbiol. Biotechnol.* 23(12):1705-1710.
158. Tang J, Qi S, Li Z, An Q, Xie M, Yang B, & Wang Y (2014) Production, purification and application of polysaccharide-based bioflocculant by *Paenibacillus mucilaginosus*. *Carbohydr. Polym.* 113:463-470.
159. Ahn S, Suh H-H, Lee C-H, Moon S-H, Kim H-S, Ahn K-H, Kwon G-S, Oh H-M, & Yoon B-D (1998) Isolation and characterization of a novel polysaccharide producing *Bacillus polymyxa* A49 KCTC 4648P. *J. Microbiol. Biotechnol.* 8(2):171-177.
160. Liang T-W & Wang S-L (2015) Recent advances in exopolysaccharides from *Paenibacillus* spp.: production, isolation, structure, and bioactivities. *Mar. Drugs* 13(4):1847-1863.
161. Morillo J, Aguilera M, Ramos-Cormenzana A, & Monteoliva-Sánchez M (2006) Production of a metal-binding exopolysaccharide by *Paenibacillus jamilae* using two-phase olive-mill waste as fermentation substrate. *Curr. Microbiol.* 53(3):189-193.
162. Wang C-L, Huang T-H, Liang T-W, Fang C-Y, & Wang S-L (2011) Production and characterization of exopolysaccharides and antioxidant from *Paenibacillus* sp. TKU023. *New Biotechnol.* 28(6):559-565.
163. Pooja KP & Chandra TS (2009) Production and partial characterization of a novel capsular polysaccharide KP-EPS produced by *Paenibacillus pabuli* strain ATSKP. *World J. Microbiol. Biotechnol.* 25(5):835-841.
164. Lee IY, Seo WT, Kim GJ, Kim MK, Ahn SG, Kwon GS, & Park YH (1997) Optimization of fermentation conditions for production of exopolysaccharide by *Bacillus polymyxa*. *Bioprocess Eng.* 16(2):71-75.

165. Raza W, Makeen K, Wang Y, Xu Y, & Qirong S (2011) Optimization, purification, characterization and antioxidant activity of an extracellular polysaccharide produced by *Paenibacillus polymyxa* SQR-21. *Bioresour. Technol.* 102(10):6095-6103.
166. Kim S-W, Ahn S-G, Seo W-T, Kwon G-S, & Park Y-H (1998) Rheological properties of a novel high viscosity polysaccharide, A49-Pol, produced by *Bacillus polymyxa*. *J. Microbiol. Biotechnol.* 8(2):178-181.
167. Madden JK, Dea ICM, & Steer DC (1986) Structural and rheological properties of the extracellular polysaccharides from *Bacillus polymyxa*. *Carbohydr. Polym.* 6(1):51-73.
168. Liu J, Luo J, Ye H, Sun Y, Lu Z, & Zeng X (2009) Production, characterization and antioxidant activities in vitro of exopolysaccharides from endophytic bacterium *Paenibacillus polymyxa* EJS-3. *Carbohydr. Polym.* 78(2):275-281.
169. Liu J, Luo J, Ye H, Sun Y, Lu Z, & Zeng X (2010) Medium optimization and structural characterization of exopolysaccharides from endophytic bacterium *Paenibacillus polymyxa* EJS-3. *Carbohydr. Polym.* 79(1):206-213.
170. Chang Z-Q, Lee J-S, Hwang M-H, Hong J-H, Jung H-K, Lee S-P, & Park S-C (2009) A novel β -glucan produced by *Paenibacillus polymyxa* JB115 induces nitric oxide production in RAW264.7 macrophages. *J. Vet. Sci.* 10(2):165.
171. Morillo Pérez J, García-Ribera R, Quesada T, Aguilera M, Ramos-Cormenzana A, & Monteoliva-Sánchez M (2008) Biosorption of heavy metals by the exopolysaccharide produced by *Paenibacillus jamilae*. *World J Microbiol. Biotechnol.* 24(11):2699-2704.
172. Aguilera M, Monteoliva-Sanchez M, Suarez A, Guerra V, Lizama C, Bennasar A, & Ramos-Cormenzana A (2001) *Paenibacillus jamilae* sp. nov., an exopolysaccharide-producing bacterium able to grow in olive-mill wastewater. *Int. J. Syst. Evol. Microbiol.* 51(Pt 5):1687-1692.
173. Yegorenkova IV, Tregubova KV, Matora LY, Burygin GL, & Ignatov VV (2008) Composition and immunochemical characteristics of exopolysaccharides from the rhizobacterium *Paenibacillus polymyxa* 1465. *Microbiology* 77(5):553-558.
174. Yegorenkova I, Tregubova K, Matora L, Burygin G, & Ignatov V (2011) Biofilm formation by *Paenibacillus polymyxa* strains differing in the production and rheological properties of their exopolysaccharides. *Curr. Microbiol.* 62(5):1554-1559.
175. Kahng G-G, Lim S-H, Yun H-D, & Seo W-T (2001) Production of extracellular polysaccharide, EPS WN9, from *Paenibacillus* sp. WN9 KCTC 8951P and its usefulness as a cement mortar admixture. *Biotechnol. Bioprocess Eng.* 6(2):112-116.
176. Weon-Taek S, Kahng G-G, Nam S-H, Choi S-D, Suh H-H, Kim S-W, & Park Y-H (1999) Isolation and characterization of a novel exopolysaccharide-producing *Paenibacillus* sp. WN9 KCTC 8951P. *J. Microbiol. Biotechnol.* 9(6):820-825.
177. Sukplang P & Vela GR (2000) Production and characterization of a novel extracellular polysaccharide produced by *Paenibacillus velaei*, sp. nov. Ph. D. thesis, University of North Texas.
178. Aziz R, Bartels D, Best A, DeJongh M, Disz T, Edwards R, Formsma K, Gerdes S, Glass E, Kubal M, Meyer F, Olsen G, Olson R, Osterman A, Overbeek R, McNeil L, Paarmann D, Paczian T, Parrello B, Pusch G, Reich C, Stevens R, Vassieva O, Vonstein V, Wilke A, & Zagnitko O (2008) The RAST Server: Rapid Annotations using Subsystems Technology. *BMC Genomics* 9(1):75.
179. Cobb RE, Wang Y, & Zhao H (2015) High-efficiency multiplex genome editing of *Streptomyces* species using an engineered CRISPR-Cas system. *ACS Synth. Biol.* 4(6):723-728.

180. Kim OS, Cho YJ, Lee K, Yoon SH, Kim M, Na H, Park SC, Jeon YS, Lee JH, Yi H, Won S, & Chun J (2012) Introducing EzTaxon-e: a prokaryotic 16S rRNA gene sequence database with phylotypes that represent uncultured species. *Int. J. Syst. Evol. Microbiol.* 62(3):716-721.
181. Boe L, Gros MF, te Riele H, Ehrlich SD, & Gruss A (1989) Replication origins of single-stranded-DNA plasmid pUB110. *J. Bacteriol.* 171(6):3366-3372.
182. Altschul SF, Gish W, Miller W, Myers EW, & Lipman DJ (1990) Basic local alignment search tool. *J. Mol. Biol.* 215(3):403-410.
183. Apweiler R, Bairoch A, Wu CH, Barker WC, Boeckmann B, Ferro S, Gasteiger E, Huang H, Lopez R, Magrane M, Martin MJ, Natale DA, O'Donovan C, Redaschi N & Yeh L-SL (2004) UniProt: the Universal Protein knowledgebase. *Nucleic Acids Res.* 32(suppl_1):D115-D119.
184. Yu C-S, Lin C-J, & Hwang J-K (2004) Predicting subcellular localization of proteins for Gram-negative bacteria by support vector machines based on n-peptide compositions. *Prot. Sci.* 13(5):1402-1406.
185. Kanehisa M & Goto S (2000) KEGG: Kyoto Encyclopedia of Genes and Genomes. *Nucleic Acids Res.* 28(1):27-30.
186. Rühmann B, Schmid J, & Sieber V (2014) Fast carbohydrate analysis via liquid chromatography coupled with ultra violet and electrospray ionization ion trap detection in 96-well format. *J. Chrom. A* 1350(0):44-50.
187. Rühmann B, Schmid J, & Sieber V (2016) Automated modular high throughput exopolysaccharide screening platform coupled with highly sensitive carbohydrate fingerprint analysis. *JoVE* (110):e53249.
188. DuBois M, Gilles KA, Hamilton JK, Rebers PA, & Smith F (1956) Colorimetric method for determination of sugars and related substances. *Anal. Chem.* 28(3):350-356.
189. Bradford MM (1976) A rapid and sensitive method for the quantitation of microgram quantities of protein utilizing the principle of protein-dye binding. *Anal. Biochem.* 72(1):248-254.
190. Toukach P, Joshi HJ, Ranzinger R, Knirel Y, & von der Lieth C-W (2007) Sharing of worldwide distributed carbohydrate-related digital resources: online connection of the Bacterial Carbohydrate Structure DataBase and GLYCOSCIENCES. *Nucleic acids Res.* 35(suppl 1):D280-D286.
191. Stewart EJ (2012) Growing unculturable bacteria. *J. Bacteriol.* 194(16):4151-4160.
192. Rühmann B, Schmid J, & Sieber V (2015) High throughput exopolysaccharide screening platform: From strain cultivation to monosaccharide composition and carbohydrate fingerprinting in one day. *Carbohydr. Polym.* 122(0):212-220.
193. Wilson K (2001) Preparation of Genomic DNA from Bacteria. *Curr. Protoc. Mol. Biol.*, John Wiley & Sons, Inc., Hoboken.
194. Patel RK & Jain M (2012) NGS QC toolkit: a toolkit for quality control of next generation sequencing data. *PLoS ONE* 7(2):e30619.
195. Martin M (2011) Cutadapt removes adapter sequences from high-throughput sequencing reads. *EMBnet* 17(1):pp. 10-12.
196. Cox MP, Peterson DA, & Biggs PJ (2010) SolexaQA: At-a-glance quality assessment of Illumina second-generation sequencing data. *BMC Bioinform.* 11(1):485.
197. Zerbino DR & Birney E (2008) Velvet: algorithms for de novo short read assembly using de Bruijn graphs. *Genome Res.* 18(5):821-829.

198. Overbeek R, Begley T, Butler RM, Choudhuri JV, Chuang H-Y, Cohoon M, de Crécy-Lagard V, Diaz N, Disz T, Edwards R, Fonstein M, Frank ED, Gerdes S, Glass EM, Goesmann A, Hanson A, Iwata-Reuyl D, Jensen R, Jamshidi N, Krause L, Kubal M, Larsen N, Linke B, McHardy AC, Meyer F, Neuweyer H, Olsen G, Olson R, Osterman A, Portnoy V, Pusch GD, Rodionov DA, Rückert C, Steiner J, Stevens R, Thiele I, Vassieva O, Ye Y, Zagnitko O, & Vonstein V (2005) The subsystems approach to genome annotation and its use in the project to annotate 1000 genomes. *Nucleic Acids Res.* 33(17):5691-5702.
199. Rütting M, Schmid J, Rühmann B, Schilling M, & Sieber V (2016) Controlled production of polysaccharides—exploiting nutrient supply for levan and heteropolysaccharide formation in *Paenibacillus* sp. *Carbohydr. Polym.* 148:326-334.
200. Tallgren AH, Airaksinen U, von Weissenberg R, Ojamo H, Kuusisto J, & Leisola M (1999) Exopolysaccharide-producing bacteria from sugar beets. *Appl. Environ. Microbiol.* 65(2):862-864.
201. MA J-j & YIN R-c (2011) Primary study on extracellular polysaccharide producing bacteria in different environments. *J. Anhui Uni.* (Natural Science Edition) 3.
202. Garai-Ibabe G, Areizaga J, Aznar R, Elizaquivel P, Prieto A, Irastorza A, & Dueñas MT (2010) Screening and selection of 2-branched (1,3)- β -D-glucan producing lactic acid bacteria and exopolysaccharide characterization. *J. Agr. Food Chem.* 58(10):6149-6156.
203. van Geel-Schutten GH, Flesch F, ten Brink B, Smith MR, & Dijkhuizen L (1998) Screening and characterization of *Lactobacillus* strains producing large amounts of exopolysaccharides. *Appl. Microbiol. Biotechnol.* 50(6):697-703.
204. Reuber TL & Walker GC (1993) Biosynthesis of succinoglycan, a symbiotically important exopolysaccharide of *Rhizobium meliloti*. *Cell* 74(2):269-280.
205. Stredansky M & Conti E (1999) Succinoglycan production by solid-state fermentation with *Agrobacterium tumefaciens*. *Appl. Microbiol. Biotechnol.* 52(3):332-337.
206. Vincze E & Bowra S (2006) Transformation of rhizobia with broad-host-range plasmids by using a freeze-thaw method. *Appl. Environ. Microbiol.* 72(3):2290-2293.
207. Bräutigam E, Fiedler F, Woitzik D, Flammann HT, & Weckesser J (1988) Capsule polysaccharide-protein-peptidoglycan complex in the cell envelope of *Rhodobacter capsulatus*. *Arch. Microbiol.* 150(6):567-573.
208. Suh IS, Herbst H, Schumpe A, & Deckwer WD (1990) The molecular weight of xanthan polysaccharide produced under oxygen limitation. *Biotechnol. Lett.* 12(3):201-206.
209. Zheng Z, Jiang Y, Zhan X, Ma L, Wu J, Zhang L, & Lin C (2014) An increase of curdlan productivity by integration of carbon/nitrogen sources control and sequencing dual fed-batch fermentors operation. *Appl. Biochem. Microbiol.* 50(1):35.
210. Wu J, Zhan X, Liu H, & Zheng Z (2008) Enhanced production of curdlan by *Alcaligenes faecalis* by selective feeding with ammonia water during the cell growth phase of fermentation. *Chin. J. Biotechnol.* 24(6):1035-1039.
211. Lee J-h & Lee IY (2001) Optimization of uracil addition for curdlan (β -1 \rightarrow 3-glucan) production by *Agrobacterium* sp. *Biotechnol Lett.* 23(14):1131-1134.
212. Zhang H-T, Zhan X-B, Zheng Z-Y, Wu J-R, English N, Yu X-B, & Lin C-C (2012) Improved curdlan fermentation process based on optimization of dissolved oxygen combined with pH control and metabolic characterization of *Agrobacterium* sp. ATCC 31749. *Appl. Microbiol. Biotechnol.* 93(1):367-379.
213. Naessens M, Cerdobbel A, Soetaert W, & Vandamme EJ (2005) *Leuconostoc* dextranase and dextran: production, properties and applications. *J. Chem. Technol. Biotechnol.* 80(8):845-860.

214. Karthikeyan RS, Rakshit SK, & Baradarajan A (1996) Optimization of batch fermentation conditions for dextran production. *Bioprocess Eng.* 15(5):247-251.
215. Liu L, Liu Y, Li J, Du G, & Chen J (2011) Microbial production of hyaluronic acid: current state, challenges, and perspectives. *Microb. Cell Fact.* 10:99-99.
216. Bajaj IB, Saudagar PS, Singhal RS, & Pandey A (2006) Statistical approach to optimization of fermentative production of gellan gum from *Sphingomonas paucimobilis* ATCC 31461. *J. Biosci. Bioeng.* 102(3):150-156.
217. Giavasis I, Harvey LM, & McNeil B (2006) The effect of agitation and aeration on the synthesis and molecular weight of gellan in batch cultures of *Sphingomonas paucimobilis*. *Enzyme Microb. Technol.* 38(1):101-108.
218. García-Ochoa F, Santos VE, Casas JA, & Gómez E (2000) Xanthan gum: production, recovery, and properties. *Biotechnol. Adv.* 18(7):549-579.
219. Roseiro JC, Esgalhado ME, Amaral Collaço MT, & Emery AN (1992) Medium development for xanthan production. *Process Biochem.* 27(3):167-175.
220. Banik RM, Santhiagu A, & Upadhyay SN (2007) Optimization of nutrients for gellan gum production by *Sphingomonas paucimobilis* ATCC-31461 in molasses based medium using response surface methodology. *Bioresour. Technol.* 98(4):792-797.
221. Rütering M, Schmid J, Gansbiller M, Braun A, Kleinen J, Schilling M, & Sieber V (2018) Rheological characterization of the exopolysaccharide Paenan in surfactant systems. *Carbohydr. Polym.* 181(1):719-726.
222. Bonacucina G, Martelli S, & Palmieri GF (2004) Rheological, mucoadhesive and release properties of Carbopol gels in hydrophilic cosolvents. *Int. J. Pharm.* 282(1):115-130.
223. Kim J-Y, Song J-Y, Lee E-J, & Park S-K (2003) Rheological properties and microstructures of Carbopol gel network system. *Colloid. Polym. Sci.* 281(7):614-623.
224. Bao H, Li L, Gan LH, & Zhang H (2008) Interactions between ionic surfactants and polysaccharides in aqueous solutions. *Macromolecules* 41(23):9406-9412.
225. Goddard ED (1994) Polymer/surfactant interaction - Its relevance to detergent systems. *J. Am. Oil Chem. Soc.* 71(1):1-16.
226. Mukherjee I, Sarkar D, & Moulik SP (2010) Interaction of gums (Guar, Carboxymethylhydroxypropyl Guar, Diutan, and Xanthan) with surfactants (DTAB, CTAB, and TX-100) in aqueous medium. *Langmuir* 26(23):17906-17912.
227. Morris GA, Adams GG, & Harding SE (2014) On hydrodynamic methods for the analysis of the sizes and shapes of polysaccharides in dilute solution: A short review. *Food Hydrocoll.* 42, Part 3:318-334.
228. Kostanski LK, Keller DM, & Hamielec AE (2004) Size-exclusion chromatography - a review of calibration methodologies. *J. Biochem. Bioph. Methods* 58(2):159-186.
229. Rinaudo M (2001) Relation between the molecular structure of some polysaccharides and original properties in sol and gel states. *Food Hydrocoll.* 15(4-6):433-440.
230. Duus JØ, Gotfredsen CH, & Bock K (2000) carbohydrate structural determination by NMR spectroscopy: modern methods and limitations. *Chem. Rev.* 100(12):4589-4614.
231. Rinaudo M, Milas M, Lambert F, & Vincendon M (1983) Proton and carbon-13 NMR investigation of xanthan gum. *Macromolecules* 16(5):816-819.

-
232. Jansson P-E, Lindberg B, & Sandford PA (1983) Structural studies of gellan gum, an extracellular polysaccharide elaborated by *Pseudomonas elodea*. *Carbohydr. Res.* 124(1):135-139.
233. Chandrasekaran R, Puigjaner LC, Joyce KL, & Arnott S (1988) Cation interactions in gellan: An x-ray study of the potassium salt. *Carbohydr. Res.* 181(Supplement C):23-40.
234. Milas M & Rinaudo M (1979) Conformational investigation on the bacterial polysaccharide xanthan. *Carbohydr. Res.* 76(1):189-196.
235. Sharmin F, Wakelin S, Huygens F, & Hargreaves M (2013) Firmicutes dominate the bacterial taxa within sugar-cane processing plants. *Sci. Rep.* 3:3107.
236. Aleti G, Sessitsch A, & Brader G (2015) Genome mining: Prediction of lipopeptides and polyketides from *Bacillus* and related Firmicutes. *Comput. Struct. Biotechnol. J.* 13:192-203.
237. Oh J-H & van Pijkeren J-P (2014) CRISPR–Cas9-assisted recombineering in *Lactobacillus reuteri*. *Nucleic Acids Res.* 42(17):e131.
238. Altenbuchner J (2016) Editing of the *Bacillus subtilis* genome by the CRISPR-Cas9 system. *Appl. Environ. Microbiol.* 82(17):5421-5427.
239. Pyne ME, Bruder MR, Moo-Young M, Chung DA, & Chou CP (2016) Harnessing heterologous and endogenous CRISPR-Cas machineries for efficient markerless genome editing in *Clostridium*. *Sci. Rep.* 6:25666.
240. Chen W, Zhang Y, Yeo W-S, Bae T, & Ji Q (2017) Rapid and efficient genome editing in *Staphylococcus aureus* by using an engineered CRISPR-Cas9 system. *JACS* 139(10):3790-3795.
241. Kim S-B & Timmusk S (2013) A simplified method for gene knockout and direct screening of recombinant clones for application in *Paenibacillus polymyxa*. *PLoS ONE* 8(6):e68092.
242. Zarschler K, Janesch B, Zayni S, Schäffer C, & Messner P (2009) Construction of a gene knockout system for application in *Paenibacillus alvei* CCM 2051T, Exemplified by the S-layer glycan biosynthesis initiation enzyme WsfP. *Appl. Environ. Microbiol.* 75(10):3077-3085.
243. Fu Y, Foden JA, Khayter C, Maeder ML, Reyon D, Joung JK, & Sander JD (2013) High-frequency off-target mutagenesis induced by CRISPR-Cas nucleases in human cells. *Nat. Biotechnol.* 31:822.
244. Cho SW, Kim S, Kim Y, Kweon J, Kim HS, Bae S, & Kim J-S (2014) Analysis of off-target effects of CRISPR-Cas-derived RNA-guided endonucleases and nickases. *Genome Res.* 24(1):132-141.
245. Yang T, Rao Z, Zhang X, Xu M, Xu Z, & Yang ST (2017) Metabolic engineering strategies for acetoin and 2,3-butanediol production: advances and prospects. *Crit. Rev. Biotechnol.* 37(8):990-1005.
246. Hertlein G, Seiffert M, Gensel S, Garcia-Gonzalez E, Ebeling J, Skobalj R, Kuthning A, Süßmuth RD, & Genersch E (2016) Biological role of paenilarvins, iturin-like lipopeptide secondary metabolites produced by the honey bee pathogen *Paenibacillus larvae*. *PLoS ONE* 11(10):e0164656.

7 Abbreviations

%	percent
°C	degree Celsius
η_0	zero shear viscosity
μg	microgram
μL	microliter
μM	micromolar, micromole per liter
ABC	ATP-binding cassette
ABTS	2,2-azino-bis-(3-ethylbenzthiazoline)-6-sulfonic acid
Ac	acetate
AM	active matter
amp	ampicillin
Ara	L-arabinose
ATP	adenosine triphosphate
bp	base pair
C*	critical polymer concentration
Cas9	CRISPR associated
CPS	capsular polysaccharide
CRISPR	clustered regularly interspaced short palindromic repeats
crRNA	CRISPR RNA
DA-64	N-(carboxymethylamino-carbonyl)-4,4'-bis-(dimethylamino)-diphenylamine sodium salt
DTT	dithiothreitol
ddH ₂ O	ultra-pure water
Da	Dalton
DMSO	dimethyl sulfoxide
DNA	deoxyribonucleic acid
EDTA	ethylenediaminetetraacetic acid
EPS	exopolysaccharide
ESI	electrospray ionization
FTIR	fourier-transform infrared spectroscopy
Fuc	L-fucose
fwd	forward
g	gram
G'	storage modulus
G''	loss modulus
Gal	D-galactose
GC	gas chromatography
Gl	Glycerate
Glc	D-glucose
GlcA	D-glucuronic acid

GlcNAc	N-acetyl-D-glucosamine
Glyc	glycerol
GPC	gel permeation chromatography
GRAS	generally regarded as safe
GT	glycosyl transferase
h	hours
HB	3-hydroxybutyrate
HDR	homology directed repair
HT	high throughput
Hz	hertz
IAA	Indole-3-acetic acid
IEC	Ion Exclusion Chromatography
kan	kanamycin
kb	kilobases
L	liter
LB	Lysogen broth
LPS	lipopolysaccharide
Man	D-mannose
ManA	mannuronic acid
MALLS	multi angle laser light scattering
mg	milligram
min	minutes
mL	milliliter
mM	millimolar. millimol per liter
MOPS	3-(N-morpholino)-propane-sulfonic acid
MS	mass spectrometer
neo	neomycin
NHEJ	non-homologous end joining
nm	nanometer
NMR	nuclear magnetic resonance
OPX	outer membrane polysaccharide export
Pa	Pascal
PCP	polysaccharide co-polymerase
PCR	polymerase chain reaction
PMP	1-phenyl-3-methyl-pyrazolone
pO ₂	partial pressure of oxygen
Pyr	pyruvate
RAST	rapid annotation using subsystem technology
rev	reverse
RNA	ribonucleic acid
rpm	rounds per minute
RT	room temperature

SDS	sodium dodecyl sulfate
sec	second
SEC	size exclusion chromatography
sgRNA	single guide RNA
Suc	sucrose
Succ	succinate
t	ton
TALENs	TAL effector nucleases
tet	tetracycline
TFA	trifluoroacetic acid
tracrRNA	trans-activating crRNA
TRIS	Tris(hydroxymethyl)aminomethane
UA	uronic acid
UHPLC	Ultra High Performance Liquid Chromatography
UV	ultra violet
v/v	volume per volume
w/v	weight per volume
w%	weight percent
x g	x g-force
Xyl	D-xylose
ZFNs	zinc finger nucleases

8 List of Figures

Figure 1.1 Chemical structure of Xanthan repeating unit.	16
Figure 1.2. Higher ordered structures formed by interrupted polysaccharides, based on the theory of junction zones.	17
Figure 1.3. Rheological behavior of thickening polysaccharides.	18
Figure 1.4. Gel textures produced by various hydrocolloids.	19
Figure 1.5. Molecular mechanisms of polysaccharide production.	20
Figure 1.6. Mixing in stirred tank fermenters.	23
Figure 1.7. Mechanisms involved in adaptive immunity of type II CRISPR-Cas system.	28
Figure 3.1. Basis for the strain selection.	51
Figure 3.2. Genome map and putative EPS cluster of <i>Paenibacillus</i> sp. 2H2.	80

9 List of Tables

Table 1.1. Important marketed bacterial exopolysaccharides with corresponding application fields and properties.	24
Table 1.2. Summary of exopolysaccharides produced by <i>Paenibacillus</i> strains.	32
Table 2.1. Equipment used in this study.	34
Table 2.2. Software and databases used in this study.	35
Table 2.3. Bacterial strains used in this study.	36
Table 2.4. Chemicals and reagents used in this study.	37
Table 2.5. Kits, enzymes and special consumables used in this study.	38
Table 2.6. Plasmids used in this study.	40
Table 4.1. Process characteristics of selected bacterial exopolysaccharides from detailed studies.....	109